The role of arginine methylation in alternative splicing

DISSERTATION

zur Erlangung des akademischen Grades

Doktor der Naturwissenschaften

(Dr. rer. nat.)

vorgelegt von

KATARZYNA KROWICKA

Universität Bielefeld

Fakultät für Biologie

Oktober 2019

DEDICATION

Dla mojej kochanej Mamy, bez której bym tego nie rozpoczela

Oraz

Dla mojego przyszlego Meza, bez którego bym tego nie ukonczyla

Contents

1. Summary

Gene expression is affected on many different levels. Transcriptional and post-transcriptional regulation are followed by translational control and post-translational regulatory mechanisms. It has been shown that reactions occurring on post-transcriptional and post-translational levels are necessary for normal plant development and help them to adapt to environmental changes.

Recent findings provide a link between post-transcriptional and post-translational regulation. To investigate the impact of posttranslational modifications on the function of splicing factors in *Arabidopsis thaliana*, the importance of arginine methylation in the RNA-binding protein GLYCINE-RICH RNA-BINDING PROTEIN 7 (GRP7) was analysed. The arginines at position 141 in GRP7 and in its homolog GLYCINE-RICH RNA-BINDING PROTEIN 8 (GRP8) have been shown to be symmetrically methylated by PROTEIN ARGININE METHYLTRANSFERASE 5 (PRMT5).

Transgenic plants with mutations causing amino acid exchange of arginine at the position 141 provided non-methylated versions of GRP7 and were used for evaluation of the importance of methylation status at this residue. Plants miss-expressing *PRMT5* and *GRP7/GRP8* were used to study possible interactions. To determine the importance of PRMT5-mediated arginine methylation of GRP7 and GRP8 for controlling physiological responses, flowering time control, pathogen defense and response to salt stress were analysed in transgenic plants.

The obtained results showed that arginine methylation of GRP7 does not affect flowering time, germination rates and primary root development under normal and stress conditions. The methylation mutants were indistinguishable from the wild type in these investigated processes. The complementation lines and overexpressing lines, carrying the mutated versions of GRP7 flowered as fast as their respective controls. However, applying biotic and abiotic stress to the plants that lack PRMT5 and GRP7 revealed a hierarchal set up between both proteins in some instances. The double mutant plants exhibited the phenotype of the *prmt5* loss-of-function mutants after pathogen infection and exposure to high salinity. The collected results suggest that *PRMT5* is epistatic to *GRP7*. Possible hierarchical interaction between PRMT5 and GRP7/GRP8 was assessed by analyses of alternative splicing of common target pre-mRNAs. It seems that PRMT5 and GRP7/GRP8 influence alternative splicing of *AKIN11,* a direct target of GRP7, in a hierarchical manner.
Moreover, the obtained results show that salt stress promotes alternative splicing for additional plasticity in responding to external stimulus. Although we are at the beginning of understanding the importance of alternative splicing for plant

physiological functions, it is possible that the response to stress conditions require elevated alternative splicing for decreasing energy costs and/or enriching proteome complexity.

Further analyses of the importance of arginine methylation in GRP7/GRP8 will be possible with the *prmt5 grp7 grp8* triple mutant, which was generated using the CRISPR/Cas9 system in this work. This will help us to better understand mechanisms at post-transcriptional and post-translational levels.

2. Zusammenfassung

Die Genexpression wird auf vielen verschiedenen Ebenen beeinflusst. Translationale kontroll- und posttranslationale Regulierungsmechanismen folgen transkriptionaler und posttranskriptionaler Regulation. Es konnte gezeigt werden, dass die Reaktionen, welche auf posttranskriptionaler und posttranslationaler Ebene stattfinden, für eine normale Pflanzenentwicklung notwendig sind und der Pflanze dabei helfen, sich an Umweltveränderungen anzupassen.

Neuste Erkenntnisse zeigen einen Zusammenhang zwischen posttranskriptionaler und posttranslationaler Regulation. Um den Einfluss von posttranslationalen Modifikationen auf die Funktion von Spleißfaktoren in *Arabidopsis thaliana* zu untersuchen, wurde die Bedeutung der Argininmethylierung in dem RNA-bindenden Protein GLYCIN-RICH RNA-BINDING PROTEIN 7 (GRP7) analysiert. Es konnte gezeigt werden, dass die Arginine in GRP7 und dessen Homolog GLYCIN-RICH RNA-BINDING PROTEIN 8 (GRP8) an Position 141 durch die PROTEIN-ARGININ-METHYLTRANSFERASE 5 (PRMT5) symmetrisch methyliert sind.

Transgene Pflanzen mit Mutationen, welche den Aminosäureaustausch von Arginin an Position 141 verursachen, resultierten in einer nicht methylierten Version von GRP7 und wurden verwendet, um die Bedeutung dieser Methylierung zu untersuchen. Pflanzen, welche *PRMT5* und *GRP7/GRP8* nicht exprimierten, wurden auf mögliche Wechselwirkungen untersucht. Um die Bedeutung der PRMT5-vermittelten Argininmethylierung von GRP7 und GRP8 für die Kontrolle physiologischer Reaktionen zu bestimmen, wurde der Blühzeitpunkt, die Pathogenabwehr und die Reaktion auf Salzstress in transgenen Pflanzen analysiert.

Die Ergebnisse zeigten, dass die Argininmethylierung von GRP7 den Blühzeitpunkt, die Pathogenabwehr, die Keimraten und die Primärwurzelentwicklung unter normalen und unter Stressbedingungen nicht beeinflusst. Die Mutanten waren bei den untersuchten Prozessen nicht vom Wildtyp zu unterscheiden. Die Komplementationslinien und die überexprimierenden Linien, welche die mutierte Variante von GRP7 getragen haben, blühten zum gleichen Zeitpunkt wie die Kontrolllinien. In einigen Fällen zeigten Pflanzen, welche weder PRMT5 noch GRP7 exprimierten, unter biotischem und abiotischem Stress einen hierarchischen Aufbau zwischen diesen beiden Proteinen. Pflanzen mit dieser Doppelmutation zeigten sowohl nach einer Infektion durch Erreger als auch nach der Exposition von hohem Salzgehalt den Phänotyp der *prmt5 loss-of-function* Mutante. Die gesammelten Ergebnisse lassen vermuten, dass *PRMT5* epistatisch über *GRP7* steht. Mögliche hierarchische Wechselwirkungen zwischen PRMT5 und GRP7/GRP8 wurden durch Analysen des

alternativen Spleißens gemeinsamer Ziel-Prä-mRNAs untersucht. Es scheint, dass PRMT5 und GRP7/GRP8 das alternative Spleißen von *AKIN11*, einem direkten Ziel von GRP7, auf hierarchische Weise beeinflussen.
Darüber hinaus zeigen die erzielten Ergebnisse, dass Salzstress das alternative Spleißen fördert, um zusätzliche Plastizität bei der Reaktion auf externe Reize zu erzielen. Wir stehen erst am Anfang, die Bedeutung des alternativen Spleißens für pflanzenphysiologische Funktionen zu verstehen. Aber es ist möglich, dass die Reaktion auf Stressbedingungen ein vermehrtes alternatives Spleißen erfordert, um die Energiekosten zu senken und/oder die Komplexität der Proteome zu erhöhen.
Die in dieser Arbeit mit dem CRISPR/Cas9-System erstellte Dreifachmutante *prmt5 grp7 grp8* ermöglicht weitere Analysen zur Bedeutung der Argininmethylierung in GRP7/GRP8. Dies wird helfen, die Mechanismen auf posttranskriptionaler und posttranslationeller Ebene besser zu verstehen.

3. Introduction

3.1. Alternative splicing as a part of post-transcriptional regulation in *Arabidopsis thaliana*

In eukaryotes, gene expression is controlled at many levels, by chromatin remodelling, transcriptional control, RNA processing, translational control and post-translational modifications. In the eukaryotic mRNA life cycle, precursor mRNA (pre-mRNA) is transcribed by RNA polymerase II in the nucleus, during which first RNA-processing steps are already taking place. Afterwards, the pre-mRNA undergoes further processing before the mature mRNA is transported to the cytoplasm where it is used for translation or degraded (Wahl et al., 2009).
Post-transcriptional control of gene expression includes pre-mRNA splicing, capping and polyadenylation, mRNA transport, and influences virtually all aspects of the mRNA life cycle such as stability, localisation, translation or decay (Figure 3.1). RNA-binding proteins (RBPs) are the main mediators of posttranscriptional processes. RBPs contain well-defined sequence motifs involved in RNA binding, which allows for direct interactions between RBPs and target RNAs or modulating the function of other regulatory factors (Figure 3.1) (Lorković and Barta, 2002).

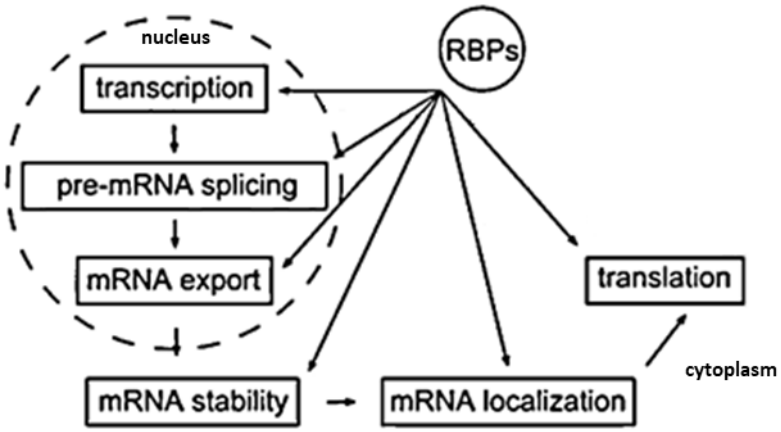

Figure 3.1 The mechanisms of post-transcriptional regulation. (Staiger and Köster, 2011; modified)

3.1.1. Constitutive and alternative splicing

Splicing takes place in the nucleus and is the process of creating a mature mRNA from the pre-mRNA, where introns are being removed and exons are joined together. Splicing is carried out by spliceosome components and other RBPs regulating pre-mRNA splicing. The spliceosome is a ribonucleoprotein complex, consisting of five uridine-rich small nuclear ribonucleoproteins (U snRNPs) U1, U2, U4, U5 and U6 snRNPs and other non-snRNP proteins. Each snRNP is assembled of non-coding small

nuclear RNA (snRNA) and RBPs. The SM proteins (B/B′, D3, D2, D1, E, F, and G) assemble into a ring-shaped heteroheptamer on snRNA U1, U2, U4 and U5 creating the respective snRNP. The snRNA U6 associates with SM-like proteins (LSM) (Henriques and Mas, 2013; Kornblihtt et al., 2013; Will and Lührmann, 2011).

The splicing process requires not only the spliceosome components but also well-defined splice sites (Figure 3.2.A). The exon-intron borders in the pre-mRNA are determined by short sequences, which can be recognized by snRNPs. The 5' splice site is located at the beginning of the intronic region and contains a relatively short 5' splice site consensus sequence. The 3' splice site is located at the end of the intronic region and it is defined by the branch site, the polypyrimidine tract and the 3' splice site consensus sequence (Konarska, 1998; Moore et al., 1993; Senapathy et al., 1990).

The splicing process starts with recruiting all necessary spliceosome components. The U1 snRNP binds to a complementary sequence in the pre-mRNA 5' splice site and two subunits of the U2 auxiliary factor (U2AF) bind to the 3' splice site, creating the complex E (Figure 3.2.B). The addition of U2 snRNP to the branch point changes complex E into the pre-spliceosome complex A. In the next step, U4, U5 and U6 snRNPs bind to the U2 snRNP, composing the pre-catalytic spliceosome complex B. The complex B turns into its active form, when U1 and U4 snRNPs disassociate and Nineteen Complex (NTC) joins the remaining spliceosome components. In the next two steps, the pre-mRNA undergoes the splicing process. Firstly, the 5' splice site is hydrolyzed and the intron 5' end is bound to an adenosine residue – the branch site. Secondly, the 3' splice site is cleaved, and the bordering exons are ligated in the initial order. The U2, U5, U6 snRNP and NTC disconnect from the mature mRNA, the intron lariat is released and degraded. The used spliceosome components become a part of a new spliceosome complex (Figure 3.2.B) (Meyer et al., 2015; Moore et al., 1993).

The spliceosome assembly is controlled by splicing signals, generated through protein binding (*trans*-acting factors) to *cis*-regulatory sequences: intronic splicing enhancers (ISE), exonic splicing enhancers (ESE), exonic splicing silencers (ESS) and/or intronic splicing silencers (ISS). Some *trans*-acting factors can either activate or repress the use of the splice site, but some of them can do both and the final effect depends on the nature of the bound *cis*-regulatory sequence. To the group of *trans*-acting factors belong amongst others: serine-arginine-rich (SR) proteins with an Arg/ Ser-rich (RS) domain and one or two RNA recognition motifs (RRMs), as well as heterogeneous nuclear ribonucleoproteins (hnRNPs), which contain various RRMs and K homology RNA-binding domains. SR and hnRNPs proteins bind to pre-mRNA and depending on their binding position, they can positively or negatively influence a recruiting of spliceosome

components to nearby splice sites (Barta et al., 2010; Fairbrother et al., 2002; Lavigueur et al., 1993; Lorković and Barta, 2002; Wang et al., 2004; Xue et al., 2009).

The degree of identity between the splice site sequence and the consensus sequence determines the binding affinity of splicing factors, making the splice site stronger or weaker. Strong splice sites are thought to be used for constitutive splicing. The efficiency of the weak sites can be modulated by *cis*-regulatory sequences and *trans*-acting factors. The localisation of both strong and weak splice sites can influence the choice of alternative splice sites, leading to alternative splicing (AS) (Fairbrother et al., 2002; Kornblihtt et al., 2013).

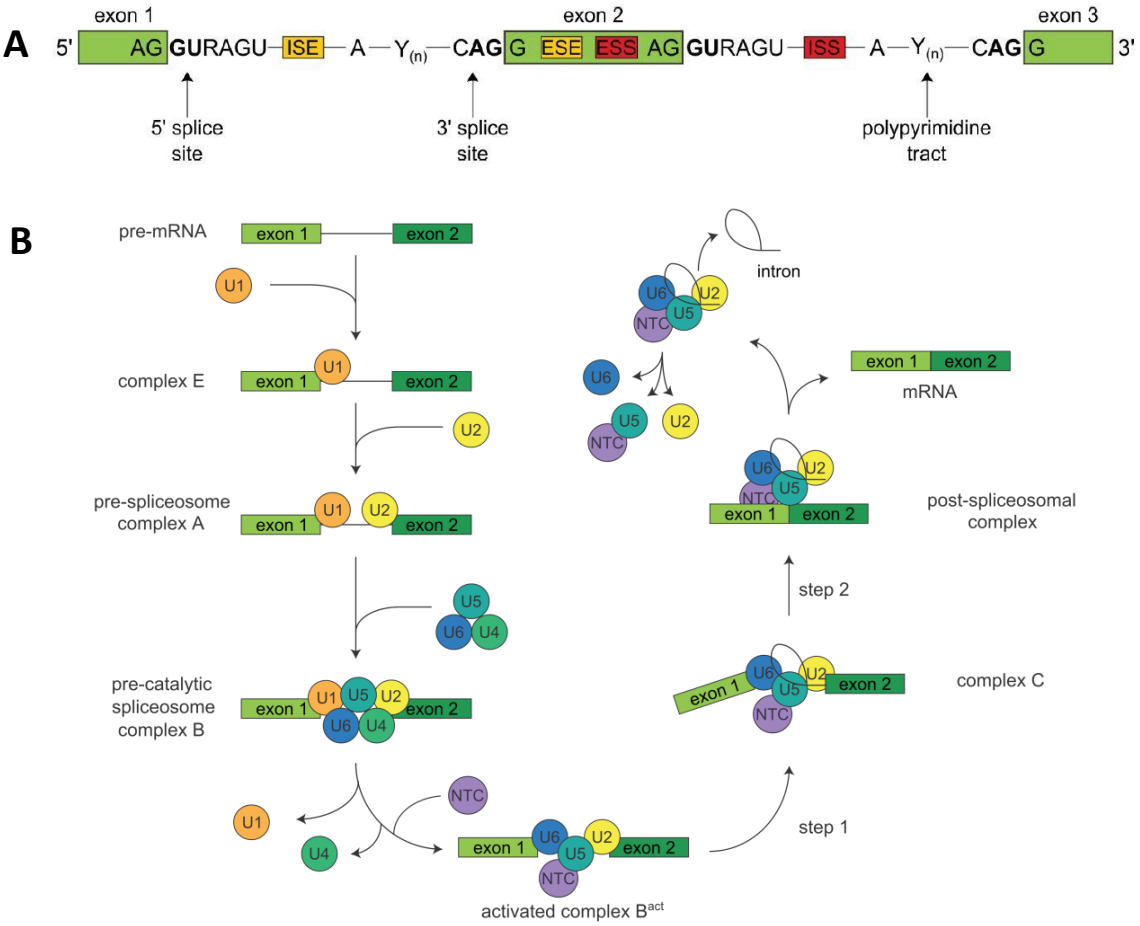

Figure 3.2 Pre-mRNA splicing. (**A**) Splice sites and regulatory elements involved in splicing. R- purine (A/G), Y – pyrimidine (C/T), ISE - intronic splicing enhancer, ESE exonic splicing enhancer, ESS - exonic splicing silencer, ISS - intronic splicing silencer (Meyer et al., 2015); (**B**) Mechanism of pre-mRNA splicing. The spliceosome components are recruited to pre-mRNA, composed of complexes E, A, B and B^{act}, respectively. Intron removal starts with the cleavage at the 5' splice site, followed by forming complex C. Next, pre-mRNA is cleaved at the 3' splice site and then exons are ligated. Finally, the mature mRNA is released, and spliceosome

components are used in another round. NTC- The Nineteen Complex See text for more details (Meyer et al., 2015; modified).

As it has been described above, constitutive splicing (CS) is the process of removing all introns from pre-mRNA and connecting exons. AS takes place when at least one of the constitutive splice sites is omitted by the spliceosome complex. The possibility of using other splice sites leads to the production of different transcripts from the same precursor, encoded by one gene. Transcripts from AS lack a part of the sequence and/or contain additional fragments. Different types of AS are characterized by intron retention (IR), exon skipping (ES), mutually exclusive exons (MEE), usage of alternative 5' slice site (Alt. 5'ss) and/or alternative 3' splice site (Alt. 3'ss) (Figure 3.3) (Black, 2005).

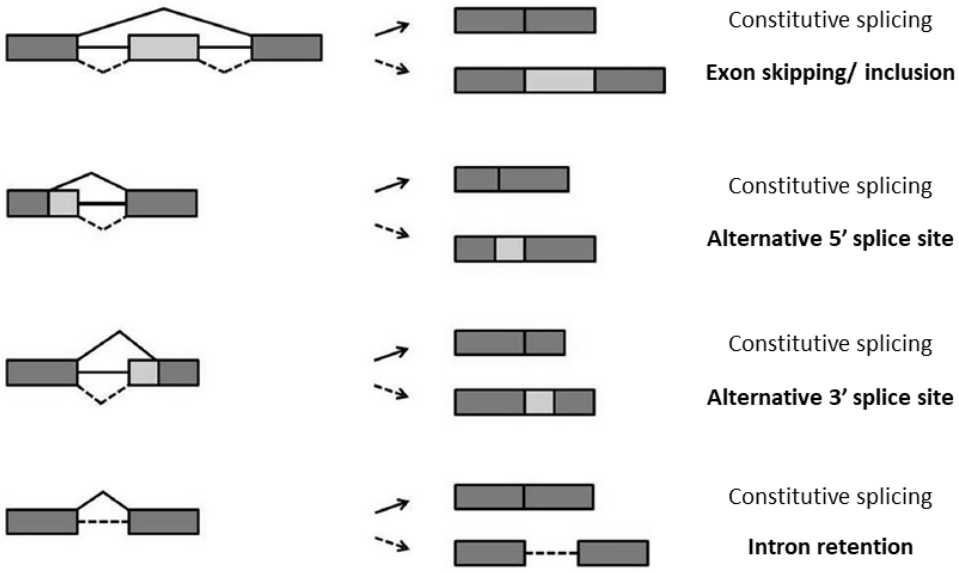

Figure 3.3 Different transcript variants from alternative splicing. Dark gray boxes – exons, light gray boxes – alternative exon regions, lines – introns, solid diagonal lines – constitutive splicing events, dotted line – alternative splicing events (Nolte and Staiger, 2015; modified).

The initial recognition of introns and exons is essential for correct splicing. Binding of specific proteins to a pre-mRNA can prevent recognition of 5' and 3' splice sites in the intron, thus constitutive splicing is not performed, and the intron is retained in the mature mRNA (Black, 2003). Moreover, it has been shown that exonic splicing enhancers (ESE) are required to prevent exon skipping by positive regulation of the splicing process at neighbouring splice sites. Exons, which do not contain ESE are not recognized and therefore they might be absent in the mature mRNA (Black, 2005; Ibrahim et al., 2005). On the other hand, exonic splicing silencers (ESS) suppress an inclusion of pseudoexons in CS and inhibit the splicing process at neighbouring splice sites, leading to AS (Wang et al., 2004).

Cryptic sites are located within intronic sequences and are not used during CS. Due to the negative influence of silencer elements as well as the lack of enhancers, those cryptic sites are not recognised as an element of an exon (Black, 2005).

AS has been shown to regulate transcriptome diversity. Variations in the stability of different mRNA splice variants can modify the transcriptome capacity as well. Changes in the open reading frame (ORF) can result in a frameshift mutation, possibly with a premature termination codon (PTC). However, mRNA stability, nuclear localisation and/or translational processes might be affected even if AS occurred in non-coding regions. For example, an intron retention can also be a cause of PTC in mRNAs. Those mRNAs are usually targeted for degradation via nonsense-mediated decay (NMD), what decrease an amount of truncated proteins (Figure 3.4) (Cartegni et al., 2002; Filichkin et al., 2010; Reddy, 2007). AS transcripts can also be confined in the nucleus, what makes them inaccessible to NMD. It has been shown, that such a mechanism can be development and time dependent (Göhring et al., 2014; Hartmann et al., 2018; Yang et al., 2017).

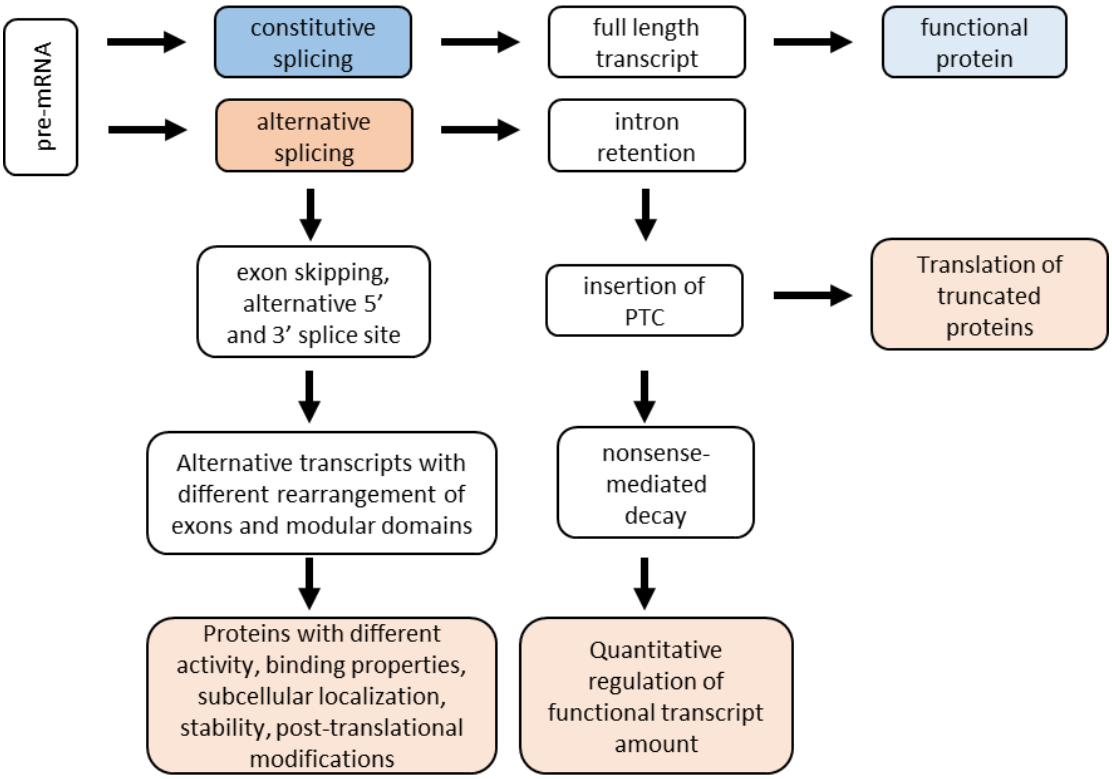

Figure 3.4 Capability of alternative splicing to adjust transcriptome and proteome. PTC - premature termination codon, (Mastrangelo et al., 2012; modified).

Moreover, it is possible that AS increases the proteome complexity through the synthesis of proteins with altered domain structures. However, those suppositions

remain elusive in plants (Chaudhary et al., 2019; Laloum et al., 2018). During splicing, the choice of alt. ss results in an inclusion or an exclusion of RNA fragment, and thus a synthesised protein can have a different set of features. It is predicted that such a protein can exhibit different enzymatic and/or binding activities, can be localised in different cellular compartments, with changed stability and/or post-translational modifications (Figure 3.4). Therefore, a role of a gene, which generates multiple transcripts, can be changed by shifting the ratio of constitutively and alternatively spliced isoforms (Laloum et al., 2018).

3.1.2. Functions of alternative splicing in plants

In *A. thaliana,* ~80% of nuclear genes contain intronic regions (The Arabidopsis Genome Initiative, 2000). At least 22% of total genes and 42-61% of multi-exon genes undergo alternative splicing, generating more than one transcript from the same pre-mRNA (Chamala et al., 2015; Filichkin et al., 2010; Marquez et al., 2012; Wang and Brendel, 2006). In *A. thaliana*, the most and the least abundant AS events are IR (56-65%) and ES (4-8%), respectively (Chamala et al., 2015; Wang and Brendel, 2006). However, the contribution of IR to changes in the transcriptome is low and only 23,6% of AS transcripts contain one or more retained introns (Marquez et al., 2012).

Although AS was the subject of many studies, its function has been only partly uncovered. The poor sensitivity of mass spectrometry techniques appears to be a major barrier for detecting changes is protein domains and thus proteome complexity, which are the effects of AS (Chaudhary et al., 2019). Till now, scientists have revealed that AS is required for regulating developmental changes, growth, as well as for responding to stress conditions (S. Filichkin et al., 2015; Reddy et al., 2013; Staiger and Brown, 2013). Recently, Chaudhary and co-workers proposed a double role of AS during the initial phase of stress conditions. According to their opinion, AS can limit normal protein synthesis and increase the proteomic complexity, which is possibly required under stress conditions (Chaudhary et al., 2019). This proposed scheme explains the need of maintaining low metabolic costs in addition to an elevated level of AS under stress condition.

The main function of AS seems to be the fine-tuning of the transcriptome, specifically to a changing environment. As stated by Petrillo and co-workers, light changes can regulate AS in plants to adapt to variables light conditions. An external stimulus, which affect photosynthesis and growth can be identified by chloroplasts and transferred to nucleus. Environmental changes, which disturb plastid homeostasis, initiate retrograde signals that influence AS, in particular splicing of pre-mRNAs that encode RNA-processing proteins. Those molecular re-arrangements seem to be necessary for

adjustment of plant metabolism and development to continuously changing light conditions (Petrillo et al., 2014). A recent discovery reveals the nuclear regulatory mechanism of light controlled AS. Godoy Herz and co-workers showed that light-mediated AS is regulated by Pol II elongation, where the light conditions accelerate the elongation process and increases probability of skipping week splice sites, resulting in fully spliced mRNA (Godoy Herz et al., 2019).

A well-documented example of light/dark-mediated changes in AS is pre-mRNA splicing of *At-RS31,* encoding a serine-arginine-rich splicing factor. Only one of three *At-RS31* splice variants encode an active *At*-RS31 protein. The level of the functional transcript decreases in the dark, while the total transcript level of all possible isoforms stays unchanged (Petrillo et al., 2014). Additional experiments showed that the functional transcript *At*-RS31 is responsible for plant growth and adjustment to changing light conditions (Petrillo et al., 2014). A study from 2016 showed that AS is essential for light-mediated processes, such as photomorphogenesis. Etiolated *A. thaliana* seedlings, when exposed to light, within short time exhibited a wide range of changes in AS. Along with the shift from dark to light, over 60% of the AS events switched from non-productive to protein-coding splicing variants (Hartmann et al., 2016).

Furthermore, it has been shown that AS is very important for temperature-dependent flowering. In *A. thaliana,* Col-0 two splice variants of *FLOWERING LOCUS M (FLM)* were shown to compete for connecting with the floral repressor SHORT VEGETATIVE PHASE (SVP) (Posé et al., 2013). One splice variant FLM-β, contains exon 2 and together with SVP represses flowering at low temperatures, as the FLM-β isoform is most abundant in cooler conditions. On the other hand, FLM-δ, incorporating exon 3, predominantly forms a complex with SVP at higher temperatures. Due to the fact that the third exon exhibits reduced DNA binding ability, FLM-δ-SVP was described as a dominant-negative activator of flowering (Posé et al., 2013). Capovilla and co-workers employed the CRISPR/Cas9 technology to investigate the function of the second and third exon. They showed that plants with *FLM-β* in *flm-3* loss of function mutants were late flowering, while *FLM-δ* plants in *flm-3* background were not flowering earlier than *flm-3*. Therefore, FLM-β can be considered as a flowering repressor. However, the participation of FLM-δ in the regulation of flowering time stays unclear (Capovilla et al., 2017).

AS of pre-mRNAs is increasingly recognized as an important factor in the regulation of gene expression under stress conditions, including cold, drought, heat, high salinity and pathogen infection.

A study performed on grapes (*Vitis vinifera*) showed that ~70% of genes undergo AS at high temperature. Although all splicing events were more abundant under heat,

changes in intron retentions were the most significant (Jiang et al., 2017). In the same publication, Jiang and co-workers showed that increasing ambient temperature is correlated with elevated protein levels of RNA-binding proteins SR45, SR30 and SR34 as well as the nuclear ribonucleic protein U1A, which explains why AS is more pronounced under heat stress (Jiang et al., 2017). Moreover, it has been shown that specific heat shock factors (HSFs) are regulated by AS, in both grapes and *A. thaliana* (Jiang et al., 2017; Sugio et al., 2009).

Calixto and co-workers performed RNA-seq analysis and identified ~9000 genes that were differentially expressed (DE) and/or differentially regulated by AS (DAS) in *A. thaliana* under cold stress. Among them, 1647 genes were exclusively regulated at the AS level. In the group of early response genes regulated only by AS, many cold-responsive transcription factors and RNA-binding proteins were confirmed. In some cases, significant AS changes were detected already after 40 min as well as after a two-degree change in temperature (from 20°C to 18°C). Therefore, AS was proposed to be responsible for the rapid initial response to cold (Calixto et al., 2018). In the same publication, the *U2B-LIKE* gene encoding an RNA-binding protein was identified in the group of early AS response genes. Further, *U2B-LIKE* was shown to be required for cold tolerance (Calixto et al., 2018).

Moreover, Ding and co-workers reported global changes in AS in *A. thaliana* seedlings, which were exposed to salt stress. By using the high-coverage RNA-seq data, it was determined that ~49% of intron-containing genes undergo AS in response to salt stress. 10% of the intron-containing genes were categorized as DAS and their functions were mainly linked to stress response and RNA splicing (Ding et al., 2014). Moreover, it has been shown that SR splicing factors are regulated by AS under salt stress conditions. IR, alt.5'ss and/or alt.3'ss are frequently used in pre-mRNA splicing of *SR* transcripts, what often results in PTC-containing *SR* mRNAs. (Ding et al., 2014). A recent publication shows that the spliceosome component *At*U1A controls AS under salt stress, where it regulates pre-mRNA splicing of reactive oxygen species (ROS)-related genes. Therefore, it was proposed that *At*U1A is required for salt tolerance (Gu et al., 2018).

Finally, AS is essential for maintaining pathogen resistance. The products of disease resistance *(R)* genes have been shown to be regulated by AS during the resistance response. According to the Gene-for-gene concept, R proteins specifically recognize pathogen strains with cognate avirulence (*avr*) determinants (Flor, 1971; Leister and Katagiri, 2000). The majority of *R* gene products belong to the NBS-LRR class, containing nucleotide binding site domains and multiple leucine-rich repeats (Baker et al., 1997). AS of *R* pre-mRNAs results in PTCs and then truncated proteins with fewer domains. In *A. thaliana* hundreds of *R* genes have been identified and one of them is *RESISTANCE TO PSEUDOMONAS SYRINGAE 4 (AtRPS4)*, which encodes a protein that

confers resistance to *Pseudomonas syringae* pv *tomato* DC3000 (Gassmann et al., 1999). Interestingly, it has been shown that the intronless version of *AtRPS4* cannot fully complement the *rps4* mutant. In complementation lines expressing truncated transgenes, a partial resistance was also observed. (Zhang and Gassmann, 2003). Further studies revealed that the products of the full length and truncated transcripts *AtRPS4* have different stability and functions in *RPS4*-mediated resistance (Zhang and Gassmann, 2007). Moreover, such a AS-mediated regulation of disease resistance genes was also found for other *R* genes in *A. thaliana,* as well as across plant species, e.g. *Nicotiana tabacum*, *Hordeum vulgare, Oryza sativa* (Costanzo and Jia, 2009; Dinesh-Kumar and Baker, 2000; Halterman et al., 2003; Peart et al., 2005).

3.2. The RNA binding proteins *At*GRP7 and *At*GRP8

The plant glycine-rich proteins (GRPs) are a superfamily, which is characterized by semi-repetitive glycine-rich motifs. GRPs have diverse localisation and functions, therefore the classification of plant GRPs is based on the structure of the glycine repeats and the presence of conserved motifs (Mangeon et al., 2010).

Arabidopsis thaliana GLYCINE-RICH RNA-BINDING PROTEIN 7 and 8 (*At*GRP7 and *At*GRP8) are RBPs and belong to one class, since both *At*GRP7 and *At*GRP8 contain a single RNA recognition motif (RRM) at the N-terminus with two highly conserved ribonucleoprotein consensus sequences (RNP1 and RNP2) and a glycine-rich domain at the C-terminus. These two genes share 77% homology between their DNA sequences and their protein products share a similar molecular weight, which is about 16 kDa. GRP7 and GRP8 protein sequences share 81% homology, therefore functional redundancy has been suggested (Carpenter et al., 1994; Heintzen et al., 1994; Staiger et al., 2003; Streitner et al., 2008; van Nocker and Vierstra, 1993).

Schöning and co-workers tested the RRM domain in *At*GRP7, which is a well-characterized RNA-binding domain. They showed that the exchange of arginine at the position 49, the first amino acid in the conserved ribonucleoprotein consensus sequence 1 (RNP1), to glutamine (R49Q) reduces the *At*GRP7 binding-ability to its RNA-targets (Schöning et al., 2007), which was later confirmed by *in vivo* studies (Köster et al., 2014).

The combination of individual nucleotide resolution crosslinking and immunoprecipitation (iCLIP) and RNA immunoprecipitation-sequencing (RIP-seq) experiments allowed Meyer and co-workers to identify 452 high-confidence RNA targets of *At*GRP7 *in vivo*. The group of high confidence binders included a number of transcripts related to the response to abiotic stresses (cold, salinity) and pathogen

defense (Meyer et al., 2017). It has been also shown that *At*GRP7 preferentially binds to 3'UTR regions. Moreover, *At*GRP7 targets were mostly downregulated when *At*GRP7 is overexpressed and upregulated when *At*GRP7 is absent. Therefore, it was concluded that *At*GRP7 most likely acts as a negative regulator (Meyer et al., 2017).

It has been previously shown that GRP7 is localised in the nucleus and cytoplasm (Kim et al., 2008; Ziemienowicz et al., 2003). Moreover, it has been shown that GRP7 interacts with the nuclear import receptors transportin in plant and HeLa cells (Ziemienowicz et al., 2003). Under cold stress conditions, GRP7 takes part in mRNAs export from the nucleus to the cytoplasm (Kim et al., 2008). The nucleocytoplasmic distribution of GRP7 is regulated by protein *At*JAC1 (*Arabidospis* JACALIN-LECTIN LIKE1, AT3G16470), which interacts with GRP7 in the cytoplasm. *At*JAC1 responses to jasmonic acid and other stimulus and is involved in many biological processes, including flowering. Overexpression of *At*JAC1 leads to accumulation of GRP7 in the cytoplasm and the lack of *At*JAC1 is involved with nuclear localisation of GRP7 (Xiao et al., 2015).

3.2.1. *At*GRP7 and *At*GRP8 as a part of a downstream oscillator in the circadian system in *Arabidopsis thaliana*

The circadian clock in *Arabidopsis thaliana*

The circadian clock (from „*circa diem*", about one day) is an endogenous time-keeping mechanism, with a period of ~24 hours, that is entrained to the periodic light regime of the environment and controls internal processes so that they take a place at the most appropriate time of day. This provides a competitive advantage and contributes to the fitness of the plants with maximum energy uptake and biomass production (Barak et al., 2000; Johansson and Köster, 2019).

The circadian clock works at the level of single cells. Rhythmically expressed clock genes operate through autoregulatory negative transcription-translation feedback loops, which generate rhythmic oscillations in cellular, metabolic and physiological activities (Más, 2008). By using enhancer trap lines, Michael and McClung showed that 36% of the *A. thaliana* genome is circadian-regulated (Michael and Mcclung, 2003). In plants, the circadian clock controls many biological processes such as leaf movement, stomatal and petal opening, chloroplast shape and movement, hypocotyl length and flowering (Barak et al., 2000; Dowson-Day and Millar, 1999; Engelmann et al., 1992; Hassidim et al., 2017; Kaihara and Takimoto, 1979; Vanden Driessche, 1966; Wang and Tobin, 1998).

Consisting of input pathways, a core oscillator and output pathways (Figure 3.5.A), the biological clock is an endogenous timekeeper that most organisms possess. However, it was suggested that the plant circadian clock system developed separately form the others, since no homology has been found between *A. thaliana* clock genes and biological clock components of *Drosophila,* mammals or fungi (McClung, 2006; Salomé and McClung, 2004; Schöning and Staiger, 2005; Staiger et al., 2003).

Mechanism of the circadian clock in *Arabidopsis thaliana*

The interlocked transcription-translation feedback loops are the main control system in a circadian clock. In the core oscillator, transcript abundance of clock genes changes in the rhythm of a day period. The protein of the rhythmically expressed gene regulates the expression of a second gene (negative regulator). The changes in the protein level of the negative component represses the expression of first gene and that generates ~24 hours oscillations in the biological clock (Johansson and Köster, 2019).

In *A. thaliana,* the core oscillator is based on reciprocal regulations between CIRCADIAN CLOCK ASSOCIATED 1 (CCA1), LATE ELONGATED HYPOCOTYL (LHY) and TIMING OF CAB EXPRESSION 1 (TOC1), creating a so called core loop (Figure 3.5.B). The morning phase genes *CCA1* and *LHY* are transcription factors with Myb-type DNA-binding domains, which are transiently induced by phytochromes and show a rhythmical expression with a peak at dawn. TOC1 was characterized as a response regulator protein with a CCT DNA-binding domain. TOC1 shows circadian oscillation with a peak at dusk and its expression is negatively regulated by CCA1 and LHY during the day. The protein level of LHY and CCA1 decreases towards the evening and the level of TOC1 protein increases (Alabadí et al., 2001; Gendron et al., 2012; Huang et al., 2012). It has also been shown that *LHY* and *CCA1* work in negative autoregulatory loops for their own and reciprocal gene expression regulation by forming physical interactions with other transcription factors (Adams et al., 2015).

Besides the core loop, the core oscillator is also composed of a morning and evening loop. In the morning loop, CCA1 and LHY promote expression of *PSEUDORESPONSE REGULATORS (PRRs) PRR5, PRR7* and *PRR9,* which repress *CCA1* and *LHY* (Greenham and Mcclung, 2015; Mateos et al., 2018). Many studies showed that LHY is a positive regulator of *PRRs* genes. However, work of Adams and co-workers revealed a new side of the circadian clock by presenting LHY as a direct transcriptional repressor of all *PRRs* genes (Adams et al., 2015; Mateos et al., 2018). Therefore, further studies are necessary to understand this fundamental and very complex system.

The main components of the evening loop are TOC1, LUX ARRHYTHMO (LUX), EARLY FLOWERING 3 and 4 (ELF3, EFL4). TOC1 directly or indirectly represses expression of

the morning-phase genes *CCA1, LHY, PRR5, PRR9* and *PRR7*. On the other hand, the three evening-phase elements ELF3, ELF4 and LUX form a multi-protein complex, called the evening complex (EC), which decreases the expression levels of *PRR5, PRR7, PRR9,* TOC1 and *GIGANTEA* (*GI*), resulting in re-started transcriptional activity of *CCA1* and *LHY*. TOC1 and EC, besides a negative autoregulatory function, regulate each other reciprocally (Dixon et al., 2011; Helfer et al., 2011; Herrero et al., 2012).

The rhythm of the core oscillator is passed on to output pathways, linking environmental changes with a set of diverse biological processes for controlling their timing and through this contributing to plant fitness.

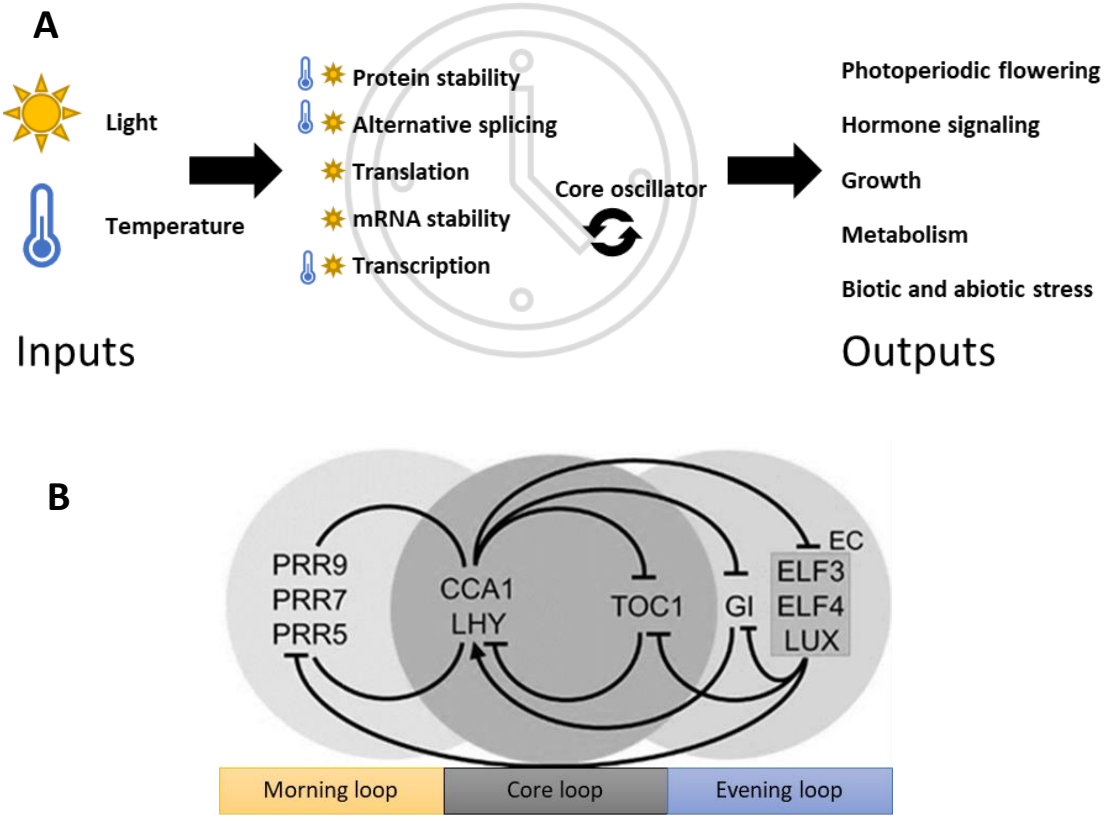

Figure 3.5 Mechanism of the circadian clock in *Arabidopsis thaliana*. (**A**) Environmental stimuli, such as light and temperature changes, are processed in the core oscillator for controlling many important biological processes (Nohales and Kay, 2016; modified). (**B**) The core oscillator is composed of three main interconnected loops (morning loop, core loop and evening loop). The core loop is based on the reciprocal regulation between CCA1/LHY and TOC1. Expressed in the morning, CCA1 and LHY positively regulate *PRR5, PRR7*, *PRR9* and they in turn repress CCA1 and LHY. In the morning, CCA1 and LHY also repress *TOC1* and *GI* and the genes coding proteins of the evening complex (EC) – *ELF3, ELF4, LUX*. During the day, the amount of EC increase to peak at the evening, repressing the expression of *GI*, *TOC1* and *PRRs* to promote then the transcription of *CCA1* and *LHY* (Johansson and Köster, 2019; modified).

Circadian clock and alternative splicing

Alternative splicing (AS) has been shown to influence circadian clock genes in plants, human, *Drosophila* and *Neurospora* for maintaining circadian rhythms and responding to external stimuli (Lee et al., 2018; Shakhmantsir et al., 2018; Shakhmantsir and Sehgal, 2019; Shang et al., 2017; Staiger and Brown, 2013; Wang et al., 2018).

In *A. thaliana,* by using high-throughput and high-resolution methods, the extensive regulation of AS on many important circadian clock genes was revealed (Filichkin et al., 2010; James et al., 2012). Studies on respective mutants showed that spliceosome components such as SKI-INTERACTING PROTEIN (SKIP) (Wang et al., 2012), SPLICEOSOME TIMEKEEPER LOCUS 1 (STIPL1) (Jones et al., 2012), SM-LIKE 4 and 5 (LSM4, LSM5) (Perez-Santángelo et al., 2014) and splicing factors PROTEIN ARGININE METHYLTRANSFERASE 5 (PRMT5) (Sanchez et al., 2010), GEM NUCLEAR ORGANELLE ASSOCIATED PROTEIN 2 (GEMIN2) (Schlaen et al., 2015), SICKLE (SIC) (Marshall et al., 2016), SERINE/ARGININE-RICH 45 (SR45) (Filichkin et al., 2015) affect AS of core clock transcripts, such as *PRR7, PRR9, TOC1, CCA1, LHY*.

Moreover, AS does not only affect the core clock genes but also regulates downstream elements of the circadian clock, i.e. *AtGRP7* and *AtGRP8,* producing NMD-inducing PTC+ transcripts (Schöning et al., 2008, 2007; Staiger et al., 2003).

*At*GRP7 and *At*GRP8 as downstream elements of circadian system

Both genes *AtGRP7* and *AtGRP8* show circadian transcript oscillations with a peak in the evening. The observed rhythmicity in *AtGRP7* and *AtGRP8* expression reflects the rhythm from the core oscillator (Carpenter et al., 1994; Heintzen et al., 1994). Using transgenic lines carrying reporter constructs, the *AtGPR7* promoter region necessary for retaining unaltered *AtGRP7* rhythmic oscillations was characterized (Staiger and Apel, 1999). Additionally, it has been shown that the core oscillator components, LHY and CCA1, influence the *AtGRP7* transcription oscillations by direct binding to two evening elements in the *AtGRP7* promoter region (Harmer et al., 2000; Schaffer et al., 1998; Wang and Tobin, 1998). Thus, transcriptional regulation is crucial for stable, rhythmical *At*GRP7 activity.

Despite being controlled by CCA1/LHY, *At*GPR7 and *At*GRP8 are not involved in the regulation of main circadian components. Therefore, it was suggested that *At*GPR7 and *At*GRP8 work as a downstream oscillator, also known as a molecular slave oscillator, integrating information from the core oscillator into an output pathway (Figure 3.6) (Heintzen et al., 1994; Schmal et al., 2013).

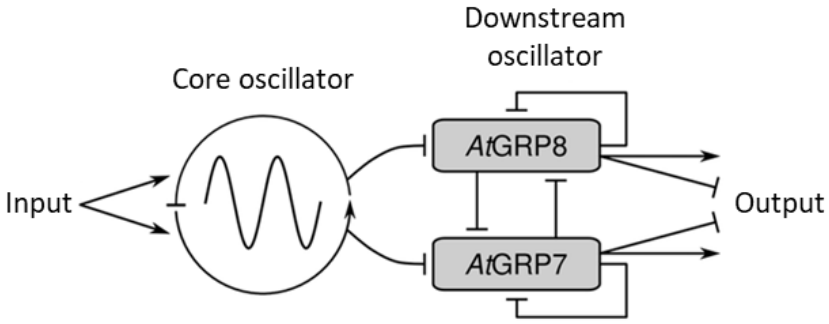

Figure 3.6 Circadian clock system with the downstream oscillator in *Arabidopsis thaliana*. The *At*GRP7 and *At*GRP8 oscillations are regulated by negative autoregulatory feedback loops and the core oscillator, integrating the input pathways. The rhythmicity in the downstream oscillator regulates expression of target genes for adapting the plant biological processes to the constantly changing environment (Schmal et al., 2013; modified).

Negative autoregulation and cross-regulation of *At*GRP7 and *At*GRP8

*At*GRP7 and *At*GRP8 undergo negative autoregulation by alternative splicing, where binding of *At*GRP7 or *At*GRP8 to their own pre-mRNA activates a cryptic 5' splice site in the intron. The resulting alternatively spliced transcript retains part of the intron including a premature termination codon and is subjected to degradation via nonsense-mediated decay (NMD) (Figure 3.7). At low *At*GRP7 protein levels, *AtGRP7* pre-mRNA is constitutively spliced and functional *At*GRP7 is produced. The accumulation of *At*GRP7 leads to alternative splicing and transcript degradation, decreasing the level of functional protein. *At*GRP8 undergoes the analogous process (Schöning et al., 2008, 2007; Staiger et al., 2003).

In addition to the autoregulatory functions of *At*GRP7 and *At*GRP8 described above, reciprocal regulation between both proteins has been shown. According to the present model, *At*GRP7 promotes unproductive splicing, where the alternatively spliced *AtGRP8* transcript is degraded by NMD, leading to decreased *At*GRP8 protein levels. Likewise, *At*GPR8 binds to the *AtGRP7* transcript and promotes the use of a cryptic 5' splice site. Through this, *At*GRP8 positively regulates alternative splicing of *AtGRP7,* leading to downregulation of *At*GRP7 protein (Schöning et al., 2008).

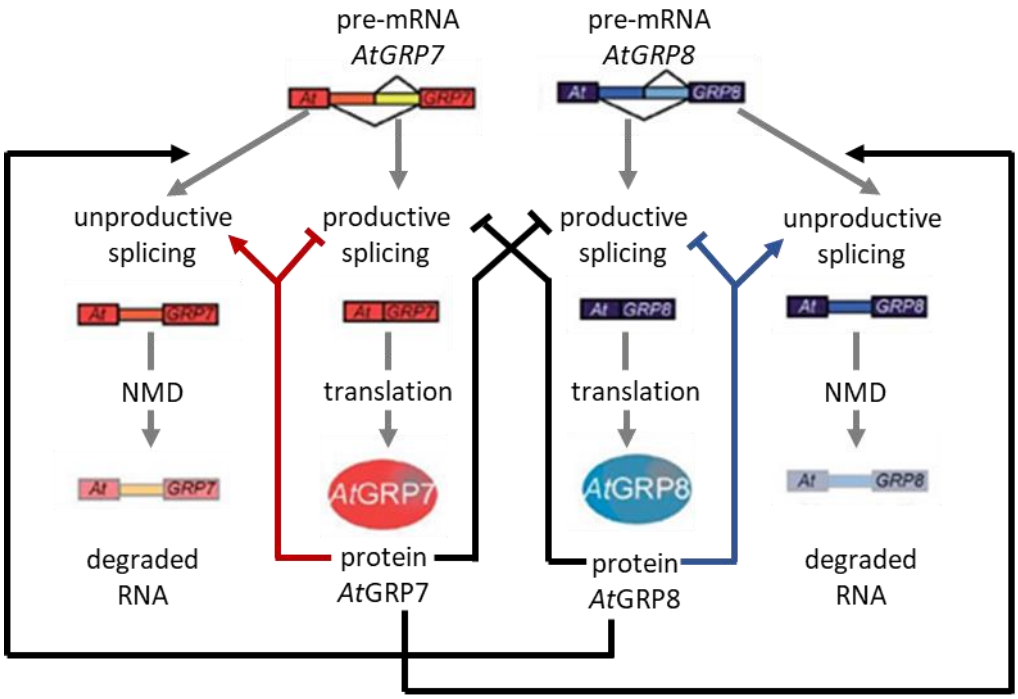

Figure 3.7 Autoregulation and cross-regulation of *At*GRP7 and *At*GPR8 via a transcription-translation feedback loop. *AtGRP7* and *AtGRP8* pre-mRNAs are processed by the constitutive or alternative splicing, generating functional proteins or alternatively spliced transcripts with a retained part of the intron, containing a premature stop codon. Grey arrows indicate productive and unproductive splicing, leading to translation or nonsense-mediated decay (NMD). Black arrows indicate cross-regulation between *At*GRP7 and *At*GRP8. Red and blue arrows indicate the autoregulation of *At*GRP7 and *At*GRP8, respectively (Schöning et al., 2008; modified).

3.2.2. Physiological functions of *At*GRP7 and *At*GRP8

Most of the publications report on the physiological functions of *At*GRP7 rather than *At*GRP8. Since *At*GRP7 and *At*GRP8 belong to the same class of proteins, share 77% of their amino acid sequence and contribute to similar molecular processes, it is expected that both proteins share at least some of their physiological functions.

Role in flowering time

Analyses of the *atgrp7-1* T-DNA mutant and RNA interference lines *AtGRP7i* and *AtGRP8i* revealed that the reduction or lack of *At*GRP7 or *At*GRP8 results in late flowering. On the other hand, plants overexpressing *At*GRP7 (*At*GRP7ox) flower earlier than wild type plants in short-day conditions (Streitner et al., 2008). Additionally, the late flowering phenotype of *atgrp7-1* can be complemented by a 3 kb genomic GRP7 fragment (Steffen and Staiger, unpubl.). Moreover, molecular analyses showed that transcript level of the floral repressor *FLOWERING LOCUS C* (*FLC*) is elevated in *atgrp7-*

1 and reduced in *At*GRP7ox. Accordingly, it is deduced that *At*GRP7 plays a positive role in the transition to the reproductive phase (Figure 3.8). The regulation of flowering time by *At*GRP7 is controlled, at least partly, by repressing *FLC* expression. Due to the fact that the photoperiodic response is not affected in *atgrp7* loss-of-function mutants and the late flowering phenotype of *atgrp7-1* can be rescued by vernalization, *At*GRP7 was suggested to be a component of the autonomous pathway (Streitner et al., 2008).

Role in response to abiotic stress

*At*GRP7 has also been shown to play a role in stress tolerance, i.e. responses to abscisic acid (ABA), high salt concentrations, dehydration and cold stress (Carpenter et al., 1994; Kim et al., 2008). *At*GRP7ox plants exposed to high salinity conditions or drought exhibited a hypersensitive phenotype with retarded germination and slower seedling growth in comparison to wild type plants and *atgrp7-1* (Kim et al., 2008). Moreover, the level of *At*GRP7 and *At*GRP8 proteins increases upon oxidative stress and cold stress (Carpenter et al., 1994; Schmidt et al., 2010; Schöning et al., 2008). Interestingly, the transcript levels of *COLD-REGULATED 15A* (*COR15A*), *RESPONSIVE TO ABA 18* (*RAB18)* and *RESPONSIVE TO DESSICATION 29A* (*RD29A*), also known as *COLD REGULATED 78* (*COR78*), were down-regulated in *At*GRP7ox plants (Streitner et al., 2010). However, the *At*GPR7ox plants seem to be more resistant to cold stress when compared to *atgrp7-1,* with hypersensitivity in low temperatures (Kim et al., 2008).

Tolerance to different abiotic stresses is also influenced by stomatal opening and closing. Kim and co-workers localised *At*GRP7 in the guard cell and reported *At*GRP7-mediated stomatal closure upon various treatments. The results suggest that *At*GRP7 is required for stomatal closing during ABA- and cold-stress. On the other hand, *At*GRP7 stimulates stomatal opening when exposed to dehydration and salt stress. In conclusion, high levels of *At*GRP7 support plant tolerance to cold stress but negatively influence plant resistance to dehydration and salt stress (Kim et al., 2008) (Figure 3.8).

Role in pathogen defense

Finally, *At*GRP7 has been shown to play a role in plant innate immunity. Plants that lack *At*GRP7 are more susceptible to *Pseudomonas syringae* bacterial infection than wild type plants. On the other hand, *At*GRP7ox plants are more resistant to *P. syringae* treatment in comparison to wild type. It has been shown that *At*GRP7 promotes translation of *FLAGELLIN SENSITIVE 2* (*FLS2*), which encodes a receptor for bacterial flagellin. Molecular analyses revealed that arginine at the position 49 (R^{49}) in the *At*GRP7 amino-acid-chain is ADP-ribosylated by HopU1, the *P. syringae* type III effector, which supresses the plants' innate immunity by modifying RBPs. The ADP-ribosylation in R^{49}, as well as mutation of R^{49}, negatively influences or even blocks the RNA-binding

function of *At*GRP7. While the endogenous *At*GRP7 can fully complement the *grp7-1* mutant, *At*GRP7 with an amino-acid-exchange at the position 49 does not rescue the susceptibility of the *grp7-1* mutant to bacterial infection. Taken together, *At*GRP7 is involved in pathogen defence and the RNA-processing mediated by *At*GRP7 might be important for plant defence transcripts and therefore for plant innate immunity (Fu et al., 2007; Jeong et al., 2011; Nicaise et al., 2013) (Figure 3.8).

It has been shown that the immune response depends on the time of day. Bacterial growth is more suppressed and the expression of defense genes (e.g. *FLG22-INDUCED RECEPTOR-LIKE 1* (*FRK1*)) is higher, when *A. thaliana* plants are syringe-infiltrated in the morning than at the evening (Korneli et al., 2014).
FRK1, the PTI (Pattern Triggered Immunity)-responsive gene, encoding a leucine-rich-repeat (LRR) receptor kinase, is involved in early defense signalling. *PATHOGENESIS-RELATED GENE 1* (*PR1*) is a defense marker gene involved in late defense signalling. Therefore *FRK1* and *PR1* are termed as early and late response genes. The expression of both flagellin-responsive defense-related genes *FRK1* and *PR1* is induced by *Pst* infection through a MAPK- (mitogen-activated protein kinase)- cascade (Asai et al., 2002; Hsu et al., 2013; Pel et al., 2014; Uknes et al., 1992; Xing et al., 2001).
Transcripts of *PATHOGENESIS-RELATED PROTEIN 1* and *2* (*PR1* and *PR2)* were found up-regulated in *At*GRP7ox and down-regulated in *grp7-1* mutants. Plants overexpressing *At*GRP7 with a mutation in the RNA-binding domain did not display up-regulated *PR1* or *PR2*. This finding suggests that the RNA-binding domain in *At*GRP7 is necessary for positive regulation of both transcripts (Streitner et al., 2010). However, RNA immunoprecipitation (RIP) analysis revealed that *PR1* transcripts are not direct targets of *At*GRP7 (Hackmann et al., 2014). Moreover, the authors showed that *PR1* is regulated by *At*GRP7 on the transcriptional level by increasing the activity of the *PR1* promoter (Hackmann et al., 2014).

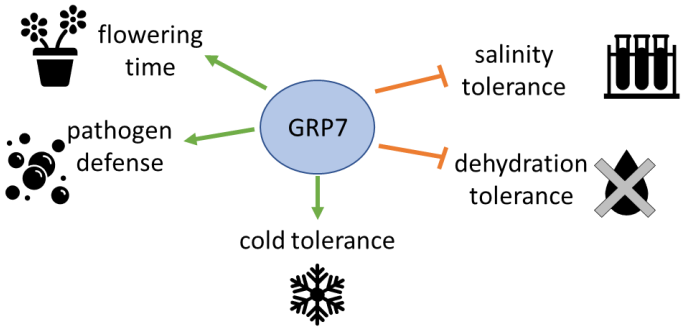

Figure 3.8 GRP7 function in a flowering time control and stress responses. See text for details.

3.2.3. Role of *At*GRP7 and *At*GRP8 in pre-mRNA splicing

*At*GRP7 and *At*GRP8 participate in alternative splicing (AS) of their own transcripts as well as affect AS of multiple other pre-mRNAs (Meyer et al., 2017; Schöning et al., 2008; Streitner et al., 2012). Their negative autoregulation and cross-regulation were described in chapter 3.2.1 .

By using a high-resolution RT-PCR-based AS panel (Simpson et al., 2008), Streitner and co-workers showed that the overexpression of *At*GRP7 significantly changes 59 AS events. Further, 30 AS events showed significant changes in plants overexpressing *At*GRP8 and 27 of them appeared also in the analyses of the *At*GRP7ox line (Streitner et al., 2012). The changes in the isoform ratios were also analysed in *atgrp7-1* 8i line, which beside T-DNA insertion in *AtGRP7* sequence carries an RNAi construct against *AtGRP8*. In *atgrp7-1* 8i line identified 17 AS events with significant changes and 14 of them were also found to be altered in *At*GRP7ox line. The changes with opposite directions in *At*GRP7ox and *atgrp7-1* 8i were observed in 10 AS event, what suggested that the identified pre-mRNAs could be direct targets for *At*GRP7 (Streitner et al., 2012). By using the RNA immunoprecipitation (RIP) (Köster and Staiger, 2014), the *in vivo* binding of *At*GRP7 was shown for 7 different transcripts and among of them was *AtGRP8* (Streitner et al., 2012). Moreover, the comparison of three different data sets showed that *At*GRP7 can affect particular AS events in the same direction or antagonistically to SR proteins or the subunits of the CAP binding complex (Raczynska et al., 2009; Simpson et al., 2008; Streitner et al., 2012). Several transcripts recognized in the AS panel as a potential *At*GRP7 targets (Streitner et al., 2012) were also identified in the pioneering study (Meyer et al., 2017). By use of RNA immunoprecipitation (RIP) and an individual nucleotide resolution crosslinking and immunoprecipitation (iCLIP) approaches, the high confidence *At*GRP7 targets were identified and for some of them, the direct influence of *At*GRP7 on their AS has been proved. The published data provides a new sight to the AS network and brings us closer to identification of the new RNA-binding sites in the new target RNAs (Meyer et al., 2017).

3.3. Protein arginine methylation derived by *At*PRMT5

Posttranslational modification of arginine (R) residues, although discovered half a century ago, has only recently been recognized to play a key role in the chromatin structure, regulation of transcription, RNA processing and transport, translation, signal transduction, DNA repair and cell differentiation (Bedford and Clarke, 2009; Bedford and Richard, 2005; Blackwell and Ceman, 2012; Lee et al., 2005; Pahlich et al., 2006; Paik and Kim, 1967; Yu, 2011).

Arginine is an α-amino acid, which contains a positively charged guanidinium group and mediates hydrogen bonding and amino-aromatic interactions. In posttranslational arginine methylation, methyl groups are added to the arginine nitrogens, resulting in one or two methyl groups bound to the guanidino nitrogen atoms (Bedford and Richard, 2005; Gary and Clarke, 1998) (Figure 3.9).

Arginine methylation is catalysed by PROTEIN ARGININE METHYLTRANSFERASES (PRMTs) with the use of *S*-adenosylmethionine (AdoMet) as a methyl donor. PRMTs have been found in higher plants, animals and fungi (Lee et al., 2005). While, the length of the individual PRMTs differs significantly, their structure contains a conserved fragment of ~310 amino acids, the PRMT core, which consists of an N-terminal methyltransferase (MTase) domain, a dimerization arm and a C-terminal β-barrel domain (Cheng et al., 2005). PRMTs are classified into two groups: type I and II. Type I PRMTs catalyse the formation of monomethylarginine (MMA) and asymmetric dimethylarginine (aDMA). Type II PRMTs catalyse the formation of MMA and symmetric dimethylarginine (sDMA) (Figure 3.9) (Bedford and Richard, 2005; Lee et al., 2005; Pek et al., 2012).

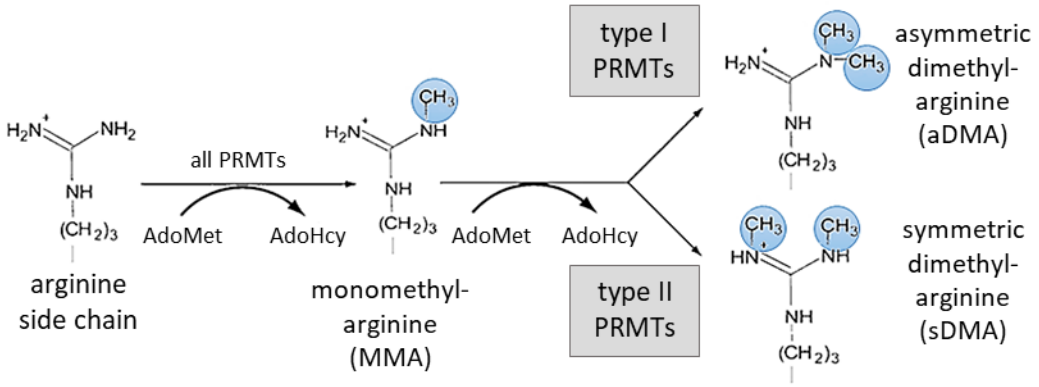

Figure 3.9 Arginine methylation catalysed by PRMTs. All PRMTs catalyse the transfer of the methyl group to arginine guanidino group to form monomethylarginine (MMA). Next, PRMTs type I and type II catalyse the formation of asymmetric dimethylarginine (aDMA) and symmetric dimethylarginine (sDMA), respectively. In all reactions, the methyl donor *S*-adenosylmethionine (AdoMet) is turned into *S*-adenosylhomocysteine (AdoHcy) (Pahlich et al., 2006; modified).

Arginine methylation interferes with the formation of hydrogen bonds and increases the hydrophobicity and bulkiness of the amino acid side chain (Pahlich et al., 2006). Accordingly, enzymatic activity (El-Andaloussi et al., 2006), stability (Sivakumaran et al., 2009), subcellular localisation (Smith et al., 2004), protein-protein- (Iberg et al., 2008) and protein-nucleic acid interactions (Gary and Clarke, 1998; Tan and Nakielny, 2006) of the target proteins can be perturbed due to steric hindrance. Substrates with methylated arginines are found in diverse classes of proteins such as histones and

cellular and nuclear proteins involved in RNA processing (Bedford and Clarke, 2009; Bedford and Richard, 2005; Gary and Clarke, 1998).

PROTEIN ARGININE METHYLTRANSFERASE 5 (PRMT5)

In mammalian cells it has been shown that PRMT5 is present in the nucleus and cytoplasm to catalyse the formation of sDMA in histone and nonhistone proteins. PRMT5 changes the expression of target proteins by providing a methyl group to histones H4, H2A, H3, as well as transcription factors and co-regulators (e.g. SPT5 transcription elongation factor and RNA polymerase II FCP phosphatase) (Amente et al., 2005; Ancelin et al., 2006; Branscombe et al., 2001; Kwak et al., 2003; Pal et al., 2004; Tan and Nakielny, 2006). PRMT5 also catalyses methylation in the myelin basic protein (MBP) and components of the pre-mRNA splicing machinery: SM protein B/B', D1, D3 (U1, U2, U4, U5 snRNP) and SM-like protein LSM4 (U6 snRNP) (Brahms et al., 2001; Friesen et al., 2001). Studies conducted in *Caenorhabditis elegans* PRMT5 showed that the exchange of conserved phenylalanine into methionine in the active site of PRMT5 leads to elevated methylase activity. More importantly, the mutated version of PRMT5 catalyses the formation of both aDMA and sDMA, showing the role of the steric limitations in the catalytic mechanism (Sun et al., 2011).

Human PRMT5 is involved in proper assembly of ribosomes and thus protein synthesis and optimal cell proliferation (Ren et al., 2010), as well as maintaining the Golgi apparatus architecture (Zhou et al., 2010) and cell cycle regulation by influencing the outcome of the DNA damage response (Jansson et al., 2008). PRMT5 orthologues in *C. elegans* negatively regulate the process of apoptosis, induced by DNA damage (Yang et al., 2009). In mice and flies, PRMT5 is essential for germ cell formation (Ancelin et al., 2006; Anne et al., 2007).

In plants, PRMTs have been shown to be involved in many important biological processes: vegetative growth, flowering time, circadian clock oscillations and response to abiotic stresses (Ahmad and Cao, 2012). Nine PRMT genes have been found in *A. thaliana* (Niu et al., 2007). Some of these have been identified in screens for mutants with altered flowering time or abiotic stress responses. Best characterized in *A. thaliana* is the type II *At*PRMT5, one of the most highly conserved genes in multicellular eukaryotes. *At*PRMT5, also termed CALCIUM UNDERACCUMULATION 1 (CAU1) and SHK1 BINDING PROTEIN 1 (SKB1), catalyses the formation of MMA and sDMA. The *AtPRMT5* contains 23 exons and encodes a protein of ~72 kDa, which shares 47% homology with the human PRMT5 (Pei et al., 2007).

3.3.1. Role of methyltransferase PRMT5 in *Arabidopsis thaliana*

In *A. thaliana, At*PRMT5 methylates histone H2A and H4, depositing symmetric dimethylation on arginine 3 in histone 4 (H4R3sm2). The arginine methylation in histones e.g. H4R3sme2 might be a linker between post-translational modifications and transcriptional, as well as post-transcriptional regulation (Deng et al., 2010; Pei et al., 2007) (Figure 3.10).

Besides that, *At*PRMT5 catalyses the formation of sDMA in non-histone proteins, such as myelin basic protein (MBP), U snRNP *At*SM proteins and RNA processing factors (Deng et al., 2010) (Figure 3.10). Controlled by post-translational modifications, SM spliceosomal proteins and RNA processing factors directly or indirectly influence pre-mRNA splicing of diverse genes, therefore the reflection of their function can be found in multiple developmental processes (Deng et al., 2010).

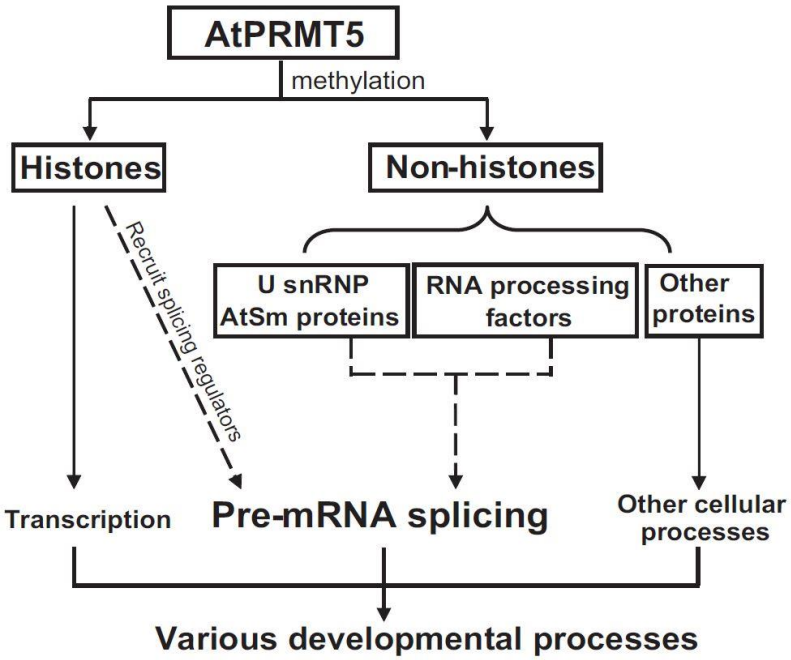

Figure 3.10 Graphic representation of the influence of *At*PRMT5 on pre-mRNA splicing. See text for details; (Deng et al., 2010).

Role in regulating splicing

A strong hint pointing to the relevance of *At*PRMT5-mediated arginine methylation of splicing factors came from data published in 2010. The results from RNA-seq analyses showed that *At*PRMT5 deficiency causes splicing defects in hundreds of genes, which are involved in many cellular and biological processes (Deng et al., 2010). The 3'ss events have been shown to be the most common in *atprmt5* in comparison to the total

number of AS events. However, it has been revealed that IR events are more abundant in *atprmt5* mutant than in the wild type (Zhang et al., 2011).

Symmetric arginine dimethylation is required for U snRNP biogenesis. Before SM (SM B/B', D1, D3) proteins can be loaded onto U1, U2, U4, U5 snRNA and SM-like protein LSM4 onto U6 snRNA, to form respective snRNPs, SM protein are symmetrically dimethylated by *At*PRMT5 (Brahms et al., 2001; Friesen et al., 2001). The absence of symmetric dimethylation in SM protein disturbs the formation of the active spliceosome and recruitment of the NineTeen complex (NTC). Without *At*PRMT5, NTC is unable to connect to U5 snRNP, which results in a global defect in pre-mRNA splicing (Figure 3.11) (Deng et al., 2016, 2010; Zhang et al., 2011).

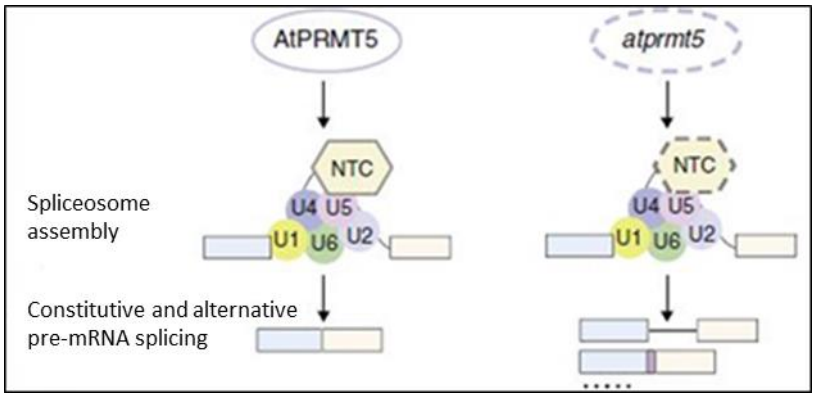

Figure 3.11 Function of *At*PRMT5 in regulating pre-mRNA splicing. The lack of *At*PRMT5 influences spliceosome assembling and leads to changes in pre-mRNA splicing (Deng and Cao, 2017; modified).

Role in plant development and flowering time

*At*PRMT5 plays an important role in the transition from the vegetative to the reproductive phase and regulates flowering time. Immunoblot analysis showed high *At*PRMT5 protein levels in flowers, roots and siliques, as well as in seedlings at an early developmental stage (5 to 20-day-old- seedlings)(Wang et al., 2007). Lack of functional *At*PRM5 induces pleiotropic developmental defects including growth retardation characterized by smaller cotyledons and rosette leaves, and shorter primary roots in comparison to wild type in the early vegetative development. Later in development, *atprmt5* exhibits dark green and curled leaves, and a late flowering phenotype (Pei et al., 2007). In contrast, plants overexpressing *AtPRMT5* in the wild type background flower earlier than wild type plants, suggesting a positive role of *At*PRMT5 in flowering timing regulation (Wang et al., 2007). Furthermore, the *atprmt5* mutant was also found to be vernalization-insensitive (Schmitz et al., 2008).

Examination of the late flowering *atprmt5* mutant on the transcriptional level showed an increased expression of flowering repressor *FLOWERING LOCUS C (FLC)*, suggesting

that *At*PRMT5 plays a role in flowering time through the autonomous pathway by repressing *FLC* transcription (Pei et al., 2007). It has been shown that *atprmt5 flc-3* double mutants flower earlier then *atprmt5,* confirming the role of *At*PRMT5 in flowering time by regulating *FLC* expression (Pei et al., 2007; Wang et al., 2007). On the molecular levels, it has been shown that *At*PRMT5 catalyses histone methylation of the *FLC* promoter, which leads to repression of *FLC* and therefore promotes flowering and is essential for the vernalization process. The high *FLC* level in *atprmt5* is only partly derepressed during exposure to the cold, i.e. plants do not flower rapidly after applied vernalization treatment and thus display a vernalization-insensitive phenotype (Schmitz et al., 2008).

It has been shown that lack of *At*PRMT5 up-regulates total *FLK* transcript level (Pei et al., 2007). A study from 2010 revealed that the observed *FLK* up-regulation was implemented by accumulation of unspliced transcripts, with the first intron retained, while the constitutively spliced form of *FLK* transcript decreased 30% in *atprmt5* mutants, resulting in enhanced *FLC* expression level and delayed flowering (Deng et al., 2010) (Figure 3.12).

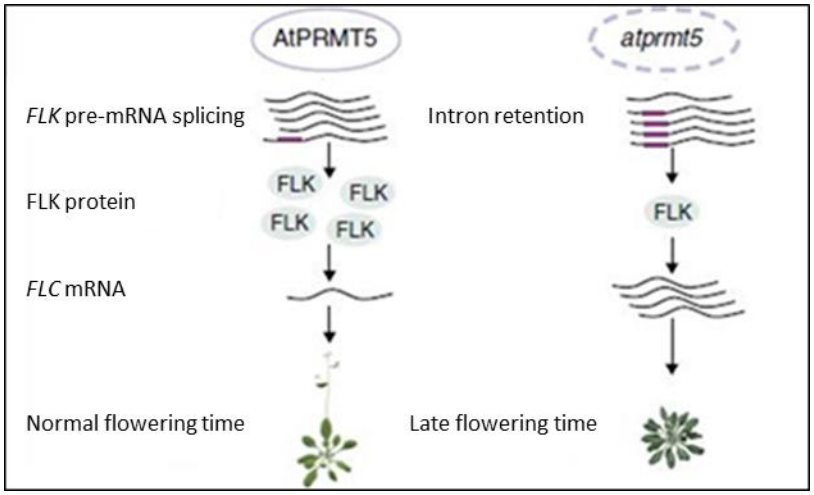

Figure 3.12 Impact of *At*PRMT5 on flowering time via regulation of pre-mRNA splicing. The lack of *At*PRMT5 influences spliceosome assembling and leads to changes in pre-mRNA splicing of *FLK*. The alternatively spliced isoforms affect down-stream processes, which results in late flowering time (Deng and Cao, 2017; modified)

Role in circadian rhythm

In 2010, two publications reported a strong influence of *At*PRMT5 on the circadian clock. It was shown that lack of *At*PRMT5 leads to lengthened periods in expression of clock genes and clock-controlled output genes, as well as cotyledon movement. The expression of the core loop genes *CCA1, LHY* and *TOC1* in *atprmt5* show a longer period in comparison to wild type. The evening loop gene *GI* and the morning loop genes *PRR7*

and *PRR9* exhibit longer periods and higher amplitudes in the *atprmt5* loss-of-function mutant. Therefore, it was assumed that *GI, PRR7* and *PRR9* are possible targets of *At*PRMT5. In addition, Sanchez and co-workers showed that *AtPRMT5* expression is controlled by circadian rhythm. In conclusion, these discoveries suggest an important role of arginine methylations for the circadian clock functioning in a feedback loop manner (Hong et al., 2010; Sanchez et al., 2010).

The circadian clock regulates rhythmical expression of *AtPRMT5* but also *At*PRMT5 can influence the core clock components. Loss of *At*PRMT5 function affects the circadian rhythm, caused at least partly by changes in alternative splicing of the morning-loop-gene *PRR9*. The alternative splice variants with an alt. 5' ss within exon 2 and/or retained intron 3 lead to a decreased number of isoforms encoding the full-length PRR9 protein and result in impaired circadian rhythms (Sanchez et al., 2010) (Figure 3.13).

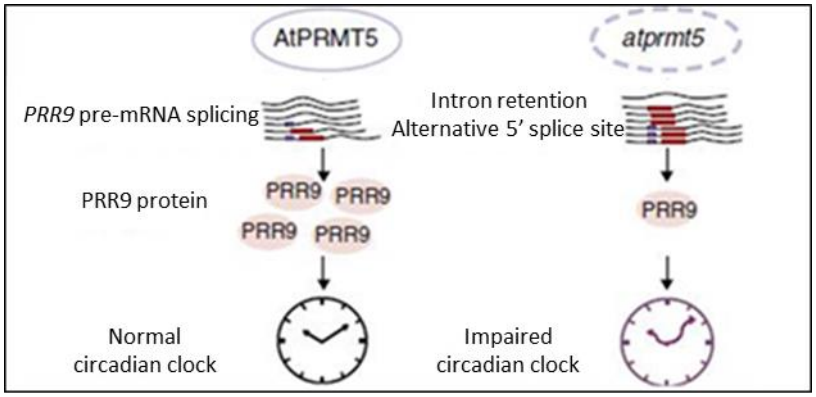

Figure 3.13 Impact of *At*PRMT5 on controlling circadian clock via regulation of pre-mRNA splicing. The lack of *At*PRMT5 influences spliceosome assembling and leads to changes in pre-mRNA splicing of *PRR9*. The alternatively spliced isoforms affect down-stream processes, which results in impaired circadian clock (Deng and Cao, 2017; modified).

Role in stress response

Beside the late flowering and growth retardation, *atprmt5* mutants show salt and ABA hypersensitivity. Under salt stress, *At*PRMT5 controls the adaptive response. The salt treatment reduces the global level of H4R3sme2. It has been shown that under salt stress conditions, the methyltransferase *At*PRMT5 disassociates from chromatin and the H4R3sme2 level decreases, resulting in transcriptional activation of *FLC* and stress-responsive genes (Zhang et al., 2011).

Hypersensitive to salt stress, *atprmt5* mutants exhibit splicing defects in genes that are involved in many biological processes, predominantly in response to abiotic stress (Deng et al., 2010). Further studies showed that *At*PRMT5 (SKB1 in the publication) is required for pre-mRNA splicing of stress-related genes e.g. *RESPONSIVE TO*

DESSICATION 22 (RD22). Moreover, *At*PRMT5 and LSM4, which is methylated by *At*PRMT5, might have overlapping roles in the tolerance of high salinity (Zhang et al., 2011) (Figure 3.14).

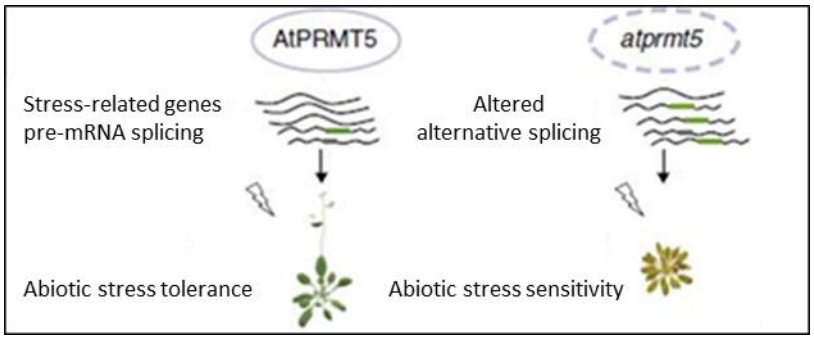

Figure 3.14 Impact of *At*PRMT5 on responding to stress via regulation of pre-mRNA splicing. The lack of *At*PRMT5 influences spliceosome assembling and leads to changes in pre-mRNA splicing of stress-related genes. The alternatively spliced isoforms affect down-stream processes, which results in abiotic stress sensitivity (Deng and Cao, 2017; modified).

*At*GRP7 and *At*GRP8 as targets for the methyltransferase *At*PRMT5

In 2010, the use of antibodies that detect symmetrically dimethylated arginines such as the SYM10 antibody, raised against a peptide containing four symmetrical dimethyl-arginine-glycine repeats, allowed the detection of a wide spectrum of targets in wild type plants, but not in the *atprmt5* mutants. Among those were numerous proteins involved in RNA processing including *At*GRP7 and *At*GRP8. Moreover, the arginine at the position 141 (R141) for both *At*GRP7 and *At*GRP8 was identified by mass spectrometry to be the residue methylated *in vivo* by PRMT5 (Deng et al., 2010).

3.4. Aim of this work

The goal of my work was to investigate the impact of posttranslational arginine methylation on the function of splicing factors in *Arabidopsis thaliana*. The presented work focuses on RNA-binding proteins *At*GRP7 and *At*GRP8 that are methylated by *At*PRMT5.

The *atprmt5* mutant shows a global defect in alternative splicing. Moreover, the *At*PRMT5 targets *At*GRP7 and *At*GRP8 also affect alternative splicing. Plants with altered *At*PRMT5 or *At*GRP7 levels exhibit both common and distinct changes in splicing of target transcripts. Accordingly, it is hypothesized that *At*PRMT5 may affect pre-mRNA splicing of certain target transcripts via modulation of *At*GRP7 and/or *At*GRP8 activity.

Both *At*PRMT5 and *At*GRP7 have been shown to be controlled by the circadian clock, have an impact on flowering time and regulate stress responses. Therefore, my thesis aims to investigate the impact of arginine methylation in *At*GRP7 and *At*GRP8 catalysed by *At*PRMT5 on controlling physiological responses such as flowering time control, stress tolerance and pathogen defense.

4. Materials and methods

4.1. Plant material

The list of *Arabidopsis thaliana* lines, used in this study, can be found in Table 4.1.

Table 4.1 *Arabidopsis thaliana* lines used in this study.

Plant line	Description
Col-0	Columbia-0 wild type
grp7-1	*At*GRP7 *loss-of-function* mutant in Col-0 (Fu et al., 2007)
grp7-1 8i	*atgrp7-1* crossed with *AtGRP8*i-l71 (RNAi construct against *At*GRP8) (Streitner et al., 2008)
prmt5-1	*At*PRMT5 *loss-of-function* mutant in Col-0 (T-DNA-Insertion) (Pei et al., 2007)
prmt5-5	*At*PRMT5 *loss-of-function* mutant in Col-0 (Nonsense mutation in the last base in the exon 20. Exchange of guanine to thymine leads to the Premature Stop Codon) (Sanchez et al., 2010)
prmt5-1 x grp7-1	*atprmt5-1* crossed with *atgrp7-1*
prmt5-5 x grp7-1	*atprmt5-5* crossed with *atgrp7-1*
prmt5-1x grp7-1 8i	*atprmt5-1* crossed with *atgrp7-1 8i*
prmt5-5 x grp7-1 8i	*atprmt5-5* crossed with *atgrp7-1 8i*
prmt5-1xgrp7-1 atgrp8	Cross *atprmt5-1 atgrp7-1* with CRISPR/Cas9 construct targeting *At*GRP8
prmt5-5xgrp7-1 atgrp8	Cross *atprmt5-5 atgrp7-1* with CRISPR/Cas9 construct targeting *At*GRP8
GRP7FL (4a)	Complementation line with full-length *AtGRP7* genomic sequence under endogenous promoter in *atgrp7-1*
GRP7FL (10c)	Complementation line with full-length *AtGRP7* genomic sequence under endogenous promoter in *atgrp7-1*
GRP7 R141A	Complementation line with full-length *AtGRP7* genomic sequence with point mutation leading to amino acid replacement R141A, under endogenous promoter in *atgrp7-1* (Exchange: arginine [R] to alanine [A] at the position 141 in *At*GRP7 amino acid chain)
GRP7 R141K	Complementation line with full-length *AtGRP7* genomic sequence with point mutation leading to amino acid replacement R141K, under endogenous promoter in *grp7-1* (Exchange: arginine [R] to lysine [K] at the position 141 in GRP7 amino acid chain)
GRP7ox (D1c or G1d)	*At*GRP7ox in Col-0 (Streitner et al., 2008)
GRP7ox *prmt5-1*	*At*GRP7ox in *prmt5-1*
GRP7ox *prmt5-5*	*At*GRP7ox in *prmt5-5*

GRP7ox R141A	*At*GRP7ox with point mutation leading to amino acid replacement R141A in Col-0 (Exchange: arginine [R] to alanine [A] at the position 141 in GRP7 amino acid chain)
GRP7ox R141K	*At*GRP7ox with point mutation leading to amino acid replacement R141K in Col-0 (Exchange: arginine [R] to lysine [K] at the position 141 in GRP7 amino acid chain)
GRP7ox R141F	*At*GRP7ox with point mutation leading to amino acid replacement R141F in Col-0 (Exchange: arginine [R] to phenylalanine [F] at the position 141 in GRP7 amino acid chain)
GRP7-GFP	*At*GRP7-GFP under control of its endogenous promoter and its *cis*-regulatory elements (5'UTR, intron, 3'UTR) in *atgrp7-1* (Streitner et al., 2012)
GRP7-GFP R141A	*At*GRP7-GFP under control of its endogenous promoter and its *cis*-regulatory elements (5'UTR, intron, 3'UTR) with point mutation leading to amino acid replacement R141A in *atgrp7-1*
GRP7-GFP R141K	*At*GRP7-GFP under control of its endogenous promoter and its *cis*-regulatory elements (5'UTR, intron, 3'UTR) with point mutation leading to amino acid replacement R141K in *atgrp7-1*
GRP7-GFP/ *prmt5-1 x grp7-1*	*At*GRP7-GFP under control of its endogenous promoter and its *cis*-regulatory elements (5'UTR, intron, 3'UTR) in *atprmt5-1 x atgrp7-1*
GRP7-GFP/ *prmt5-5 x grp7-1*	*At*GRP7-GFP under control of its endogenous promoter and its *cis*-regulatory elements (5'UTR, intron, 3'UTR) in *atprmt5-5 x atgrp7-1*

4.2. Plant growth conditions

4.2.1. Plant growth on soil

Arabidopsis thaliana seeds were uniformly distributed over the moist soil and then stratified at 4°C in the dark for 3 days. After the cold treatment, the pots were grown in a controlled environment growth cabinet at 20°C and 70% humidity under short day (8h light and 16h dark) or long day (16h light and 8h dark) conditions, chosen depending on the experiment.

4.2.2. Plant growth on MS-agar plates

For growing *Arabidopsis thaliana* plants on sterile medium, seeds were surface sterilized under sterile conditions on a clean bench. Seeds were first washed with 70% ethanol for 1 min and then with a bleach solution (6% sodium hypochlorite with 0,01% Triton X-100) for 5 min. The seeds were then washed 3 times with autoclaved distilled water, the remaining water was removed, and the seeds were kept at 4°C in the dark for 3 days. After stratification, the seeds were plated on half strength Murashige-Shoog

(MS) medium (2,2 g/L MS powder, 0,5 g/L MES (2-(N-morpholino) ethanesulfonic acid), 0,5% sucrose, 1% agar, pH 5,7) (Murashige and Skoog, 1962). The plates were placed in the Percival incubator with chosen experimental growth conditions: short day (16h light and 8h dark), long day (16h light and 8h dark) or 12:12 (12h light and 12h dark).

4.2.3. Selection of transgenic plants on selective medium

The seeds, obtained after the floral dip *Arabidopsis thaliana* transformation were plated on selective medium, containing the required antibiotic (Table 4.2).

Table 4.2 Antibiotics used in the selective mediums.

Antibiotic	Abbreviation	Concentration (μg/ml)
Ampicillin	Amp	100
Gentamycin	Gen	100
Hygromycin	Hyg	20
Kanamycin	Kan	50
Rifampicin	Rif	50

4.2.4. Harvest of plant material

The aerial parts of the plants were harvested at defined time points, frozen in liquid nitrogen and stored at -80°C. The plant material was ground with Mixer Mills (Retsch® MM 400; vibrational frequency 25Hz, grinding time 25 sec) or homogenized manually with pre-cooled mortar and pestle.

4.3. Molecular biology methods

4.3.1. Genomic DNA isolation

The harvested plant material was collected in 2 mL tubes, frozen in liquid nitrogen and ground with Mixer Mills Retsch® MM 400. For isolating genomic DNA, 500 μL Wisconsin-Buffer (200 mM Tris HCl, pH 9,0, 400 mM LiCl, 25 mM EDTA, pH 8,0, 1% SDS) were added to the plant material. The samples were homogenized by shaking and then centrifuged for 5 min at 16 000 x *g* (Ependorf 5415R). 350 μL of the supernatant were transferred to a new 1,5 mL tube. The genomic DNA was precipitated by adding 350 μL isopropanol. The samples were centrifuged for 10 min at 16 000 x *g*. The supernatant was discarded, and the pellet was washed with 70% ethanol. After the wash, the remaining alcohol was completely removed, and the pellet was resuspended in 160 μL TE buffer (10 mM Tris HCl pH 8 and 1 mM EDTA pH 8).

4.3.2. Total RNA isolation

Total RNA was isolated from 100 mg ground plant material in 2 mL tube. 1mL TriReagent (400 mM ammonium thiocyanate, 800 mM guanidinium thiocyanate, 4,35% glycerol, 100 mM sodium acetate (pH 5,2), 38% acidic phenol) was added to each tube, then the mixture was homogenized by shaking and incubated at room temperature for 5 min. The liquid phases were separated by centrifugation for 10 min at 4°C and 12 000 x *g*. The aqueous phase was transferred to a fresh tube and RNA was extracted by adding 200 μL chloroform: isoamyl alcohol (24:1), thoroughly mixing the sample for 3 min and centrifuging for 15 min at 4°C and 12 000 x *g*. The aqueous phase was transferred to a new tube and the chloroform extraction was repeated once. The RNA was precipitated with isopropanol for 45 min at room temperature. The precipitate was collected by centrifugation for 10 min at 4°C and 16 000 x *g*. The RNA pellet was washed two times with 70% ethanol, allowed to air dry for 5-10 min and then resuspended in 40 μL RNase-free water. The RNA concentration was determined by spectrophotometric measurement of the absorbance of the sample at 260 nm using the NanoDrop 1000 (Thermo Scientific). The RNA quality was assessed on a denaturing agarose gel electrophoresis.

4.3.3. Denaturing agarose gel electrophoresis for RNA analysis

The integrity of isolated RNA was checked by formaldehyde-agarose gel electrophoresis. 100 mL of the denaturing gel was prepared with 1,5 g agarose, 3,5 mL of 37% formaldehyde and 10 mL 10x MOPS buffer (100 mM 3-(N-morpholino) propanesulfonic acid (MOPS), 40 mM sodium acetate x 3 H_2O, 5 mM EDTA, pH 7,0). 2 μg of total RNA was mixed with twice the volume of the RNA sample buffer (150 μL 10x MOPS buffer, 190 μL (37%) formaldehyde, 660 μL formamide and 1 μL ethidium bromide), heated at 65°C for 15 min and then cooled down on ice. Before loading, 1/10 volume of loading dye (glycerol with bromophenol blue) was added to each RNA sample. The gel was run in 1x MOPS buffer at 80 V for 120 min.

4.3.4. cDNA synthesis

For cDNA synthesis, the RNA sample was treated first with DNase and then used for the reverse transcription. 2,2 μg of total RNA were digested with 2,2 μL RQ1-DNaseI (Promega) and 1 μL 10x RQ1-buffer (Promega) in a final volume of 10 μL. The sample was incubated at 37°C for 45 min. Afterwards, the DNase enzyme was inactivated with the Stop Solution (Promega) at 65°C for 10 min.

After DNase treatment, the RNA sample was mixed with 1 μL Oligo(dT)$_{12\text{-}18}$ primer (10 μM), 4 μL dNTPs (5 mM) and then incubated at 65°C for 5 min. Next, 4 μL 5x RT-

buffer, 1 μL DTT (100 mM) and 0,5 μL AMV Reverse Transcriptase (Roboklon) were added to the sample. Following incubation conditions were used to reverse transcribe the RNA samples: 42°C for 15 min, 50°C for 45 min, 80°C for 10 min and cooling down on ice. Synthesised cDNA was diluted 1:10 with water and used for further analyses.

4.3.5. Real Time quantitative PCR (RT-qPCR)

The RT-qPCRs were performed using the iTaq Universal SYBR Green Supermix (Bio-Rad) (Table 4.3 and Table 4.4) or with EvaGreen Dye (Biotium) and GoTaq (Promega) (Table 4.5 and Table 4.6) in the CFX96 Real Time Cycler (Bio-Rad). All used primers are listed in the appendix. The $\Delta\Delta C_t$ method was used to calculate the relative transcript level (Livak and Schmittgen, 2001). The expression levels of the housekeeping genes *PP2A* and *ACT2* (*PROTEIN PHOSPHATASE 2A* and *ACTIN 2*) were used for normalization.

Table 4.3 RT-qPCR mix with iTaq SYBR Green.

Ingredients	
Forward Primer	0,4 μM
Reverse Primer	0,4 μM
2x iTaq Supermix	1x
cDNA	1-2 μL
water	up to 10 μL

Table 4.4 RT-qPCR program with iTaq SYBR Green.

Cycles	Temperature	Time
1x	95°C	3 min
45x	95°C 60°C + Plate Read	15 sec 30 sec
1x 1x 1x 1x	95°C 60°C 65-95°C, 0,5°C increment + Plate Read 12°C	30 sec 30 sec 5 sec ∞

Table 4.5 RT-qPCR mix with EvaGreen and GoTaq.

Ingredients	
Forward Primer	0,25 μM
Reverse Primer	0,25 μM
5xGoTaq Flexi Buffer	1x
dNTPs (5 mM)	0,2 mM
$MgCl_2$ (25 mM)	2,5 μM
cDNA	2 μL
Eva Green (20x)	1x
GoTaq (5U/μL)	1U
water	up to 10 μL

Table 4.6 RT-qPCR program with EvaGreen and GoTaq

Cycles	Temperature	Time
1x	94°C	2 min
45x	94°C 60°C 72°C + Plate Read	15 sec 30 sec 30 sec
1x 1x 1x 1x	95°C 60°C 65-95°C, 0,5°C increment + Plate Read 12°C	30 sec 30 sec 5 sec ∞

4.3.6. Semiquantitative PCR (sqPCR)

Semiquantitative polymerase chain reaction (sqPCR) was used as an approach for the measurement of expression level for specified genes in the flowering time experiments, as well as in analyses of alternative splicing.
The reaction mix with GoTaq DNA Polymerase (Promega) and the program used for sqPCRs are listed in Table 4.7 and Table 4.8. Annealing temperatures were optimized for each primer set based on the melting temperature (T_m). The elongation time depended on the size of amplified DNA fragment (1 min/kb). The number of cycles was determined experimentally. C1000 Touch Thermal Cycler (BioRad) was used to perform sqPCRs. The expression levels of *PP2A* and *ACT2* housekeeping genes were used for normalization. The sqPCR products were visualized on 1,5% sodium-borate agarose gels (details in 4.3.7).

Table 4.7 sqPCR mix with GoTaq

Ingredients	
Forward Primer	0,25 μM
Reverse Primer	0,25 μM
5xGoTaq Flexi Buffer	1x
dNTPs (5 mM)	0,2 mM
$MgCl_2$ (25mM)	2,5 mM
GoTaq (5 U/μL)	2 U
cDNA	1-2 μL
water	up to 20 μL

Table 4.8 sqPCR program with GoTaq

Cycles	**Temperature**	**Time**
1x	95°C	2 min
28-35 x	95°C 55-65°C 72°C	30 sec 30 sec 30-60 sec
1x 1x	95°C 12°C	4 min ∞

4.3.7. Electrophoresis with agarose gel

The 0,8-2% agarose gels with ethidium bromide (EtBr) were used for DNA visualisation. Agarose gels were prepared with TAE buffer (Tris-Acetat-EDTA; 40 mM Tris, 20 mM acetic acid and 1 mM EDTA), sodium-borate buffer (10 mM NaOH and 10 mM boric acid) or with TBE buffer (88 mM Tris, 88 mM boric acid and 2 mM EDTA). The electrophoresis was performed at 80-120V for the required time. Next, the gels were exposed to UV light and the pictures were taken. The size of DNA bands was check with GeneRuler 100 bp Plus DNA Ladder (Thermo Scientific).

4.3.8. DNA extraction from agarose gel

The agarose gel was run to separate the DNA of interest with 1x TAE running buffer (Tris-Acetat-EDTA; 40 mM Tris, 20 mM acetic acid and 1 mM EDTA). The indicated DNA band was cut out from the agarose gel on a UV plate. According to The Tiburon-

Shark-method, the gel fragment was transferred into a 0,2 mL PCR-tube with a hole on the bottom, filled with glass wool. To shred and melt the agarose gel, the PCR-tube was placed into a 1,5 mL Eppendorf tube and centrifuged at 2800 x *g* for 45 sec. Afterwards, the 0,2 mL PCR-tube was discarded, the total volume of the liquid was measured and an equal amount of phenol: chloroform: isoamyl alcohol (25:24:1) was added. The sample content was mixed by vortexing for 20 sec and then centrifuged for 5 min at 16000 x *g*. The upper phase was transferred into a new 1,5 mL Eppendorf tube and the total volume was measured. 0,5 x volumes of 3M sodium acetate (pH 5,2) and 3,75 x volumes of 100% were added. The sample was stored overnight at -20°C. On the next day, the sample was centrifuged for 30 min at 4°C and 16000 x *g*. The supernatant was discarded, and the pellet was washed twice with 150 μL of 70% Ethanol (-20°C) and centrifuged for 2 min at 4°C and 16000 x *g*. The supernatant was removed completely, the pellet was briefly dried and then resuspended in 15 μL water. The DNA concentration was determined by spectrophotometric measurement of the absorbance of the sample at 260 nm using the NanoDrop 1000 (Thermo Scientific).

4.4. Biochemical methods

4.4.1. Protein isolation

Protein isolation was performed by mixing 30 mg ground plant material with 200 μL Protein extraction buffer (62,5 mM Tris-HCl (pH 6,8), 20% (w/v) glycerol, 2% (w/v) SDS and 1% (v/v) β-mercaptoethanol). The homogeneous solution was boiled at 95°C for 10 min and then cooled down briefly. To pellet plant tissue debris, the sample was centrifuged for 10 min at maximum speed. The supernatant was transferred to a new tube and stored at -20°C.

4.4.2. Total protein quantification

The total protein concentration was determined in the GLOMAX R-MULTI DETECTION system (Promega) with the Pierce 660 nm Protein Assay (Thermo Scientific) combined with Ionic Detergent Combability Reagent (Thermo Scientific), according to the producer's instruction. The protein assay standard curve was prepared with bovine serum albumin (BSA) in the protein extraction buffer in three different concentrations 3, 2 and 1 mg/mL.

4.4.3. SDS-PAGE

The sodium dodecyl sulfate–polyacrylamide gel was prepared between two sealed glass plates. At first, the lower separating gel (12 or 15% acrylamide/bis-acrylamide 37.5:1, 375 mM Tris/HCL (pH 8,8), 0,1% SDS, 0,025% tetramethylethylenediamine (TEMED)

and 0,001% ammonium persulfate (APS))) was poured and covered with a few drops of 100% isopropanol, which eliminated formed bubbles. When the separating gel polymerised, the isopropanol was completely removed. The 5% stacking gel (5% acrylamide/bis-acrylamide 37.5:1, 125 mM Tris/HCL (pH 6,8), 0,1% SDS, 0,025% TEMED and 0,001% APS) was poured on the top of separating gel. Before the stacking gel polymerised, a comb was placed between glass plates in the gel. The protein samples were mixed in equal volumes with the sample buffer (185 mM Tris-HCl (pH6,8), 30% glycerine, 2% SDS and 150 μL/mL β-mercaptoethanol), boiled at 95°C for 5 min and loaded into the gel for separation of denatured proteins. The electrophoresis was performed in 1x the running buffer (25 mM Tris and 192 mM glycine) with use of The BioRad Mini Protean set or the self-made vertical chambers.

4.4.4. Western blot analysis

After SDS-PAGE, separated proteins were transferred onto a polyvinylidene difluoride (PVDF) membrane during blotting procedure in 1x Western Transfer buffer (25 mM Tris, 192 mM Glycine, 0,05% SDS and 20% methanol). Next, the membrane was blocked for 1 h in a solution of 2% non-fat dried milk powder and TBST buffer (50 mM Tris-HCl (pH 7,5), 150 mM NaCl and 0,1% Tween 20) to prevent non-specific antibody binding. The primary and secondary antibodies were diluted in 2% non-fat dried milk powder in TBST buffer (Table 4.9) The membrane was incubated with the primary antibody for 1 h under constant shaking and then washed three times for 10 min each in TBST buffer. Next, the membrane was incubated with the secondary antibody for 30 min, followed by four washes in TBST for 15 min each. Detection was performed with a chemiluminescence reaction, where reagent A (99 mM Tris-HCl (pH 8,8), 0,198 mM Coumaric acid in dimethyl sulfoxide (DMSO), 1,25 mM Luminol in DMSO) and reagent B (3% (v/v) H_2O_2) were mixed and poured over the membrane. The chemiluminescent signal was detected with a Stella 3200 (Raytest).

Table 4.9 The primary and secondary antibodies.

Type	Antibody	Dilution	Reference / source
Primary antibody	α-*At*GRP7	1:2000	Rabbit antipeptide antibody (Streitner et al., 2008)
	α-*At*GRP8	1:2000	Rabbit antipeptide antibody (Streitner et al., 2008)
	α-LHCP	1:20000	Rabbit polyclonal antibody (Heintzen et al., 1994)
	α-GFP	1:2000	Mouse monoclonal antibody, Roche
Secondary antibody	α-Rabbit IgG	1:5000	Secondary antibody, Sigma-Aldrich
	α-Mouse IgG	1:2500	Secondary antibody, Sigma-Aldrich

Finally, the membrane was stained for 30 min with amido-black solution (1% (v/v) amidoblack, 45% (v/v) methanol and 10% (v/v) acetic acid) and then washed in destaining solution (45% (v/v) methanol and 10% (v/v) acetic acid). Amido-black staining as well as the light-harvesting complex protein LHCP were used as loading controls and for normalization.

4.4.5. Coomassie Blue staining of SDS-PAGE

For Coomassie blue staining, the SDS-PAGE gel was incubated for 30 min in Coomassie blue solution (0,1% Coomassie Brilliant Blue R250, 50% (v/v) methanol and 10% (v/v) acetic acid) under constant shaking and then incubated in destaining solution (45% (v/v) methanol and 10% (v/v) acetic acid) until the bands are clearly visible.

4.5. Transformation of bacteria

4.5.1. Plasmids isolation

Plasmid isolation from *E. coli* was performed from 5 mL overnight bacterial cultures using the Invisorb® Spin Plasmid Mini Two Kit (STRATEC Molecular GmbH). Bacterial cells were harvested in 2 mL Eppendorf tube by centrifugation for 1 min at 13000 rpm. The supernatant was completely removed, and the bacterial pellet was resuspended in 250 μL Solution A. Next, 250 μL Solution B was added and the sample content was gently mixed. 250 μL Solution C was added and the tube content was gently mixed by inverting. The sample was centrifuged for 5 min at 13000 rpm. The clarified supernatant was transferred onto a Spin Filter, incubated for 1 min at room-temperature and centrifuged for 1 min at 11000 rpm. The flow-through was discarded, 750 μL Wash Solution were added on the column and then centrifuged for 1 min at 11000 rpm. The flow-through was discarded and the sample was centrifuged two more times for 3 min at 13000 rpm to dry the filter. The Spin Filter was placed into a new 1,5 mL tube, 50 μL sterile water were added to the middle of the column and incubated at room temperature for 2 min. Afterwards, the sample was centrifuged at 11000 rpm for 2 min, the Spin Filter was discarded and the DNA plasmid concentration was determined by spectrophotometric measurement of the absorbance of the sample at 260 nm using the NanoDrop 1000 (Thermo Scientific).

4.5.2. Transformation of *Escherichia coli*

For heat-shock transformation, chemically competent *E. coli* TOP10 cells were used, which gained the competence by $CaCl_2$ treatment.
In preparation for the transformation, the chemically competent cells were thawed on ice. Next, 3 μL of ligation product or plasmid of interest was added, cells were gently

mixed and incubated for 20 min on ice. Afterwards, heat-shock was performed by placing the cells at 42°C for 90 sec. Samples were put back on ice for 4 min and 300 µL LB medium was added (10 g/L tryptone/peptone from Casein, 5 g/L yeast extract and 10 g/L NaCl). Next, the tubes were placed in a shaking incubator at 37°C for 50 min. The recovered bacterial samples (60 µL and 300 µL) were plated on LB agar plates (10 g/L tryptone/peptone from Casein, 5 g/L yeast extract, 10 g/L NaCl and 14 g/L agar-agar) containing the appropriate antibiotic (Table 4.2). Plates were kept overnight at 37°C. Afterwards, colonies were counted and checked by colony PCR. Positive clones were multiplied, plasmids were isolated (details in 4.5.1) and checked by several restriction digests and by Sanger sequencing. The confirmed plasmids were transformed into *Agrobacterium tumefaciens*.

4.5.3. Transformation of *Agrobacterium tumefaciens*

For heat-shock transformation, chemically competent *A. tumefaciens* GV3103 cells were used, which gained the competence by $CaCl_2$ treatment.
Chemically competent cells were thawed on ice, 5 µL of plasmid DNA was added, followed by gentle mixing and incubation on ice for 5 min. Afterwards, heat-shock was performed by placing the cells in liquid nitrogen for 5 min and then incubating them at 37°C for 5 min. 1 mL LB medium containing 0,5 mg/L $MgSO_4$ was added and cells were placed in a shaking incubator at 28°C for 90 min. The recovered bacteria samples were centrifuged at 6000 rpm for 30 sec. 600 µL of the supernatant was discarded. The bacterial pellet was resuspended in the rest of supernatant and plated (60 µL and 300 µL) on LB agar plates (10 g/L tryptone/peptone from Casein, 5 g/L yeast extract, 10 g/L NaCl and 14 g/L agar-agar) containing the appropriate antibiotic (Table 4.2). Plates were incubated for two days at 28°C. Afterwards, colonies were counted and checked by colony PCR. Positive clones were multiplied, plasmids were isolated (details in 4.5.1) and checked by several restriction digests. The confirmed plasmids were transformed into *Arabidopsis thaliana.*

4.6. Plant infiltration with *Pseudomonas syringe*

Preparation of plants *Arabidopsis thaliana*
Seeds of indicated plant lines were sowed on soil and grown under short-day conditions (details in 4.2.1). 5/6-week-old plants were used for bacterial infiltration. One biological replicate consisted of 12 plants from each line. Only healthy plants with equal rosette sizes were selected for the infiltration.

Preparation of bacteria *Pseudomonas syringe*
Three days before the infiltration, 5 mL King's B medium (20 g/L proteose peptone, 1,5 g/L dipotassium hydrogen phosphate, 1,5 g/L magnesium sulphate, pH 7,2) with

rifampicin (details in 4.2.3) was inoculated with *P. syringe* pv. tomato DC3000. After two days of growth at 28°C in a shaking incubator, the pre-culture was extended up to 50 mL and incubated at 28°C for one more day.
Bacterial cells were harvested by centrifugation at 4°C and 4000 x *g* for 10 min. The supernatant was removed, and the pellet was resuspended in 15 mL 10mM $MgCl_2$ solution, centrifuged at 4°C and 4000 x *g* for 10 min and the supernatant was discarded. The wash of bacterial cells was repeated once more. Next, the bacterial cell pellet was resuspended in 50 mL 10mM $MgCl_2$. That bacterial solution was diluted 1:3 with 10mM $MgCl_2$ and used in photometric measurements of OD_{600} (optical density λ600 nm). The bacterial culture was diluted to a final OD_{600} of 0,05 and used for plant infiltration.

Infiltration process

One biological replicate included infiltration of 6 plants from each line with 10mM $MgCl_2$ (mock treatment) and infiltration of another 6 plants from each line with *P. syringe* bacterial solution OD_{600} 0,05. All rosette leaves were infiltrated at zt1 (Zeitgeber time 1, 1 h after lights on). Infiltration was done by gentle pressing of the indicated liquid into the leaf abaxial side with a 1 mL blunt end needleless syringe. After infiltration, all residue liquid was removed from the rosette leaves and the plants were returned to their original growing conditions.

Harvest of plant material

The infiltrated leaves were harvested at two different time points: 4 h after infiltration (zt5) and 24 h after infiltration (zt1). The harvested leaves were immediately frozen in liquid nitrogen and then stored at -80°C.

Molecular analyses

The collected plant material was ground and used for RNA isolation (details in 4.3.2). The integrity of isolated RNA was check with a denaturing gel (details in 4.3.3) and RNA samples were used for cDNA synthesis (details in 4.3.4). sqPCR with cDNA samples was performed to amplify *FRK1* (AT2G19190) and *PR1* (AT2G14610) transcripts. *ACT2* (AT3G18780) was used as a loading control. The sqPCR products were visualised on 1,5% agarose sodium-borate gel (details in 4.3.6). The transcript levels were quantified by RT-qPCR, where *PP2A* was used as a control (details in 4.3.5). The primers used for sqPCR and RT-qPCR are listed in the appendix.

4.7. Generation of transgenic plants

4.7.1. Transformation of *Arabidopsis thaliana*

Arabidopsis thaliana plants were vacuum infiltrated with bacterial solution of *A. tumefaciens,* carrying the gene of interest in a binary vector (Bechtold and Pelletier, 1998).

Preparation of *Arabidopsis thaliana* plants

A. thaliana plants were grown on soil for two weeks under short-day conditions and then transferred to long-day conditions. Before transformation, all siliques were removed from the plants.

Preparation of *Agrobacterium tumefaciens*

5 mL LB medium containing $MgSO_4$ and antibiotics (Kan/Gen/Rif - Table 4.2) were inoculated with *A. tumefaciens* harbouring the recombinant plasmid and incubated for two days at 28°C on a rotary shaker. The 5 mL preculture was used for inoculation of 500 mL LB medium with selective antibiotics (Kan/Gen/Rif), which was then incubated for 24 h at 28°C with vigorous agitation. Afterwards, the bacterial culture was centrifuged at 5000 rpm in a GSA rotor (Sorvall) for 20 min at 4°C and the cell pellet was resuspended in 500 mL infiltration medium (½ x MS-medium (pH 5,7), 5% (w/v) sucrose, 44 nM BAP (benzylaminopurine) 200 μ/L Silwet, pH 5,7).

Transformation

A beaker with *A. tumefaciens* suspension was placed into a desiccator. The aerial parts of the plants were dipped in bacterial solution and placed on the side of the desiccator. Next, the closed desiccator was connected to a water vacuum pump and the plants were vacuum infiltrated for 2 min. Afterwards, the vacuum was released and excess infiltration solution on the plants was gently removed with a paper towel. The plants were placed in a plastic tray and kept in a darkness for 24 h. After that time, plants were brought back to long-day conditions.

Selection of transformants

After 1,5-2 months, seeds were harvested from transformed plants (T_1 seeds). The T_1 seeds were sterilized and plated on ½ MS plates with Augmentin and selective antibiotic (e.g. hygromycin for HPT1 vector). 2-week-old T_1 seedlings were transferred to soil and grown in long-day conditions. The T_2 seeds were harvested from T_1 plants, sterilized and plated on ½ MS plates with selective antibiotic. The numbers of germinated seeds, antibiotic resistant and non-resistant seedlings were counted, and numbers were used for determination of the transgenic insert status. Plants that segregated with a 3:1 ratio in the T_2 generation and yielded seeds that were all

resistant, were defined as homozygous transgenic plants carrying a single copy of the T-DNA insertion. Only homozygous plants were used for further experiments. Western blot analyses were performed on plants of the T_2 or further generations to check the protein level of the introduced transgenes.

4.7.2. Generation of the *prmt5 grp7 grp8* triple mutants with the CRISPR/Cas9 system

A. tumefaciens GV3101 pSoup carrying plasmid pYB196_sgRNA7 (Jan Reineke and Christiane Nöh, unpublished) was used to generate the CRISPR/Cas9 plants. Plasmid pYB196 harbours sgRNA sequence 5'–ATTGGTTGAGTACCGGTGCTTTGT–3' targeting the first exon in *AtGRP8* gene, controlled by the Arabidopsis U6-26 promoter. Plasmid contains also *Cas9* gene driven by the *ICU2*-promoter and *bar* gene providing Basta® resistance.
A. thaliana plants *prmt5-1 x grp7-1* and *prmt5-5 x grp7-1* were transformed via Agrobacterium-mediated transformation (details in 4.7.1). Harvested T_1 seeds were used for further analyses.

Selection and genotyping in T_1 generation
Seeds of T_1 generation were sowed on soil and 10-week-old seedlings were sprayed with Basta® solution (20 mg/L BASTA® 200 (Bayer CropScience), 0,1% Tween 20). The spaying was repeated on day 12 and 14. Next, the Basta® resistant plants were selected, the plant material was harvested and used for DNA isolation (details in 4.3.1).

To confirm the presents of sgRNA in transgenic plants, the isolated DNA from Basta® resistant plants was used in PCRs with primers F_NotI_pEN and R_NotI_pEN (sequences in Appendix). The reaction mix and the program used for PCRs are listed in Table 4.10 and Table 4.11. The PCR products were visualized on 1,2% TBE (Tris/Borate/EDTA) agarose gels (details in 4.3.7).

Table 4.10 PCR mix

Ingredients	
10x Taq-Buffer	1x
$MgCl_2$	1 mM
dNTPs	0,2 mM
Forward Primer	0,5 μM
Reverse Primer	0,5 μM
Taq Polymerase	0,3 μL
cDNA	1,5 μL
water	up to 15 μL

Table 4.11 PCR program

Cycles	Temperature	Time
1x	94°C	5 min
30x	94°C	30 sec
	50°C	45 sec
	72°C	30 sec
1x	72°C	5 min
1x	12°C	∞

Further analyses were performed only for the T_1 plants, which carried sgRNA. To show mutations in *AtGRP8,* a fragment of the *AtGRP8* gene was amplified using primers CCRB_5'UTR and Agrp_95 (sequences in Appendix). The reaction mix and the program used for PCRs are listed in Table 4.10 and Table 4.11. The PCR products were visualized by using polyacrylamide gel electrophoresis (PAGE). 15% PAGE gel contained: 15% acrylamide/bisacrylamide (37,5:1), 1x TBE, 0,08% ammonium persulfate and 0,08% TEMED. Before loading samples on the gel, the PCR products were denatured at 95°C for 5 min and then renatured at the room temperature. For each sample, 3 μL of PCR product was mixed with 1,2 μL 10x loading dye. Next, the samples were loaded on the PAGE gel in 1x TBE running buffer. The gel was run at 150 V for 150 min. Further, the gel was incubated in ethidium bromide bath for 10 min and then exposed to UV light and the pictures were taken. The size of DNA bands was check with GeneRuler 100 bp Plus DNA Ladder (Thermo Scientific).

Selection and genotyping in T_2 generation

Seeds of T_2 generation were sowed on soil and 10-week-old seedlings were sprayed with Basta® solution, as described above. The resistant plants were again analysed for the presence of sgRNA. Further, to identify the mutations in *AtGRP8*, DNA from T_2 plants were analysed in PAGE-assays in two rounds.

In the round one, homozygous and heterozygous mutants were identified through visualization of the heteroduplex migration pattern on the PAGE gel. DNA from T_2 plants was used to amplify the *AtGRP8* fragment and the PCR products were run on the 15% PAGE gel, as described above. In the round two, PCR products from the wild types and from the T_2 plants were mix. The heteroduplex migration pattern on the PAGE gel allowed for identification of homozygous mutants. DNA from T_2 plants and wild type plants were used in PCR with CCRB_5'UTR and Agrp_95 primers to amplify the *AtGRP8* fragment. 3 μL of the PCR product from T_2 plant was mixed with 3 μL of the PCR product from the wild type, and then denatured at 95°C for 5 min and renatured at the room temperature. Next, 2 μL of loading dye was added to 4 μL of the renatured PCR mix and loaded on the 15% PAGE gel. The gel was run at 150 V for 150 min. Further, the gel was incubated in ethidium bromide bath for 10 min and then exposed to UV light and the pictures were taken. The size of DNA bands was check with GeneRuler 100 bp Plus DNA Ladder (Thermo Scientific).

The *At*GRP8 protein level was evaluated in T_2 generation. Proteins were extracted and analysed via Western blot (details in 4.4.3 and 4.4.4). The homozygous status of the *GRP8* locus was examined by Sanger sequencing of the PCR products including the target sequence.

4.8. Flowering time analysis

Seeds of homozygous lines were sown on soil and stratified at 4°C for 3 days. Plants were grown in short-day conditions (details in 4.2.1). After 14 days, seedlings were transferred to single pots filled with soil. Flowering time analyses were performed on 20 plants for each line. At bolting, rosette leaves were counted.
For Western blot analysis, aerial parts of ten 18-day-old seedlings of each plant line at zt7 (Zeitgeber time 7, 7 h after lights on) were collected. Proteins were extracted and analysed via Western blot (details in 4.4.3 and 4.4.4). The RNA was isolated from 5-week-old rosettes, collected from five plants for each plant line at zt7. The RNA samples were reverse transcribed (details in 4.3.2 and 4.3.4) and the synthesised cDNAs were used for PCRs and then visualized on agarose ethidium bromide (EtBr) gels.

4.9. Salt stress analyses

4.9.1. Germination assay under salt stress conditions

Seeds of indicated plant lines were sterilized and stratified (details in 4.2.2). 30 seeds of each line were plated on a quarter of a ½ MS plate without NaCl, with 150 mM NaCl, or with 200 mM NaCl. One biological replicate consisted of three technical replicates with three different NaCl concentrations. After plating, germination assays were conducted in long-day conditions. Every day for two weeks, the number of germinated seeds was counted.

4.9.2. Root length under salt stress conditions

Seeds of indicated plant lines were sterilized, stratified and plated on ½ MS medium (details in 4.2.2). After 4 days of growing in long-day conditions, 45 seedlings were transferred on ½ MS vertical plates with and without 100 mM NaCl and the plates were situated vertically in the same growing conditions. After additional seven days, the plates with 11-day-old seedlings were photographed and the pictures were analysed with the public domain software ImageJ (http://rsb.info.nih.gov/ij).

4.9.3. Analysis of alternative splicing under salt stress conditions

Seeds of indicated plant lines were sterilized, stratified, plated on ½ MS medium and grown in long-day conditions (details in 4.2.2). 11-day-old seedlings were transferred at zt4 (Zeitgeber time 4, 4 h after lights on) on ½ MS plates with and without 200 mM NaCl and put back to the same growing conditions for additional 6 h. At zt10, aerial parts of seedlings were harvested and immediately frozen in liquid nitrogen, stored at -80°C.

RNA was isolated from the collected plant material and later used for cDNA synthesis (details in 4.3.2 and 4.3.4). The alternative isoforms of *FLK* (AT3G04610), *AKIN11* (AT3G29160) and *VFP5* (AT5G05550) were analysed with sqPCRs and visualized on agarose gels with EtBr. The ratio of CS and AS isoforms were calculated based on the bands' intensity, measured with the public domain software ImageJ (http://rsb.info.nih.gov/ij).

4.10. Alternative splicing analysis

Seeds of indicated plant lines were sterilized, stratified, plated on ½ MS medium and grown in 12 h :12 h conditions for 16 days (details in 4.2.2). The aerial parts of 16-day-old seedlings were harvested at zt11. RNA was isolated from the collected plant material and later used for cDNA synthesis (details in 4.3.2 and 4.3.4). The alternative isoforms of *AKIN11* (AT3G29160) and *VFP5* (AT5G05550) were analysed with sqPCRs and visualized on agarose gels with EtBr. The ratio of CS and AS isoforms were calculated based on the bands' intensity, measured with the public domain software ImageJ (http://rsb.info.nih.gov/ij).

5. Results

It has been shown that the arginine residue at position 141 (R141) in the *At*GRP7 amino-acid chain is symmetrically dimethylated by methyltransferase *At*PRMT5 and that the lack of *At*PRMT5 leads to no arginine methylation in *At*GRP7 (Figure 5.1) (Deng et al., 2010).

To investigate the physiological function of the arginine methylation at position 141 in *At*GRP7, I used complementation lines expressing mutated versions of *AtGRP7* under the control of the endogenous promoter. Constructs expressing *At*GRP7 protein variants which can no longer be methylated were generated by exchanging R141 for alanine (R141A) and lysine (R141K), respectively (Figure 5.1). A change from arginine to phenylalanine (R141F) mimics symmetric dimethylation of arginine, since phenylalanine and methylated arginine have similarly sized hydrocarbon chains. Moreover, phenylalanine has bulky hydrophobic properties, mimicking the symmetric dimethylation of arginine. Therefore it has been used to test the effects of constitutive arginine methylation (Figure 5.1).

To investigate the role of *At*PRMT5-mediated arginine methylations, I used the loss-of-function mutants *prmt5-1* and *prmt5-5*, generated by T-DNA insertion and point mutation, respectively (Alonso et al., 2003; Pei et al., 2007). The single mutants *grp7-1* and *prmt5* were compared to double mutants, generated by crossing *prmt5* mutants with *grp7-1* (*prmt5-1 x grp7-1* and *prmt5-5 x grp7-1*). In my analyses, I also used *grp7-1* 8i lines, which contains an RNAi construct decreasing the levels of *At*GRP8 protein, which is partially redundant to *At*GRP7 and up-regulated in *grp7-1*(Streitner et al., 2008). Additionally, I used *prmt5* mutants crossed with *grp7-1* 8i (*prmt5-1 x grp7-1* 8i and *prmt5-5 x grp7-1* 8i). The crosses mentioned above have been previously generated in our laboratory (Christine Nolte and Kristina Neudorf, unpublished). All *Arabidopsis thaliana* lines used in this study are listed in Table 4.1.

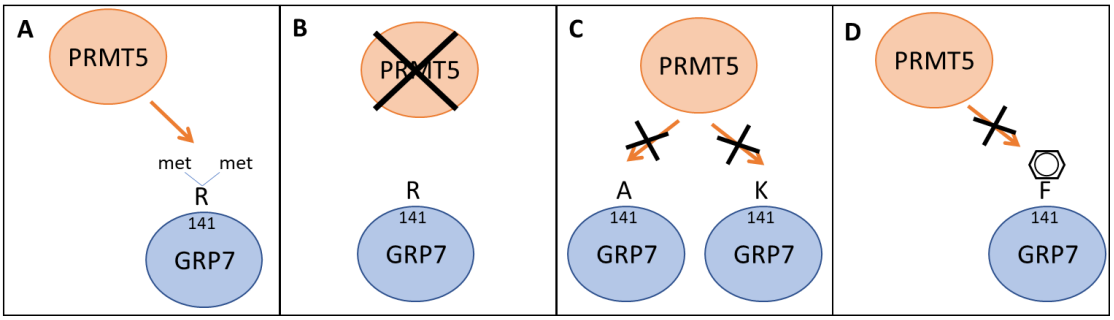

Figure 5.1 GRP7 is a target for methyltransferase PRMT5. (**A**) PRMT5 dimethylates arginine at the position 141 in GRP7; (**B**) the lack of PRMT5 results in no arginine methylation in GRP7; (**C**) the exchange of arginine at position 141 in GRP7 to alanine or lysine provides non methylated residue; (**D**) the exchange of arginine at position 141 in GRP7 to phenylalanine, mimicking arginine methylation.

5.1. Generation of transgenic *At*GRP7-GFP plants with mutations in the methylated arginine 141 residue

In order to analyse the importance of arginine methylation mediated by *At*PRMT5 at position 141 in *At*GRP7 for its cellular and physiological functions, I generated transgenic plants expressing *At*GRP7-GFP fusion proteins where arginine has been exchanged to alanine (R141A) or lysine (R141K), respectively, providing residues that can no longer be methylated.

To generate the pRT_GRP7^{R141A}-GFP cloning vector, I cloned a DNA fragment from the JM11ΔPst *At*GRP7^{R141A} vector into pRT_GRP7-GFP (Figure 5.2). The pRT_GRP7-GFP construct contains the genomic *At*GRP7 sequence with *cis*-regulatory elements (5'UTR, intron and 3'UTR) under control of the endogenous *AtGRP7* promoter. The plasmid JM11ΔPst *At*GRP7^{R141A} contains the genomic sequence of *AtGRP7,* where arginine [AGA] at the position 141 has been mutated to alanine [GCT].
To generate pRT_GRP7^{R141K}-GFP arginine [AGA] at the position 141 was mutated to lysine [AAG] in an analogous manner (Figure 5.2).
All three vectors, JM11ΔPst *At*GRP7^{R141A}, JM11ΔPst *At*GRP7^{R141K} and pRT_GRP7-GFP have been previously generated in our laboratory (Christine Nolte, unpublished).

For construction of pRT_GRP7^{R141A}-GFP and pRT_GRP7^{R141K}-GFP, JM11ΔPst *At*GRP7^{R141A} and JM11ΔPst *At*GRP7^{R141K}, respectively, were double digested with *BbsI* and *HpaI*. The resulting 211 bp DNA fragments containing the *AtGRP7* sequence with the R141A and R141K mutations were purified from agarose gels and then cloned into pRT_GRP7-GFP after its digestion with *BbsI* and *HpaI* and dephosphorylation.

The correct orientation of the ligated DNA fragment was confirmed by restriction digests and Sanger-sequencing. In preparation for plant transformation, GRP7^{R141A}-GFP and GRP7^{R141K}-GFP were cloned into the binary vector HPT1 using the restriction enzymes *HindIII* and *XbaI*. The resulting vectors, pHPT1-GRP7^{R141A}-GFP and pHPT1-GRP7^{R141K}-GFP were transformed into *E. coli* and then transformed into *A. tumefaciens.* After each transformation colonies were checked by restriction digests. The constructs were transformed into *grp7-1* plants using *Agrobacterium*-mediated transformation.

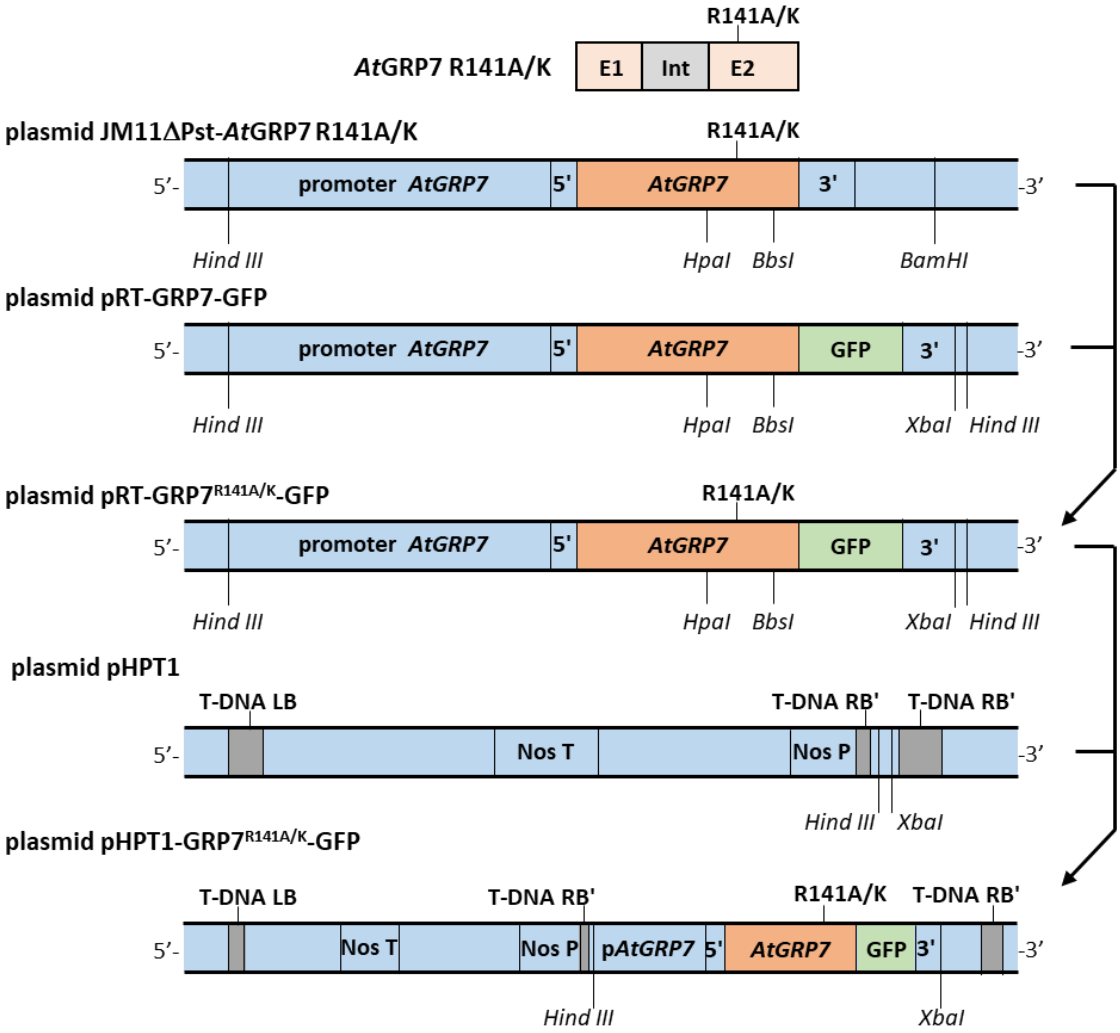

Figure 5.2 Cloning strategy for generating AtGRP7 R141A -GFP and AtGRP7 R141K -GFP. Used abbreviations: E1- Exon 1, Int- Intron, E2- Exon 2, 5'- 5'UTR, 3'-3'UTR, Nos T- Nos Terminator Nos P- Nos Promoter, p*AtGRP7*-promoter *AtGRP7*. See text for details.

5.2. Flowering time analysis in plants with mutations in the methylated arginine 141 residue in *At*GRP7

Mutants that lacks *GRP7* flower later than wild type plants (Streitner et al., 2008). It has been shown that the lack of *GRP7* expression in *grp7-1* mutants can be fully complemented by a genomic *GRP7* fragment (Steffen and Stagier, unpublished). To test whether the non-methylated variants of GRP7 are able to complement the late flowering phenotype of the *grp7-1* mutant, flowering time experiments were conducted (Figure 5.3).

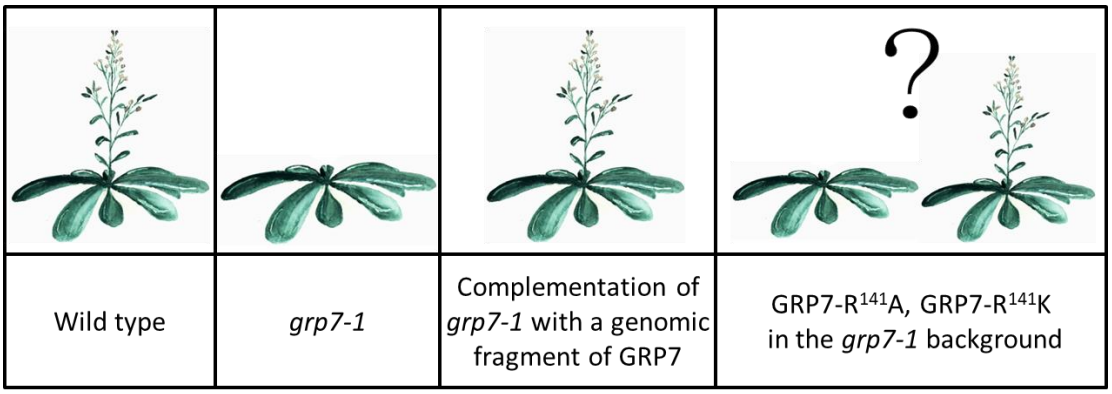

Figure 5.3 Graphic representation of the flowering time analysis.

On the molecular level, it has been shown that GRP8 protein level and *GRP8* transcript level are increased in *grp7-1* compared to wild type, due to the release from GRP7 repression (Streitner et al., 2008). The phenotype of *grp7-1* can be fully rescued by the endogenous genomic *GRP7* fragment expressed under the *GRP7* promoter. In contrast to *grp7-1* mutants, plants overexpressing GRP7 (GRP7ox) display decreased GRP8 protein and *GRP8* transcript levels. Due to the negative *GRP7* autoregulation, the endogenous *GRP7* transcript level in GRP7ox plants is down regulated as well. In the flowering time experiments, I aimed to examine, whether the non-methylated versions of *GPR7* can fully complement the *grp7-1* mutant and down-regulate the GRP8 protein and *GRP8* transcript levels.

To analyse the importance of R141 methylation in GRP7 for flowering time, I used three different sets of transgenic plants.
In the first set, I used *grp7-1* lines complemented with *AtGRP7* variants, where R141 has been mutated to either alanine ($GRP7^{R141A}$ (*grp7-1*)) or lysine ($GRP7^{R141K}$ (*grp7-1*)) expressed under the *AtGRP7* promoter. The lines have been previously generated in our laboratory by Christine Nolte and Frederik Dombert (unpublished).
As controls served two independent complementation lines termed GRP7 FL4a (*grp7-1*) and GRP7 FL10c (*grp7-1*) expressing the full-length genomic *AtGRP7* sequence

under the *AtGRP7* promoter in the *grp7-1* background. These lines have been previously generated in our laboratory (Alexander Steffen, unpublished).

For the second experiment, I used complementation lines expressing the same GRP7 variants as above but fused to GFP (GREEN FLUORESCENT PROTEIN). These constructs, termed *pGRP7::GRP7*^{R141A}*-GFP* and *pGRP7::GRP7*^{R141K}*-GFP,* were introduced into the *grp7-1* background (details in 5.1). *At*GRP7-GFP (*grp7-1*) plants carrying a full-length genomic *AtGRP7* sequence fused to *GFP* under *AtGRP7* promoter (Streitner et al., 2012) served as a control.
Additionally, to compare the function of R141 methylation in GRP7 to the effect of PRMT5 on flowering time, I also used lines expressing GRP7-GFP under the endogenous promotor in the double mutant background *prmt5-1 x grp7-1* and *prmt5-5 x grp7-1* (previously generated in our laboratory by Kristina Neudorf and Christine Nolte).

The third flowering time analysis was conducted with a set of plants overexpressing *GRP7* variants with mutated R141, termed *At*GRP7^{R141A}ox, *At*GRP7^{R141K}ox and *At*GRP7^{R141F}ox, which were previously generated in our laboratory (Christine Nolte and Frederik Dombert, unpublished). These plants carry the *AtGRP7* coding sequence (CDS) with the respective mutations (R141A, R141K, R141F) and are expressed under control of the constitutive Cauliflower Mosaic Virus (CaMV) 35S promoter in the Col-0 background. The exchange of arginine to phenylalanine (F) mimics arginine methylation and was used to test the effects of constitutive arginine methylation at the position 141 in GRP7. The *At*GRP7ox lines D1c and G1d, which express the *AtGRP7* CDS under the constitutive CaMV 35S promoter (Streitner et al., 2008), were used as controls.

5.2.1. Flowering time analysis in GRP7^{R141A} and GRP7^{R141K} (*grp7-1*) complementation lines

In the first flowering time experiment, *grp7-1* plants had more rosette leaves than Col-0 when bolting, as previously published (Streitner et al., 2008) (Figure 5.4). Complementation plant lines GRP7 FL4a and FL10c with the full-length genomic *GRP7* sequence under *GRP7* promoter in *grp7-1* background, were used as controls and showed no change in flowering time compared to Col-0. Therefore, the original genomic *GRP7* sequence in GRP7 FL4a and FL10c lines fully complemented the *grp7-1* mutant, since the late flowering phenotype of *grp7-1* was abolished. The complementation lines GRP7^{R141A} and GRP7^{R141K} flowered significantly earlier than *grp7-1* and had a similar number of rosette leaves as Col-0 and GRP7 FL4a and FL10c at bolting (Figure 5.4).

A

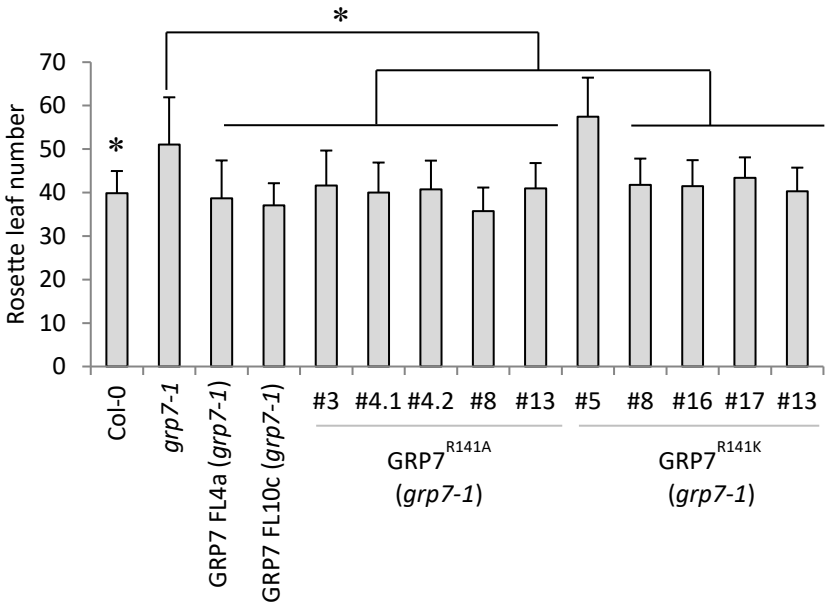

B

plant line	Rosette leaf number				
	n	Mean	Median	± SD	*p*-value
Col-0	15	39,9	39,0	5,1	0,0002
grp7-1	15	51,1	48,0	10,9	
GRP7 FL4a (*grp7-1*)	15	38,7	38,0	8,7	0,0000
GRP7 FL10c (*grp7-1*)	15	37,1	37,0	5,1	0,0000
$GRP7^{R141A}$ (*grp7-1*) #3	15	41,7	38,0	8,0	0,0027
$GRP7^{R141A}$ (*grp7-1*) #4.1	19	40,0	40,0	6,9	0,0001
$GRP7^{R141A}$ (*grp7-1*) #4.2	17	40,8	40,0	6,6	0,0004
$GRP7^{R141A}$ (*grp7-1*) #8	18	35,7	37,5	5,4	0,0000
$GRP7^{R141A}$ (*grp7-1*) #13	15	41,0	43,0	5,8	0,0010
$GRP7^{R141K}$ (*grp7-1*) #5	15	57,5	60,0	9,0	0,0975
$GRP7^{R141K}$ (*grp7-1*) #8	17	41,8	42,0	6,1	0,0021
$GRP7^{R141K}$ (*grp7-1*) #16	15	41,5	40,0	6,0	0,0020
$GRP7^{R141K}$ (*grp7-1*) #17	15	43,4	44,0	4,7	0,0255
$GRP7^{R141K}$ (*grp7-1*) #13	15	40,3	40,0	5,4	0,0004

Figure 5.4 Flowering times of the complementation lines $GRP7^{R141A}$ and $GRP7^{R141K}$. Homozygous transgenic plants were grown under short-day conditions (8 h light and 16 h dark rhythm). The rosette leaf number was determined at bolting. (**A**) Bars represent means ± SD of rosette leaf number, scored for a minimum of 15 plants. One-way ANOVA followed by a post-hoc Dunnet test was used to show statistically significant results, $*p < 0{,}05$; $GRP7^{R141A}$

and GRP7^{R141K} lines were compared to *grp7-1* (**B**) Table contains names of plant lines, *n* numbers of counted plants, means and medians ± SD of rosette leaf numbers.

However, the immunoblot analysis showed varying GRP7 protein levels in GRP7^{R141A} and GRP7^{R141K} (Figure 5.5). Moreover, it can be observed that the level of GRP8 protein depends on the level of GRP7 and it is inversely proportional. On the transcriptional level, the differences in the amount of *GRP7* mRNA in the independent transgenic lines explain the differences in GRP7 protein level (Figure 5.6). Like antagonistic GRP7 and GRP8 protein levels, the amount of *GRP7* and *GRP8* transcripts is also inversely proportional.

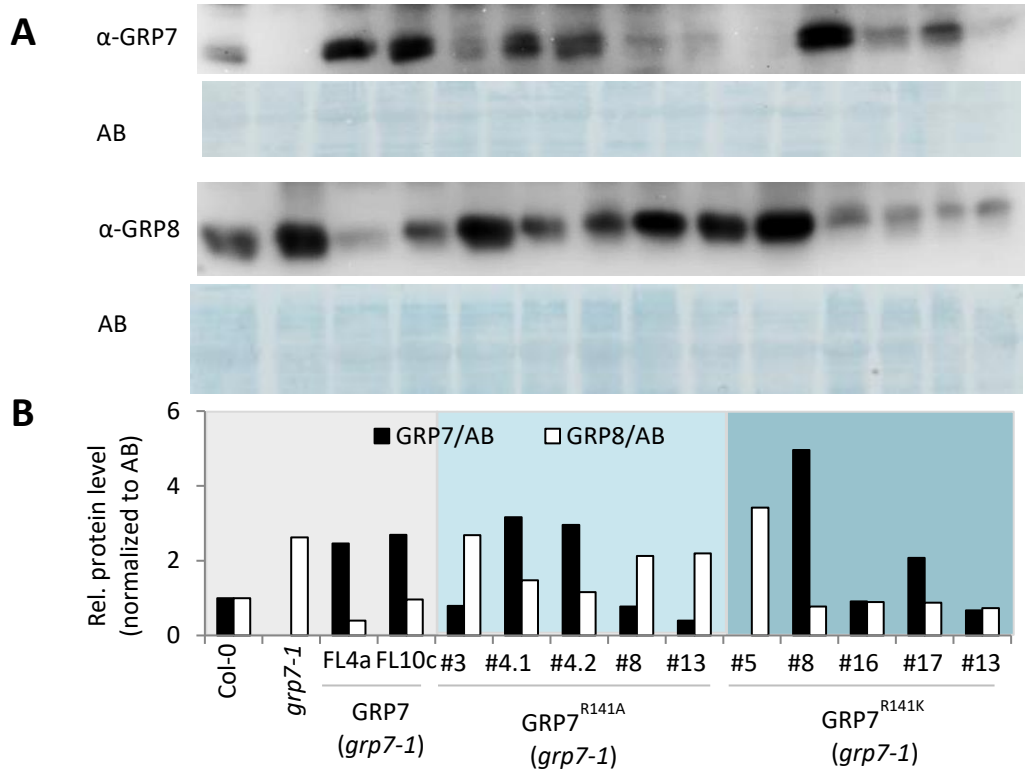

Figure 5.5 Levels of GRP7 and GRP8 proteins in complementation lines GRP7^{R141A} and GRP7^{R141K}. The total protein extracts were isolated from 18-days-old seedlings grown under short day conditions (8 h light and 16 h dark rhythm). (**A**) The protein level of GRP7 and GRP8 was examined by Western blot with anti-GRP7 (α-GRP7) and anti-GRP8 (α-GRP8) antibodies. Amido black was used as a loading control. Uncropped pictures Figure A. 1. (**B**) The signal intensities were analyzed with ImageJ (http://rsb.info.nih.gov/ij). Data was normalized to amido black and presented as a bar chart.

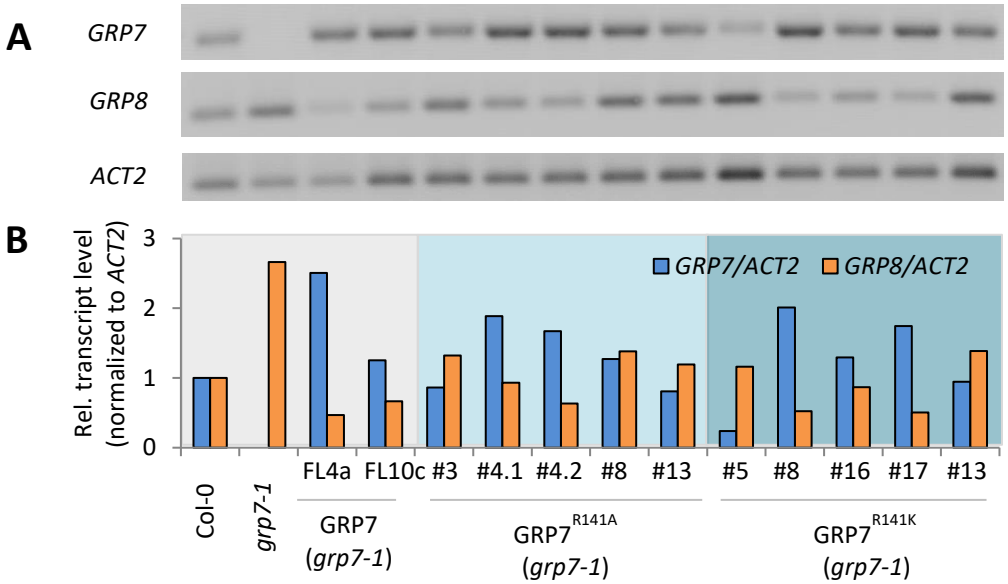

Figure 5.6 Transcript level of *GRP7* and *GRP8* in complementation lines GRP7^{R141A} and GRP7^{R141K}. The RNA samples were isolated from 5-week-old seedlings grown under short day conditions (8 h light and 16 h dark rhythm). (**A**) Total RNA was reverse transcribed and used for measuring *GRP7* and *GRP8* levels by semi-quantitative PCR. *ACTIN2* (*ACT2*) was used as a loading control. Uncropped pictures Figure A. 2. (**B**) The public domain software ImageJ (http://rsb.info.nih.gov/ij) was used for measurement of signal intensities. Data was normalized to *ACT2*.

5.2.2. Flowering time analysis in GRP7^{R141A}-GFP and GRP7^{R141K}-GFP (*grp7-1*) complementation lines.

In the second flowering time experiment, the *grp7-1* plants complemented with GRP7-GFP were used as a control and flowered earlier then *grp7-1* plants. Therefore, the GRP7-GFP construct also rescued the late flowering phenotype of *grp7-1* (Figure 5.7). However, the plants that lack functional PRMT5 protein, GRP7-GFP (*prmt5-1 x grp7-1*) and GRP7-GFP (*prmt5-5 x grp7-1*), flowered with greater rosette leaf number in comparison to GRP7-GFP (*grp7-1*) and *grp7-1*, indicating that the lack of PRMT5 leads to a delay in flowering time. On the other hand, the rosette leaf number of the GRP7^{R141A}-GFP (*grp7-1*) and GRP7^{R141K}-GFP (*grp7-1*) plants was significantly different from *grp7-1* and comparable to GRP7-GFP (*grp7-1*) (Figure 5.7).

A

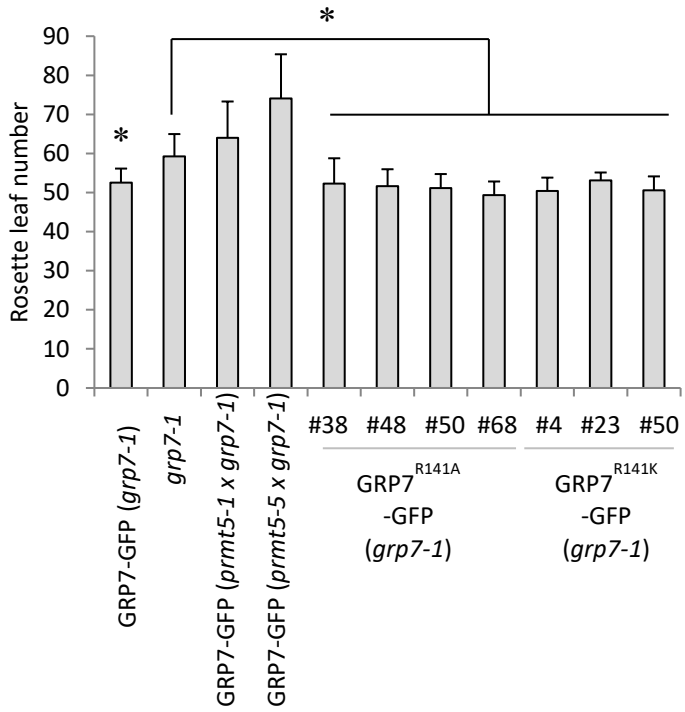

B

plant line	Rosette leaf number				
	n	Mean	Median	± SD	*p*-value
GRP7-GFP (*grp7-1*)	15	52,5	51,0	3,6	0,0139
grp7-1	15	59,3	58,0	5,7	
GRP7-GFP (*prmt5-1 x grp7-1*)	17	64,0	64,0	9,3	0,1420
GRP7-GFP (*prmt5-5 x grp7-1*)	14	74,1	74,0	11,3	0,0000
$GRP7^{R141A}$-GFP (*grp7-1*) #38	15	52,3	52,0	6,5	0,0094
$GRP7^{R141A}$-GFP (*grp7-1*) #48	15	51,7	52,0	4,3	0,0037
$GRP7^{R141A}$-GFP (*grp7-1*) #50	15	51,1	52,0	3,6	0,0015
$GRP7^{R141A}$-GFP (*grp7-1*) #68	15	49,3	50,0	3,5	0,0001
$GRP7^{R141K}$-GFP (*grp7-1*) #4	19	50,4	50,0	3,4	0,0002
$GRP7^{R141K}$-GFP (*grp7-1*) #23	15	53,1	53,0	2,0	0,0321
$GRP7^{R141K}$-GFP (*grp7-1*) #50	15	50,5	51,0	3,6	0,0005

Figure 5.7 Flowering times of the transgenic $GRP7^{R141A}$-GFP and $GRP7^{R141K}$-GFP plants. Homozygous transgenic plants were grown under short-day conditions (8 h light and 16 h dark rhythm). The rosette leaf number was determined at bolting. (**A**) Bars represent means ± SD of rosette leaf number, scored for a minimum of 15 plants. One-way ANOVA followed by a post-hoc Dunnet test was used to show statistically significant results, $*p < 0,05$; $GRP7^{R141A}$-GFP and $GRP7^{R141K}$-GFP lines were compared to *grp7-1*. (**B**) Table contains names of plant lines, *n* numbers of counted plants, means and medians ± SD of rosette leaf numbers.

The immunoblot analysis showed that lack of GRP7 in the *grp7-1* caused an increase in GRP8 protein level (Figure 5.8). In the complementation lines GRP7^{R141A}-GFP (*grp7-1*) and GRP7^{R141K}-GFP (*grp7-1*), protein levels of GRP7 and GRP8 were comparable to the control line GRP7-GFP (*grp7-1*). This suggests that the mutated versions of GRP7 are able to control the amount of functional *GRP8* transcripts via alternative splicing.

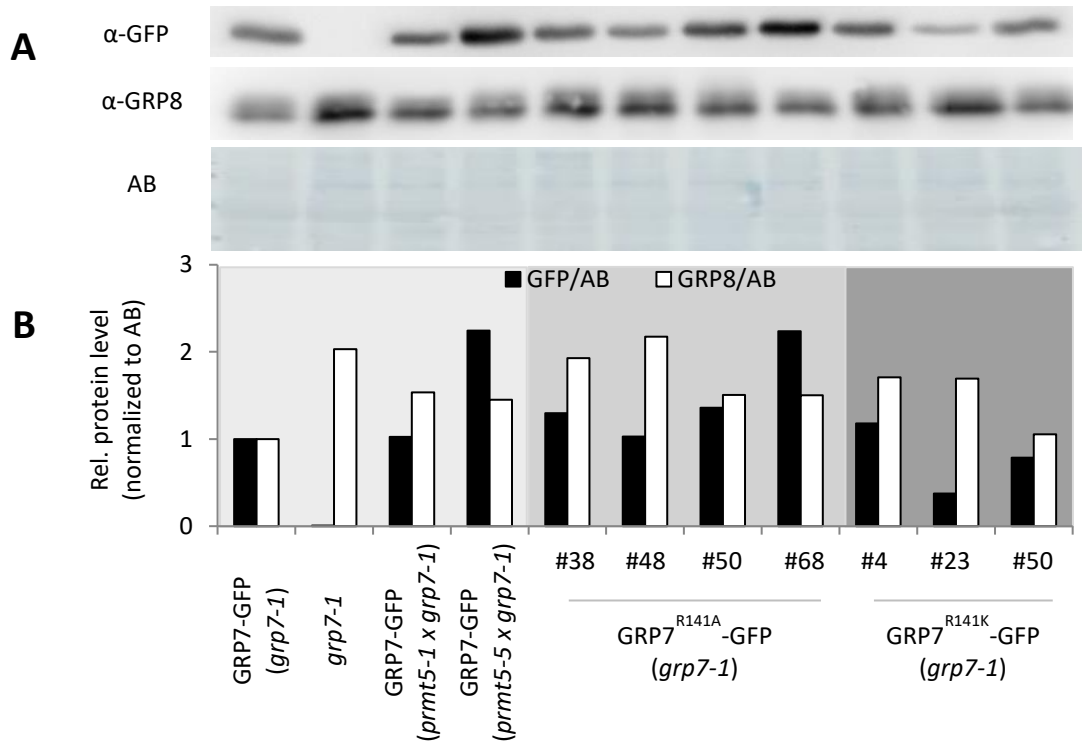

Figure 5.8 Levels of GRP7 and GRP8 proteins in the transgenic GRP7^{R141A}-GFP and GRP7^{R141K}-GFP plants. The total protein extracts were isolated from 18-days-old seedlings grown under short day conditions (8 h light and 16 h dark rhythm). (**A**) The protein level of GRP7 and GRP8 was examined by Western blot with anti-GFP (α-GFP) and anti-GRP8 (α-GRP8) antibodies, respectively. Amido black was used as a loading control. Uncropped pictures Figure A. 3. (**B**) The signal intensities were analysed with software ImageJ (http://rsb.info.nih.gov/ij). Data was normalized to amido black and presented as a bar chart.

Similar to the immunoblot analysis, the examination of *GRP7* and *GRP8* transcripts showed that the *GRP7* pre-mRNA in GRP7^{R141A}-GFP (*grp7-1*) and GRP7^{R141K}-GFP (*grp7-1*) were expressed at different levels in the independent transformants (Figure 5.9). However, the *GRP8* transcript level was not increased, as observed in *grp7-1* plants, indicating that the mutated versions of *GRP7* complemented the *grp7-1* phenotype.

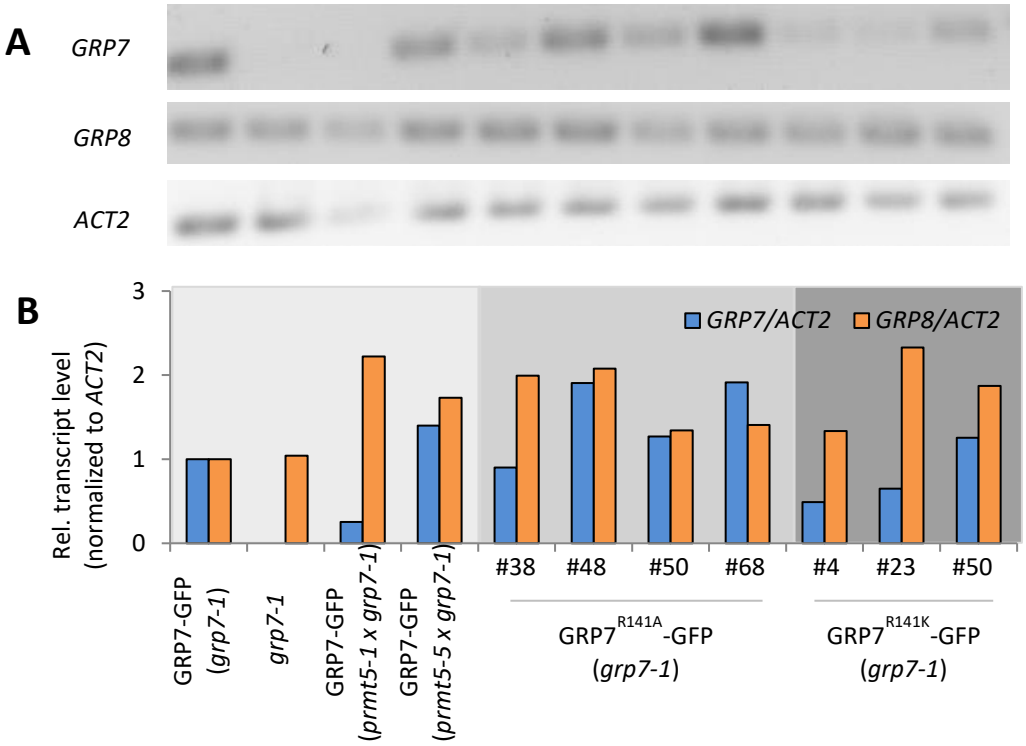

Figure 5.9 Transcript level of *GRP7* and *GRP8* in the transgenic GRP7^{R141A}-GFP and GRP7^{R141K}-GFP plants. The RNA samples were isolated from 5-week-old seedlings grown under short day conditions (8 h light and 16 h dark rhythm). (**A**) Total RNA was reverse transcribed and used for measuring *GRP7* and *GRP8* levels by semi-quantitative PCR. *ACTIN2* (*ACT2*) was used as a loading control. Uncropped pictures Figure A. 4. (**B**) The public domain software ImageJ (http://rsb.info.nih.gov/ij) was used for measurement of signal intensities. Data was normalized to *ACT2*.

5.2.3. Flowering time analysis in GRP7^{R141A}ox, GRP7^{R141K}ox and GRP7^{R141F}ox overexpressing lines

The third flowering time experiment showed that the plants overexpressing *GRP7* (GRP7ox D1c and G1d) flower earlier, with less leaves, than the wild type Col-0 (Figure 5.10). Plants overexpressing mutated versions of *GRP7*, GRP7^{R141A}ox, GRP7^{R141K}ox and GRP7^{R141F}ox, also had fewer rosette leaves at flowering time and showed significant differences to Col-0.

A

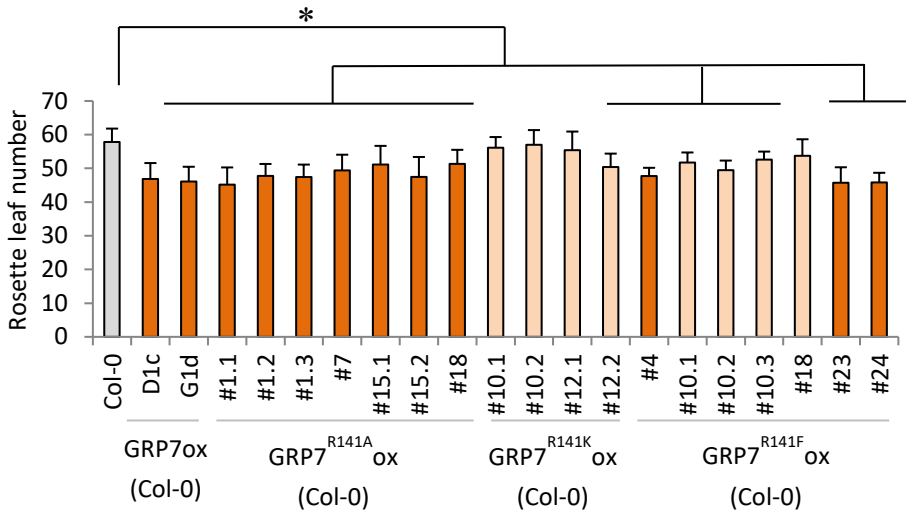

B

	Rosette leaf number				
plant line	*n*	Mean	Median	± SD	*p*-value
Col-0	20	57,9	58,5	4,0	
GRP7ox D1c	20	46,9	46,5	4,7	0,0000
GRP7ox G1d	20	46,1	46,5	4,4	0,0000
GRP7^{R141A}ox #1.1	17	45,2	44,0	5,1	0,0000
GRP7^{R141A}ox #1.2	17	47,8	48,0	3,5	0,0000
GRP7^{R141A}ox #1.3	15	47,4	48,0	3,7	0,0000
GRP7^{R141A}ox #7	15	49,4	48,0	4,7	0,0000
GRP7^{R141A}ox #15.1	15	51,1	49,5	5,5	0,0002
GRP7^{R141A}ox #15.2	15	47,5	48,0	5,9	0,0000
GRP7^{R141A}ox #18	15	51,3	52,0	4,2	0,0002
GRP7^{R141K}ox #10.1	15	56,1	56,0	3,2	0,9642
GRP7^{R141K}ox #10.2	15	57,0	56,0	4,4	1,0000
GRP7^{R141K}ox #12.1	15	55,4	56,0	5,5	0,6646
GRP7^{R141K}ox #12.2	15	50,4	50,0	4,0	0,0000
GRP7^{R141F}ox #4	18	47,7	48,0	2,4	0,0000
GRP7^{R141F}ox #10.1	15	51,7	52,0	3,0	0,0005
GRP7^{R141F}ox #10.2	15	49,5	49,0	2,9	0,0000
GRP7^{R141F}ox #10.3	15	52,6	53,0	2,4	0,0054
GRP7^{R141F}ox #18	15	53,7	55,0	4,9	0,0644
GRP7^{R141F}ox #23	15	45,7	46,0	4,6	0,0000
GRP7^{R141F}ox #24	15	45,8	46,0	2,7	0,0000

Figure 5.10 Flowering times of the lines overexpressing GRP7^{R141A} and GRP7^{R141K}. Homozygous transgenic plants were grown under short-day conditions (8 h light and 16 h dark rhythm). The rosette leaf number was determined at bolting. (**A**)

Bars represent means ± SD of rosette leaf number, scored for a minimum of 15 plants. Orange - plants strongly overexpressing GRP7, light orange - plants overexpressing GRP7 less than controls D1c and G1c, grey - wild type level of protein GRP7. One-way ANOVA followed by a post-hoc Dunnet test was used to show statistically significant results, * $p < 0{,}05$; GRP7^{R141A}ox, GRP7^{R141K}ox and GRP7^{R141F}ox lines were compared to *grp7-1*. (**B**) Table contains names of plant lines, *n* numbers of counted plants, means and medians ± SD of rosette leaf numbers.

The immunoblot analysis showed that the overexpression of GRP7 decreases the level of GRP8 protein (Figure 5.11 and Figure 5.12). The level of GRP7 in Col-0 was undetectable due to the low efficiency of the anti-GRP7 antibody. Unlike the others, plants #10.1, #10.2 and #12.1, coming from two independent transformation events, flowered with a rosette leaf number similar to Col-0. The explanation of this deviation is the fact that the GRP7 protein level in #10.1, #10.2 and #12.1 was considerably lower than in other lines. Therefore, the differences in the rosette leaf numbers between #10.1, #10.2, #12.1 plants and Col-0 were not significant.

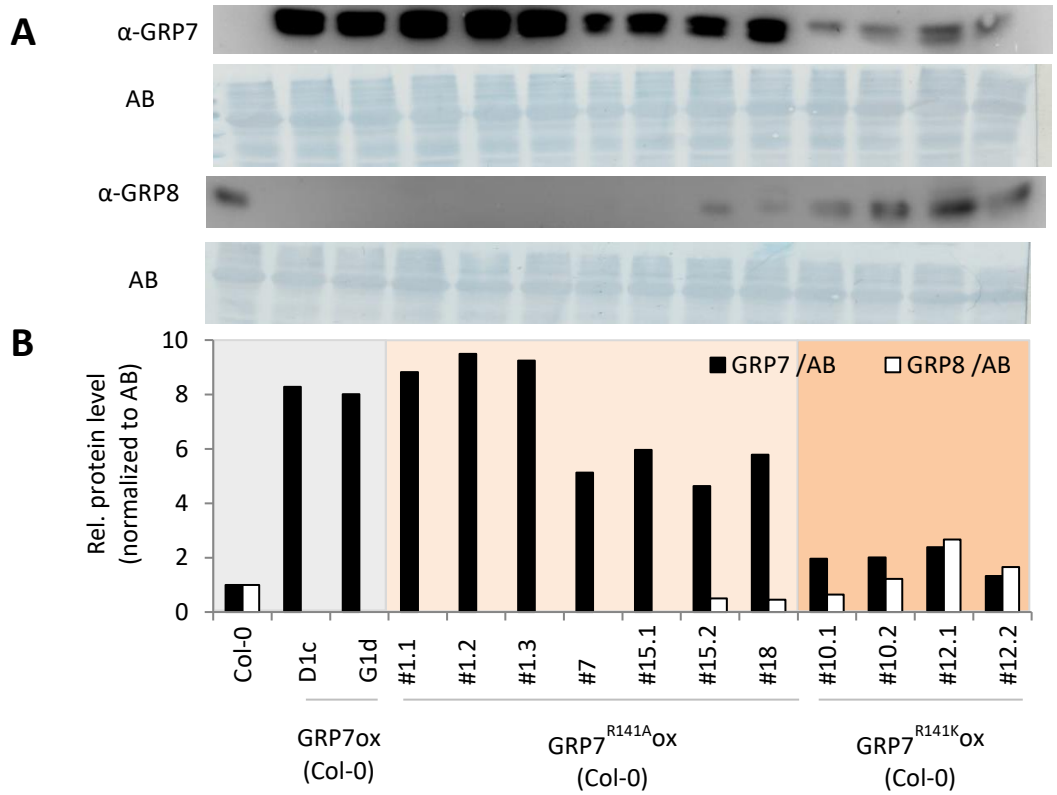

Figure 5.11 Levels of GRP7 and GRP8 proteins in lines overexpressing GRP7^{R141A} and GRP7^{R141K}. The total protein extracts were isolated from 18-days-old seedlings grown under short day conditions (8 h light and 16 h dark rhythm). (**A**) The protein level of GRP7 and GRP8 was examined by Western blot with anti-GRP7 (α-GRP7) and anti-GRP8 (α-GRP8) antibodies. Amido black was used as a loading control. Uncropped pictures Figure A. 5. (**B**) The signal intensities were analysed with software ImageJ (http://rsb.info.nih.gov/ij). Data was normalized to amido black and presented as a bar chart.

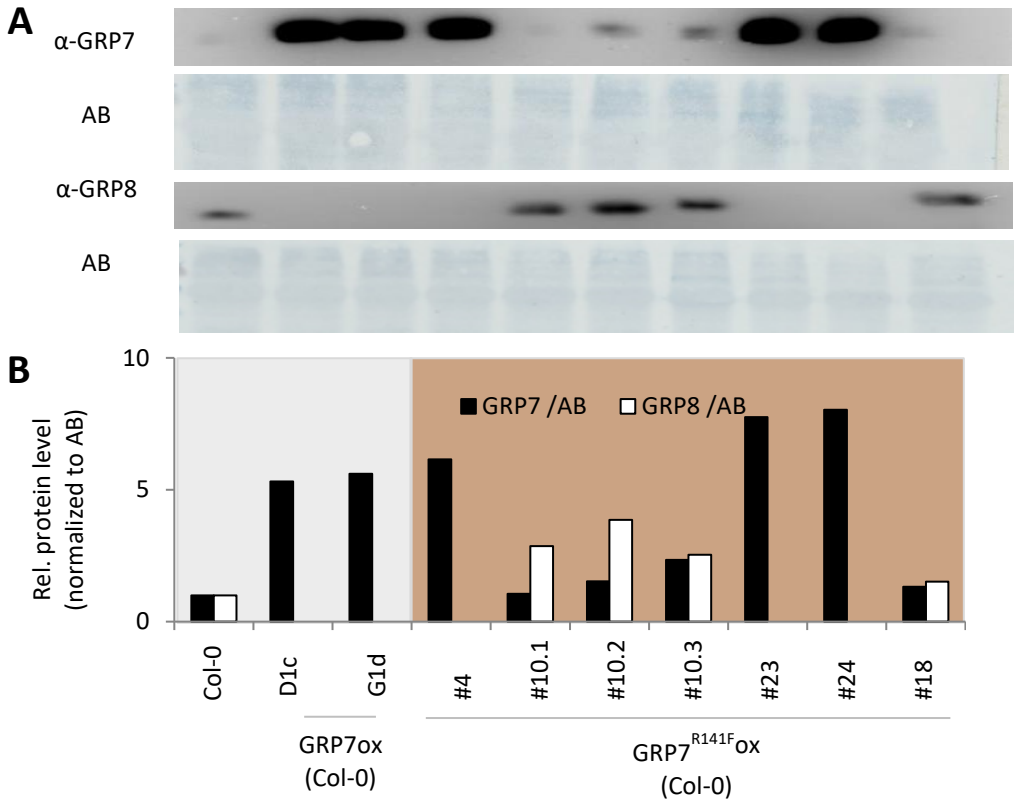

Figure 5.12 Levels of GRP7 and GRP8 proteins in lines overexpressing GRP7^{R141F}. The total protein extracts were isolated from 18-days-old seedlings grown under short day conditions (8 h light and 16 h dark rhythm). (**A**) The protein level of GRP7 and GRP8 was examined by Western blot with anti-GRP7 (α-GRP7) and anti-GRP8 (α-GRP8) antibodies. Amido black was used as a loading control. Uncropped pictures Figure A. 5. (**B**) The signal intensities were analysed with software ImageJ (http://rsb.info.nih.gov/ij). Data was normalized to amido black and presented as a bar chart.

GRP7^{R141A}ox, GRP7^{R141K}ox and GRP7^{R141F}ox plants, which showed a high GRP7 level in the immunoblot analysis, had decreased levels of GRP8 protein (Figure 5.11 and Figure 5.12) and a reduced level of *GRP8* transcripts (Figure 5.13). The high level of GRP7 protein created a negative feedback loop reducing the amount of the endogenous functional transcript. Because of that, the level of endogenous *GRP7* transcript was decreased.

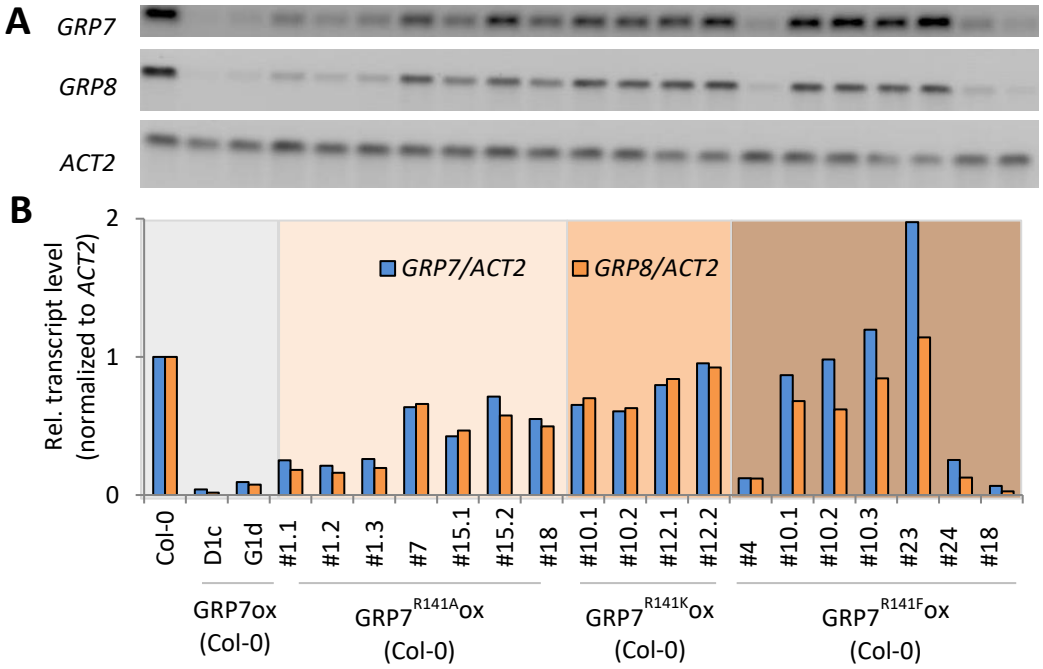

Figure 5.13 Transcript level of *GRP7* and *GRP8* in lines overexpressing GRP7^{R141A}, GRP7^{R141K} and GRP7^{R141F}. The RNA samples were isolated from 5-week-old seedlings grown under short day conditions (8 h light and 16 h dark rhythm). (**A**) Total RNA was reverse transcribed and used for measuring *GRP7* and *GRP8* levels by semi-quantitative PCR. *ACTIN2* (*ACT2*) was used as a loading control. Uncropped pictures Figure A. 6. (**B**) The public domain software ImageJ (http://rsb.info.nih.gov/ij) was used for measurement of signal intensities. Data was normalized to *ACT2*.

In conclusion, the overexpressed mutated versions of GRP7 (GRP7^{R141A} and GRP7^{R141K}) seem to be fully functional and rather than the methylation status of arginine at position 141 in GRP7, the level of GRP7 protein seems to matter.

In summary, all three flowering experiments showed that the exchange of arginine at position 141 to alanine, lysine or phenylalanine in the GRP7 protein did not affect the number of rosette leaves at bolting, where the complementation lines flowered at the same time as wild type and the overexpressing lines flowered at the same time as GRP7ox plants. Additionally, the mutations did not affect *GRP7* and *GRP8* transcripts levels in comparison to the respective controls.
Therefore, it is concluded that the presence or absence of the methylation at the position 141 in GRP7, delivered by PRMT5, does not influence the flowering time.

5.3. Analysis of the role of arginine methylation in response to biotic stress (pathogen defense)

It has been shown that *grp7-1* mutants are more susceptible to pathogen infections. On the other hand, plants overexpressing GRP7 are more resistant than wild type and *grp7-1* under biotic stress (Fu et al., 2007; Nicaise et al., 2013). Furthermore, it has been shown that *prmt5* plants exhibit enhanced resistance against *Hyaloperonospora arabidopsidis,* thus PRMT5 has been proposed as a negative regulator of plant immunity (Huang et al., 2016). Latest publication from Hu and co-workers shows that PRMT5 is also a negative regulator of bacterial resistance, therefore its RNA and protein level decreases 12 h after bacterial infection. Moreover, it has been shown that this sudden drop of PRMT5 reduces arginine methylation level in PRMT5-target ARGONAUTE 2 (AGO2), thereby prevents degradation of AGO2 and AGO2-associated sRNAs (Hu et al., 2019).

To determine the importance of arginine methylation for the response to biotic stress, *A. thaliana* plants were infected with *Pseudomonas syringe* pv. tomato DC3000 (*Pst*) by leaf infiltration. Four different genotypes were used in the experiment: wild-type Col-0, the T-DNA knock-out mutants *grp7-1* and *prmt5-1* and the double mutant *prmt5-1 x grp7-1*. 10 mM magnesium chloride was used as a mock treatment. Severe disease symptoms were observable 48 h after the infiltration (Figure 5.14).

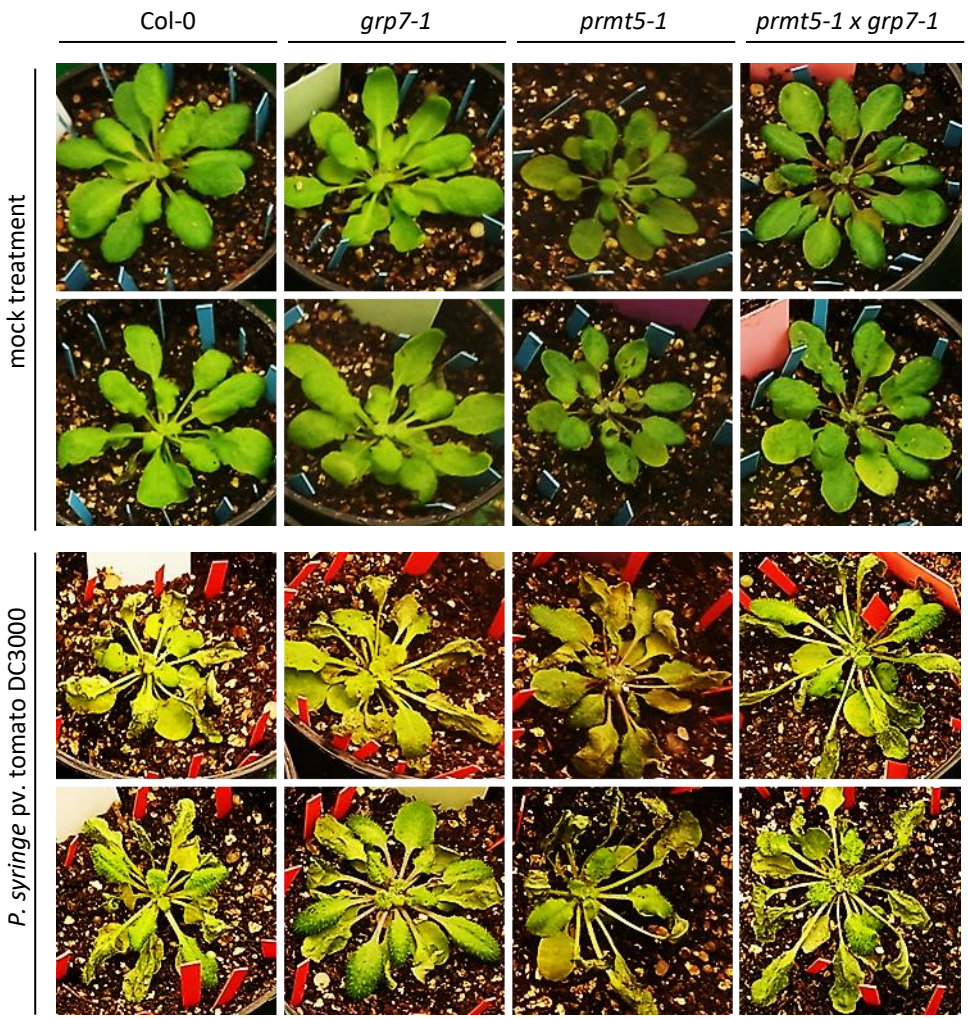

Figure 5.14 Disease symptoms in plants infiltrated with *Pseudomonas syringe* pv. tomato DC3000 and magnesium chloride (mock treatment). Pictures have been taken 48 h after plant infiltration. Representative pictures from three independent experiments are shown.

To examine the plant response to pathogen infection on the molecular level, the expression levels of the PTI (Pattern Triggered Immunity)-responsive gene *FLG22-INDUCED RECEPTOR-LIKE 1 (FRK1)* and a defense marker gene *PATHOGENESIS-RELATED GENE 1 (PR1)* were analysed. At the indicated times (4 h and 1 day after infiltration), plant material was harvested and used for RNA isolation. The *PR1* and *FRK1* expression levels were determined in Col-0, *grp7-1*, *prmt5-1* and *prmt5-1 x grp7-1* plants by RT-qPCR and normalized to *PP2A* levels.

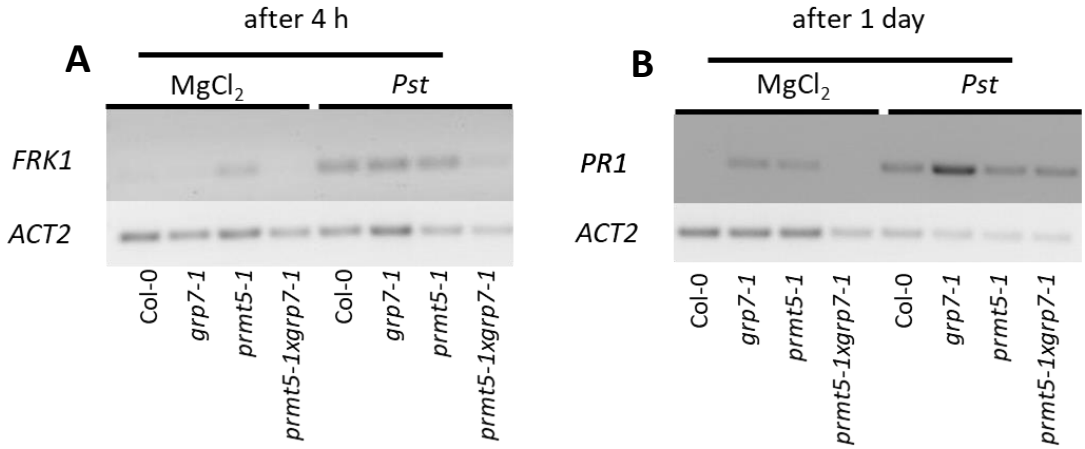

Figure 5.15 *FRK1* and *PR1* transcript levels in plants infiltrated with *P. syringae* pv. *tomato* DC3000. *A. thaliana* plants were infiltrated with bacterial solution (*Pst*) (bacteria resuspended in 10 mM $MgCl_2$) and pure 10 mM $MgCl_2$ (mock). The RNA samples were isolated from infiltrated rosette leaves (**A**) harvested 4 hours after infiltration and (**B**) 1 day after infiltration. The total RNA was reverse transcribe and used for semi-quantitative PCR for *FRK1* and *PR1*. *ACTIN2* (*ACT2*) was used as a loading control.

Plants from all four different genotypes treated with *Pst* showed increased *PR1* transcript levels, in comparison to the mock treatment (Figure 5.15, Figure 5.16 and Figure 5.17). Despite small differences visible on a gel picture (Figure 5.15), no significant changes in steady-state *PR1* transcript abundance were detected between the four different genotypes (Figure 5.17). However, data of independent biological replicates shows tendency, where *PR1* is higher upregulated in *grp7-1* plants in comparison to Col-0 and the *PR1* transcript levels in *prmt5-1* and *prmt5-1 x grp7-1* are not as high as in Col-0 (Figure 5.16).

Analysis of *FRK1* expression in Col-0, *grp7-1, prmt5-1* and *prmt5-1 x grp7-1* showed increased levels in plants treated with *Pst* but not with the mock solution (Figure 5.15, Figure 5.16 and Figure 5.17). The amount of *FRK1* transcripts in *grp7-1, prmt5-1* and *prmt5-1 x grp7-1* was not as high as in Col-0 control plants. A statistically significant difference was observed between Col-0 and the double mutant *prmt5-1 x grp7-1*. The upregulation of *FRK1* recorded in the single mutants *grp7-1* and *prmt5-1* after *Pst* treatment was not as high as in Col-0, however the detected differences were not statistically significant. Analysis of *FRK1* expression in independent biological replicates confirms the described above tendencies (Figure 5.16).

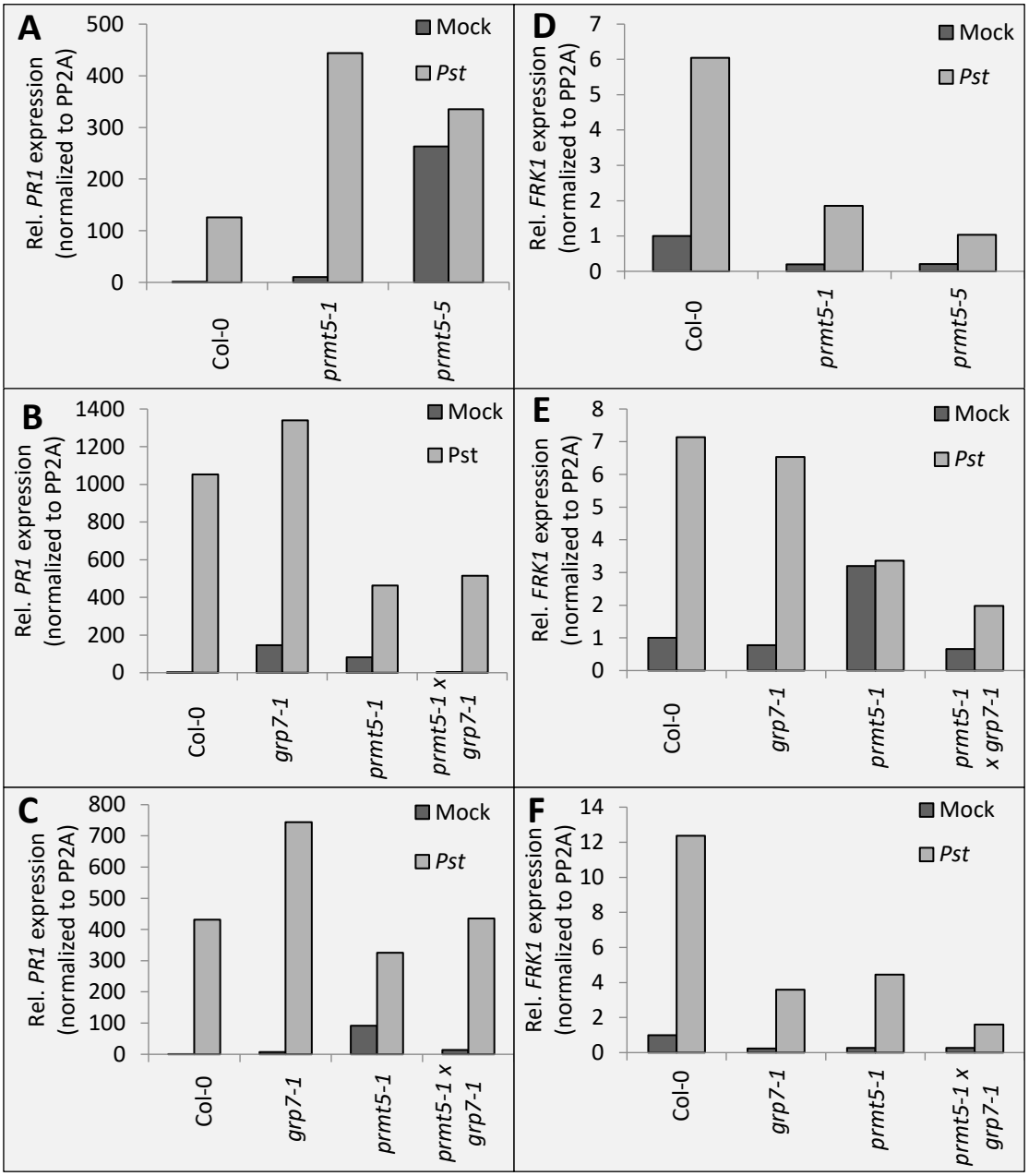

Figure 5.16 Relative *PR1* and *FRK1* transcript level in three independent biological replicates. (**A, B, C**) Relative *PR1* transcript level in plants 4 hours after infiltration; (**D, E, F**) relative *FRK1* transcript level in plants 1 day after infiltration with bacterial solution (*Pst)* or magnesium chloride (mock). The RNA samples were isolated from infiltrated rosette leaves. The expression level was measured by quantitative RT–qPCR and normalized to *PP2A* levels. The bar charts show independent biological replicates.

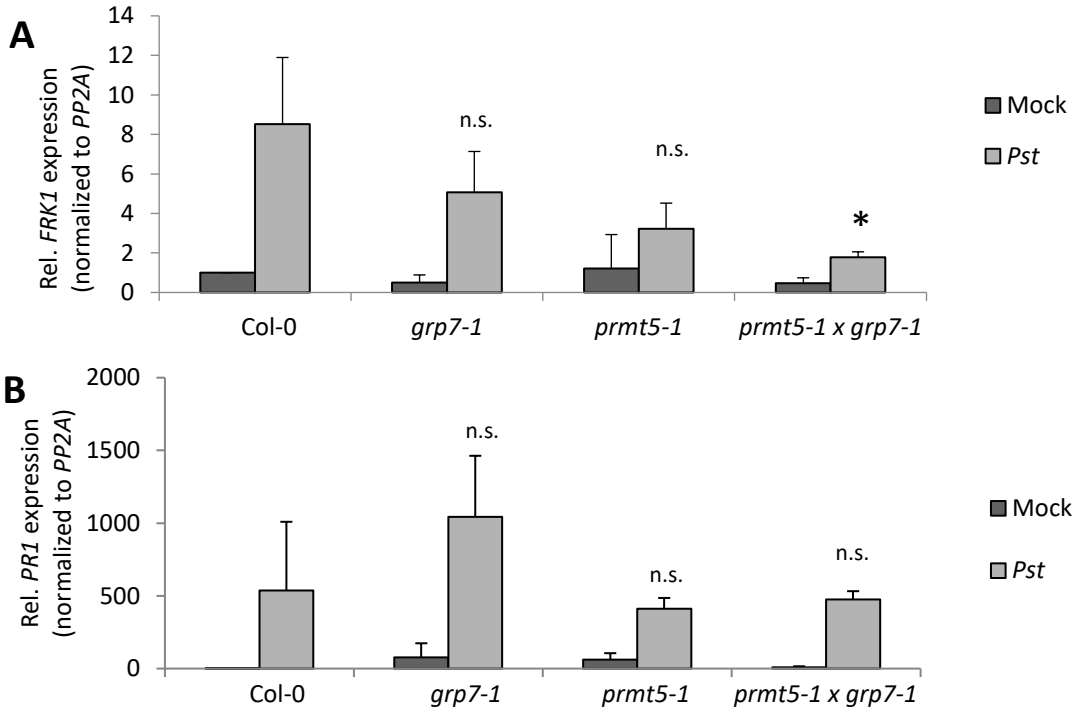

Figure 5.17 Relative transcript levels of *FRK1* and *PR1*. (**A**) The plant material was harvested 4 hours after infiltration (**B**) and 1 day after infiltration with bacterial solution (*Pst)* or magnesium chloride (mock). The expression level was measured by quantitative RT–qPCR and normalized to *PP2A* levels. The bar chart shows the mean expression based on three biological replicates for Col-0 and *prmt5-1* and two biological replicates for *grp7-1* and *prmt5-1 x grp7-1*. Each biological replicate consisted of two technical replicates each ± SD, compared to wild type. Statistical analysis was done with two-tailed Student's t test; * $p < 0{,}05$. n.s., not significant.

The presented results suggest that lack of GRP7 and PRMT5 negatively influence the pathogen response in *A. thaliana,* as manifested by lower *FRK1* expression in *grp7-1, prmt5-1* and *prmt5-1 x grp7-1,* compared to Col-0. In opposition to this stand the results of *PR1* expression level. Differences between Col-0 and mutants although not significant, suggest that GRP7 and PRMT5 could work in opposite direction, where GRP7 could be a negative regulator and PRMT5 positive regulator of plant immunity. Interestingly, the transcript levels of *FRK1* and *PR1* detected in *prmt5-1 x grp7-1* plants resemble *prmt5-1* pattern, rather than intermediate phenotype or expression levels observed in *grp7-1*. This suggests that *PRMT5* could be epistatic to *GRP7,* where both proteins would work in the same pathway for controlling plant defence transcriptome.

5.4. Analysis of the role of *At*GRP7 arginine methylation in the response to abiotic stress (salt stress)

5.4.1. Seeds germination under salt stress conditions

Multiple studies have shown that lack of PRMT5 leads to hypersensitivity to abiotic stresses (Hu et al., 2017; Zhang et al., 2011). The opposite effect has been described for the T-DNA mutant *grp7-1*, where the lack of GRP7 resulted in a higher resistance to salt stress in comparison to wild-type plants (Kim et al., 2008).
Furthermore, it has been reported that *prmt5* mutants show growth retardation in comparison to wild type (Pei et al., 2007). Indeed, grown on ½ MS medium, the *prmt5-1* and *prmt5-1 x grp7-1* seedlings were smaller in comparison to Col-0 or *grp7-1* (Figure 5.18). Interestingly, the double mutant *prmt5-1 x grp7-1* did not show the intermediate phenotype but the same as *prmt5-1,* suggesting an interaction of both proteins in the examined developmental stage. On the other hand, the complementation lines GRP7-GFP (*grp7-1),* GRP7^{R141A}-GFP (*grp7-1*) and GRP7^{R141K}-GFP did not differ form *grp7-1* (Figure 5.18).

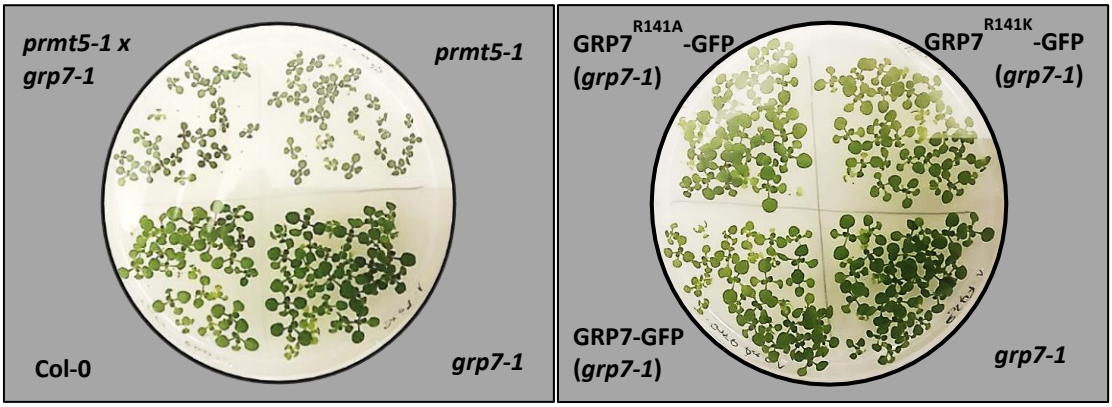

Figure 5.18 Growth retardation of *prmt5* seedlings. From each line, 30 sterilized seeds were plated on ½ MS plates. Plants were grown at 20°C under long day conditions (16 h light, 8 h dark). Pictures have been taken at day 14.

The pleiotropic phenotype of *prmt5* mutants, which is also observable in the double mutant *prmt5-1 x grp7-1,* suggests that *PRMT5* is epistatic to *GRP7*. However, the status of arginine methylation at the position 141 in GRP7 derived by PRMT5 seems to not have an influence on the growth process, while the lack of PRMT5 protein leads to strong changes in seedlings development.

To determine the functional role of GRP7 arginine methylation derived by PRMT5 under salt stress conditions, I investigated the seed germination rate and root length of Col-0, *grp7-1, prmt5-1* and *prmt5-1 x grp7-1*, as well as of GRP7-GFP (*grp7-1),* GRP7^{R141A}-GFP (*grp7-1*) and GRP7^{R141K}-GFP (*grp7-1*).

The salt concentrations were chosen based on previous experiments, conducted in our laboratory (Melina Martin, unpublished). The results showed that 150 mM and 200 mM NaCl affect germination in *grp7* and *grp8* mutants. However, 100 mM NaCl was not enough to display such differences between Col-0 and *grp7-1* (Melina Martin, unpublished). Therefore in this study, the germination rate was examined for seeds germinating on a control plate containing only ½ MS, as well as on ½ MS medium containing 150 and 200 mM NaCl (Figure 5.19). On each medium, 30 seeds of the indicated genotypes were plated. The presented results are obtained from three biological replicates, with three technical replicates each. The germination rate was calculated as a percentage of seeds germinated on the indicated day to the total number of germinated seeds.

The supplementation of ½ MS medium with NaCl salt decreased the germination rates for all lines and was inversely proportional to the increasing amount of salt. Under salt stress conditions, *grp7-1* seeds had significantly higher germination rates (90% in 150 mM NaCl and 84% in 200 mM NaCl at day 2) and *prmt5-1* seeds had significantly lower germination rates (45% and 25%) in comparison to the wild-type (56% and 42%). The seeds from the double mutant plants *prmt5-1 x grp7-1* exposed to salt stress germinated slower (27% and 27% at day 2) than the wild-type seeds and showed hypersensitivity to salt stress, like *prmt5-1* (Figure 5.19).

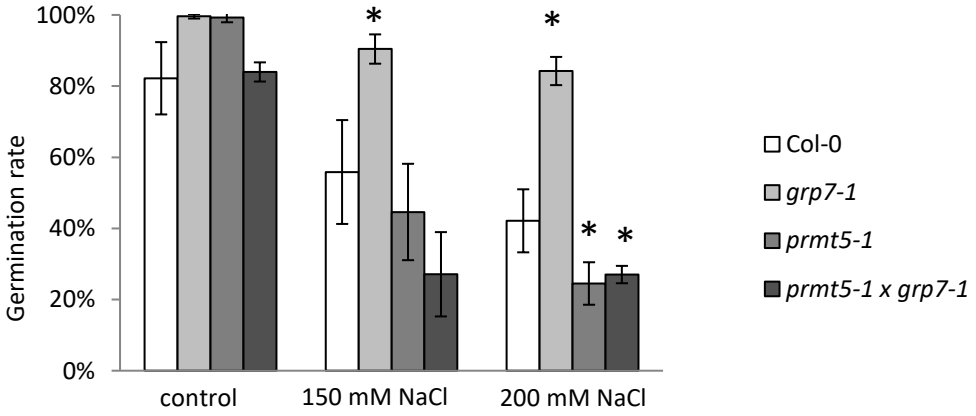

Figure 5.19 Germination rate of transgenic seeds exposed to salt stress. Germination rate was counted as a percentage of germinated seeds at day 2 to the total number of germinated seeds after 14 days. Error bars indicate SD of three biological replicates with thee technical replicates each with 30 seeds plated per line; two-tailed Student's test; *p < 0,05.

On the control plates, 80-100% seeds of Col-0, *grp7-1, prmt5-1* and *prmt5-1 x grp7-1* germinated on day 2. On the same day, seeds exposed to salt stress conditions (150 and 200 mM NaCl), showed the biggest differences in the germination rate between indicated lines (Figure 5.20).

The germination process was slowed down under salt stress conditions, proportionally to applied salt concentration. The supplementation with 150 mM and 200 mM NaCl caused that 80-100% seeds germinated on day 3 and 4, respectively (Figure 5.20).

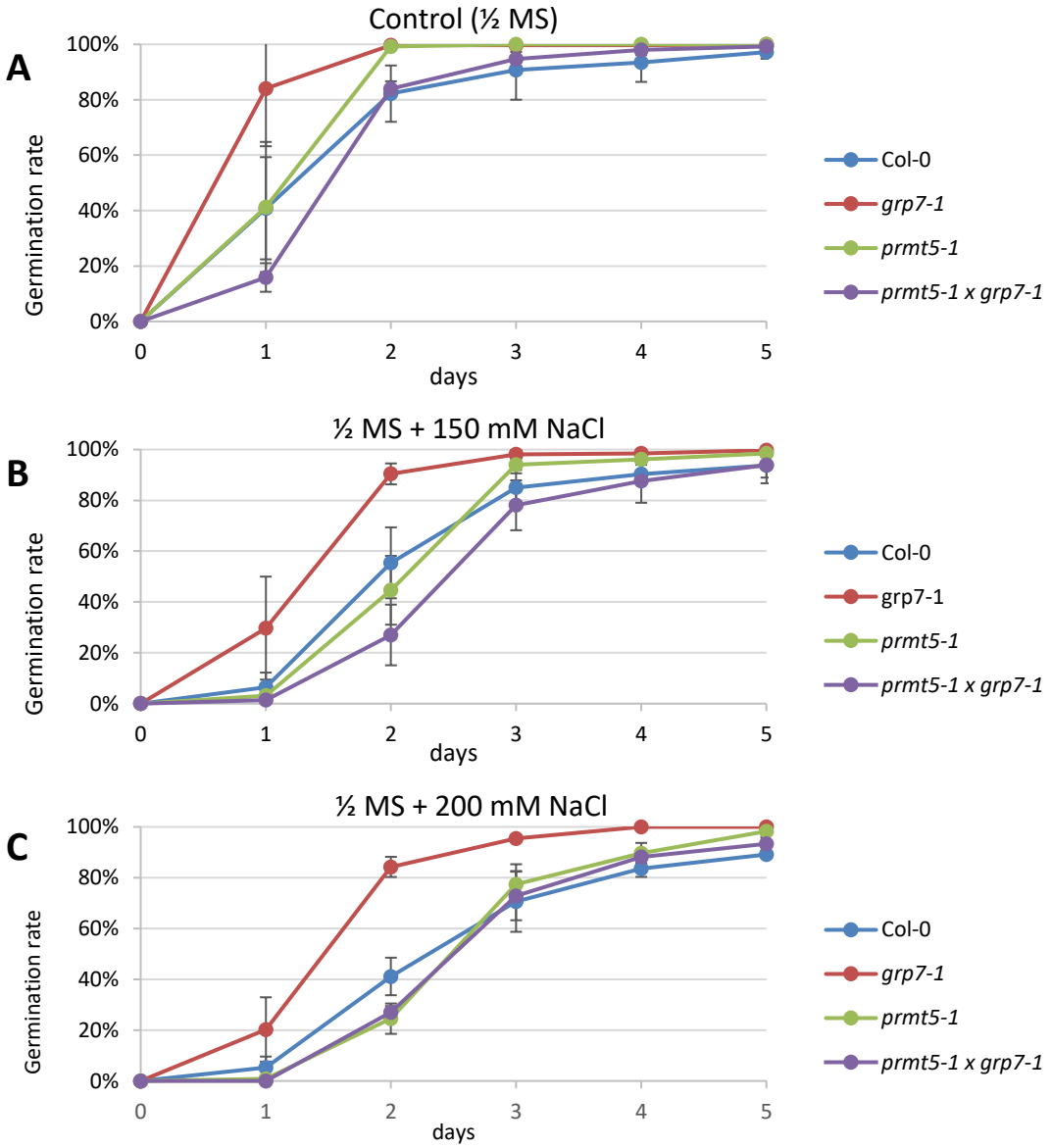

Figure 5.20 The impact of GRP7 and PRMT5 on the seed germination process under control and salt stress conditions. The germination was tested on (**A**) control plates ½ MS, as well as ½ MS medium supplemented with (**B**) 150 mM NaCl and (**C**) 200 mM NaCl. The germination rate was calculated as a percentage of germinated seeds at the indicated day to the total number of germinated seeds after 14 days. Error bars indicate SD of three biological replicates with thee technical replicates each with 30 seeds plated per line.

Seeds from all genotypes that germinated on control plates generated roots and shoots with green cotyledons and leaves. On the contrary, after 14 days all seed germinated

on ½ MS medium supplemented with 150 or 200 mM NaCl had suppressed growth and never developed a proper root system or leaves (Figure 5.21).

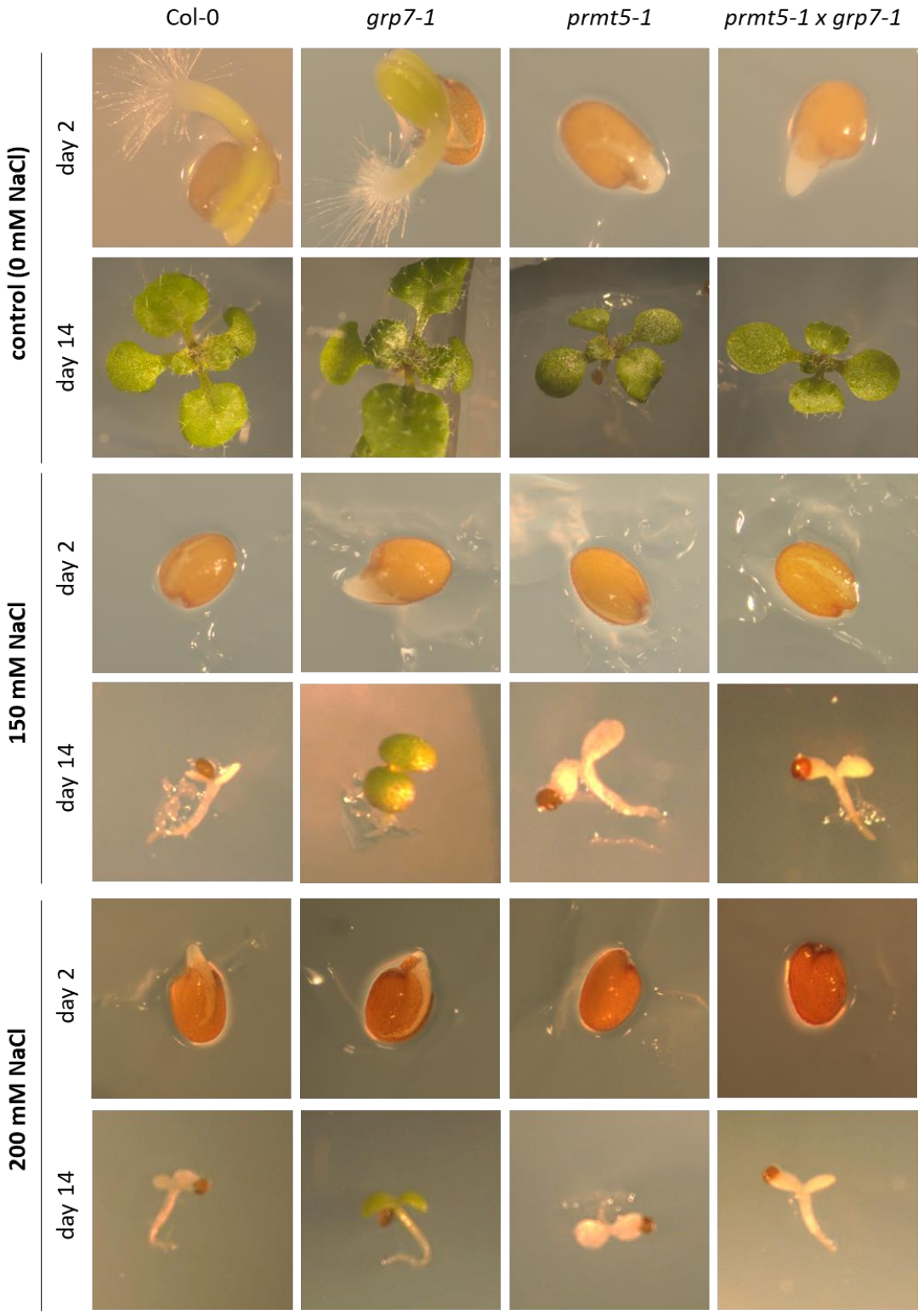

Figure 5.21 The phenotypic analysis of transgenic seeds germinating under salt stress conditions. Seeds from indicated lines were plated on ½ MS medium

(control) and medium supplemented with 150 mM or 200 mM NaCl. Pictures were taken at day 2 and 14.

By comparison, GRP7-GFP (*grp7-1),* GRP7^{R141A}-GFP (*grp7-1*) and GRP7^{R141K}-GFP (*grp7-1*) lines had lower germination rates than *grp7-1* (Figure 5.22). Although germination rates of seeds plated on ½ MS with 150 mM NaCl were not statistically different, a growth on 200 mM NaCl revealed significant differences in germination rates between *grp7-1* and complementation lines. Seeds of GRP7-GFP (*grp7-1*), germinating on plates supplemented with 150 mM or 200 mM NaCl, showed similar germination rates (62%; 48%) to GRP7^{R141A}-GFP (*grp7-1*) (67%; 42%) and GRP7^{R141K}-GFP (*grp7-1*) (77% and 59%).

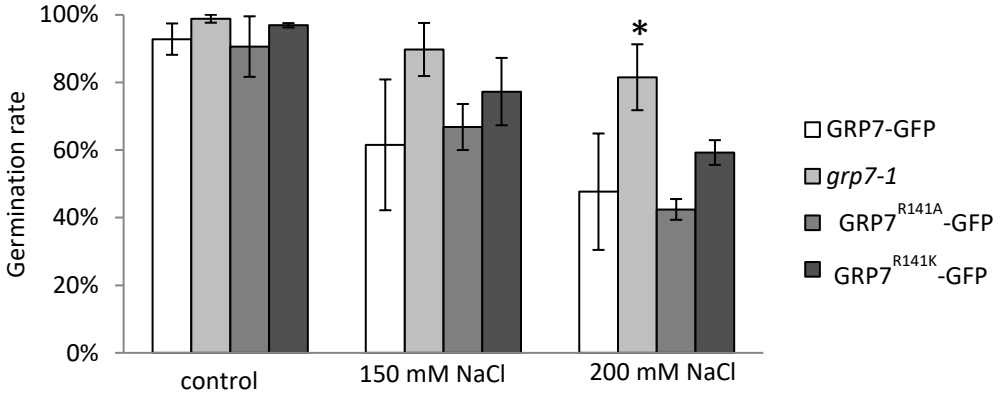

Figure 5.22 Germination rate of transgenic seeds exposed to salt stress. Germination rate was counted as a percentage of germinated seeds at day 2 to the total number of germinated seeds after 14 days. Error bars indicate SD of three biological replicates with thee technical replicates each with 30 seeds plated per line; two-tailed Student's test; *p < 0,05; **p < 0,01.

On the control plates, almost all seeds of GRP7-GFP (*grp7-1),* GRP7^{R141A}-GFP (*grp7-1*) and GRP7^{R141K}-GFP (*grp7-1*) lines germinated on day 2. Under salt stress conditions (150 and 200 mM NaCl) on day 2, seeds showed the biggest differences in the germination rate between indicated lines (Figure 5.23).

Similarly to the first germination assay, slower germination under salt stress conditions was observed (Figure 5.23). On the plates with 150 mM and 200 mM NaCl, 80-100% seeds germinated on day 3 and 4, respectively.

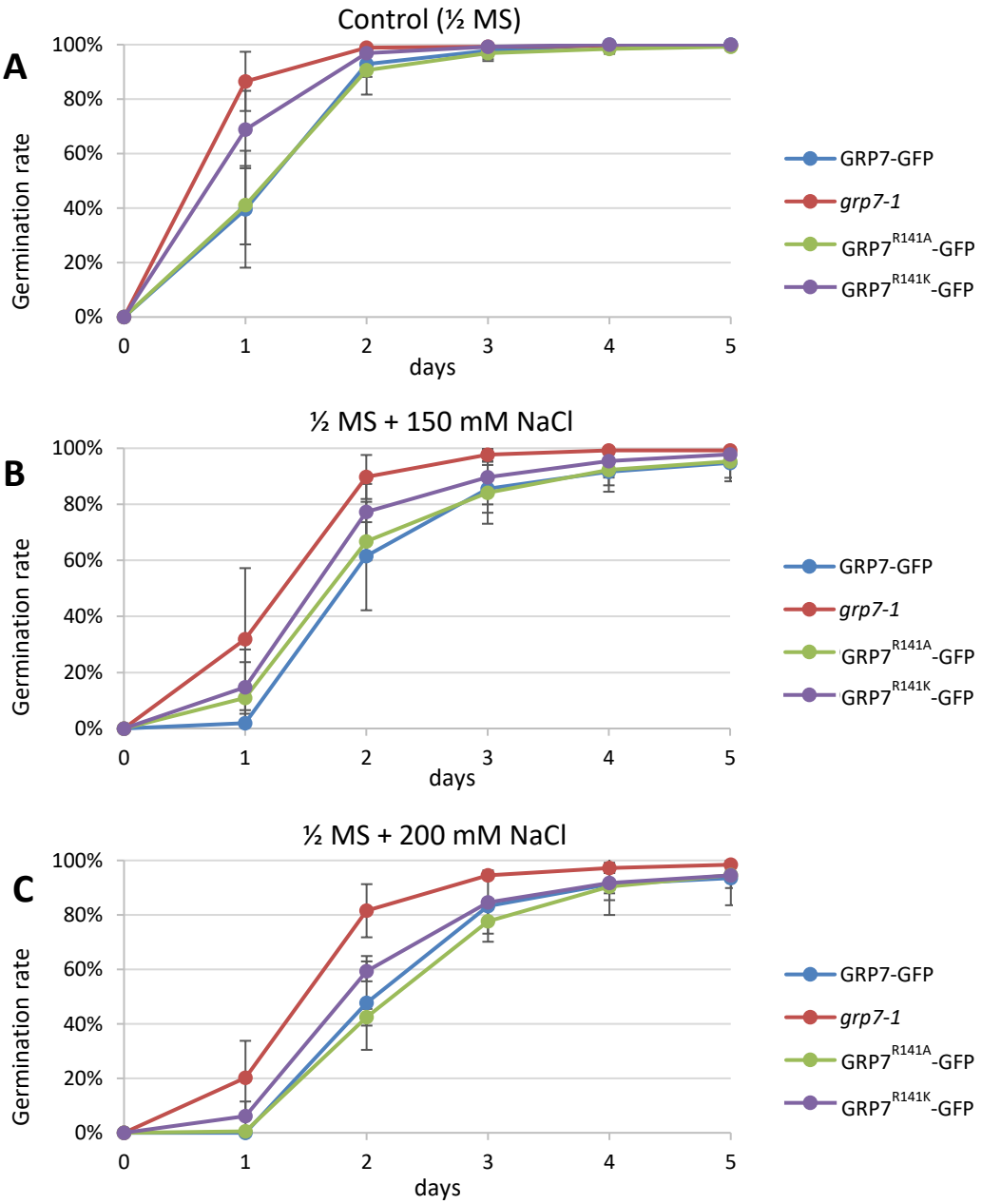

Figure 5.23 The impact of arginine 141 in GRP7 on the seed germination process under control and salt stress conditions. The germination was tested on (**A**) control plates ½ MS, as well as ½ MS medium supplemented with (**B**) 150 mM NaCl and (**C**) 200 mM NaCl. The germination rate was calculated as a percentage of germinated seeds at the indicated day to the total number of germinated seeds after 14 days. Error bars indicate SD of three biological replicates with thee technical replicates each with 30 seeds plated per line.

In conclusion, based on the experiments described above, methylation of arginine 141 in GRP7 does not affect the germination process. However, the lack of methyltransferase PRMT5 delays the germination process, therefore less *prmt5-1* seeds germinated on day 2, in comparison to Col-0. An important result brought the analysis

of *prmt5-1 x grp7-1*. The double mutant did not show the intermediate phenotype but displayed the phenotype of the single mutant *prmt5-1,* suggesting that *PRMT5* is epistatic to *GRP7*.

5.4.2. Primary root length under salt stress conditions

It has been previously shown that application of 100 mM NaCl allows for evaluating the impact of salt stress on a root growth in *grp7-1* and *prmt5-1* (Cao et al., 2006; Hu et al., 2017). Therefore, to assess the influence of salt stress on the root length of the GRP7 arginine methylation mutants, 4-day-old seedlings, grown on ½ MS medium, were transferred to ½ MS vertical plates with or without 100 mM NaCl and cultured for an additional 7 days.

The primary root lengths of wild-type (Col-0) and *grp7-1* seedlings grown on control plates (without NaCl supplementation) did not differ from each other (5,8 cm and 5,7 cm, respectively). However, both *prmt5-1* and *prmt5-1 x grp7-1* lines showed shorter primary roots on the control plates (3,1 cm and 3,2 cm, respectively) in comparison to the wild-type and *grp7-1*. Under salt stress conditions, the primary root length decreased for all lines. Furthermore, the primary roots of *prmt5-1* and *prmt5-1 x grp7-1* grown on medium with 100 mM NaCl were significantly shorter (1,2 cm and 1,3 cm) than the roots of wild-type and *grp7-1* (2,8 cm and 2,9 cm) (Figure 5.24). The length of the primary roots of wild type and *grp7-1* seedlings was reduced by about half (48% and 51%, respectively) under salt stress conditions compared to control plates. However, the primary roots of *prmt5-1* and *prmt5-1 x grp7-1* under salt stress conditions grown only up to 39% and 41% of the root length on control plates. The 10% difference in the primary root length, resulting from PRMT5 absence suggests that PRMT5 is required in cellular processes involved in response to salt stress.

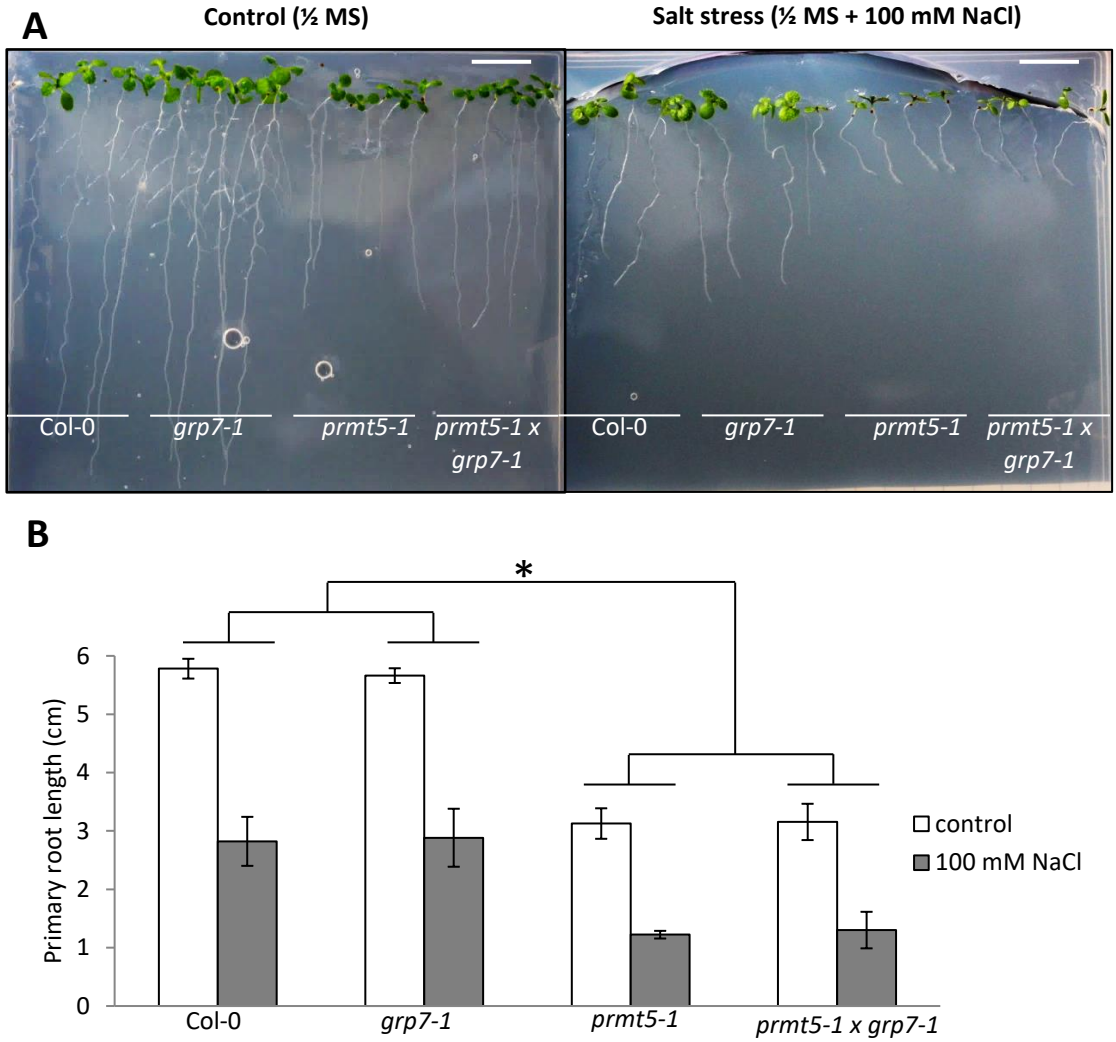

Figure 5.24 Primary root length in transgenic seedlings grown under salt stress conditions. (**A**) Germinated on ½ MS medium, 4-day-old seedlings were transferred on vertical plates with or without 100 mM NaCl and grown for another 7 days. Pictures were taken at day 11. Scale bar indicates 1 cm. (**B**) Root length was measured using the public domain software ImageJ (http://rsb.info.nih.gov/ij). The column chart shows the mean from three biological replicates with three technical replicates each ± SD. Statistical analysis was done with two-tailed Student's *t* test; *p < 0,05.

The primary root length did not differ between *grp7-1* and the complementation lines GRP7-GFP (*grp7-1)*, GRP7^{R141A}-GFP (*grp7-1*) and GRP7^{R141K}-GFP (*grp7-1*) under control conditions, as well as under high salinity. The reductions in root lengths under salt stress conditions were not significantly different between indicated lines (Figure 5.25). The results suggest that GRP7 does not have an impact on the primary root growth under normal and salt stress conditions.

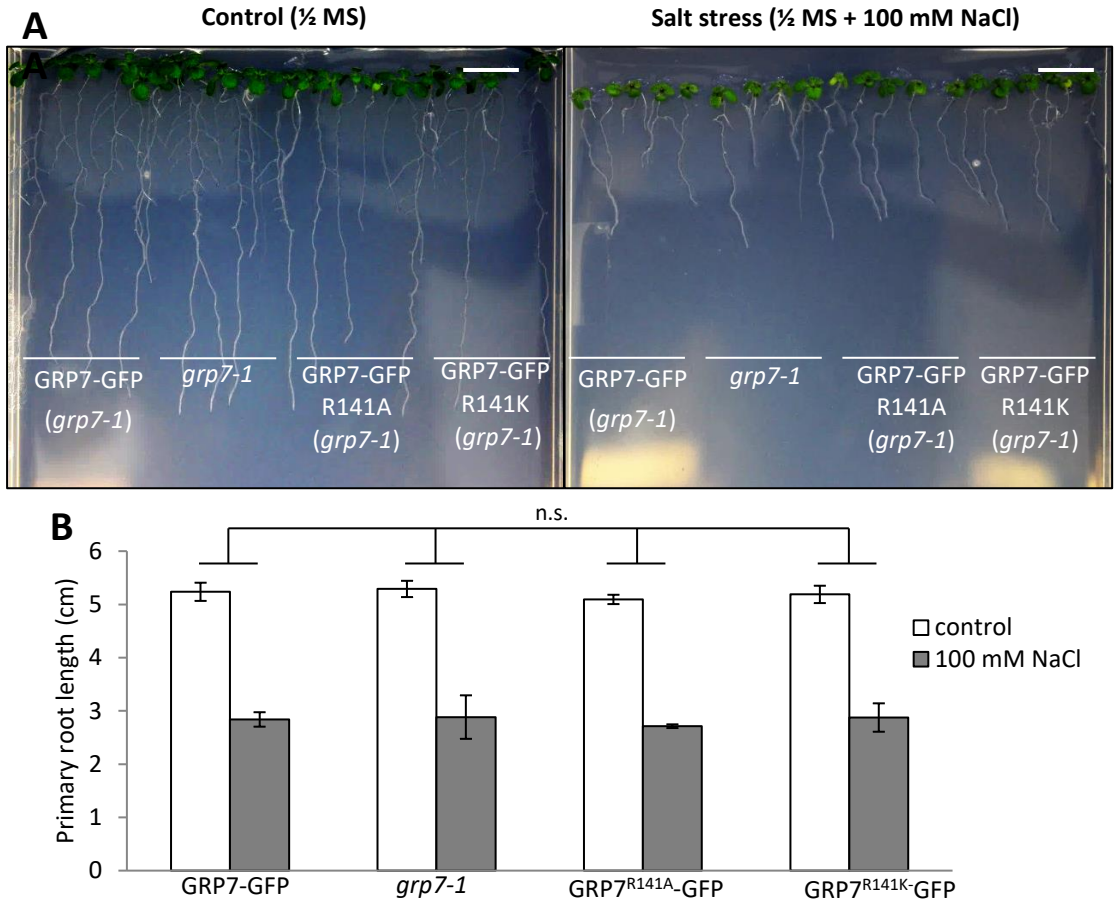

Figure 5.25 Primary root length in transgenic seedlings grown under salt stress conditions. (**A**) Germinated on ½ MS medium, 4-day-old seedlings were transferred on vertical plates with or without 100 mM NaCl and grown for another 7 days. Pictures were taken at day 11. Scale bar indicates 1 cm. (**B**) Root length was measured using the public domain software ImageJ (http://rsb.info.nih.gov/ij). The column chart shows the mean from three biological replicates with three technical replicates each ± SD. Statistical analysis was done with two-tailed Student's *t* test; n.s., not significant.

The analysis of the primary root length showed that the different GRP7 arginine methylation mutants GRP7^{R141A}-GFP (*grp7-1*) and GRP7^{R141K}-GFP (*grp7-1*) exhibited the same phenotype as GRP7-GFP (*grp7-1*) and *grp7-1* plants under control and salt stress conditions. Therefore, it can be concluded that GRP7 does not affect the primary root length. On the other hand, the results of germination rate under salt stress conditions suggest that GRP7 can be a negative regulator of the germination process, when seeds are exposed to a high salinity. The germination rate analysis also showed that methylation status at arginine 141 in GRP7 does not affect germination under control or salt stress conditions.

In contrast, less seeds of *prmt5-1* and *prmt5-1 x grp7-1* than Col-0 and *grp7-1* germinated on day 2 under salt stress conditions, suggesting that the germination process was slowed down in the mutants that lack functional PRMT5 protein. Although

grp7-1 seeds germinated faster than seeds from all other analysed lines in control and salt stress conditions, the effect of GRP7 absence is masked by the lack of PRMT5 protein in the double mutant *prmt5 x grp7-1*. On the other hand, seedlings of *prmt5-1* and *prmt5-1 x grp7-1* exhibited shorter roots than Col-0 and *grp7-1*, suggesting a role of PRMT5 in a root system development under control and salt stress conditions. This implies that both proteins have rather opposite functions for the regulation of salt tolerance at different developmental stages. Due to the fact that in the germination assay *prmt5-1 x grp7-1* mutant showed the phenotype of *prmt5-1*, it can be hypothesized that GRP7 acts down-stream of PRMT5. However, it seems that arginine methylation of GRP7 by PRMT5 does not influence any of the tested processes.

5.5. Alternatively spliced transcripts regulated by *At*GRP7 and *At*PRMT5

It has been shown that both GRP7 and PRMT5 play important roles in pre-mRNA splicing. Due to the fact that GRP7 and GRP8 were identified as targets for PRMT5, my aim was to examine the possible influence of the interaction between GRP7/GRP8 and PRMT5 on alternative splicing (AS).

To identify AS events, which are affected by GRP7 and PRMT5, I used two datasets obtained through the high-resolution RT-PCR AS panels (Sanchez et al., 2010; Streitner et al., 2012). A study published in 2010 identified 44 splicing events, which were significantly different between *prmt5* mutants and wild type (Sanchez et al., 2010). On the other hand, 17 splicing events were identified to be significantly different between *grp7-1* 8i mutant and wild type (Streitner et al., 2012).

The RNA-sequencing datasets for *prmt5* and *grp7-1* 8i mutants were compared to identify transcript isoforms that were significantly different between the mutants and the corresponding wild types, respectively (Figure 5.26).

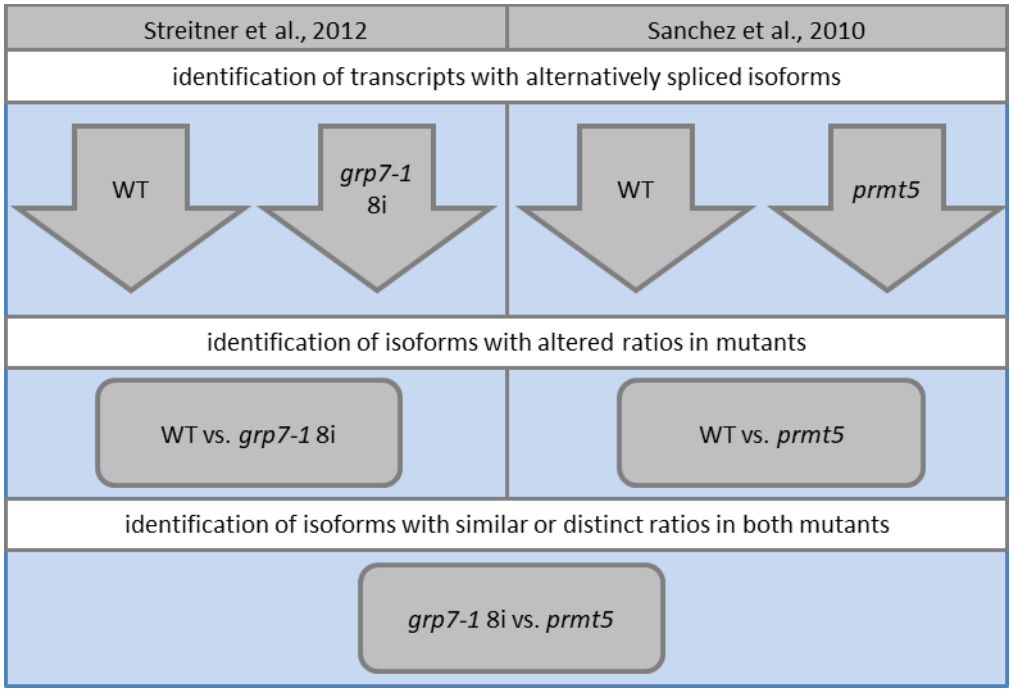

Figure 5.26 Scheme of data analysis steps. Data obtained through high-resolution RT-PCR AS panels for *prmt5* and *grp7-1* 8i was analysed to identify the alternatively spliced events common and distinct in *prmt5* and *grp7-1* 8i mutants, as well as significantly different from respective wild type controls.

Through the comparison of significantly altered events in *prmt5* and *grp7-1* 8i, four splicing events were found to be common for both mutants (Figure 5.27), which were used as candidates for being regulated by GRP7 arginine methylation.

Among 17 AS events, which were significantly different between *grp7-1* 8i and corresponding wild type, 13 AS events were not identified in the set of AS events in *prmt5* mutant. On the other hand, 40 out of 44 AS events were classified as exclusively appearing in *prmt5* mutant (Figure 5.27).

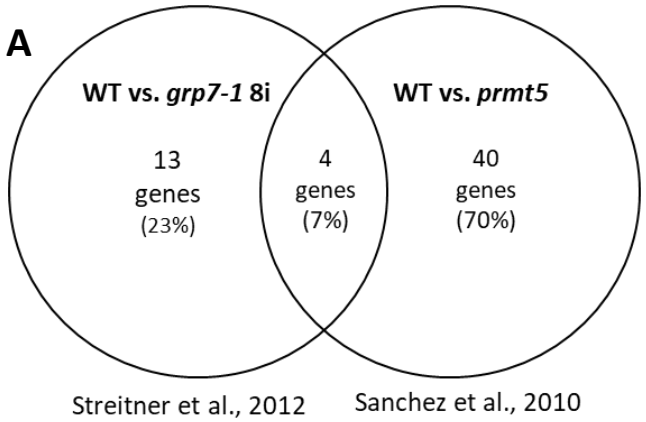

B

AGI	Gene	Splicing event
AT3G29160	*AKIN11*	Alt. 5'ss
AT5G05550	*VFP5*	ES
AT3G12570	*FYD*	Alt. 3'ss
AT4G24740	*FC2*	ES

Figure 5.27 Alternatively spliced events in *prmt5* and *grp7-1* 8i. (**A**) Overlap between two RNA-sequencing datasets for *prmt5* and *grp7-1* 8i mutants; (**B**) AS events common for *prmt5* and *grp7-1* 8i.

The four selected AS events were identified in the transcripts of *FYD, AFC2 (Arabidopsis FUS3-COMPLEMENTING GENE 2), VFP5 (VirF-INTERACTING PROTEIN 5)* and *AKIN11* (*Arabidopsis SNF1 KINASE HOMOLOG 11*). Interestingly, the *in vivo* analysis done by Streitner and co-workers (2012), showed that the *FYD, VFP5* and *AKIN11* transcripts are potential direct targets of GRP7. Moreover, AS of *AFC2* requires GRP7 RNA-binding activity but *AFC2* does not seem to be a direct target of GRP7 (Streitner et al., 2012).
The use of an alternative 3'ss within the second intron of the *FYD* 5'UTR region yields a transcript with a 29 bp longer 5'UTR, in comparison to the transcript resulting from the constitutive 3'ss. According to the data from Streitner et al., 2012 and Sanchez et al., 2010, the amount of the longer *FYD* transcript decreases (-10%) in *prm5-5* mutants and increases (+10%) in *grp7-1* 8i mutants, in comparison to respective wild types (Table 5.1). *AFC2,* which encodes a LAMMER-type protein kinase, was analysed for skipping of exons 5 and 6, leading to a PTC. The lack of PRMT5 results in higher levels (+16%) of the shorter *AFC2* transcripts without exons 5 and 6. In contrast, a reduced number (-11%) of exon 5 and exon 6 skipping events was found in *grp7-1* 8i lines. Another exon skipping event was analysed for *VPF5* transcripts, encoding a transcription factor. Skipping of exon 2 in *VFP5* takes place more often (+33%) in *prmt5-5* than in wild type and it is less frequent (-15%) in *grp7-1* 8i, when compared to the wild type. Finally, the fourth selected splicing event is the usage of an alternative 5'ss within the first intron in the *AKIN11* 5'UTR region, yielding a transcript that is 148 bp longer. The number of longer transcripts increases (+18%) in *prmt5-5* and decreases (-27%) in *grp7-1* 8i.

Table 5.1 Four AS events selected for *prmt5-5* and *grp7-1* 8i mutants. Data from Streitner et al., 2012 and Sanchez et al., 2010.

Gene	Splicing event	Isoforms	Sanchez et al., 2010		Streitner et al., 2012	
			Ratio in wild type	Ratio in *prmt5-5*	Ratio in wild type	Ratio in *grp7-1* 8i
FYD	Alt. 3'ss	159 bp / 188 bp	40% / 60%	51% / 49%	43% / 57%	33% / 67%
				+11%		-10%
AFC2	ES	143 bp / 309 bp	17% / 83%	33% / 67%	19% / 81%	7% / 93%
				+16%		-12%
VFP5	ES	210 bp / 308 bp	63% / 37%	96% / 4%	64% / 36%	50% / 50%
				+33%		-14%
AKIN11	Alt. 5'ss	159 bp / 307 bp	28% / 72%	10% / 90%	30% / 70%	57% / 43%
				-18%		+27%

5.5.1. Analysis of alternative splicing

Data obtained through the comparison of alternative splicing defects in *prmt5-5* and *grp7-1* 8i was used for further analyses to investigate the interaction between PRMT5 and GRP7/GRP8 proteins. Genetic epistasis was tested with *prmt5 x grp7-1* and *prmt5* x *grp7-1* 8i mutants based on the ratios of alternatively spliced isoforms from *AKIN11* and *VFP5* genes (Figure 5.28.A).

Due to the fact that *AKIN11* and *VFP5* showed the biggest changes in isoform ratios in *grp7-1, prmt5-1* and respective wild types, these two genes were analysed first. *FYD* and *AFC2* encode 4 and 10 different transcripts, respectively and the analysis of splicing event in *FYD* requires detection of isoforms, which differ 29 bp in length. Moreover, the ~10% differences in ratios were difficult to assess on gel pictures. Therefore, data presented in this chapter was limited to *AKIN11* and *VFP5*.

The proteins PRMT5, GRP7 and/or GRP8 could influence alternative splicing independently from each other or collectively in one pathway, which would result in an additive effect or an individual pattern, where the effect of one gene could be masked by the other. The independent effects of *prm5-5* and *grp7-1* 8i mutants are known from the high-resolution RT-PCR AS panels (Sanchez et al., 2010; Streitner et al., 2012). To predict the additive effect in *prmt5-5 x grp7-1* 8i, the calculated changes in *prmt5-5* and *grp7-1* 8i were added together for corresponding isoforms (Figure 5.28.B).

A

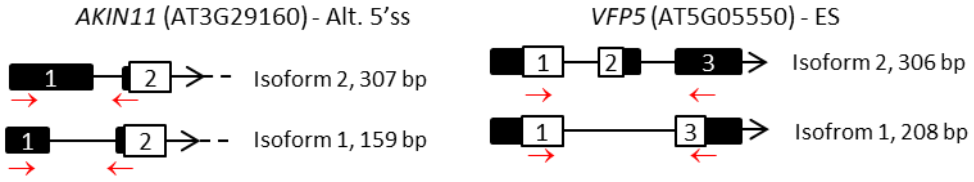

B

AKIN11	Streitner et al., 2012		Sanchez et al., 2010		Predictions of the additive effect
	WT	*grp7-1* 8i	WT	*prmt5-5*	*prmt5-5 x grp7-1* 8i
Isoform 1, 159 bp	30%	57%	28%	10%	~ 40%
Isoform 2, 307 bp	70%	43%	72%	90%	~ 60%
	Isoform 1 (+27%) Isoform 2 (-27%)		Isoform 1 (-18%) Isoform 2 (+18%)		Isoform 1 (+9%) Isoform 2 (-9%)

VFP5	Streitner et al., 2012		Sanchez et al., 2010		Predictions of the additive effect
	WT	*grp7-1* 8i	WT	*prmt5-5*	*prmt5-5 x grp7-1* 8i
Isoform 1, 208 bp	64%	50%	63%	96%	~ 80%
Isoform 2, 306 bp	36%	50%	37%	4%	~ 20%
	Isoform 1 (-14%) Isoform 2 (+14%)		Isoform 1 (+33%) Isoform 2 (-33%)		Isoform 1 (+19%) Isoform 2 (-19%)

Figure 5.28 Analysed splicing events for *AKIN11* and *VFP5*. (**A**) Schematic representation of analysed isoforms with alternative 5' splice site in *AKIN11* and exon skipping in *VFP5*. Red arrows indicate primers used in sqPCR. White boxes display codding regions and the black boxes show the 5' and 3' untranslated regions. Lines indicate introns and the black arrows show the reverse orientations of *AKIN11* and *VFP5*;(**B**) Prediction of the additive effect in *prmt5-5 x grp7-1* 8i mutant, based on the alternative splicing results from *prmt5-5* (Sanchez et al., 2010) and *grp7-1* 8i (Streitner et al., 2012).

Validation of the splicing panel data was performed by sqPCR. 16-day-old seedlings from indicated plant lines were used as a plant material (details in 4.10) and the synthesised cDNAs were used in sqPCR for amplification of *AKIN11* and *VFP5* transcripts (Figure 5.29).

In accordance with published data (Sanchez et al., 2010; Streitner et al., 2012), the usage of an alternative 5'ss within the first intron in the *AKIN11* 5'UTR region, giving a longer transcript, was more abundant in wild type (Col-0) (83%) than in *grp7-1* or *grp7-1* 8i (56% and 62%, respectively) (Figure 5.29). The lack of functional PRMT5 in *prmt5-1* and *prmt5-5* was correlated with the predominant choice of the alternative 5'ss in the first intron (89% and 85%). However, in contrast to the predicted additive effects, the isoform ratio detected in the double mutants mostly resembled the isoform ratio observed in the *prmt5* single mutants. The longer splicing variants, containing a fragment of the first intron, were predominant in *prmt5-1 x grp7-1, prmt5-1 x grp7-1*

8i, *prmt5-5 x grp7-1* and *prmt5-5 x grp7-1* 8i (77%, 95%, 88% and 86%, respectively) (Figure 5.29).

According to data from Streitner et. al., 2012, skipping of exon 2 in *VFP5* was expected to occur less often in *grp7-1* 8i mutants than in wild type. However, no significant differences between wild type, *grp7-1* and *grp7-1* 8i were observed (35%, 36% and 39%, respectively). On the other hand, almost complete exon 2 skipping was expected for single *prmt5* mutants based on Sanchez et. al., 2010. This was indeed observed in *prmt5-1* and *prmt5-5* mutants, where the isoform ratio shifted in favour of the shorter isoform (94% and 92%) in comparison to wild type (35%). Analysis of the isoform ratio in the double mutants again did not bring the predicted additive effects but displayed the pattern detected in *prmt5* single mutants. Skipping of exon 2 in *VFP5* occurred in preponderant number in *prmt5-1 x grp7-1, prmt5-1 x grp7-1* 8i, *prmt5-5 x grp7-1* and *prmt5-5 x grp7-1* 8i (89%, 92%, 91% and 91%, respectively) (Figure 5.29).

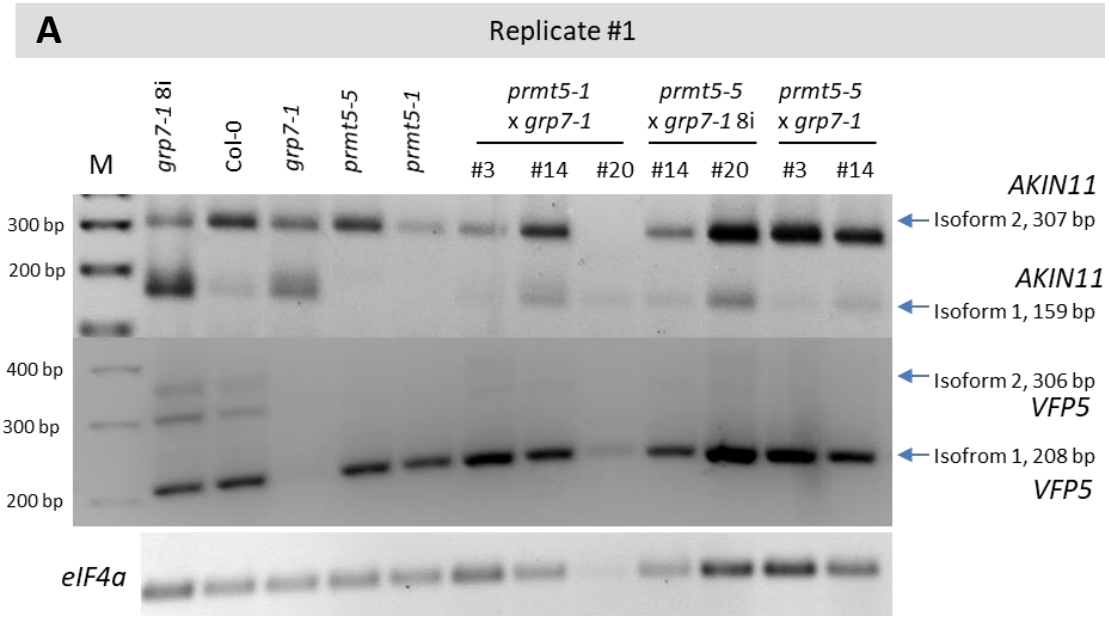

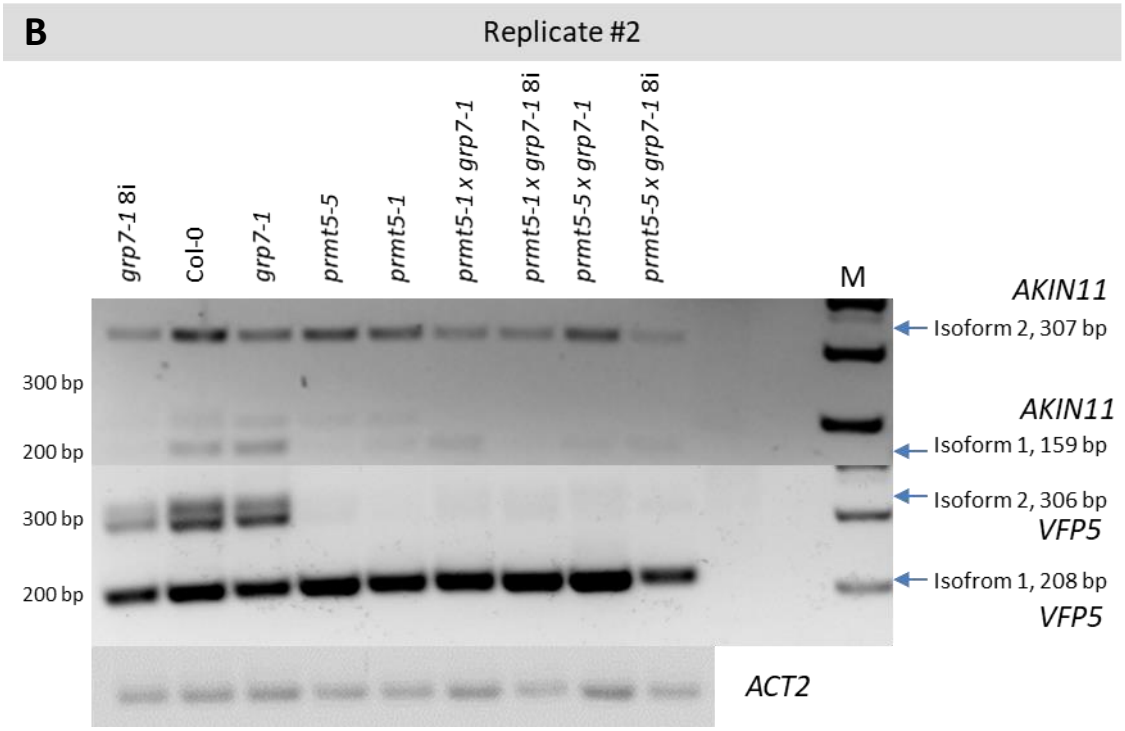
B
Replicate #2
grp7-1 8i
Col-0
grp7-1
prmt5-5
prmt5-1
prmt5-1 x grp7-1
prmt5-1 x grp7-1 8i
prmt5-5 x grp7-1
prmt5-5 x grp7-1 8i
M
AKIN11
Isoform 2, 307 bp
AKIN11
Isoform 1, 159 bp
Isoform 2, 306 bp
VFP5
Isofrom 1, 208 bp
VFP5
300 bp
200 bp
300 bp
200 bp
ACT2

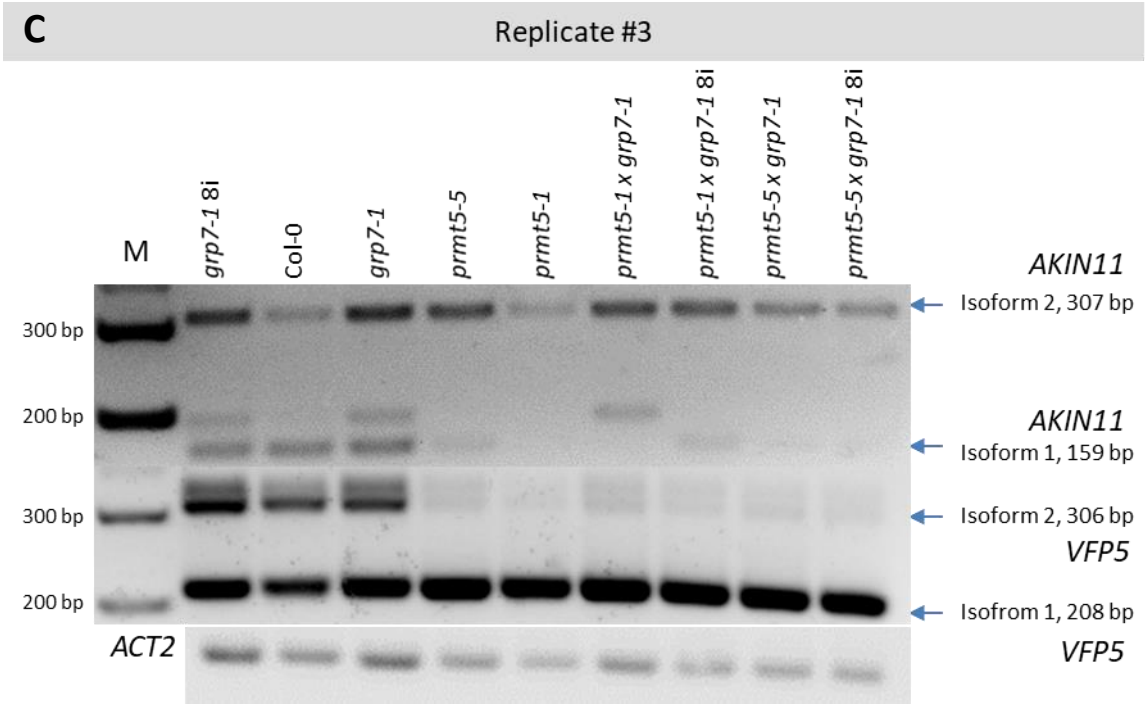
C
Replicate #3
M
grp7-1 8i
Col-0
grp7-1
prmt5-5
prmt5-1
prmt5-1 x grp7-1
prmt5-1 x grp7-1 8i
prmt5-5 x grp7-1
prmt5-5 x grp7-1 8i
AKIN11
Isoform 2, 307 bp
AKIN11
Isoform 1, 159 bp
Isoform 2, 306 bp
VFP5
Isofrom 1, 208 bp
VFP5
300 bp
200 bp
300 bp
200 bp
ACT2

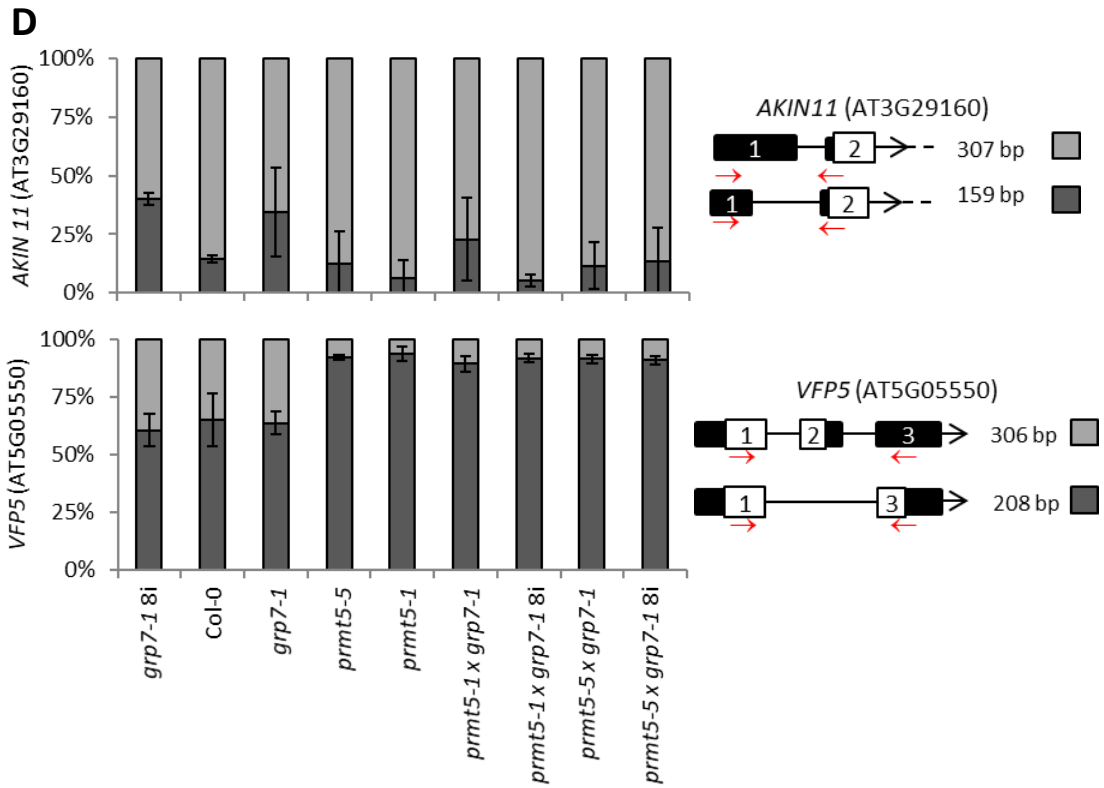

Figure 5.29 Effect of GRP7, GRP8 and PRMT5 on alternative splicing of *AKIN11* and *VFP5*. (**A, B, C**) RNA was isolated from 16-day-old seedlings and reverse transcribed. Synthesised cDNA was used in sqPCR for amplification of *AKIN11* and *VFP5* transcripts. M - 100 bp marker. Pictures **A, B** and **C** represent three biological replicates (for uncropped pictures see Figure A. 7 and Figure A. 8). (**D**) The signal intensities were measured using public domain software ImageJ (http://rsb.info.nih.gov/ij). Data was collected from three biological replicates (± SD).

The results obtained for *AKIN11* and *VFP5* show that the double mutants *prmt5 x grp7-1* and *prmt5 x grp7-1* 8i, and the single mutants *prmt5-5* and *prmt5-1* preferentially exhibit similar ratios of alternatively spliced variants. Although *AKIN11* and *VFP5* transcripts are direct targets of GRP7, PRMT5 seems to have a greater influence on their pre-mRNA splicing. The fact that the double mutants do not show the predicted intermediate effect, suggests that *PRMT5* and *GRP7* function in one pathway, where *PRMT5* is epistatic to *GRP7*.

5.5.2. Analysis of alternative splicing under salt stress conditions

To investigate the role of arginine methylation in GRP7 in AS under salt stress conditions, transgenic seedlings were exposed to high salinity and transcript ratios of selected genes were analysed.

The experiment consisted of three experimental groups. The influence of arginine methylation on AS under salt stress conditions was examined with two sets Col-0, *grp7-*

1, prmt5-1, prmt5-1 x grp7-1 and Col-0, *grp7* 8i, *prmt5-5*, *prmt5-5 x grp7-1* 8i. The changes in AS resulting from arginine methylation in GRP7 under salt stress were analysed with the third set GRP7-GFP, *grp7-1,* $GRP7^{R141A}$-GFP and $GRP7^{R141K}$-GFP. The 11-day-old seedlings were transferred on ½ MS plates with or without 200 mM NaCl for 6 h and then the aerial parts were harvested and used for RNA isolation. Reverse transcribed cDNA samples were used in sqPCR. The signal intensities were measured using the public domain software ImageJ (details in 4.9.3).

An alternative 5' splice site (alt. 5' ss) in *AKIN11* and an exon skipping event in *VFP5,* which have been previously described (chapter 5.5.1), were tested in seedlings exposed to salt stress conditions. The third analysed event was intron 1 retention in the *FLK* mRNA.
It has been shown that the total *FLK* transcript level increases in *atprmt5* mutants (Pei et al., 2007). However, the upregulated transcript level of *FLK* is a sum of a decreased transcript level of the constitutively spliced isoform and an increased level of *FLK* transcripts with retained intron 1. The alternatively spliced variant of *FLK* is not able to downregulate the *FLC* transcript level and therefore negatively influences flowering (Deng et al., 2010). Moreover, it was shown by a genome wide association study (GWAS) that *FLK* is possibly involved in salinity tolerance (Julkowska et al., 2016).

Alternative splicing under salt stress conditions in *prmt5-1 x grp7-1*

The first analysed AS event was intron 1 retention in *FLK*. In Col-0 and *grp7-1,* intron 1 is removed from pre-mRNA by splicing. Only 8% and 9% of *FLK* transcripts contained the intron 1 in Col-0 and *grp7-1,* respectively. However, a lack of PRMT5 in *prmt5-1* and *prmt5-1 x grp7-1* increased number of IR, where 17% and 13% of *FLK* transcripts included intron 1 (Figure 5.30). Under salt stress conditions, the amount of IR in Col-0 and *grp7-1* the same, while the amount of IR event increased +9% and +8% in *prmt5-1* and *prmt5-1 x grp7-1* in comparison to the control (Figure 5.30).
The second analysed AS event was the usage of an alternative 5'ss within the first intron in the *AKIN11* 5'UTR region. In Col-0, the alternative 5'ss was found in 51% of *AKIN11* transcripts. The longer isoform with alternative 5'ss was less abundant in *grp7-1* (38%). On the other hand, *prmt5-1* and *prmt5-1 x grp7-1* were characterised by high levels of isoforms with alternative 5'ss (85% and 81%, respectively). Under salt stress conditions, the ratio of *AKIN11* isoforms shifted in favor of the alternative 5'ss in all lines. However, the amount of the longer isoform increased about two times more in Col-0 and *grp7-1* (+19% and +20%), than in *prmt5-1* and *prmt5-1 x grp7-1* (+11% and +12%) (Figure 5.30).
The last analysed AS event was the skipping of exon 2 in *VFP5*. In Col-0 and *grp7-1,* exon 2 was included in 41% and 38% of *VFP5* transcripts. In contrast, exon 2 was

skipped in almost all *VFP5* transcripts in *prmt5-1* and *prmt5-1 x grp7-1* (98% and 97%, respectively). In Col-0 and *grp7-1* seedlings exposed to salt stress, an increased number of ES events (+24% and +11%, respectively) was detected. In case of *prmt5-1* and *prmt5-1 x grp7-1,* no changes in isoform ratios were observed (Figure 5.30).

The presented results cannot be directly compared to the results from the alternative splicing experiments described above (chapter 5.5.1), because the experiments were performed under different conditions (details in chapters 4.9.3 and 4.10). Therefore, differences in controls in *AKIN11* can be observed. However, the comparison between Col-0, *grp7-1* and *prmt5-1* mutants reveals similar tendencies in *AKIN11* isoform ratios.

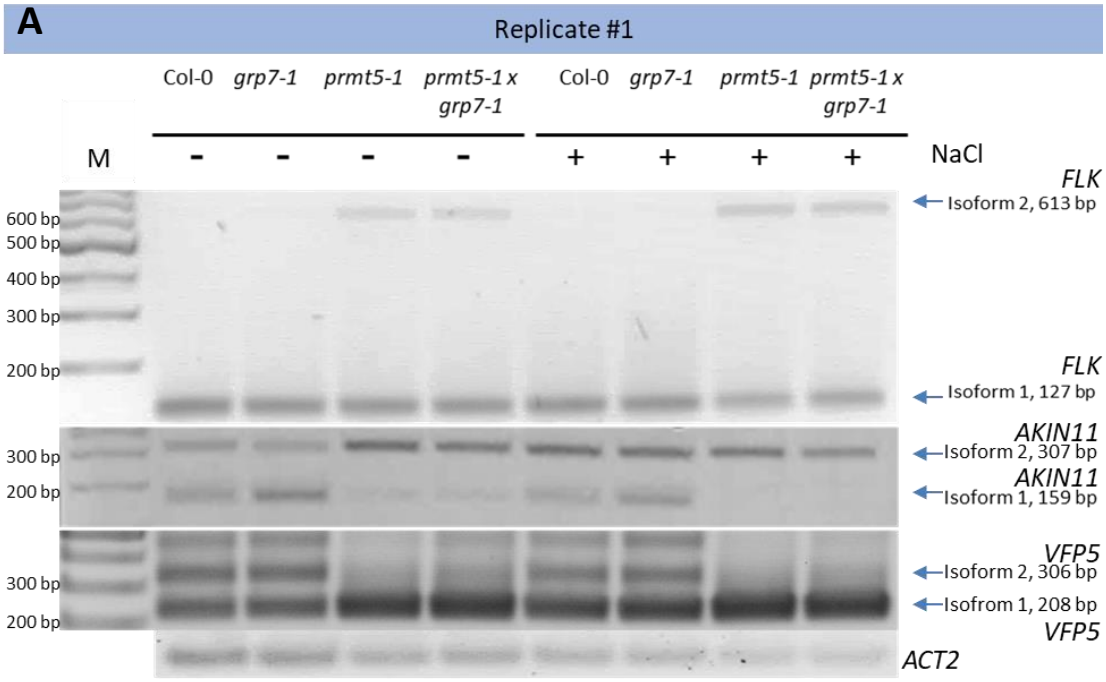

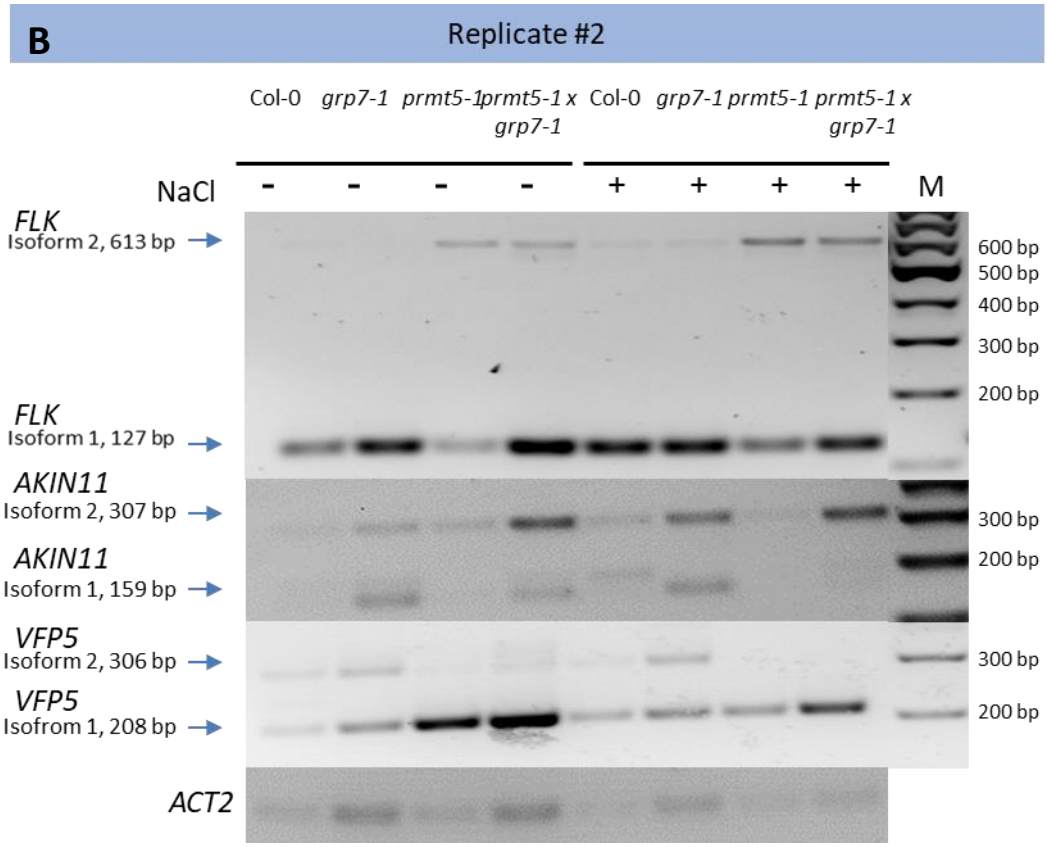
B
Replicate #2
Col-0
grp7-1
prmt5-1
prmt5-1 x grp7-1
Col-0
grp7-1
prmt5-1
prmt5-1 x grp7-1
NaCl
- - - - + + + +
M
FLK
Isoform 2, 613 bp
FLK
Isoform 1, 127 bp
AKIN11
Isoform 2, 307 bp
AKIN11
Isoform 1, 159 bp
VFP5
Isoform 2, 306 bp
VFP5
Isofrom 1, 208 bp
ACT2
600 bp
500 bp
400 bp
300 bp
200 bp
300 bp
200 bp
300 bp
200 bp

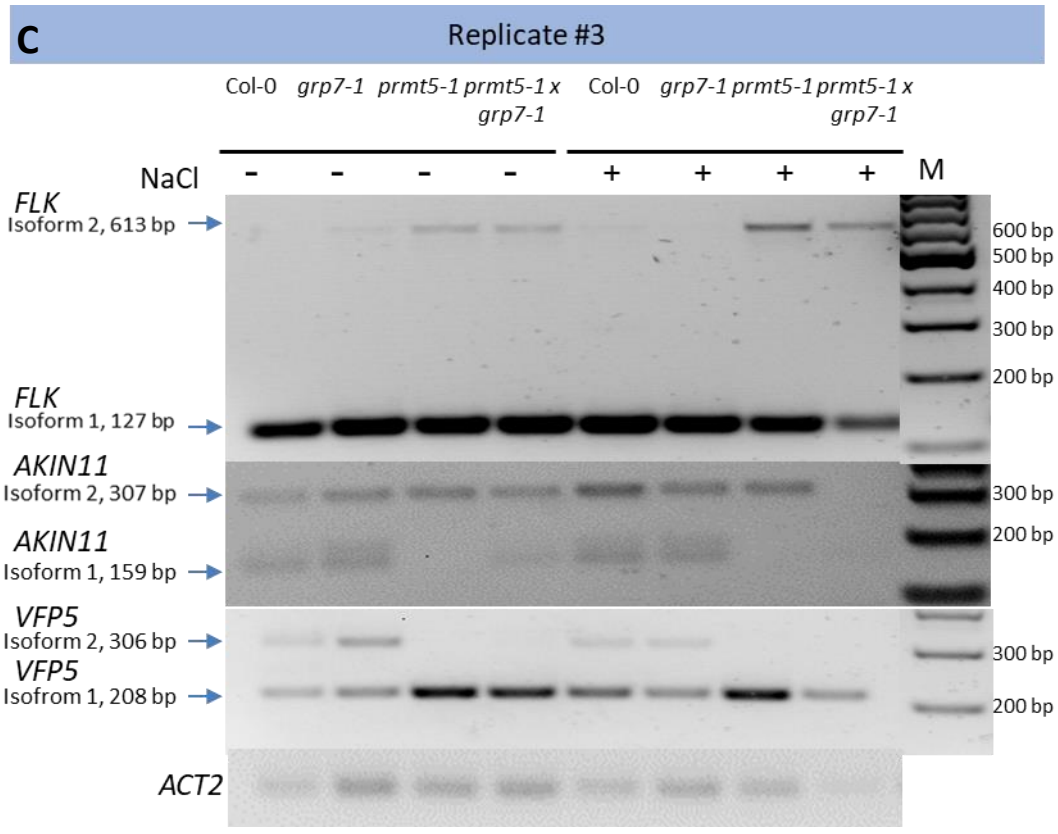
C
Replicate #3
Col-0
grp7-1
prmt5-1
prmt5-1 x grp7-1
Col-0
grp7-1
prmt5-1
prmt5-1 x grp7-1
NaCl
- - - - + + + +
M
FLK
Isoform 2, 613 bp
FLK
Isoform 1, 127 bp
AKIN11
Isoform 2, 307 bp
AKIN11
Isoform 1, 159 bp
VFP5
Isoform 2, 306 bp
VFP5
Isofrom 1, 208 bp
ACT2
600 bp
500 bp
400 bp
300 bp
200 bp
300 bp
200 bp
300 bp
200 bp

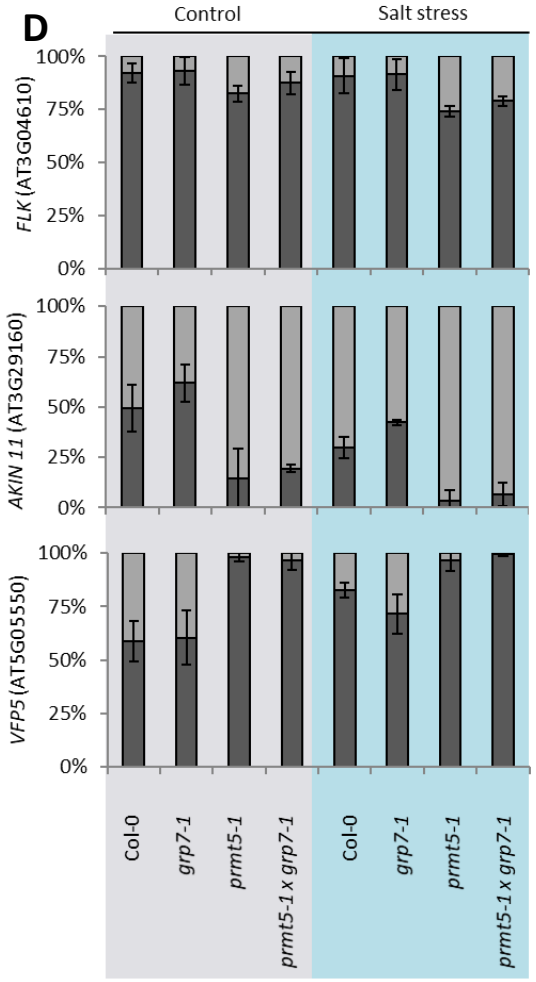

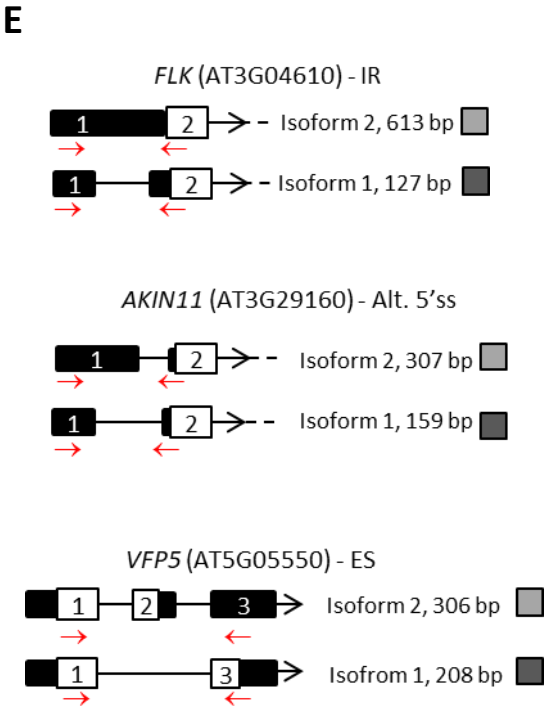

F

Gene	Splicing event	isoform	Control (0 mM NaCl) Col-0	*grp7-1*	*prmt5-1*	*prmt5-1 x grp7-1*	Salt stress (200 mM NaCl) Col-0	*grp7-1*	*prmt5-1*	*prmt5-1 x grp7-1*
FLK	IR	#1	92%	93%	83%	87%	91%	92%	74%	79%
		#2	8%	7%	17%	13%	9%	8%	26%	21%
AKIN 11	Alt. 5'ss	#1	49%	62%	15%	19%	30%	42%	4%	7%
		#2	51%	38%	85%	81%	70%	58%	96%	93%
VFP5	ES	#1	59%	61%	98%	97%	83%	72%	97%	100%
		#2	41%	39%	2%	3%	17%	28%	3%	1%

Figure 5.30 Effect of GRP7 and PRMT5 on alternative splicing of *FLK, AKIN11* and *VFP5* under salt stress conditions. (**A, B, C**) 11-day-old seedlings were transferred on ½ MS plates with or without 200 mM NaCl for 6 h and aerial parts were harvested. Synthesised cDNAs were used in sqPCR for amplification of *FLK, AKIN11* and *VFP5* transcripts. Pictures **A, B** and **C** represent three biological replicates. Uncropped pictures Figure A. 9, Figure A. 11, Figure A. 12. (**D**) Isoform ratios for *FLK, AKIN11* and *VFP5*. The signal intensities were measured using public domain software ImageJ (http://rsb.info.nih.gov/ij). Data collected from three biological replicates (± SD). (**E**) Schematic representation of analysed isoforms

with alternative 5' splice site in *AKIN11*, exon skipping in *VFP5* and intron retention in *FLK*. Red arrows indicate primers used in sqPCR. White boxes indicate codding regions and the black boxes indicate the 5' and 3' untranslated regions. Lines show introns and the black arrows indicate the reverse orientations of *AKIN11, VFP5* and *FLK*. (**F**) Data table shows the ratios of AS events detected in *FLK, AKIN11* and *VFP5* in analysed lines under control and salt stress conditions.

In all analysed cases, the ratios of AS events in Col-0 and *grp7-1* were considerably different from *prmt5-1* and *prmt5-1 x grp7-1,* whereas results of the two last lines were always very similar to each other. Interestingly, the *prmt5-1 x grp7-1* double mutant displays defects in AS detectable also in *prmt5-1* but not in *grp7-1*. The double mutant does not show an intermediate phenotype but rather displays only the effects of the *prmt5* mutation. Together with the observations from the previous chapters, these results reinforce the assumption that *PRMT5* is epistatic to *GRP7*.

It is noteworthy that all analysed AS events were more abundant in *prmt5-1* and *prmt5-1 x grp7-1,* than in Col-0 and *grp7-1*. This suggests that PRMT5 has a great impact on AS of *FLK, AKIN11* and *VFP5,* possibly greater than GRP7. Furthermore, AS events became even more abundant under stress conditions. As a result of salt stress, the frequency of IR in *FLK* increased, an alternative 5'ss in *AKIN11* was chosen more often and the number of the exon 2 skipping event in *VFP5* was also elevated. It seems that PRMT5 negatively regulates AS of the transcripts mentioned above. However, it is possible that under high salinity also other pathways are activated, which positively influence AS.

Alternative splicing under salt stress conditions in *prmt5-5 x grp7-1* 8i

The intron 1 retention in *FLK,* the usage of an alternative 5'ss within the first intron in the *AKIN11* 5'UTR region and the skipping of the exon 2 in *VFP5* were analysed in Col-0, *grp7-1* 8i, *prmt5-5* and *prmt5-5 x grp7-1* 8i under control and salt stress conditions.

The intron 1 in *FLK* was spliced out almost from all pre-mRNA in Col-0 and *grp7-1* (91% and 91%, respectively). The *FLK* transcripts with retained intron 1 were more abundant in *prmt5-5* and *prmt5-5 x grp7-1* 8i (18% and 14%), than in Col-0 or *grp7-1* 8i (9% and 9%). Under salt stress conditions, the intron 1 was retained only in 6% and 5% of the *FLK* transcripts in Col-0 and *grp7-1,* respectively. Under the same conditions, the increase of the intron 1 retention was detected in *prmt5-5* and *prmt5-5 x grp7-1* 8i (20% and 24%, respectively).

The usage of an alternative 5'ss within the first intron in the *AKIN11* 5'UTR region in Col-0 appeared in 53% of *AKIN11* transcripts. In *grp7-1* 8i, the alternative 5'ss was used only in 34% of *AKIN11* transcripts. On the other hand, in *prmt5-5* and *prmt5-5 x grp7-1* 8i the alternative 5'ss was detected in 57% and 74% *AKIN11* transcripts, respectively. Under salt stress conditions, the usage of the alternative 5'ss increased in all lines. In Col-0 and *grp7-1* 8i, the alternative 5'ss appeared in 59% and 51% of *AKIN11* transcripts, respectively. The high salinity drastically increased the usage of alternative 5'ss in *prmt5-5* and *prmt5-5 x grp7-1* 8i. The longer isoforms were detected in 84% and 92% *AKIN11* transcripts.

Under normal conditions, in Col-0 and *grp7-1* 8i the skipping of the exon 2 in *VFP5* appeared in 57% and 56% of *VFP5* transcripts. On the other hand, the exon 2 was retained in 11% and 15% *VFP5* transcripts in *prmt5-5* and *prmt5-5 x grp7-1* 8i. As a result of high salt stress, the exon 2 skipping in *VFP5* was much higher in comparison to the results obtained under normal conditions. The exon 2 was skipped in 77% and 79% of *VFP5* transcripts in Col-0 and *grp7-1* 8i, respectively. The same AS event under salt stress conditions in *prmt5-5* and *prmt5-5 x grp7-1* 8i was even more abundant (89% and 91%, respectively).

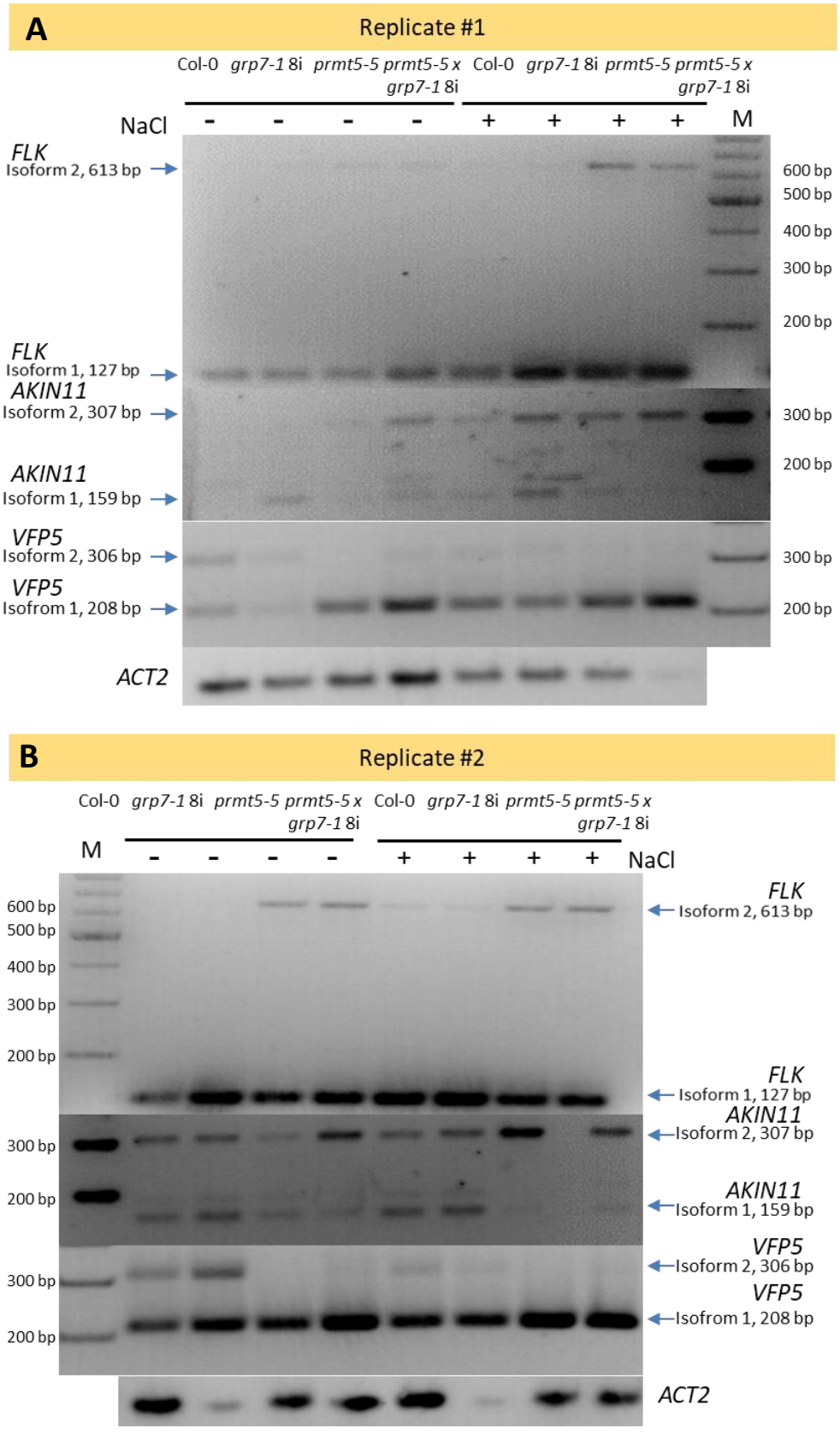
A
Replicate #1
Col-0
grp7-1 8i
prmt5-5
prmt5-5 x grp7-1 8i
Col-0
grp7-1 8i
prmt5-5
prmt5-5 x grp7-1 8i
NaCl
- - - - + + + +
M
FLK
Isoform 2, 613 bp
FLK
Isoform 1, 127 bp
AKIN11
Isoform 2, 307 bp
AKIN11
Isoform 1, 159 bp
VFP5
Isoform 2, 306 bp
VFP5
Isofrom 1, 208 bp
ACT2
600 bp
500 bp
400 bp
300 bp
200 bp
300 bp
200 bp
300 bp
200 bp
B
Replicate #2
Col-0
grp7-1 8i
prmt5-5
prmt5-5 x grp7-1 8i
Col-0
grp7-1 8i
prmt5-5
prmt5-5 x grp7-1 8i
M
- - - - + + + +
NaCl
600 bp
500 bp
400 bp
300 bp
200 bp
300 bp
200 bp
300 bp
200 bp
FLK
Isoform 2, 613 bp
FLK
Isoform 1, 127 bp
AKIN11
Isoform 2, 307 bp
AKIN11
Isoform 1, 159 bp
VFP5
Isoform 2, 306 bp
VFP5
Isofrom 1, 208 bp
ACT2

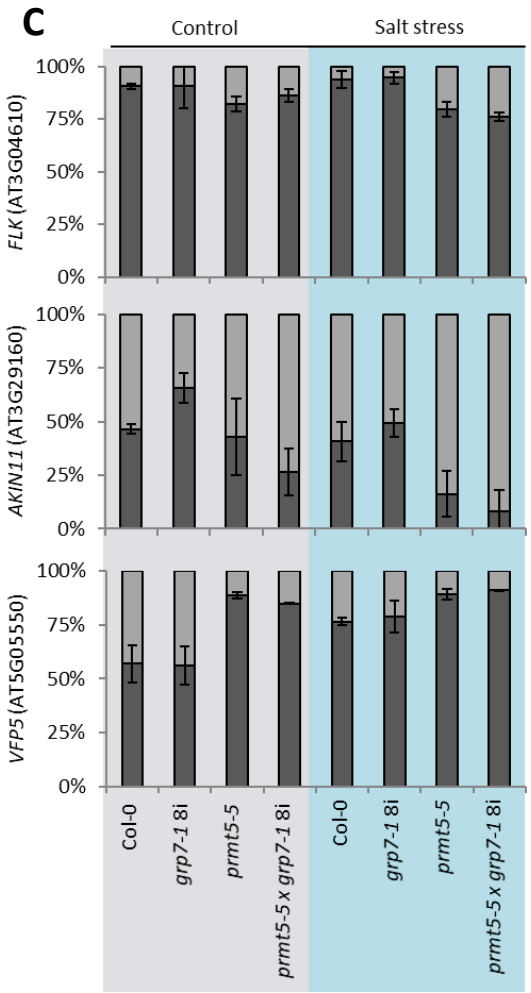

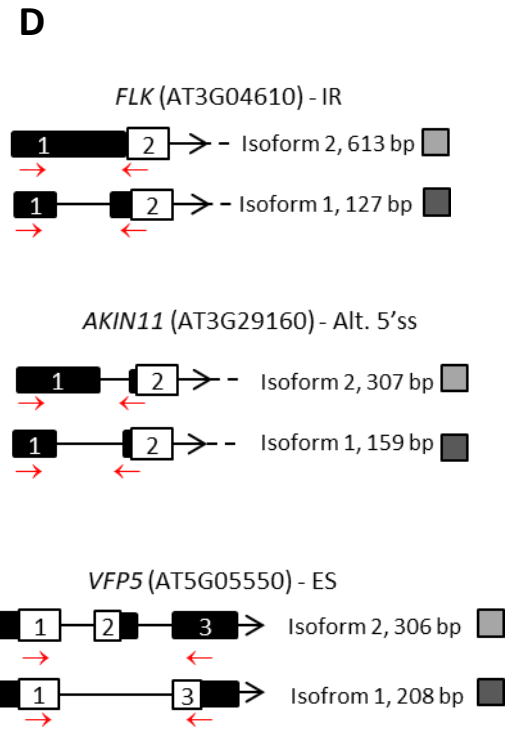

E

Gene	Splicing event	isoform	Control (0 mM NaCl)				Salt stress (200 mM NaCl)			
			Col-0	*grp7-1* 8i	*prmt5-5*	*prmt5-5 x grp7-1* 8i	Col-0	*grp7-1* 8i	*prmt5-5*	*prmt5-5 x grp7-1* 8i
FLK	IR	#1	91%	91%	82%	86%	94%	95%	80%	76%
		#2	9%	9%	18%	14%	6%	5%	20%	24%
AKIN 11	Alt. 5'ss	#1	47%	66%	43%	26%	41%	49%	16%	8%
		#2	53%	34%	57%	74%	59%	51%	84%	92%
VFP5	ES	#1	57%	56%	89%	85%	77%	79%	89%	91%
		#2	43%	44%	11%	15%	23%	21%	11%	9%

Figure 5.31 Effect of GRP7, GRP8 and PRMT5 on alternative splicing of *FLK*, *AKIN11* and *VFP5* under salt stress conditions. (**A**, **B**) 11-day-old seedlings were transferred on ½ MS plates with or without 200 mM NaCl for 6 h and aerial parts were harvested. Synthesised cDNAs were used in sqPCR for amplification of *AKIN11* and *VFP5* transcripts. Pictures **A** and **B** represent two biological replicates. Uncropped pictures Figure A. 13. (**C**) Isoform ratios for *FLK*, *AKIN11* and *VFP5*. The signal intensities were measured using public domain software ImageJ (http://rsb.info.nih.gov/ij). Data collected from two biological replicates (± SD). (**D**) Schematic representation of analysed isoforms with

alternative 5' splice site in *AKIN11*, exon skipping in *VFP5* and intron retention in *FLK*. Red arrows indicate primers used in sqPCR. White boxes indicate codding regions and the black boxes indicate the 5' and 3' untranslated regions. Lines show introns and the black arrows indicate the reverse orientations of *AKIN11, VFP5* and *FLK*. (**E**) Data table shows the ratios of AS events detected in *FLK, AKIN11* and *VFP5* in analysed lines under control and salt stress conditions.

The isoform ratios of all analysed AS events in Col-0 and *grp7-1* 8i were considerably different from *prmt5-5* and *prmt5-5 x grp7-1* 8i. The opposite effect was observed for *AKIN11* transcripts in *grp7-1* 8i and *prmt5-5*. Furthermore, rather than additive effects, the *prmt5-5 x grp7-1* 8i mutant displayed the same isoform ratios detected in *prmt5-5* mutant.

Under salt stress conditions, the AS events became more abundant in all lines. However, *prmt5-5* and *prmt5-5 x grp7-1* 8i had always the highest rates of AS events. The *prmt5-5 x grp7-1* 8i mutant did not display an intermediate phenotype, neither under normal nor stress conditions.

The comparison of the results from the first and the second experimental sets brings minimal differences between respective plant lines, *grp7-1* and *grp7-1* 8i, *prmt5-5* and *prmt5-1*. Moreover, the lack of major differences between *prmt5-1 x grp7-1* and *prmt5-5 x grp7-1* 8i suggests that GRP8 does not influence the tested AS events in a substantial way.

Alternative splicing under salt stress in GRP7-GFP complementation lines with mutated methylated arginine

The same AS events as described above were analysed in complementation lines expressing GRP7-GFP with mutations in methylated R141 (GRP7^{R141A}-GFP, GRP7^{R141K}-GFP) using GRP7-GFP and *grp7-1* as controls.

Analysis of intron 1 retention in the *FLK* transcript revealed only small differences between lines with a percentage of IR from 4% up to 9% in all analysed lines, both under control and high salinity conditions. Therefore, based on these results it seems that arginine methylation in GRP7 has little or no influence on AS of *FLK* (Figure 5.32).

An alternative 5'ss within the first intron of *AKIN11* was used in about half of the transcripts in GRP7-GFP plants. In the case of *grp7-1,* slight increase of the short isoform (+8%) with the constitutive splice site was detected in comparison to GRP7-GFP. Only small differences in alternatively spliced isoform ratios were observed between GRP7-GFP, GRP7^{R141A}-GFP and GRP7^{R141K}-GFP lines (-5% and +4%, respectively). Under salt stress conditions, a shift in favor of the longer isoform with an alternative 5'ss was detected in all lines. However, the change in GRP7-GFP was significantly larger (+32%), than in the case of *grp7-1,* GRP7^{R141A}-GFP and GRP7^{R141K}-

GFP (+17%, +12% and +10%, respectively). This could suggest that methylation at arginine 141 in GRP7 is important for *AKIN11* pre-mRNA splicing (Figure 5.32).

Finally, the frequencies of exon 2 skipping in the *VFP5* transcript in GRP7-GFP, *grp7-1,* GRP7^{R141A}-GFP and GRP7^{R141K}-GFP were very similar, lying between 61% and 70%. Under salt stress, exon 2 was skipped more often than in control conditions. In GRP7-GFP, GRP7^{R141A}-GFP and GRP7^{R141K}-GFP, the percentage of ES was increased to 75%-78%. An even higher frequency of ES was detected in *grp7-1* (82%). Since GRP7^{R141A}-GFP and GRP7^{R141K}-GFP seem to complement the *grp7-1* phenotype to the same extent as GRP7-GFP, arginine methylation in GRP7 appears to not influence AS of *VFP5* (Figure 5.32).

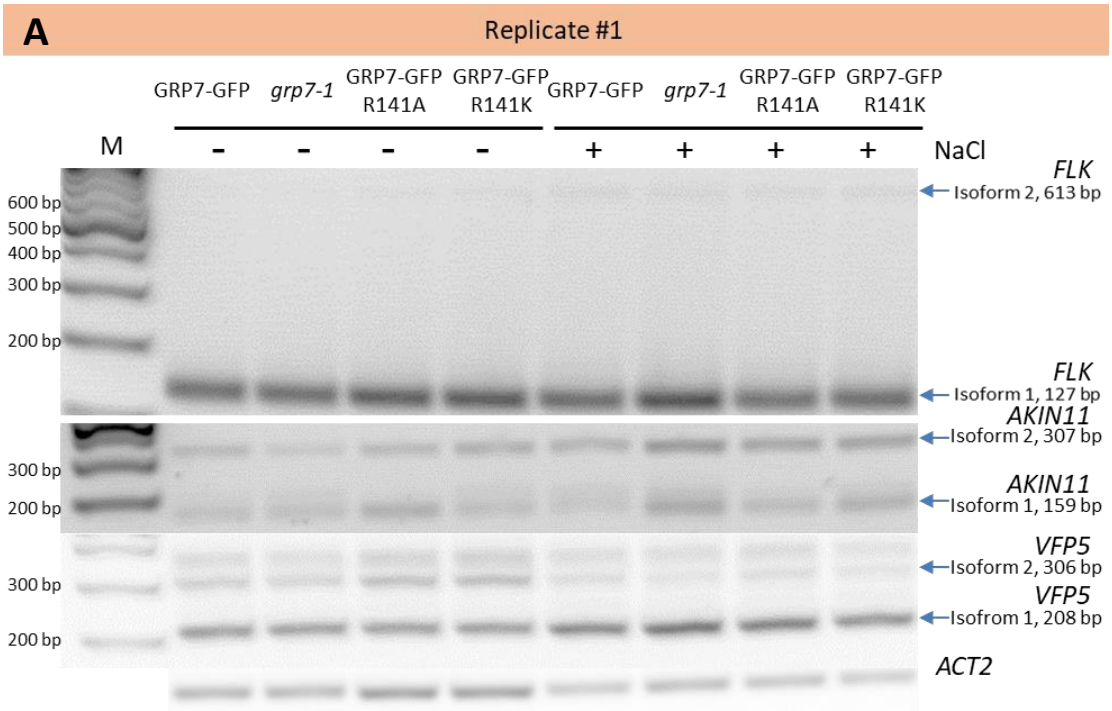

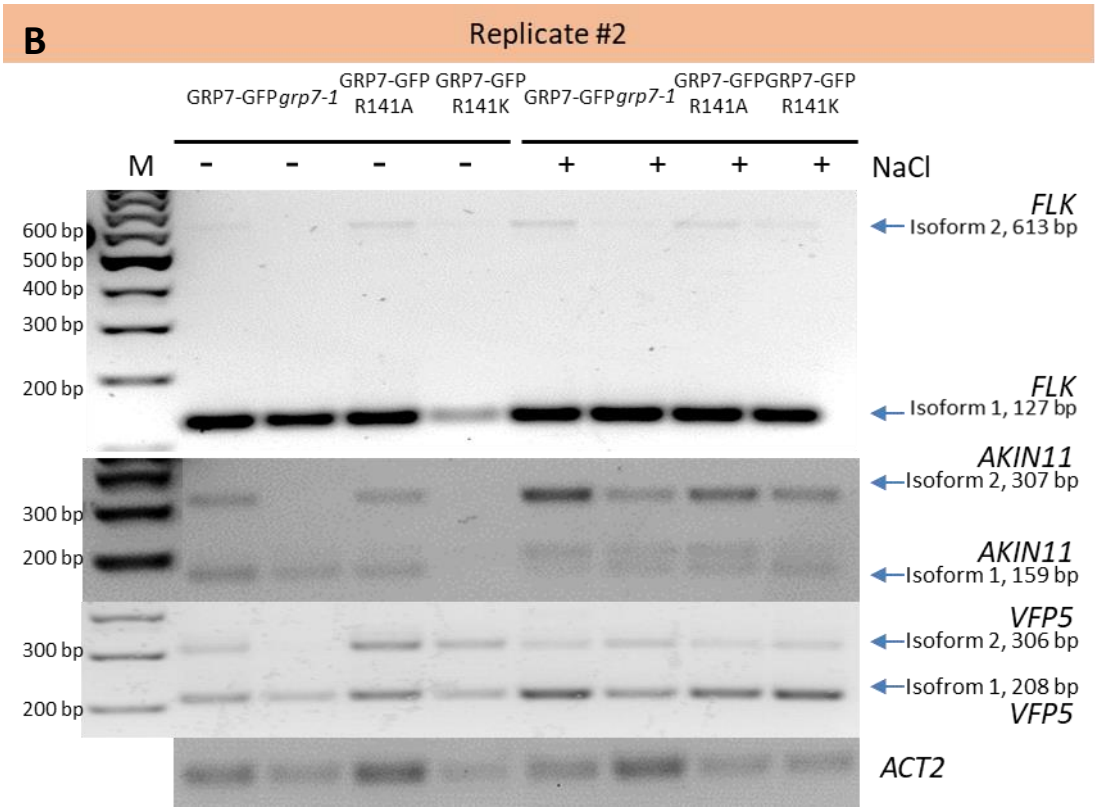
B
Replicate #2
GRP7-GFP
grp7-1
GRP7-GFP R141A
GRP7-GFP R141K
GRP7-GFP
grp7-1
GRP7-GFP R141A
GRP7-GFP R141K
M
- - - - + + + +
NaCl
600 bp
500 bp
400 bp
300 bp
200 bp
FLK
Isoform 2, 613 bp
FLK
Isoform 1, 127 bp
300 bp
200 bp
AKIN11
Isoform 2, 307 bp
AKIN11
Isoform 1, 159 bp
300 bp
200 bp
VFP5
Isoform 2, 306 bp
Isofrom 1, 208 bp
VFP5
ACT2

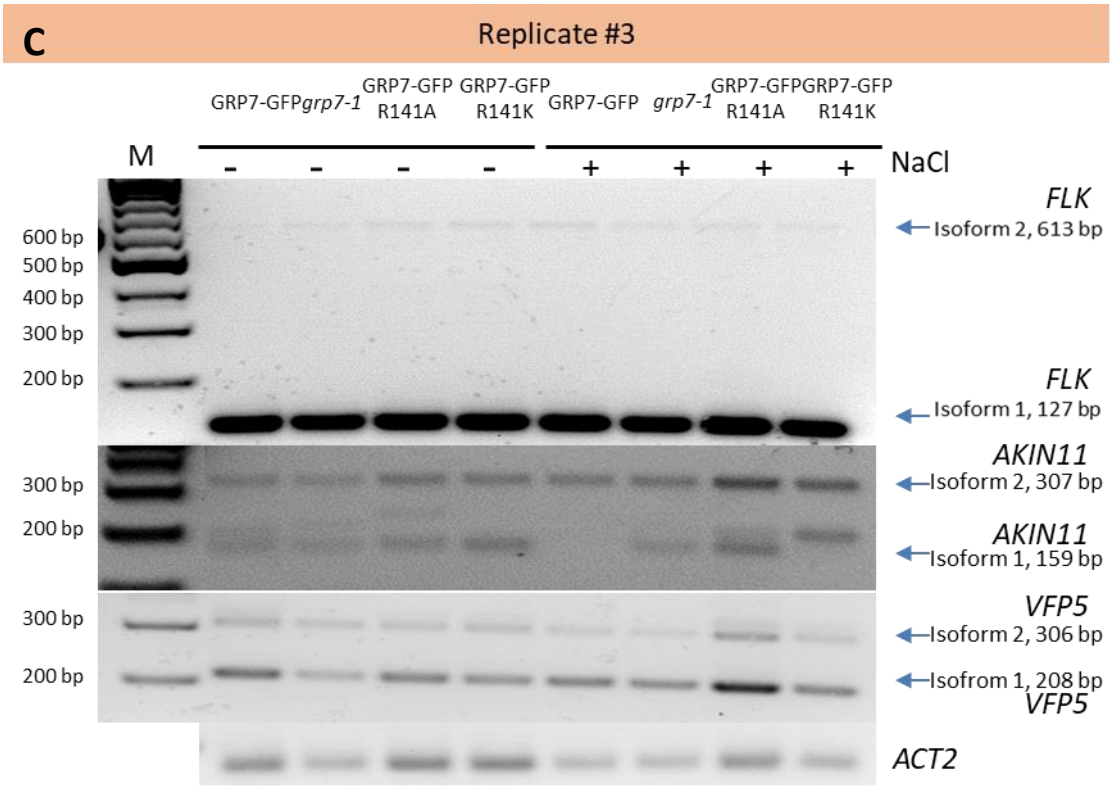
C
Replicate #3
GRP7-GFP
grp7-1
GRP7-GFP R141A
GRP7-GFP R141K
GRP7-GFP
grp7-1
GRP7-GFP R141A
GRP7-GFP R141K
M
- - - - + + + +
NaCl
600 bp
500 bp
400 bp
300 bp
200 bp
FLK
Isoform 2, 613 bp
FLK
Isoform 1, 127 bp
300 bp
200 bp
AKIN11
Isoform 2, 307 bp
AKIN11
Isoform 1, 159 bp
300 bp
200 bp
VFP5
Isoform 2, 306 bp
Isofrom 1, 208 bp
VFP5
ACT2

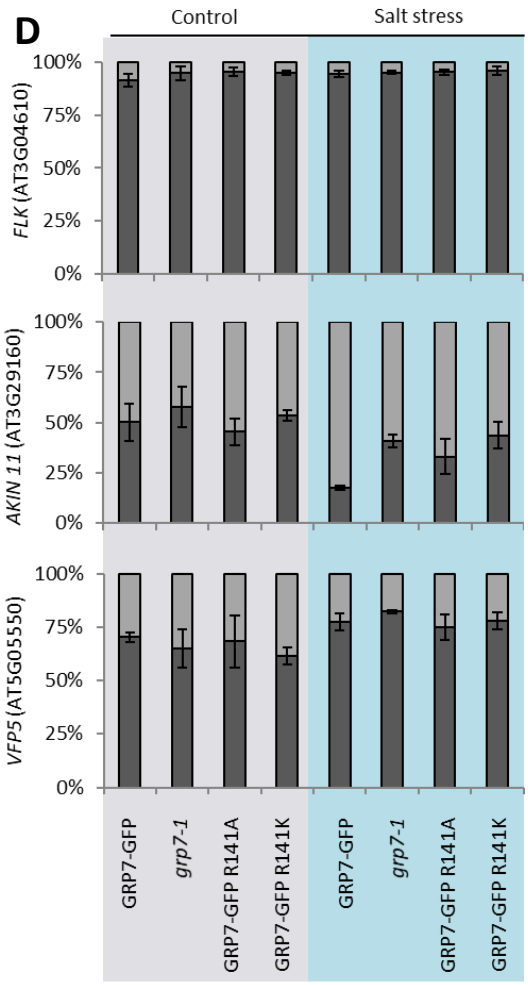

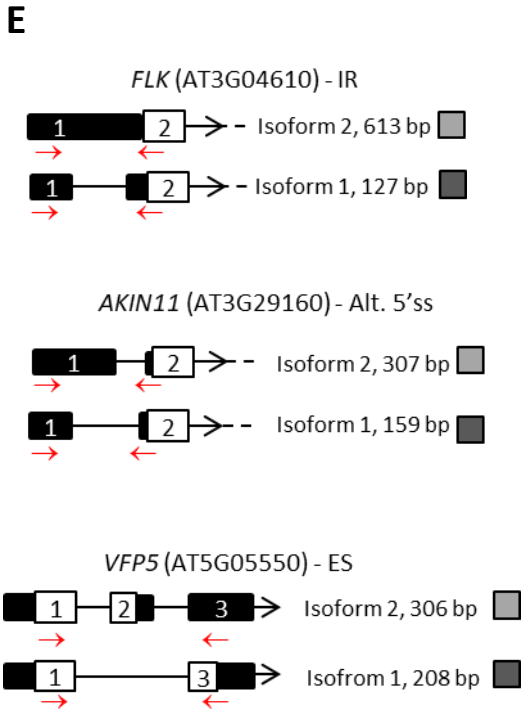

F

Gene	Splicing event	isoform	Control (0 mM NaCl)				Salt stress (200 mM NaCl)			
			GRP7-GFP	*grp7-1*	GRP7-GFP R141A	GRP7-GFP R141K	GRP7-GFP	*grp7-1*	GRP7-GFP R141A	GRP7-GFP R141K
FLK	IR	#1	91%	95%	95%	95%	94%	95%	95%	96%
		#2	9%	5%	5%	5%	6%	5%	5%	4%
AKIN 11	Alt. 5'ss	#1	50%	58%	45%	54%	18%	41%	33%	44%
		#2	50%	42%	55%	46%	82%	59%	67%	56%
VFP5	ES	#1	70%	65%	68%	61%	77%	82%	75%	78%
		#2	30%	35%	32%	39%	23%	18%	25%	22%

Figure 5.32 Effect of arginine methylation in GRP7 on alternative splicing of *FLK, AKIN11* and *VFP5* under salt stress conditions. (**A, B, C**) 11-day-old seedlings were transferred on ½ MS plates with or without 200 mM NaCl for 6 h and aerial parts were harvested. Synthesised cDNAs were used in sqPCR for amplification of *AKIN11* and *VFP5* transcripts. Pictures **A, B** and **C** represent three biological replicates. Uncropped pictures Figure A. 10, Figure A. 11, Figure A. 12. (**D**) Isoform ratios for *FLK, AKIN11* and *VFP5*. The signal intensities were measured using public domain software ImageJ (http://rsb.info.nih.gov/ij). Data collected from three biological replicates (± SD). (**E**) Schematic representation of analysed

isoforms with alternative 5' splice site in *AKIN11*, exon skipping in *VFP5* and intron retention in *FLK*. Red arrows indicate primers used in sqPCR. White boxes indicate codding regions and the black boxes indicate the 5' and 3' untranslated regions. Lines show introns and the black arrows indicate the reverse orientations of *AKIN11, VFP5* and *FLK*. (**F**) Data table shows the ratios of AS events detected in *FLK, AKIN11* and *VFP5* in analysed lines under control and salt stress conditions.

In the third experimental group, changes in ratios of AS events were much smaller, in comparison to the first and second experimental group. The presented results show that exchange of arginine 141 in GRP7 does not influence AS of *AKIN11, FLK* and *VFP5* transcripts. However, under salt stress small differences can be observed in *AKIN11* isoform ratios between GRP7-GFP and GRP7^{R141A}-GFP and GRP7^{R141K}-GFP. It seems that high salinity could influence the effectiveness of GRP7, depended on arginine methylation, for its controlling of *AKIN11* AS. This possible scenario requires further analyses though. Such correlations were not observed for either *FLK* or *VFP5*.

5.6. Generation of *prmt5 grp7 grp8* triple mutants using the CRISPR/Cas9 system

At the time of my work, there was no complete loss-of-function mutant for GRP8, since the artificial miRNAs or RNAi constructs were not able to completely eliminate GRP8 expression (Streitner et al., 2008). Therefore, the clustered regularly interspaced short palindromic repeats (CRISPR)-Cas9 (CRISPR associated) protein system was applied to generate *prmt5 grp7 grp8* lines.

CRISPR/Cas9 has been shown to be an effective tool for introducing heritable mutations in plants (Fauser et al., 2014; Hyun et al., 2015; Schiml et al., 2014; Steinert et al., 2015). By using a single guide RNA (sgRNA) and the Cas9 DNA endonuclease, the CRISPR/Cas9 system can target a specific sequence in the genome and perform a double-strand break to deleted or insert a DNA sequence, which disrupts or alters gene function. To generate a double-strand break, Cas9 requires the 3' protospacer adjacent motif (PAM) sequence, consisting of an NGG trinucleotide localised downstream of the target sequence (Cong et al., 2013; Jinek et al., 2013).

To create the *prmt5 grp7 grp8* triple knock-out mutants, homozygous *prmt5-1 grp7-1* and *prmt5-5 grp7-1* plants were transformed with the pYB196 vector, which carries the sgRNA7 under control of the U6-26 promoter, targeting the first exon in the *GRP8* sequence (Figure 5.33). The pYB196_sgRNA7 vector also harbours a *bar* gene providing Basta® resistance and the *Cas9* gene from *Streptococcus pyogenes* under control of the *ICU2* promoter. *U6 snRNA* and *ICU2* are widely conserved in higher plants and encode a splicing factor and a catalytic subunit of DNA polymerase α, respectively (Barrero et al., 2007; Hyun et al., 2013; Li et al., 2007; Waibel and Filipowicz, 1990). Therefore, the use of U6-26 and *ICU2* promoters increases the chance of the Cas9-mediated double-strand break occurring during core cellular processes such as pre-mRNA splicing and DNA replication. The U6-26 and *ICU2* promoters are activated during cell proliferation, initiating the mutagenesis process throughout both embryogenesis and the plant life cycle. As a result of the U6-26 and *ICU2* promoters' activity, somatic mutations can also occur in shoot apical meristem, which later give a rise to the floral primordia. In flowers, the mutations can be transmitted into gametes and therefore they become heritable (Hyun et al., 2015).

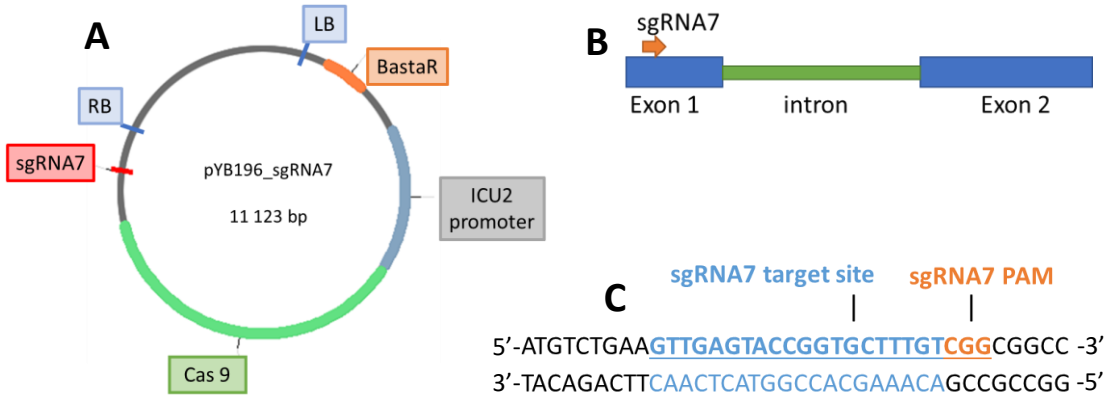

Figure 5.33 CRISPR Cas9 system. (**A**) Plasmid pYB196_sgRNA7. LB-left border, RB- right border, BastaR- Basta resistance, ICU2- INCURVATA2; (**B**) Location of sgRNA7 binding to the *AtGRP8* sequence, controlled by U6-26 promoter; (**C**) Fragment of *AtGRP8* nucleic acid sequence with marked sgRNA7 target site and PAM sequence.

To select positive transformants, plants from the T_1 and T_2 generation were sprayed with Basta® and tested for the presence of the sgRNA in the genomic DNA (gDNA) (details in 4.7.2).

The chosen T_2 plants were further analysed for the homozygous state of *GRP8*. DNA samples from T_2 plants were used to amplify *GRP8* fragments with primers flanking the first exon (details in 4.7.2). PCR products were denatured and renatured, and then visualized by polyacrylamide gel electrophoresis (PAGE). Differences in migration patterns of homo- and heteroduplexes allow the assessment of the homozygous or heterozygous state at the *GRP8* locus in T_2 plants (Figure 5.34, Figure 5.35, Figure 5.36, Figure 5.37 and Figure A. 14).

Next, potential homozygous plants were tested for mutations in *GRP8* introduced by the CRISPR/Cas9 system (details in 4.7.2). To distinguish between homozygous mutants and wild types, PCR products from T_2 plants (*prmt5-1 grp7-1 grp8* or *prmt5-5 grp7-1 grp8*) were mixed with the PCR products from wild types (in this case *prmt5-1 grp7-1* or *prmt5-5 grp7-1*). Mixed PCR products were denatured and renatured, and then visualized with the PAGE-assay. The analyses of the migration pattern with homo- und heteroduplexes allowed for selection of homozygous mutants (Figure 5.34, Figure 5.38 and Figure 5.39). Finally, GRP8 protein level was tested with immunoblot analyses (Figure 5.40) and DNA sequencing was performed for promising homozygous *prmt5 grp7 grp8* mutants (Figure 5.41, Figure 5.42 and Figure 5.43).

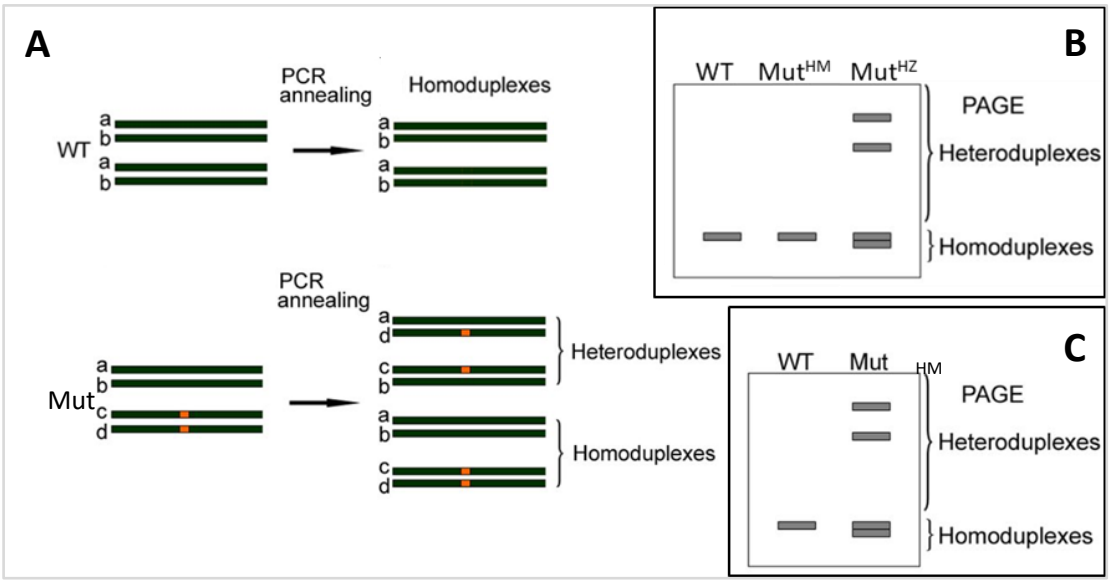

Figure 5.34 Identification of homozygous mutants among CRISPR/Cas9 plants. (**A**) Homoduplexes and heteroduplexes after denaturation and renaturation. Black bars - four DNA strands (a, b, c, d); orange boxes - monoallelic mutations (Zhu et al., 2015; modified). (**B**) Identification of heterozygous mutants with PAGE-assay. PCR products from homozygous mutants and wild types are visualized as single bands. Due to lack of full complementarity between DNA strands in heterozygous mutants, PCR products migrate slower in PAGE gels and create a heteroduplex migration pattern (Zhu et al., 2015; modified). (**C**) Identification of homozygous mutants with PAGE-assay. PCR product from a mutant was mixed with PCR product from wild type, and then denatured and renatured. Single base pair differences between a mutant and wild type are a cause for creating heteroduplexes on the PAGE gel (Zhu et al., 2015; modified).

Identification of homozygous *prmt5 grp7 grp8* mutants

By spraying the plants of the T_1 generation with Basta®, 17 *prmt5-1 grp7-1 grp8* and four *prmt5-5 grp7-1 grp8* resistant plants were identified, coming from nine and three independent T_0 transformants, respectively. The sgRNA sequence was identified in the gDNA from three *prmt5-1 grp7-1 grp8* and two *prmt5-5 grp7-1 grp8* resistant plants by PCR with primers flanking sgRNA within inserted T-DNA (Figure 5.35). In the T_2 generation, 84 plants coming from five independent parental T_0 lines were Basta® resistant. 59 out of 84 tested T_2 plants contained the sgRNA sequence in their gDNA (Table 5.2, Figure 5.35 and Figure A. 14).

Table 5.2 The Basta® resistant plants from T_2 generation containing sgRNA

	prmt5-5 grp7-1 grp8		*prmt5-1 grp7-1 grp8*		
parental lines	4A	33A	18A	27A	35A
T_2 plants with sgRNA	1, 2, 3, 4, 5, 6, 7, 8, 9, 10, 11, 12, 14, 15, 16	1, 2, 3, 5, 6, 7, 9, 10, 11, 12, 13, 14	1, 2, 3, 4, 5, 12, 13, 14, 15, 17	1, 2, 3, 5, 7, 9, 10, 11, 12, 15, 16, 17	1, 2, 4, 6, 7, 8, 10, 11, 12, 13

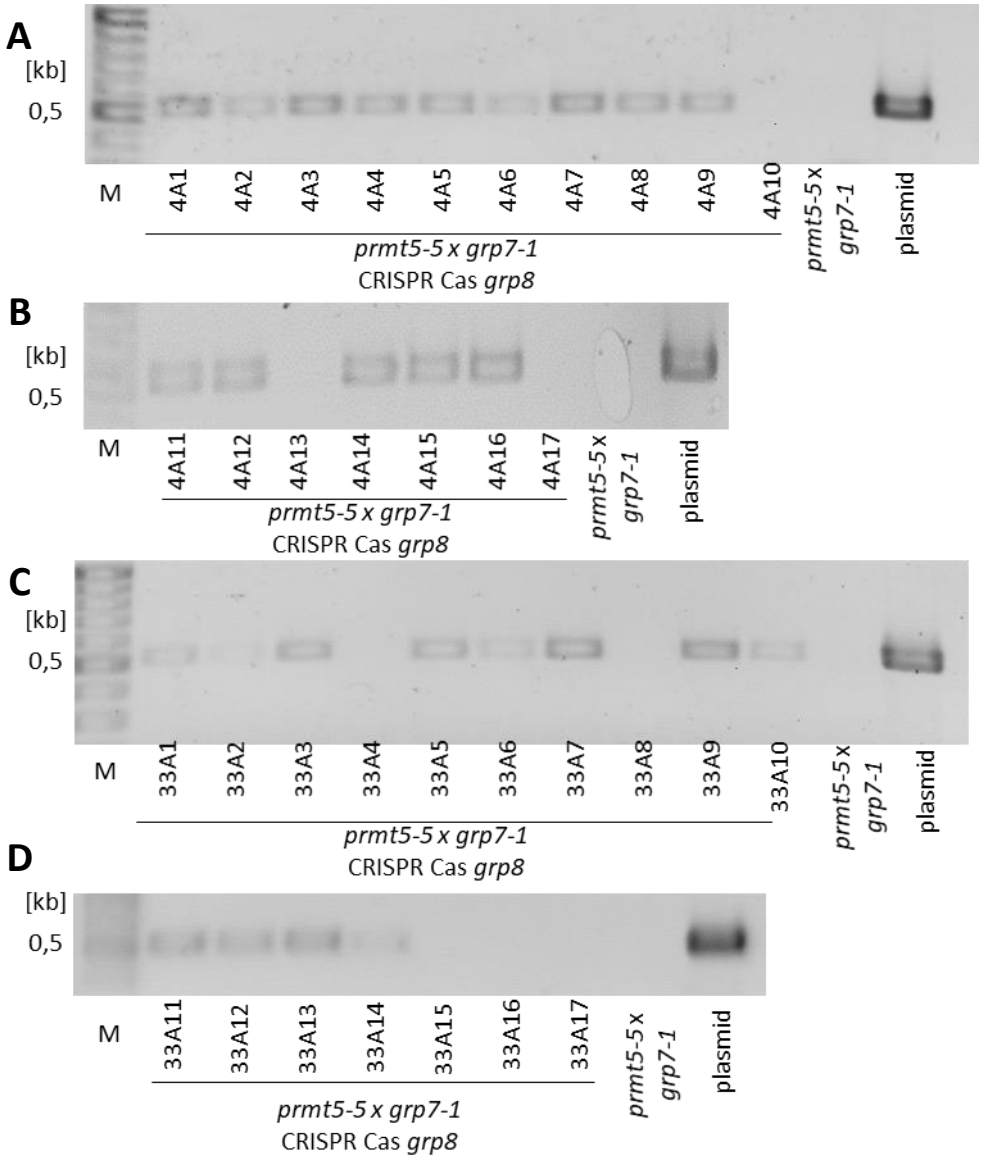

Figure 5.35 Amplification of sgRNA fragments in plants of the T_2 generation. Detection of the T-DNA with the sgRNA in transgenic plants was performed by PCR with F_NotI_pEN and R_NotI_pEN primers using DNA isolated from T_2 plants (**A** and **B**) 4A1-4A17 and (**C** and **D**) 33A1-33A17. The plasmid #2020 containing the sgRNA sequence served as a positive control, while DNA from the *prmt5-5 x grp7-1* mutant was used as a negative control. M- marker 100 bp. The same analysis was performed for *prmt5-1 x grp7-1* CRISPR Cas *grp8* T_2 plants (see Appendix Figure A. 14).

Next, the T_2 plants with sgRNA (Table 5.2) were used to investigate the status at the *GRP8* locus. To do this, fragments of the *GRP8* sequence were amplified by PCR with primers spanning exon 1. PCR products were denatured, renatured and visualized on a 15% PAGE gel (Figure 5.36 and Figure 5.37).

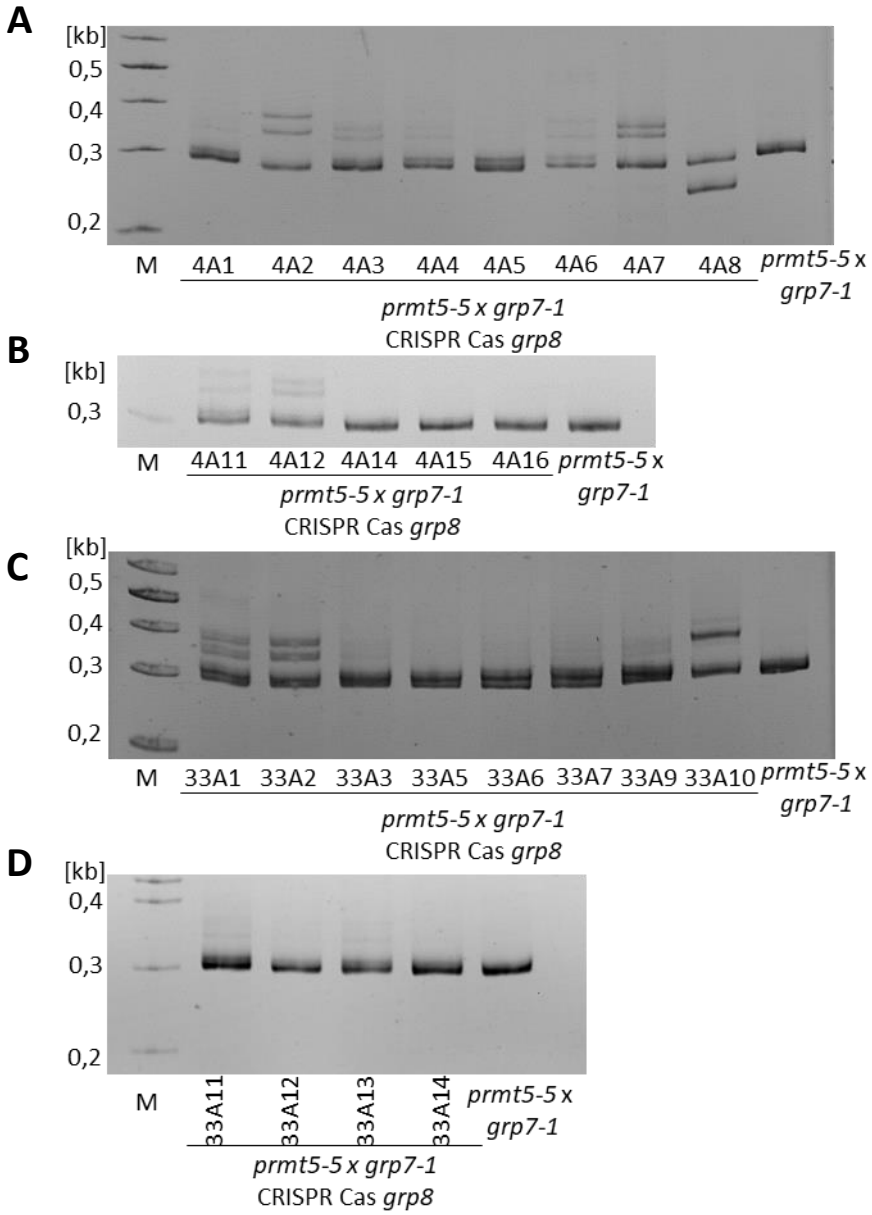

Figure 5.36 Identification of the homozygous state at the *GRP8* locus in T_2 generation of *prmt5-5 grp7-1 grp8* mutants. (**A**-**D**) The fragment of the *GRP8* sequence was amplified by PCR with CCRB_5'UTR and Agrp_95 primers using DNA isolated from T_2 plants (**A** and **B**) 4A1-4A16 and (**C** and **D**) 33A1-33A14. PCR products were denatured, renatured and visualized on a 15% PAGE gel to identify the homozygous state at the *GRP8* locus. M- marker 100 bp.

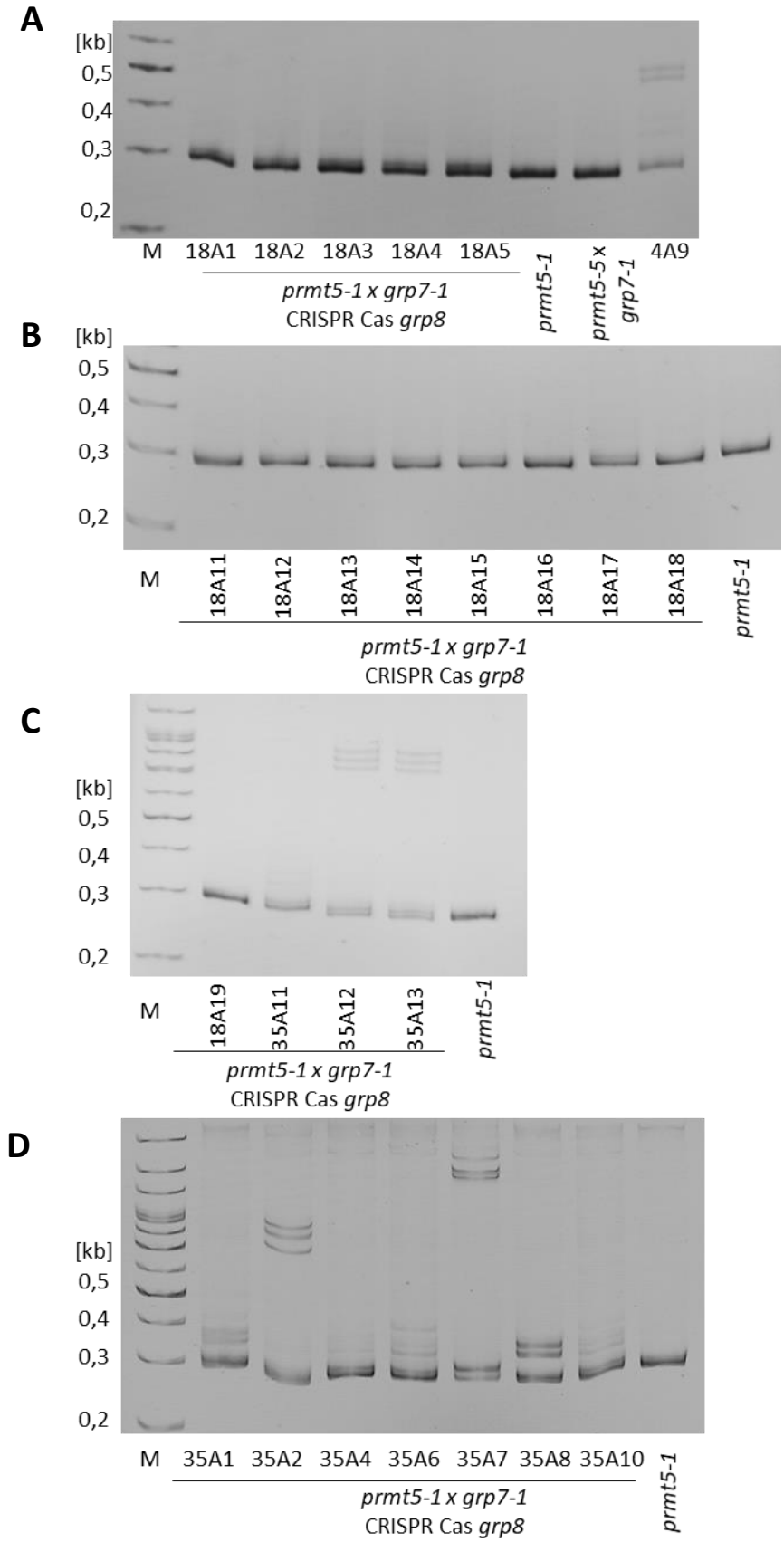
A
[kb]
0,5
0,4
0,3
0,2
M
18A1
18A2
18A3
18A4
18A5
prmt5-1
prmt5-5 x grp7-1
4A9
prmt5-1 x grp7-1
CRISPR Cas grp8
B
[kb]
0,5
0,4
0,3
0,2
M
18A11
18A12
18A13
18A14
18A15
18A16
18A17
18A18
prmt5-1
prmt5-1 x grp7-1
CRISPR Cas grp8
C
[kb]
0,5
0,4
0,3
0,2
M
18A19
35A11
35A12
35A13
prmt5-1
prmt5-1 x grp7-1
CRISPR Cas grp8
D
[kb]
0,5
0,4
0,3
0,2
M
35A1
35A2
35A4
35A6
35A7
35A8
35A10
prmt5-1
prmt5-1 x grp7-1
CRISPR Cas grp8

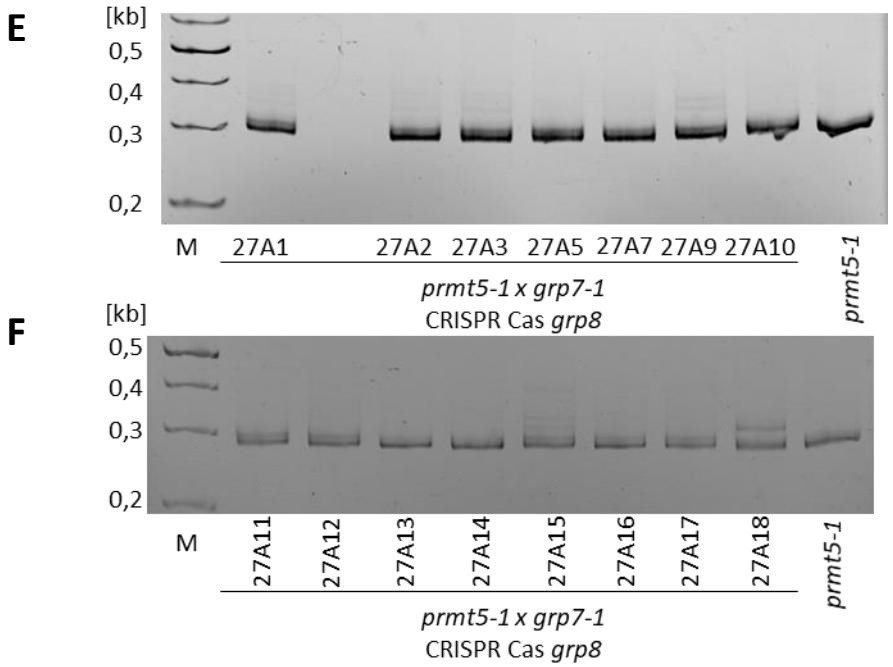

Figure 5.37 Identification of the homozygous state at the *GRP8* locus in T_2 generation of *prmt5-1 grp7-1 grp8* mutants. (**A**-**F**) The fragment of the *GRP8* sequence was amplified by PCR with CCRB_5'UTR and Agrp_95 primers using DNA isolated from T_2 plants (**A, B** and **C**) 18A1-18A19, (**C** and **D**) 35A1-33A13, (**E** and **F**) 27A1-27A18. PCR products were denatured, renatured and visualized on a 15% PAGE gel to identify the homozygous state at the *GRP8* locus. M- marker 100 bp.

The homozygous state at the *GRP8* locus was identified in 35 out of 59 tested T_2 plants (Table 5.3).

Table 5.3 T_2 plants with the homozygous state at the *GRP8* locus

	prmt5-5 grp7-1 grp8		*prmt5-1 grp7-1 grp8*		
parental lines	4A	33A	18A	27A	35A
T_2 plants with homozygous state at the *GRP8* locus	1, 5, 14, 15, 16	3, 5, 6, 7, 9, 12, 14	1, 2, 3, 4, 5, 11,12, 13, 14, 15, 16, 17, 18, 19	5, 7, 10, 11, 13, 14, 16, 17	4

These lines were then further analysed for the presence of a homozygous mutation in *GRP8*. To do this, fragments of the *GRP8* sequence were amplified by PCR with the same primers as above which are flanking exon 1. PCR products from the T_2 generation were mixed with PCR products from *prmt5-1 grp7-1* or *prmt5-5 grp7-1* mutants. The mixtures of PCR products were denatured, renatured and visualized on a 15% PAGE gel (Figure 5.38 and Figure 5.39).

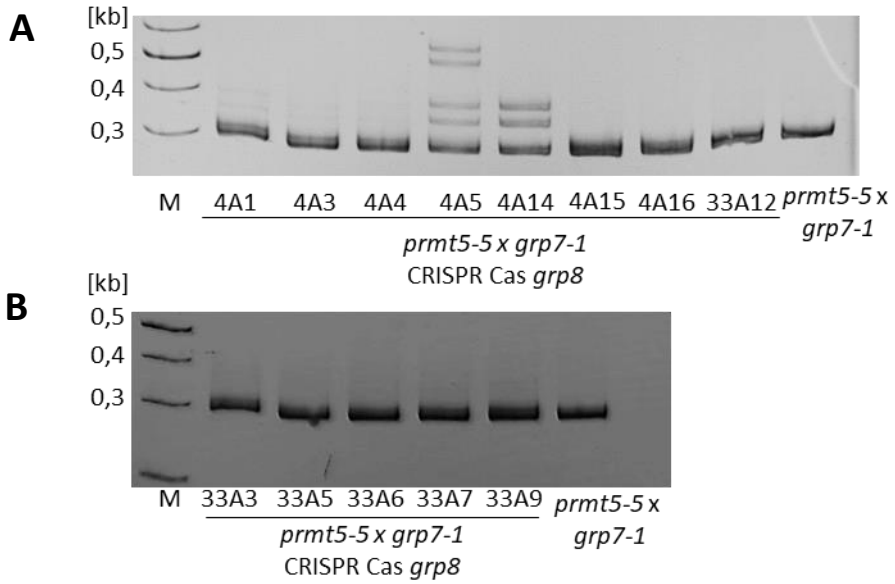

Figure 5.38 Identification of homozygous mutations at the *GRP8* locus in the T_2 generation of *prmt5-5 grp7-1 grp8* mutants. (**A**, **B**) *GRP8* fragments were PCR-amplified with CCRB_5'UTR and Agrp_95 primers using DNA isolated from T_2 plants (**A**) 4A1-4A16 and (**A, B**) 33A3-33A12 and *prmt5-5 grp7-1*. PCR products from the T_2 generation were mixed with PCR products from *prmt5-5 x grp7-1*. The mixtures of PCR products were denatured, renatured and visualized on a 15% PAGE gel to identify homozygous mutants. M- marker 100 bp.

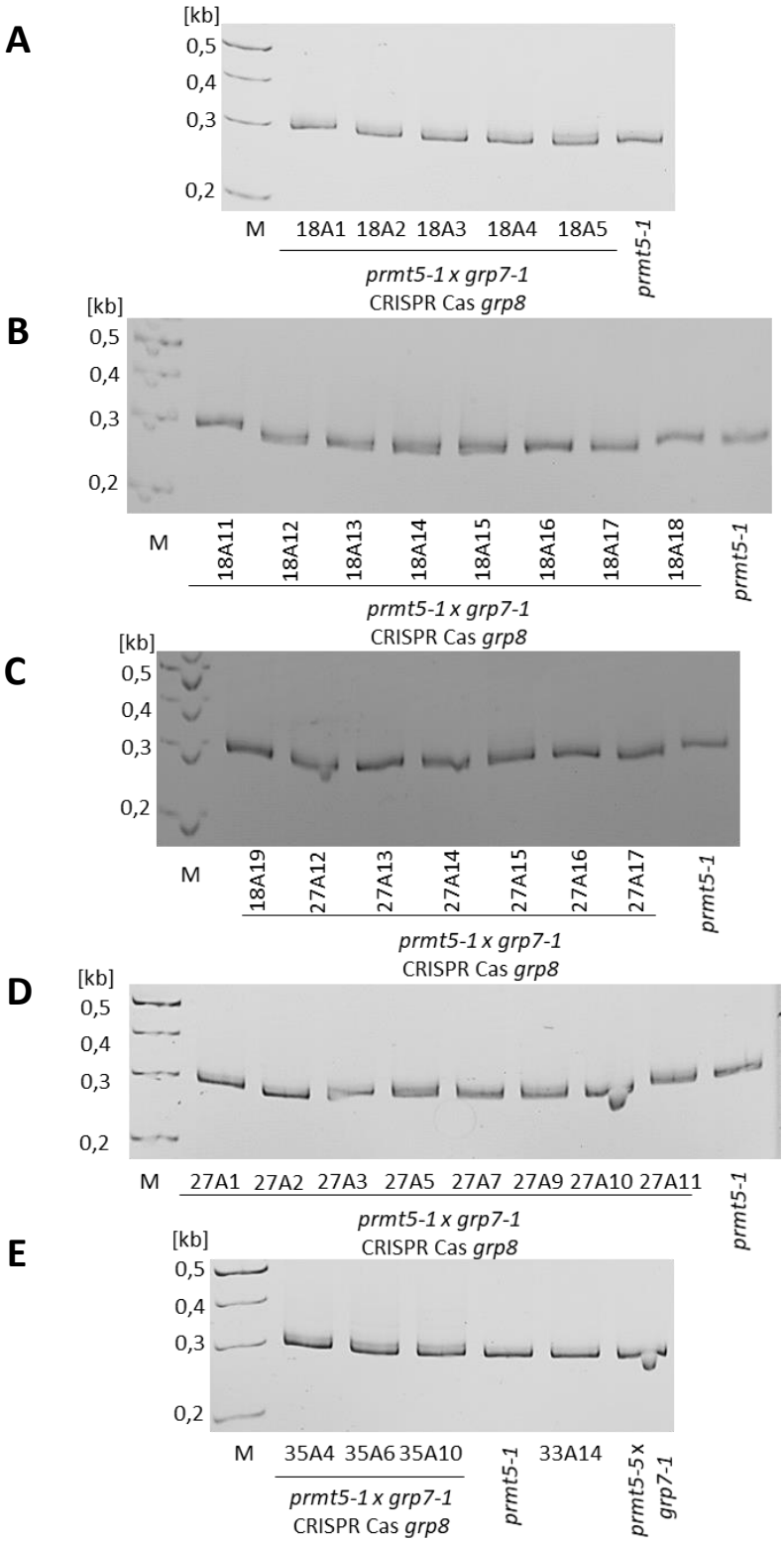

Figure 5.39 Identification of homozygous mutations at the *GRP8* locus in the T_2 generation of *prmt5-1 grp7-1 grp8* mutants. (**A**-**E**) *GRP8* fragments were PCR-amplified with CCRB_5'UTR and Agrp_95 primers using DNA isolated from T_2 plants (**A, B** and **C**) 18A1-18A19, (**C** and **D**) 27A1-27A17, (**E**) 35A4-35A10 and *prmt5-1 grp7-1*. PCR products from the T_2 generation were mixed with PCR

products from *prmt5-1 grp7-1*. The mixtures of PCR products were denatured, renatured and visualized on a 15% PAGE gel to identify homozygous mutants. M-marker 100 bp.

By mixing PCR products from mutant lines with PCR products from *prmt5-5 grp7-1*, homozygous mutations in *GRP8* were identified in lines 4A1, 4A5 and 4A14. The PAGE-assay showed also that 33A9 line could be a potential homozygous mutant (Figure 5.38 and Figure 5.39).

To determine the influence of the mutations on GRP8 protein expression, protein levels were compared by Western blot analysis. The immunoblot analyses showed that 10 T_2 plants from two independent parental T_0 lines did not express GRP8 protein (Figure 5.40). They were *prmt5-5 grp7-1 grp8* plants 4A1, 4A2, 4A5, 4A7, 4A13, 4A14, 4A15, 4A16, 4A17 and 33A9.

In plants 4A1, 4A5 and 4A14, which were determined as homozygous mutants no GRP8 protein was detected, confirming the successful knock-out of *GRP8* (Figure 5.40). Interestingly, GRP8 protein was also not detectable in 4A2, 4A7, 4A15 and 4A16 (Figure 5.40). In case of 4A2 and 4A7, both plants contained mutations in the *GRP8* sequences in the heterozygous states. It is possible that 4A2 and 4A7 were transheterozygous plants with two different mutated alleles at the *GRP8* locus. Therefore, no functional GRP8 was detected in 4A2 and 4A7. In case of 4A15 and 4A16, it was assumed that both plants were homozygous mutants. However, no homoduplex migration pattern was visible, when PCR products from 4A14 and 4A16 were mixed with PCR products from *prmt5-5 grp7-1* (Figure 5.36 and Figure 5.38).

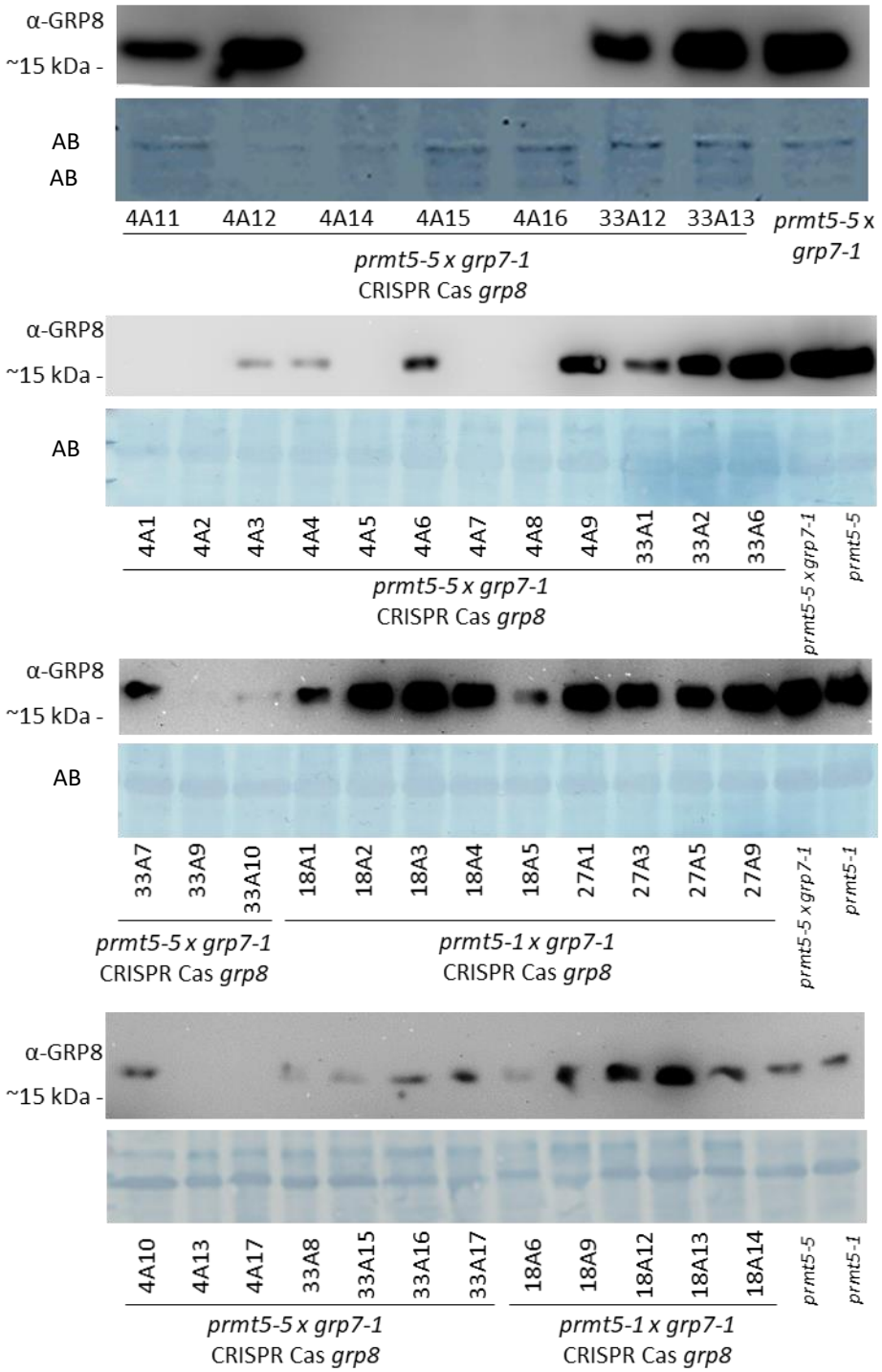

Figure 5.40 Detection of GRP8 protein level in T_2 generation of *prmt5 grp7 grp8* plants. Arrows point 10 plants *prmt5 grp7 grp8* that lack GRP8. Amidoblack (AB) staining served as a loading control.

For lines 4A1, 4A14 and 33A9, DNA fragments containing the first exon of *GRP8* were amplified and then analysed by DNA sequencing. The sequence alignment with the endogenous *GRP8* sequence showed that line 4A1 carried a 1 bp deletion, causing a

frame shift and resulting in a different amino acid chain (Figure 5.41). The consequence of that was the lack of GRP8 protein in the Western blot analysis (Figure 5.40).

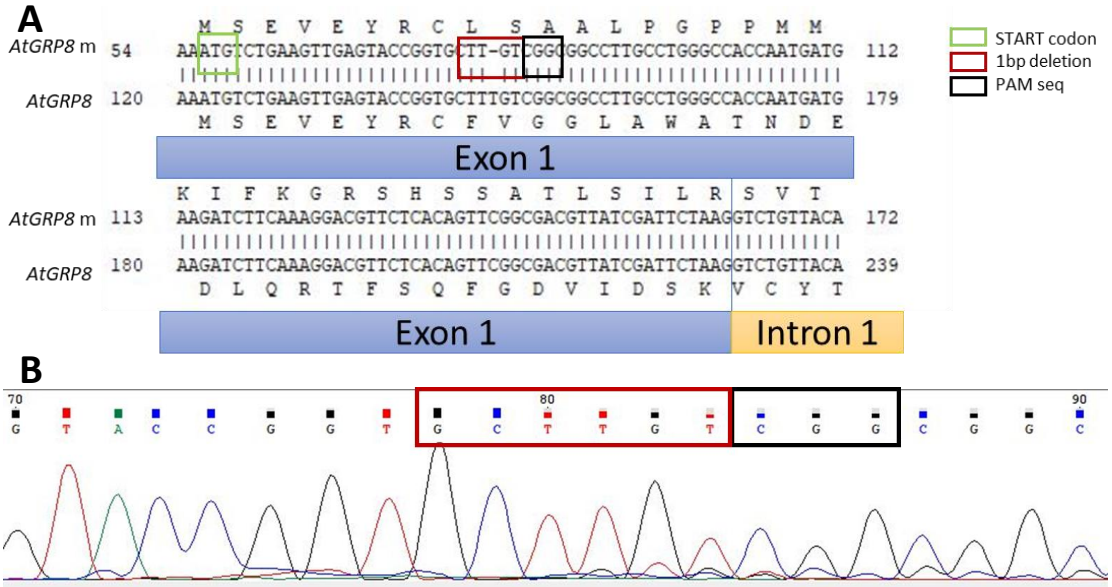

Figure 5.41 Sequence confirmation of 1 bp deletion in the plant 4A1 from T_2 generation. (**A**) Sequence alignment of *AtGRP8* (endogenous *GRP8*) and *AtGRP8* m (mutated *GRP8* in T_2 plant 4A1). (**B**) Chromatogram from DNA sequencing of *GRP8* DNA fragment isolated from the plant 4A1. Blue boxes - the first exon in *AtGRP8,* yellow box - the first intron in *AtGRP8.* Green frame - ATG sequence, red frame - the lack of one thymine, black frame - CGG, the PAM sequence.

DNA sequencing of the mutation in line 4A14 revealed a homozygous 2 bp deletion causing a frame shift that results in a premature stop codon. The resulting truncated protein would only be 17 amino acids long, whereas the endogenous GRP8 is built of 169 amino acids (Figure 5.42).

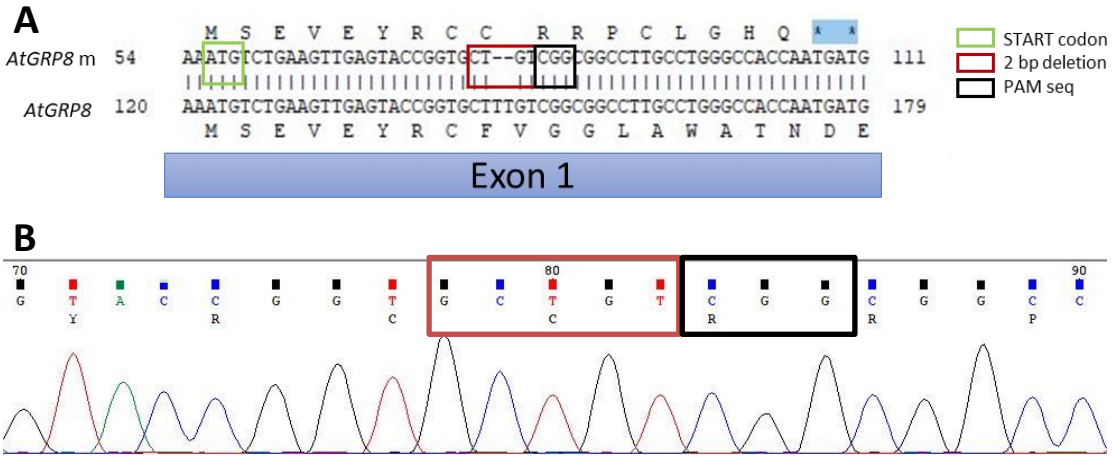

Figure 5.42 Sequence confirmation of 2 bp deletion in the plant 4A14 from T_2 generation. (**A**) Sequence alignment of *AtGRP8* (endogenous *GRP8*) and *AtGRP8* m (mutated *GRP8* in T_2 plant 4A14). (**B**) Chromatogram from DNA sequencing of

GRP8 DNA fragment isolated from the plant 4A14. Blue boxes - the first exon in *AtGRP8.* Green frame - ATG sequence, red frame - the lack of two thymines, black frame - CGG, the PAM sequence.

For line 33A9, the sequence alignment of mutated and endogenous *GRP8* sequences showed that 33A9 carried a 1 bp deletion, causing a frame shift and resulting in a different amino acid chain compared to the endogenous GRP8 protein (Figure 5.43). However, the chromatogram from 33A9 DNA sequencing showed that the analysed line is a heterozygous mutant. Therefore, to find a homozygous mutant, it would be necessary to examine the next generation of 33A9.

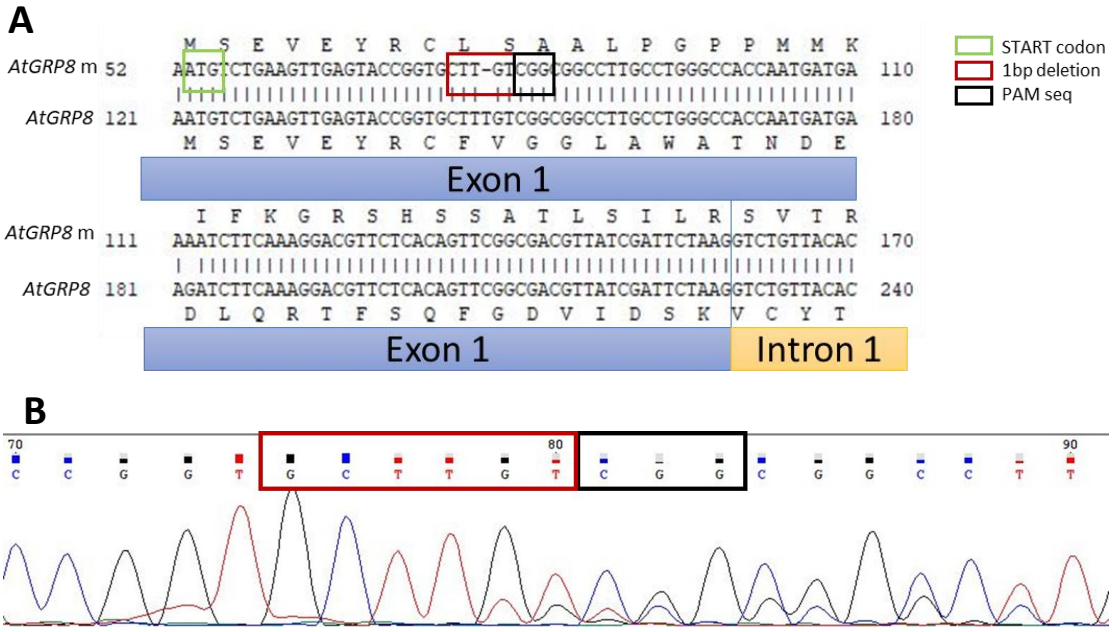

Figure 5.43 Sequence confirmation of 1 bp deletion in the plant 33A9 from T_2 generation. (**A**) Sequence alignment of *AtGRP8* (endogenous *GRP8*) and *AtGRP8* m (mutated *GRP8* in T_2 plant 33A9). (**B**) Chromatogram from DNA sequencing of *GRP8* DNA fragment isolated from the plant 33A9. Blue boxes - the first exon in *AtGRP8,* yellow box - the first intron in *AtGRP8.* Green frame - ATG sequence, red frame - the lack of one thymine, black frame - CGG, the PAM sequence

Moreover, it has been previously shown that the double mutant *prmt5 x grp7-1* flowers later than *grp7-1* and much later than Col-0 (Christine Nolte and Frederik Dombert, unpublished). Late flowering was also observed in the homozygous *prmt5-5 x grp7-1 grp8* (4A14) triple mutant, which flowers later than *prmt5-5 x grp7-1* (Figure 5.44). The beginning of flowering in *prmt5 x grp7-1 grp8* mutants was observed after 6 months of growth and the seeds were ready to harvest after another 3 months. The late flowering phenotype, which was observed in *prmt5 x grp7-1 grp8,* had been previously described in our laboratory for the *prmt5 x grp7-1* 8i mutant (Christine Nolte and Frederik Dombert, unpublished). Although a comparative experiment has not been

performed yet, it seems that the effect observed in the RNAi line was not as strong as in the CRISPR Cas line.

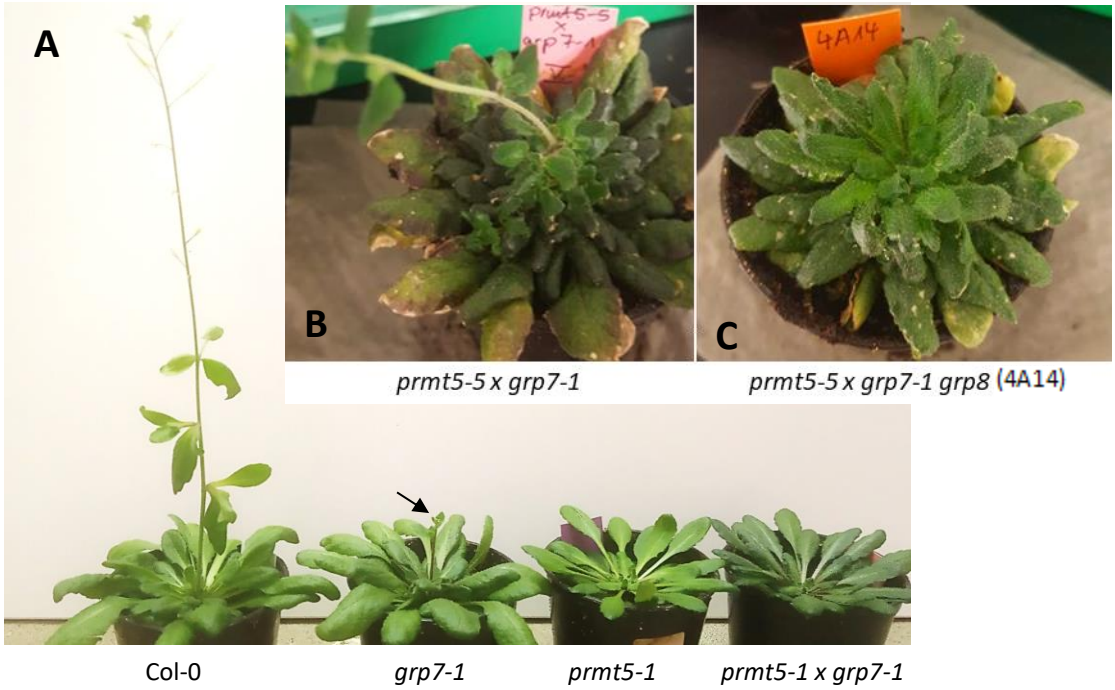

Figure 5.44 Phenotype of homozygous *prmt5-5 x grp7-1/grp8* mutant 4A14. (**A**) Double mutants *prmt5-1 x grp7-1* flower later than Col-0 and *grp7-1*. Picture of 12-week-old plants grown under short-day conditions. An arrow points a shoot apex of *grp7-1* (**B** and **C**) Pictures of 15-week-old plants *prmt5-5 x grp7-1* and *prmt5-5 x grp7-1/grp8* (4A14), grown under long-day conditions. Pictures B and C were kindly provided by Pia Gülpen.

In conclusion, the application of CRISPR/Cas9 system for creating *prmt5 grp7 grp8* plants was successful. The majority of plants in the T_2 generation were heterozygous mutants. However, two plants were confirmed as homozygous mutants. Furthermore, it is possible that *prmt5 grp7 grp8* plants flower later than *prmt5 grp7* 8i or *prmt5 grp7* mutants. Therefore, it seems that GRP8 could have an additional influence on flowering process.

6. Discussion

PRMT5 catalyses the formation of symmetric dimethylarginine in histone and non-histone proteins. PRMT5-substrates are many RNA-processing factors including GRP7 and GRP8, which are methylated by PRMT5 at the arginine 141 residue. The lack of functional PRMT5 is directly correlated with the lack of methylation in arginine 141 in GRP7 and GRP8 (Deng et al., 2010). Both the methyltransferase PRMT5 as well as its targets GRP7 and GRP8 are involved in many physiological processes, like floral transition and response to biotic and abiotic stresses (Carpenter et al., 1994; Fu et al., 2007; Hu et al., 2019; Kim et al., 2008; Streitner et al., 2008; Wang et al., 2007; Zhang et al., 2011). PRTM5, GRP7 and GRP8 are regulated by the circadian clock and influence alternative splicing of target pre-mRNAs (Deng et al., 2010; Heintzen et al., 1994; Hong et al., 2010; Meyer et al., 2017; Sanchez et al., 2010; Schmal et al., 2013; Streitner et al., 2012).

In the work presented here, it was analysed whether PRMT5-mediated arginine methylation of GRP7 is necessary for its function in controlling flowering time, pathogen defense and salt stress response. By using transgenic plants with mutations causing amino acid exchange of arginine at the position 141 to alanine or lysine (R141A and R141K), the functionality of the non-methylated versions of GRP7 was examined. Additionally, an exchange from arginine to phenylalanine (R141F) provided a hydrocarbon chain mimicking arginine methylation in GRP7, which was used to investigate the effects of constitutive arginine methylation. Furthermore, a possible hierarchical interaction between PRMT5 and GRP7 has been investigated. Plants with altered PRMT5 or GRP7 and GRP8 levels exhibit both common and distinct changes in splicing of target transcripts. To test whether PRMT5 may affect pre-mRNA splicing of certain target transcripts via modulation of GRP7 and/or GRP8 activity, *prmt5 grp7* and *prmt5 grp7* 8i mutants were used in the alternative splicing analyses.

6.1. Methylation of arginine R141 in GRP7 does not influence flowering time

GRP7 and PRMT5 have been shown as positive regulators of flowering time. The lack of GRP7 or PRMT5 is correlated with a late flowering phenotype. On the other hand, the overexpression of GRP7 or PRMT5 results in early flowering (Streitner et al., 2008; Wang et al., 2007). GRP7 was shown to be a direct target of PRMT5 and arginine 141 in GRP7 is the only arginine methylated by PRMT5 in the GRP7 amino acid chain (Deng et al., 2010).

Experiments performed in our laboratory showed that the lack of both proteins results in an additive effect, causing later flowering in comparison to *grp7-1* and *prmt5* single mutants. Therefore, it was assumed that PRMT5 and GRP7 control the process of flowering independently (Frederik Dombert and Christine Nolte, unpublished).

The flowering time experiments performed with plants containing non-methylated versions of GRP7 ($GRP7^{R141A}$ or $GRP7^{R141K}$) and $GRP7^{R141F}$ mimicking arginine methylation revealed that the arginine methylation in GRP7 does not affect the floral transition. In all three flowering experiments, plants carrying R141A, R141K and R141F mutations presented the phenotypes of respective controls, meaning that the amino acid exchanges did not alter the floral transition process. The rosette leaf number was depended on the GRP7 level, showing a stoichiometric relation. However, no correlation between methylation status and rosette leaf number has been observed.

Recent publication shows that both GRP7 and its paralog GRP8 participate in timing of floral initiation. The miss-expression of *GRP7* and *GRP8* in *grp7-1* 8i mutant results in an additional delay in floral transition, in comparison to the late flowering *grp7-1* single mutant (Steffen et al., 2019). Furthermore, both GRP7 and GRP8 undergo negative autoregulation by alternative splicing, therefore overexpression of GRP7 is correlated with downregulation of the endogenous *GRP7* transcripts. On the other hand, GRP7 and GRP8 promote alternative splicing of the reciprocal transcripts, thus overexpression of GRP7 decreases the number of functional *GRP8* transcripts (Schöning et al., 2008, 2007; Staiger et al., 2003). The obtained results show that the methylation of arginine 141 does not influence GRP7 autoregulation and its cross-regulation with GRP8. In plants overexpressing mutated versions of GRP7, the transcript level of *GRP7* and *GRP8* as well as GRP8 protein level were downregulated, as it occurs in plants overexpressing wild type GRP7. The intensity of downregulation was directly correlated with the GRP7 overexpression level.
GRP7 has been shown to regulate flowering time at least partly in an *FLC*-dependent manner (Streitner et al., 2008). However, the role of GRP8 in regulating *FLC* transcript level is not clear, since *FLC* expression in *grp7-1* 8i was not found to be significantly

different from *grp7-1* (Steffen et al., 2019). Furthermore, GRP7 was shown to affect flowering time in a hierarchical interaction with FLOWERING LOCUS D (FLD) in parallel to the components of the autonomous pathway, such as FLOWERING LOCUS CA (FCA), FLOWERING LOCUS PA (FPA) and FLOWERING LOCUS KH DOMAIN (FLK) and to affect the floral initiation through alternative splicing of floral repressor *FLOWERING LOCUS M (FLM)* (Steffen et al., 2019).
On the other hand, PRMT5 has been shown to methylate H3R4 and downregulate *FLC* expression, which affects flowering time (Pei et al., 2007; Wang et al., 2007). However, other *Arabidopsis* PRMTs, like PRMT4a,4b and PRMT10 also control the flowering time in an *FLC*-dependent manner (Niu et al., 2012, 2008, 2007). Moreover, the lack of PRMT5 and PRMT10 results in an additive effect, therefore it is expected that PRMT5 and PRMT10 regulate *FLC* expression in parallel (Niu et al., 2007). In this study, the *FLC* transcript levels in plants expressing the non-methylated versions of GRP7 were also assessed. However, the status of arginine methylation in GRP7 had no influence on *FLC* levels (data not shown).
In conclusion, the presence or absence of arginine methylation in GRP7 does not influence flowering time control.

6.2. PRMT5 and GRP7 influence pathogen defense

Multiple studies showed that GRP7 acts as positive and PRMT5 as a negative regulator of plant immune response against pathogens. It has been published that the loss of function *grp7-1* mutant is more susceptible to *Pseudomonas syringae* pv. tomato DC3000 *(Pst)* and the *prmt5* mutants exhibit higher resistance against pathogen infections (Fu et al., 2007; Hu et al., 2019; Huang et al., 2016; Jeong et al., 2011). However, two days after infiltration of Col-0, *grp7-1*, *prmt5-1* and *prmt5-1 x grp7-1* plants with *Pst* DC3000, the disease symptoms were similar in all tested lines (Figure 5.14).

Furthermore, GRP7 is a substrate for the mono-ADP-ribosyltransferase *P. syringae* type III effector HopU1. By ADP-ribosylation of conserved arginine 49 in GRP7, HopU1 represses plant immunity. The arginine 49 in GRP7 is required for RNA-binding activity and an amino-acid exchange at that residue repress GRP7 binding ability, thus the mutated version of GRP7 does not rescue the *grp7-1* phenotype (Jeong et al., 2011).

It has been shown that *Pst* infection activates mitogen-activated protein kinases and calcium-depended protein kinases resulting in induced innate immunity marker genes like *FRK1* (Asai et al., 2002). Such actions can contribute to systemic acquired resistance (SAR), which is an induced immunity against subsequent pathogenic

infection. SAR promotes expression of SAR marker genes such as pathogenesis-related (PR) genes (Thomma et al., 2001).

To assess the *Pst*-triggered defense, the expression levels of the early response gene *FRK1* were analysed. Korneli and co-workers showed that in plants after infiltration with *Pst* DC3000, *FRK1* transcript levels are time dependent (Korneli et al., 2014). The highest *FRK1* enrichment was detected 4 h after infiltration, which was in accordance with the results established in our laboratory (Christane Nöh, unpublished).

Due to the fact that GRP7 positively regulates plant immune responses, the lack of GRP7 in *grp7-1* mutant should negatively affect the *FRK1* upregulation after *Pst* infiltration. However, the *FRK1* transcript levels in Col-0 and *grp7-1* were not significantly different (Figure 5.17). Furthermore, PRMT5 has been shown to influence pathogen defense negatively, therefore its lack should increase the *FRK1* expression level. However, the *FRK1* expression levels in *prmt5-1* were not significantly different from Col-0. Interestingly, the enrichment of *FRK1* after *Pst* infiltration was significantly lower in *prmt5-1 x grp7-1,* in comparison to Col-0, showing an additive effect of the results obtained in this study for *prmt5-1* and *grp7-1* single mutants (Figure 5.17).

Moreover, the lack of GRP7 in *grp7-1* was shown to be related to a lower expression level of the late response gene *PR1* in comparison to Col-0 after *Pst* infiltration (Streitner et al., 2012). However, in the presented study, *PR1* expression levels in Col-0 and *grp7-1* were not significantly different (Figure 5.17). Furthermore, according to Huang et al., 2016, the pathogen infection should increase *PR1* expression level to a larger extent in *prmt5* mutant than in Col-0, but no significant difference was observed in this study. Interestingly, the transcript level of *PR1* detected in *prmt5-1 x grp7-1* plants resemble *prmt5-1* pattern.

The observed *PR1* and *FRK1* transcript levels were not in accordance with the published data. Biotic stresses are characterized by lower reproducibility of results compared to abiotic stresses. In the presented work, the experimental settings were the same for all biological replicates. However, the infiltrations were performed on 5-6-week-old plants. Therefore, the age of plants was different between the biological replicates. To provide the same handling, all plants were syringe-infiltrated by one person, thus the time points of single plant infiltrations were not equal. The preparation of *Pst* solution used for plant infiltration was based on a measured optical density of bacterial culture. Hence, it is possible that use of flg22, a peptide fragment of flagellin, which triggers an innate immune response, could provide clearer and more consistent results.

Recently published data shows that PRMT5 act as a negative regulator of plant immune response against *P. syringae*. Thus after bacterial infection, *PRMT5* transcript level and

protein level decrease rapidly. The reduced PRMT5 level is linked with a lower arginine methylation level in PRMT5-target ARGONAUTE 2 (AGO2), which prevents degradation of AGO2 and AGO2-associated sRNAs (Hu et al., 2019). It is possible that arginine methylation in GRP7 mediated by PRMT5 also influence pathogen resistance in plants, therefore additional experiments are required.

6.3. GRP7 and PRMT5 influence plant survival under salt stress conditions

6.3.1. GRP7 and PRMT5 impact the germination rate under salt stress conditions

Apart from the participation in flowering time control and pathogen defense, PRMT5 and GRP7 are also known as regulators of the germination process. The influence of both proteins on germinating seeds was analysed by using crosses between *prmt5-1* and *grp7-1*. The importance of the PRMT5-mediated methylation of arginine 141 in GRP7 for the same process was analysed with non-methylated versions of GRP7.

PRMT5 and GRP7 control germination under high salt stress in a hierarchical manner

In the germination assays described in this thesis, *grp7-1* seeds germinated faster than Col-0 seeds under salt stress conditions, suggesting that under high salinity GRP7 might act as a negative regulator of germination. The obtained results are analogous to previous studies, demonstrating that the lack of GRP7 is directly correlated with a better germination rate under salt stress conditions. Kim and co-workers showed that *grp7* knock-out and knock-down mutants germinate faster under salt stress conditions than Col-0. They also reported that the germination rate of GRP7ox seeds was much lower compared to Col-0 (Kim et al., 2008). Interestingly, similar observations have been made by analysing *A. thaliana* Col-0 plants overexpressing *Medicago sativa GRP* (Long et al., 2013).

Although no differences were visible under normal growth conditions between 14-day-old Col-0 and *grp7-1* seedlings*,* the growth retardation was already noticeable for *prmt5-1* and *prmt5-1 x grp7-1* seedlings (Figure 5.18)*,* in accordance with previous studies on *prmt5* mutants (Pei et al., 2007; Wang et al., 2007). Interestingly, Yue and co-workers showed that PRMT5 decreases *CORYNE (CRN)* expression levels by dimethylation of H4R4, which is important for the correct development of the shoot apical meristem (SAM). In *prmt5* mutants, the SAM size is smaller, which is probably why we were able to observe differences between Col-0, *prmt5-1* and *prmt5-1 x grp7-1* seedlings (Figure 5.18).

On the other hand, under salt stress conditions, the loss of function *prmt5-1* mutant seeds germinated slower than Col-0 seeds, suggesting that PRMT5 act as a positive regulator of the germination process. Similar results have been published by Zhang et al., 2011 and Hu et al., 2017, who showed that *prmt5* mutants exhibit a hypersensitive phenotype to salt stress.
The *prmt5-1 x grp7-1* mutant clearly displayed the same sensitivity to salt stress as the *prmt5-1* mutant, rather than the *grp7-1* resistance. The results from these germination assays suggest that *PRMT5* possibly is epistatic to *GRP7*. Due to the fact that the biggest differences between plant lines were observed on day 2, it would definitely be worth to test the GRP7 level at that physiological stage. However, many seeds would be needed to meet the methodological requirements.

PRMT5-mediated arginine methylation in GRP7 does not influence germination

In contrast to the results from the *prmt5-1 x grp7-1* germination assay described above, arginine methylation in GRP7 did not appear to impact the germination process. It seems that the lack of methylation at the position 141 in GRP7 does not influence the analysed developmental process. The non-methylated variants of GRP7 germinated as fast as the respective control. A possible explanation could be that arginine 141 in GRP7 is not methylated during the germination process. Therefore, it would be interesting to investigate this in the future.

6.3.2. PRMT5 influences the primary root length independently of GRP7

As salt stress influenced the germination process in *prmt5-1* mutants, the primary root development was also assessed. Li and co-workers showed that the lack of PRMT5 is responsible for DNA damage-induced cell death of stem cells in the *prmt5* root meristem (Li et al., 2016). In the work presented here, the length of primary roots of *prmt5-1* seedlings was 53% of wild type roots. Under salt stress conditions, the root length of wild type and *prmt5-1* seedlings grown on medium supplemented with 100 mM NaCl was 48% and 39% of the seedlings grown on control plates, respectively. The obtained results are similar to the results from other publications, which showed that *prmt5* seedlings grown on control medium have shorter roots than wild type. Moreover, the primary roots growing on medium supplemented with 100 mM NaCl reach only 20% of their normal length in *prmt5,* but 40-50% in wild type (Hu et al., 2017; Zhang et al., 2011). This is consistent with another study showing that under salt stress (100 mM NaCl) *prmt5* roots can grow up to 30% of their normal length and wild type up to 80% (Hernando et al., 2015). These results demonstrate that the *prmt5* mutant is hypersensitive to salt stress, indicating that PRMT5 is required for proper development of the root system under control and salt stress conditions.

As the lack of GRP7 under salt stress conditions influenced the germination process, the primary root development was also evaluated in *grp7-1* mutants. It has been shown that *At*GRP7 is present in both the nucleus and cytoplasm of the root cells (Kim et al., 2008) and its protein levels transiently increase in roots under salt stress (Jiang et al., 2007). Moreover, similar effect was described in *Solanum lycopersicum* L., where the salt stress also elevated the GRP7 protein levels in roots from Levovil and Roma genotypes (Manaa et al., 2011).

Despite of the potential impact of GRP7 on the root development under salt stress conditions, no influence of GRP7 on the primary root length has been observed. In this study, wild type and *grp7-1* seedlings developed primary roots with similar lengths under control and stress conditions. Analyses of the importance of arginine methylation in GRP7 for the primary root length showed no significant difference between GRP7-GFP seedlings and their non-methylated versions GRP7^{R141A}-GFP and GRP7^{R141K}-GFP. The observation that GRP7 is not involved in primary root development is consistent with the fact that the primary root length of *prmt5-1 x grp7-1* seedlings resembled that of *prmt5-1* under control or salt stress conditions. Therefore, the same root length in *prmt5-1* and *prmt5-1 x grp7-1* is not caused by hierarchical interactions between GRP7 and PRMT5, but rather by the fact that only PRMT5 is involved in the examined process.

In conclusion, PRMT5 appears to be a positive regulator of germination and primary root growth under salt stress conditions, what is well correlated with the salt-sensitive phenotype of *prmt5* mutants. In contrast, *grp7-1* mutants displayed salt resistance. The presented results imply that GRP7 negatively influences plant survival under salt stress conditions during the germination process, however it does not play an important role in the primary root development. According to both germination and primary root length analyses, the lack of methylation in arginine 141 in GRP7 does not affect any of the tested developmental process.

6.4. GRP7 and PRMT5 influence alternative splicing of *AKIN11* and *VFP5*

As it has been already shown, GRP7 influences AS of its own transcripts and other pre-mRNA-targets (Schöning et al., 2008, 2007; Streitner et al., 2012). Splicing defects in hundreds of genes detected in *prmt5* mutants contributed to determination of PRMT5 as an important regulator of AS (Deng et al., 2010; Sanchez et al., 2010).

By analysing data from Streitner et al., 2012 and Sanchez et al., 2010, which were obtained through high-resolution RT-PCR AS panels, four splicing events with altered isoform ratios in both *prmt5* and *grp7-1* mutants were identified. They were an alternative 3'ss within the second intron of the *FYD* 5'UTR region, an alternative 5' ss

within the first intron in the *AKIN11* 5'UTR region, skipping of exon 2 in *VFP5* and skipping of exons 5 and 6 in *AFC2*. Due to technical limitations, the assessment of the influence of GRP7, GRP8 and PRMT5 on AS was possible only for splicing events in *AKIN11* and *VFP5*.

AKIN11 encodes the α-subunit of the SNF1-related protein kinase 1 (SnRK1) complex. The usage of alternative 5'ss in the untranslated region in *AKIN11*, leading to an inclusion of the part of intron 1, does not affect ORF structure. Therefore, both splice variants possibly generate the same AKIN11 protein with three domains, protein kinase domain, kinase-associated 1 (KA1) and ubiquitin-associated (UBA) (Williams et al., 2014).

VFP5 is a member of the trihelix family of transcription factors that binds to the virulence protein effector VirF with F-box domain, required during *Agrobacterium* infection. The role of VFP5 is not clear. However, it was shown that VFP5 and its homolog VFP3 control expression level of many genes involved in wide range of cellular processes, suggesting that VFP3 and VFP5 are involved in regulation of plant cell homeostasis (García-Cano et al., 2015). A recent study showed that *VFP5* is upregulated during salicylic acid (SA)-response (Hickman et al., 2019). Another study showed that VFP5 (EIN2 NUCLEAR ASSOCIATED PROTEIN 2 (ENAP2)) interacts with the positive regulator of ethylene signalling ETHYLENE INSENSTIVE 2 (EIN2) *in vitro* (Zhang et al., 2016), which is involved in salt and osmotic stress tolerance, heat tolerance and stomatal closure (Cao et al., 2007; Kazan, 2015; Suzuki et al., 2005). Moreover, *ein2* mutants display salt sensitivity, suggesting that EIN2 promotes plant tolerance to high salinity (Cao et al., 2007). Recently, *VFP5* was found to be differentially alternatively spliced after 3 h upon cold treatment (Calixto et al., 2018). *VFP5* expression is also suppressed after 3-9 h (Calixto et al., 2018; Zhao et al., 2016), suggesting that *VFP5* might be a cold-response gene.
The skipping of exon 2 in *VFP5* is a result of alternative splicing of intron 2 and 3. In *VFP5*, exon 2 encodes the C-terminus and part of the 3'UTR. The transcript including exon 2 encodes the full-length VFP5 protein consisting of 249 amino acids. The lack of exon 2 causes a 9 bp difference in the length of the CDS, resulting in 246 amino acids, where the first 242 amino acids are identical for both VFP5 protein variants. However, the role of different *VFP5* splice isoforms has not been described yet.

The analyses of selected splicing events for *AKIN11* and *VFP5* in *prmt5 x grp7-1* and *prmt5 x grp7-1* 8i mutants showed that the detected isoform ratios resemble those of *prmt5* single mutants. The fact that the predicted additive effect was not observed suggests hierarchical interactions between *PRMT5* and *GRP7*. It is possible that *PRMT5*

is epistatic to *GRP7* and by participating in AS regulation, they influence isoform ratios of their RNA-targets.

Moreover, it seems that the lack of PRMT5 rather than the lack of GRP7 is more important for *AKIN11* and *VFP5* pre-mRNAs splicing. A stronger shift towards alternative splicing variants was always detected in plants lacking functional PRMT5.

6.5. GRP7 and PRMT5 influence alternative splicing under salt stress conditions

Data obtained in the alternative splicing experiments under salt stress was compared to data from the alternative splicing experiment (chapter 6.4) as well as to the results from the publications of Sanchez et al., 2010 and Streitner et al., 2012. Due to the fact that the experiments were performed under different growth conditions and the control samples were treated in different ways, the percentages of isoform ratios are not always equal between the experiments.

PRMT5 and GRP7 have a distinct impact on alternative splicing of *FLK, AKIN11* and *VFP5* under salt stress conditions

FLK is an RNA binding protein, which positively regulates flowering time by decreasing *FLC* expression (Lim et al., 2004). Moreover, it has been shown that FLK might be involved in maintaining plant growth under salt stress conditions (Julkowska et al., 2016). The tested splicing event, intron 1 retention in *FLK* transcripts, has been shown as a splicing defect reducing the number of functional *FLK* transcripts and therefore functional FLK protein (Deng et al., 2010). Recently, *FLK* was found to be rapidly regulated by AS, decreasing the intron 1 retention within *FLK* transcripts under cold treatment (Calixto et al., 2018). As it was published by Deng and co-workers, the lack of PRMT5 results in a higher percentage of *FLK* transcripts with retained intron 1, compared to wild type. In the work presented here, such a correlation was observed in *prmt5-1, prmt5-5, prmt5-1 x grp7-1* and *prmt5-5 x grp7-1* 8i. The application of salt stress shifted the *FLK* isoform ratios towards the alternative isoform in all four above mentioned lines. However, no significant difference in *FLK* isoform ratio was observed between Col-0, *grp7-1* and *grp7-1* 8i. Therefore, it is assumed that GRP7 and GRP8 do not influence AS of *FLK* under normal and salt stress conditions. Hence, the effect observed in *prmt5-1 x grp7-1* and *prmt5-5 x grp7-1* 8i is not a result of the hierarchical interactions between PRMT5 and GRP7/GRP8 but rather comes from the fact that only PRMT5 participates in *FLK* pre-mRNA splicing.

It has been previously shown that *AKIN11,* encoding the α-subunit of the SNF1-related protein kinase 1 (SnRK1) complex, is a direct target of GRP7 and its AS is regulated by

GRP7 (Streitner et al., 2012). In this thesis, miss-expression of *GRP7* or both *GRP7* and *GRP8* decreased the usage of an alternative 5' ss within the first intron in the *AKIN11* 5'UTR region, similar to the data described in Streitner et al., 2012. Moreover, Streitner and co-corkers showed that the opposite isoform ratio can be observed in plants overexpressing GRP7 (Streitner et al., 2012). These findings suggest that the binding between GRP7 and *AKIN11* pre-mRNA might be relevant to AS of *AKIN11*. In contrast, the lack of PRMT5 was correlated with a prevailing usage of an alternative 5'ss in *AKIN11*, as it was described by Sanchez et al., 2010, suggesting the opposite role of PRMT5 and GRP7 in AS of *AKIN11*. Interestingly, the additive effect was not observed in *prmt5-1 x grp7-1* and *prmt5-5 x grp7-1* 8i. Instead, double and triple mutants displayed the isoform ratios recorded for the single *prmt5* mutants, suggesting that the *PRMT5* gene could be epistatic to *GRP7*.
Under salt stress, in most cases the average usage of an alternative 5' ss increased ~20%, suggesting that salt stress positively stimulates AS of *AKIN11* pre-mRNA. It seems that GRP7 promotes and PRMT5 decreases usage of the alternative 5'ss within *AKIN11*, respectively and the salt stress has an additional impact on that process. However, not all abiotic stresses affect AS of *AKIN11* in the same direction. Streitner and co-workers showed that the temperature change (from 20°C to 16°C) correlates with the decreasing usage of an alternative 5' ss within the first intron in the *AKIN11* 5'UTR region (Streitner et al., 2013). Interestingly, AKIN11 and its homolog AKIN10 have been shown also to control responses to darkness, sugar and other abiotic stresses (Baena-González et al., 2007), suggesting that AKIN11 contributes to many different stress responses.

Furthermore, according to Streitner et al., 2012, the skipping of exon 2 in *VFP5* was expected to appear more often in Col-0 than *grp7-1* 8i mutant. However, no difference in *VFP5* isoform ratios has been noted between Col-0 and *grp7-1* or *grp7-1* 8i. On the other hand, the lack of PRMT5 was linked with the almost complete skipping of exon 2 in *VFP5,* as published by Sanchez et al., 2010. It has been shown that the skipping of exon 2 in *VFP5* rapidly increases under cold treatment (Calixto et al., 2018). Salt stress also increased the skipping of exon 2 in *VFP5* in all lines, which shows the influence of applied stress to AS of *VFP5*. The lack of GRP7 caused a smaller increase of the isoforms without exon 2, in comparison to wild type under salt stress conditions. This could suggest that GRP7 is relevant to AS of *VFP5* under salt stress, but probably not under normal conditions.

In conclusion, the lack of PRMT5 influenced all tested splicing events, confirming the data from Sanchez et al., 2010. On the other hand, GRP7 seemed to have very little impact on AS of *FLK*. It has been shown that increased intron 1 retention within *FLK* transcripts, which occured under salt stress, can decrease FLK protein level and

therefore delay flowering (Deng et al., 2010). Possibly, a delay of flowering initiation could be favourable under high salinity (Kazan and Lyons, 2016; Kim et al., 2007). Moreover, the obtained here results support the conclusions from Steffen et al., 2019 that FLK and GRP7 regulate flowering time independently.

The analyses of *VFP5* alternative transcripts did not display the expected shifts in isoform ratios in *grp7-1* or *grp7-1* 8i. However, lack of PRMT5 promoted skipping of exon 2 in *VFP5*. It has been shown that VFP5 interact with the positive regulator of ethylene signalling EIN2, essential for stress responses (Cao et al., 2007; Kazan, 2015; Suzuki et al., 2005; Zhang et al., 2016). At the moment, the function of different *VFP5* isoforms is still unclear. Therefore, it would be very interesting to check how alternative VFP5 protein isoforms influence plant response to salt stress.

However, AS of *AKIN11* was antagonistically influenced by the lack of GRP7 and PRMT5, in accordance with previous publications (Sanchez et al., 2010; Streitner et al., 2012). Important insight into AS of *AKIN11* brought the analyses of *prmt5-1 x grp7-1* and *prmt5-5 x grp7-1* 8i, which showed that the lack of PRMT5 influences the AS event more than the lack of GRP7 or GRP8. The obtained results support the prediction of the hierarchical relation between PRMT5 and GRP7/GRP8. Although, the usage of alternative 5'ss in intron 1 within 5'UTR region does not change ORF structure, the function of the alternative isoform is not known yet and it would be interesting to examine this in the future. A study from 2014 showed that intron retention within 5'UTR in *ZINC-INDUCED FACILITATOR 2* (*ZIF2)* can increase its own protein expression level to enhance zinc tolerance in *A. thaliana* (Remy et al., 2014). Therefore, it would be interesting to examine, whether alternative isoform of *AKIN11* affects translation of its own mRNA as well.

Lastly, the salt stress affected all analysed splicing events in all lines by shifting the isoform ratios towards the alternative variants. The obtained results are consistent with the genome-wide analysis in *A. thaliana,* which showed that salt stress conditions increase AS to regulate genes related to stress responses and RNA splicing (Ding et al., 2014). A recent study on *A. thaliana* upon cold stress showed that a plant response to low temperature requires genome-wide changes at the transcription level and AS (Calixto et al., 2018). Similarly in other plant species, an extensive AS and a differential expression of number of genes are a part of the response to salt stress (Zhu et al., 2018), heat stress (Kannan et al., 2018), drought (Thatcher et al., 2016) and pathogen infection (Bedre et al., 2019). This shows that stress can influence AS and modulate the number of functional transcripts for a dynamic plasticity in constantly changing environmental conditions.

The methylation status in arginine 141 in GRP7 might influence alternative splicing of *AKIN11* under salt stress

GRP7 and FLK regulate flowering time in parallel (Steffen et al., 2019). As it was shown in the previous alternative splicing experiment, GRP7 does not influence AS of *FLK*. Moreover, this thesis shows that the methylation status in arginine 141 in GRP7 does not have an impact on AS of *FLK* under normal growth conditions and salt stress.
Furthermore, the skipping of exon 2 in *VFP5* seems not to be influenced by GRP7 under normal growth conditions. However, under salt stress, the lack of GRP7 possibly increases the number of shorter isoforms without exon 2 (Figure 5.32). Nevertheless, the lack of methylation in arginine 141 in GRP7 seems to be irrelevant to the *VFP5* isoform ratio.
Finally, this thesis shows that the usage of an alternative 5' ss within the first intron in the *AKIN11* 5'UTR region appears to be affected not only by the lack of GRP7 but also by the lack of methylation in arginine 141 in GRP7 under salt stress conditions (Figure 5.32).

In conclusion, the collected results suggest that AS of *AKIN11*, direct target of GRP7, might be influenced antagonistically by PRMT5 and GRP7. Moreover, the methylation status of arginine 141 in GRP7 could possibly in addition affect the mentioned process.

6.6. Late flowering of *prmt5 grp7 grp8* triple mutants

The CRISPR/Cas9 system was successfully used to introduce mutations into the *GRP8* sequence. Although the majority of the plants in the T_2 generation had heterozygous mutations, four potential homozygous plants were identified (4A1, 4A5, 4A14 and 33A9) and homozygous mutations in *GRP8* were confirmed for two of them (4A1 and 4A14). As sequencing results showed, the T_2 plants *prmt5-5 grp7-1 grp8* 4A1 and 4A14 carried a 1 bp and 2 bp deletion in the *GRP8* sequence, respectively.

Although no detailed characterization of the triple mutant compared to double mutant has been performed yet, preliminary experiments showed that the *prmt5 grp7 grp8* plants have a late flowering phenotype, later than *prmt5 grp7* mutants. If this early observation can be confirmed, then it would mean that the *prmt5 grp7 grp8* mutant shows an additive effect, where all three genes *PRMT5*, *GRP7* and *GRP8* are involved in the flowering time control. This observation goes along with the recently published results for *grp7-1* 8i, which show that the miss-expression of *GRP8* additionally delays the floral initiation (Steffen et al., 2019). Moreover, according to our early observations, *prmt5 grp7 grp8* plants could possibly flower later than *prmt5 grp7* 8i plants. However, respective experiments have to be performed to confirm this.

6.7. Conclusions and future perspectives

The role of the methylation status of arginine 141 in GRP7 was analysed at the different developmental stages and under different physiological conditions. However, the methylation status of arginine 141 in GRP7 seemed irrelevant to GRP7 functionality in all tested physiological responses. The arginine methylation is not a constant protein modification, but subject to change under different conditions. Therefore, methylation status in GRP7 should be first evaluated across plant development and under different stress conditions to well formulate experimental questions.

This study shows that the germination process is affected by PRMT5 and GRP7. However, the determination of the possible interaction between both needs further investigation, since the methylation status of arginine was not relevant to seed germination under salt stress conditions.

On the other hand, the collected results from alternative splicing assays imply that PRMT5 regulates the functionality of GRP7 protein for regulating pre-mRNA splicing of certain transcripts, such as *AKIN11*, possibly via arginine methylation. The possible interaction between GRP7 and PRMT5 might bring an additional plasticity in alternative splicing, which could influence the proteome complexity.

The possible interaction between PRMT5 and GRP7 requires a detailed study. It would be interesting to test whether the interaction between both proteins influences their binding ability to certain targets. The results from the germination-assays and the alternative splicing experiments prompted us to use RNA immunoprecipitation approach and test the GRP7 ability to binding to its own transcripts in *prmt5* mutant. Although, the obtained data was ambiguous and uncertain, some tendency was observed, which suggested that the lack of PRMT5 could negatively affect GRP7 ability to binding to its own targets (data not shown). However, a further investigation would be required to confirm this premature data.

In conclusion, the functionality of GRP7, GRP8 and PRMT5 is essential for proper plant development and the response to environmental stimuli. However, the exact interaction and relation between the methyltransferase PRMT5 and its targets GRP7 and GRP8 remains unclear.

Bibliography

Adams S., Manfield I., Stockley P. and Carré I.A. 2015. Revised Morning Loops of the Arabidopsis Circadian Clock Based on Analyses of Direct Regulatory Interactions. PLoS One 10: 1–11.

Ahmad A. and Cao X. 2012. Plant PRMTs broaden the scope of arginine methylation. J. Genet Genomics 39: 195–208.

Alabadí D., Oyama T., Yanovsky M.J., Harmon F.G., Más P. and Kay S.A. 2001. Reciprocal regulation between TOC1 and LHY/CCA1 within the Arabidopsis circadian clock. Science 293: 880–883.

Alonso J.M., Stepanova A.N., Leisse T.J., Kim C.J., Chen H., Shinn P., Stevenson D.K., Zimmerman J., Barajas P., Cheuk R., Gadrinab C., Heller C., Jeske A., Koesema E., Meyers C.C., Parker H., Prednis L., Ansari Y., Choy N., Deen H., Geralt M., Hazari N., Hom E., Karnes M., Mulholland C., Ndubaku R., Schmidt I., Guzman P., Aguilar-Henonin L., Schmid M., Weigel D., Carter D.E., Marchand T., Risseeuw E., Brogden D., Zeko A., Crosby W.L., Berry C.C. and Ecker J.R. 2003. Genome-wide insertional mutagenesis of Arabidopsis thaliana. Science 301: 653–657.

Amente S., Napolitano G., Licciardo P., Monti M., Pucci P., Lania L. and Majello B. 2005. Identification of proteins interacting with the RNAPII FCP1 phosphatase: FCP1 forms a complex with arginine methyltransferase PRMT5 and it is a substrate for PRMT5-mediated methylation. FEBS Lett. 579: 683–689.

Ancelin K., Lange U.C., Hajkova P., Schneider R., Bannister A.J., Kouzarides T. and Surani M.A. 2006. Blimp1 associates with Prmt5 and directs histone arginine methylation in mouse germ cells. Nat. Cell Biol. 8: 623–630.

Anne J., Ollo R., Ephrussi A. and Mechler B.M. 2007. Arginine methyltransferase Capsuleen is essential for methylation of spliceosomal Sm proteins and germ cell formation in Drosophila. Development 134: 137–146.

Asai T., Tena G., Plotnikova J., Willmann M.R., Chiu W., Gomez-Gomez L., Boller T., Ausubel F.M. and Sheen J. 2002. MAP kinase signalling cascade in Arabidopsis innate immunity. Nature 415: 977–983.

Baena-González E., Rolland F., Thevelein J.M. and Sheen J. 2007. A central integrator of transcription networks in plant stress and energy signalling. Nature 448: 938–942.

Baker B., Zambryski P., Staskawicz B. and Dinesh-Kumar S.P. 1997. Signaling in plant-microbe interactions. Science 276: 726–33.

Barak S., Tobin E.M., Andronis C., Sugano S. and Green R.M. 2000. All in good time : the Arabidopsis circadian clock. Trends Plant Sci. 5: 517–522.

Barrero J.M., González-Bayón R., Del Pozo J.C., Ponce M.R. and Micol J.L. 2007. INCURVATA2 encodes the catalytic subunit of DNA polymerase α and interacts with genes involved in chromatin-mediated cellular memory in Arabidopsis thaliana. Plant Cell 19: 2822–2838.

Barta A., Kalyna M. and Reddy A.S.N. 2010. Implementing a rational and consistent nomenclature for serine/arginine-rich protein splicing factors (SR proteins) in plants. Plant Cell 22: 2926–2929.

Bechtold N. and Pelletier G. 1998. In Planta Agrobacterium-Mediated Transformation of Adult Arabidopsis thaliana Plants by Vacuum Infiltration. Methods Mol. Biol. 82: 259–266.

Bedford M.T. and Clarke S.G. 2009. Protein Arginine Methylation in Mammals: Who, What, and Why. Mol Cell. 16: 1–13.

Bedford M.T. and Richard S. 2005. Arginine methylation: An emerging regulator of protein function. Mol. Cell 18: 263–272.

Bedre R., Irigoyen S., Schaker P.D.C., Monteiro-Vitorello C.B., Da Silva J.A. and Mandadi K.K. 2019. Genome-wide alternative splicing landscapes modulated by biotrophic sugarcane smut pathogen. Sci. Rep. 9: 8876.

Black D.L. 2003. Mechanisms of alternative pre-messenger RNA splicing. Annu. Rev. Biochem. 72: 291–336.

Black D.L. 2005. A simple answer for a splicing conundrum. Proc. Natl. Acad. Sci. 102: 4927–4928.

Blackwell E. and Ceman S. 2012. Arginine methylation of RNA-binding proteins regulates cell function and differentiation. Mol. Reprod. Dev. 79: 163–175.

Brahms H., Meheus L., de Brabandere V., Fischer U. and Lührmann R. 2001. Symmetrical dimethylation of arginine residues in spliceosomal Sm protein B/B' and the Sm-like protein LSm4, and their interaction with the SMN protein. RNA 7: 1531–42.

Branscombe T.L., Frankel A., Lee J.-H., Cook J.R., Yang Z., Pestka S. and Clarke S. 2001. PRMT5 (Janus Kinase-binding Protein 1) Catalyzes the Formation of Symmetric Dimethylarginine Residues in Proteins. J. Biol. Chem. 276: 32971–32976.

Calixto C.P.G., Guo W., James A.B., Tzioutziou N.A., Entizne J.C., Panter P.E., Knight H., Nimmo H.G., Zhang R. and Brown J.W.S. 2018. Rapid and Dynamic Alternative Splicing Impacts the Arabidopsis Cold Response Transcriptome. Plant Cell 30: 1424–1444.

Cao S., Jiang L.I., Song S., Jing R.A.N. and Xu G. 2006. AtGRP7 is involved in the regulation of abscisic acid and stress responses in Arabidopsis. Cell. Mol. Biol. Lett. 11: 526–535.

Cao W.H., Liu J., He X.J., Mu R.L., Zhou H.L., Chen S.Y. and Zhang J.S.

2007. Modulation of ethylene responses affects plant salt-stress responses. Plant Physiol. 143: 707–719.

Capovilla G., Symeonidi E., Wu R. and Schmid M. 2017. Contribution of major FLM isoforms to temperature-dependent flowering in Arabidopsis thaliana. J. Exp. Bot. 68: 5117–5127.

Carpenter C.D., Kreps J.A. and Simon A.E. 1994. Genes encoding glycine-rich Arabidopsis thaliana proteins with RNA-binding motifs are influenced by cold treatment and an endogenous circadian rhythm. Plant Physiol. 104: 1015–1025.

Cartegni L., Chew S.L. and Krainer A.R. 2002. Listening to silence and understanding nonsense: exonic mutations that affect splicing. Nat. Rev. Genet. 3: 285–98.

Chamala S., Feng G., Chavarro C. and Barbazuk W.B. 2015. Genome-wide identification of evolutionarily conserved alternative splicing events in flowering plants. Front. Bioeng. Biotechnol. 3: 33.

Chaudhary S., Jabre I., Reddy A.S.N., Staiger D. and Syed N.H. 2019. Perspective on Alternative Splicing and Proteome Complexity in Plants. Trends Plant Sci. 24: 496–506.

Cheng X., Collins R.E. and Zhang X. 2005. Structural and Sequence Motifs of Protein (Histone) Methylation Enzymes. Annu. Rev. Biophys. Biomol. Struct. 34: 267–294.

Cong L., Ran F.A., Cox D., Lin S., Barretto R., Habib N., Hsu P.D., Wu X., Jiang W., Marraffini L.A. and Zhang F. 2013. Multiplex Genome Engineering Using CRISPR/Cas Systems. Science 339: 819–823.

Costanzo S. and Jia Y. 2009. Alternatively spliced transcripts of Pi-ta blast resistance gene in Oryza sativa. Plant Sci. 177: 468–478.

Deng X. and Cao X. 2017. Roles of pre-mRNA splicing and polyadenylation in plant development. Curr. Opin. Plant Biol. 35: 45–53.

Deng X., Gu L., Liu C., Lu T., Lu F., Lu Z., Cui P., Pei Y., Wang B., Hu S. and Cao X. 2010. Arginine methylation mediated by the Arabidopsis homolog of PRMT5 is essential for proper pre-mRNA splicing. Proc. Natl. Acad. Sci. U. S. A. 107: 19114–19119.

Deng X., Lu T., Wang L., Gu L., Sun J., Kong X., Liu C. and Cao X. 2016. Recruitment of the NineTeen Complex to the activated spliceosome requires AtPRMT5. Proc. Natl. Acad. Sci. 113: 5447–5452.

Dinesh-Kumar S.P. and Baker B.J. 2000. Alternatively spliced N resistance gene transcripts: Their possible role in tobacco mosaic virus resistance. Proc. Natl. Acad. Sci. 97: 1908–1913.

Ding F., Cui P., Wang Z., Zhang S., Ali S. and Xiong L. 2014. Genome-wide analysis of alternative splicing of pre-mRNA under salt stress in Arabidopsis. BMC

Genomics 15: 431.

Dixon L.E., Knox K., Kozma-Bognar L., Southern M.M., Pokhilko A. and Millar A.J. 2011. Temporal repression of core circadian genes is mediated through EARLY FLOWERING 3 in Arabidopsis. Curr. Biol. 21: 120–125.

Dowson-Day M.J. and Millar A.J. 1999. Circadian dysfunction causes aberrant hypocotyl elongation patterns in Arabidopsis. Plant J. 17: 63–71.

El-Andaloussi N., Valovka T., Toueille M., Steinacher R., Focke F., Gehrig P., Covic M., Hassa P.O., Schär P., Hübscher U. and Hottiger M.O. 2006. Arginine Methylation Regulates DNA Polymerase β. Mol. Cell 22: 51–62.

Engelmann W., Simon K. and Phen C.J. 1992. Leaf movement rhythm in A.thaliana. Zeitschrift für Naturforsch. 47: 925–928.

Fairbrother W.G., Yeh R.-F., Sharp P.A. and Burge C.B. 2002. Predictive identification of exonic splicing enhancers in human genes. Science 297: 1007–1013.

Fauser F., Schiml S. and Puchta H. 2014. Both CRISPR/Cas-based nucleases and nickases can be used efficiently for genome engineering in Arabidopsis thaliana. Plant J. 79: 348–359.

Filichkin S., Priest H.D., Megraw M. and Mockler T.C. 2015. Alternative splicing in plants: directing traffic at the crossroads of adaptation and environmental stress. Curr. Opin. Plant Biol. 24: 125–135.

Filichkin S.A., Cumbie J.S., Dharmawardhana P., Jaiswal P., Chang J.H., Palusa S.G., Reddy A.S.N., Megraw M. and Mockler T.C. 2015. Environmental stresses modulate abundance and timing of alternatively spliced circadian transcripts in Arabidopsis. Mol. Plant 8: 207–227.

Filichkin S.A., Priest H.D., Givan S.A., Shen R., Bryant D.W., Fox S.E., Wong W. and Mockler T.C. 2010. Genome-wide mapping of alternative splicing in Arabidopsis thaliana. Genome Res. 20: 45–58.

Flor H.H. 1971. Current Status of the Gene-For-Gene Concept. Annu. Rev. Phytopathol. 9: 275–296.

Friesen W.J., Paushkin S., Wyce A., Massenet S., Pesiridis G.S., Van Duyne G., Rappsilber J., Mann M. and Dreyfuss G. 2001. The Methylosome, a 20S Complex Containing JBP1 and pICln, Produces Dimethylarginine-Modified Sm Proteins. Mol. Cell. Biol. 21: 8289–8300.

Fu Z.Q., Guo M., Jeong B., Tian F., Elthon T.E., Cerny R.L., Staiger D. and Alfano J.R. 2007. A type III effector ADP-ribosylates RNA-binding proteins and quells plant immunity. Nature 447: 284–288.

García-Cano E., Magori S., Sun Q., Ding Z., Lazarowitz S.G. and Citovsky V. 2015. Interaction of Arabidopsis Trihelix-Domain Transcription Factors VFP3 and VFP5 with Agrobacterium Virulence Protein VirF. PLoS One 10: e0142128.

Gary J.D. and Clarke S. 1998. RNA and protein interactions modulated by protein arginine methylation. Prog. Nucleic Acid Res. Mol. Biol. 61: 65–131.

Gassmann W., Hinsch M.E. and Staskawicz B.J. 1999. The Arabidopsis RPS4 bacterial-resistance gene is a member of the TIR-NBS-LRR family of disease-resistance genes. Plant J. 20: 265–277.

Gendron J.M., Pruneda-Paz J.L., Doherty C.J., Gross A.M., Kang S.E. and Kay S.A. 2012. Arabidopsis circadian clock protein, TOC1, is a DNA-binding transcription factor. Proc. Natl. Acad. Sci. 109: 3167–3172.

Godoy Herz M.A., Kubaczka M.G., Brzyżek G., Servi L., Krzyszton M., Simpson C., Brown J., Swiezewski S., Petrillo E. and Kornblihtt A.R. 2019. Light Regulates Plant Alternative Splicing through the Control of Transcriptional Elongation. Mol. Cell 73: 1066-1074.e3.

Göhring J., Jacak J. and Barta A. 2014. Imaging of Endogenous Messenger RNA Splice Variants in Living Cells Reveals Nuclear Retention of Transcripts Inaccessible to Nonsense-Mediated Decay in Arabidopsis. Plant Cell 26: 754–764.

Greenham K. and Mcclung C.R. 2015. Integrating circadian dynamics with physiological processes in plants. Nat. Publ. Gr. 16: 598–610.

Gu J., Xia Z., Luo Y., Jiang X., Qian B., Xie H., Zhu Jian-kang, Xiong L., Zhu Jianhua and Wang Z. 2018. Spliceosomal protein U1A is involved in alternative splicing and salt stress tolerance in Arabidopsis thaliana 46: 1777–1792.

Hackmann C., Korneli C., Kutyniok M., Köster T., Wiedenlübbert M., Müller C. and Staiger D. 2014. Salicylic acid-dependent and -independent impact of an RNA-binding protein on plant immunity. Plant. Cell Environ. 37: 696–706.

Halterman D.A., Wei F. and Wise R.P. 2003. Powdery Mildew-Induced Mla mRNAs Are Alternatively Spliced and Contain Multiple Upstream Open Reading Frames. Plant Physiol. 131: 558–567.

Harmer S.L., Hogenesch J.B., Straume M., Chang H.S., Han B., Zhu T., Wang X., Kreps J.A. and Kay S.A. 2000. Orchestrated transcription of key pathways in Arabidopsis by the circadian clock. Science 290: 2110–2113.

Hartmann L., Drewe-Boß P., Wießner T., Wagner G., Geue S., Lee H.-C., Obermüller D.M., Kahles A., Behr J., Sinz F.H., Rätsch G. and Wachter A. 2016. Alternative Splicing Substantially Diversifies the Transcriptome during Early Photomorphogenesis and Correlates with the Energy Availability in Arabidopsis. Plant Cell 28: 2715–2734.

Hartmann L., Wießner T. and Wachter A. 2018. Subcellular Compartmentation of Alternatively Spliced Transcripts Defines SERINE/ARGININE-RICH PROTEIN30 Expression. Plant Physiol. 176: 2886–2903.

Hassidim M., Dakhiya Y., Turjeman A., Hussien D., Shor E., Anidjar A.,

Goldberg K. and Green R.M. 2017. CIRCADIAN CLOCK ASSOCIATED1 (CCA1) and the Circadian Control of Stomatal Aperture. Plant Physiol. 175: 1864–1877.

Heintzen C., Melzer S., Fischer R., Kappeler S., Apel K. and Staiger D. 1994. A light- and temperature-entrained circadian clock controls expression of transcripts encoding nuclear proteins with homology to RNA-binding proteins in meristematic tissue. Plant J. 5: 799–813.

Helfer A., Nusinow D.A., Chow B.Y., Gehrke A.R., Bulyk M.L. and Kay S.A. 2011. LUX ARRHYTHMO encodes a nighttime repressor of circadian gene expression in the Arabidopsis core clock. Curr. Biol. 21: 126–133.

Henriques R. and Mas P. 2013. Chromatin remodeling and alternative splicing: Pre- and post-transcriptional regulation of the Arabidopsis circadian clock. Semin. Cell Dev. Biol. 24: 399–406.

Hernando C.E., Sanchez S.E., Mancini E. and Yanovsky M.J. 2015. Genome wide comparative analysis of the effects of PRMT5 and PRMT4/CARM1 arginine methyltransferases on the Arabidopsis thaliana transcriptome. BMC Genomics 16: 192.

Herrero E., Kolmos E., Bujdoso N., Yuan Y., Wang M., Berns M.C., Uhlworm H., Coupland G., Saini R., Jaskolski M., Webb A., Goncalves J. and Davis S.J. 2012. EARLY FLOWERING4 Recruitment of EARLY FLOWERING3 in the Nucleus Sustains the Arabidopsis Circadian Clock. Plant Cell Online 24: 428–443.

Hickman R., Mendes M.P., Verk M.C. Van, Dijken A.J.H. Van, Sora J. Di, Denby K., Pieterse C.M.J. and Wees S.C.M. Van 2019. Transcriptional Dynamics of the Salicylic Acid Response and its Interplay with the Jasmonic Acid Pathway. bioRxiv 742742.

Hong S., Song H.-R., Lutz K., Kerstetter R. a, Michael T.P. and McClung C.R. 2010. Type II protein arginine methyltransferase 5 (PRMT5) is required for circadian period determination in Arabidopsis thaliana. Proc. Natl. Acad. Sci. U. S. A. 107: 21211–21216.

Hsu F., Chou M., Chou S., Li Y., Peng H. and Shih M. 2013. Submergence Confers Immunity Mediated by the WRKY22 Transcription Factor in Arabidopsis. Plant Cell 25: 2699–2713.

Hu J., Yang H., Mu J., Lu T., Peng J., Deng X., Kong Z., Bao S., Cao X. and Zuo J. 2017. Nitric Oxide Regulates Protein Methylation during Stress Responses in Plants. Mol. Cell 67: 702–710.

Hu P., Zhao H., Zhu P., Xiao Y., Miao W., Wang Y. and Jin H. 2019. Dual regulation of Arabidopsis AGO2 by arginine methylation. Nat. Commun. 10: 1–10.

Huang S., Balgi A., Pan Y., Li M., Zhang X., Du L., Zhou M., Roberge M. and Li X. 2016. Identification of Methylosome Components as Negative

Regulators of Plant Immunity Using Chemical Genetics. Mol. Plant 9: 1620–1633.

Huang W., Pérez-García P., Pokhilko A., Millar A.J., Antoshechkin I., Riechmann J.L. and Mas P. 2012. Mapping the core of the Arabidopsis circadian clock defines the network structure of the oscillator. Science 336: 75–79.

Hyun Y., Kim J., Cho S.W., Choi Y., Kim J.-S. and Coupland G. 2015. Site-directed mutagenesis in Arabidopsis thaliana using dividing tissue-targeted RGEN of the CRISPR/Cas system to generate heritable null alleles. Planta 241: 271–284.

Hyun Y., Yun H., Park K., Ohr H., Lee O., Kim D.-H., Sung S. and Choi Y. 2013. The catalytic subunit of Arabidopsis DNA polymerase ensures stable maintenance of histone modification. Development 140: 156–166.

Iberg A.N., Espejo A., Cheng D., Kim D., Michaud-Levesque J., Richard S. and Bedford M.T. 2008. Arginine methylation of the histone H3 tail impedes effector binding. J. Biol. Chem. 283: 3006–3010.

Ibrahim E.C., Schaal T.D., Hertel K.J., Reed R. and Maniatis T. 2005. Serine/arginine-rich protein-dependent suppression of exon skipping by exonic splicing enhancers. Proc. Natl. Acad. Sci. 102: 5002–5007.

James A.B., Syed N.H., Bordage S., Marshall J., Nimmo G.A., Jenkins G.I., Herzyk P., Brown J.W.S. and Nimmo H.G. 2012. Alternative Splicing Mediates Responses of the Arabidopsis Circadian Clock to Temperature Changes. Plant Cell 24: 961–981.

Jansson M., Durant S.T., Cho E.C., Sheahan S., Edelmann M., Kessler B. and La Thangue N.B. 2008. Arginine methylation regulates the p53 response. Nat. Cell Biol. 10: 1431–1439.

Jeong B., Lin Y., Joe A., Guo M., Korneli C., Yang H., Wang P., Yu M., Cerny R.L., Staiger D., Alfano J.R. and Xu Y. 2011. Structure Function Analysis of an ADP-ribosyltransferase Type III Effector and Its RNA-binding Target in Plant Immunity. J. Biol. Chem. 286: 43272–43281.

Jiang J., Liu X., Liu C., Liu G., Li S. and Wang L. 2017. Integrating Omics and Alternative Splicing Reveals Insights into Grape Response to High Temperature. Plant Physiol. 173: 1502–1518.

Jiang Y., Yang B., Harris N.S. and Deyholos M.K. 2007. Comparative proteomic analysis of NaCl stress-responsive proteins in Arabidopsis roots. J. Exp. Bot. 58: 3591–3607.

Jinek M., East A., Cheng A., Lin S., Ma E. and Doudna J. 2013. RNA-programmed genome editing in human cells. Elife 2: e00471.

Johansson M. and Köster T. 2019. On the move through time – a historical review of plant clock research. Plant Biol. 21: 13–20.

Jones M.A., Williams B.A., McNicol J., Simpson C.G., Brown J.W.S. and

Harmer S.L. 2012. Mutation of Arabidopsis SPLICEOSOMAL TIMEKEEPER LOCUS1 causes circadian clock defects. Plant Cell 24: 4066–4082.

Julkowska M.M., Klei K., Fokkens L., Haring M.A., Schranz M.E. and Testerink C. 2016. Natural variation in rosette size under salt stress conditions corresponds to developmental differences between Arabidopsis accessions and allelic variation in the LRR-KISS gene. J. Exp. Bot. 67: 2127–2138.

Kaihara S. and Takimoto A. 1979. Environmental factors controlling the time of flower-opening in Pharbitis nil. Plant Cell Physiol. 20: 1659–1666.

Kannan S., Halter G., Renner T. and Waters E.R. 2018. Patterns of alternative splicing vary between species during heat stress. AoB Plants 10: ply013.

Kazan K. 2015. Diverse roles of jasmonates and ethylene in abiotic stress tolerance. Trends Plant Sci. 20: 219–229.

Kazan K. and Lyons R. 2016. The link between flowering time and stress tolerance. J. Exp. Bot. 67: 47–60.

Kim J.S., Jung H.J., Lee H.J., Kim K.A., Goh C., Woo Y., Oh S.H., Han Y.S. and Kang H. 2008. Glycine-rich RNA-binding protein7 affects abiotic stress responses by regulating stomata opening and closing in Arabidopsis thaliana. Plant J. 55: 455–466.

Kim S.G., Kim S.Y. and Park C.M. 2007. A membrane-associated NAC transcription factor regulates salt-responsive flowering via FLOWERING LOCUS T in Arabidopsis. Planta 226: 647–654.

Konarska M.M. 1998. Recognition of the 5' splice site by the spliceosome. Acta Biochim. Pol. 45: 869–881.

Kornblihtt A.R., Schor I.E., Alló M., Dujardin G., Petrillo E. and Muñoz M.J. 2013. Alternative splicing: A pivotal step between eukaryotic transcription and translation. Nat. Rev. Mol. Cell Biol. 14: 153–165.

Korneli C., Danisman S. and Staiger D. 2014. Differential control of pre-invasive and post-invasive antibacterial defense by the Arabidopsis circadian clock. Plant Cell Physiol. 55: 1613–1622.

Köster T., Meyer K., Weinholdt C., Smith L.M., Lummer M., Speth C., Grosse I., Weigel D. and Staiger D. 2014. Regulation of pri-miRNA processing by the hnRNP-like protein AtGRP7 in Arabidopsis. Nucleic Acids Res. 42: 9925–9936.

Köster T. and Staiger D. 2014. RNA-binding protein immunoprecipitation from whole-cell extracts. Methods Mol. Biol. 1062: 679–695.

Kwak Y.T., Guo J., Prajapati S., Park K.J., Surabhi R.M., Miller B., Gehrig P. and Gaynor R.B. 2003. Methylation of SPT5 regulates its interaction with RNA polymerase II and transcriptional elongation properties. Mol. Cell 11: 1055–1066.

Laloum T., Martín G. and Duque P. 2018. Alternative Splicing Control of Abiotic Stress Responses. Trends Plant Sci. 23: 140–150.

Lavigueur A., La Branche H., Kornblihtt A.R. and Chabot B. 1993. A splicing enhancer in the human fibronectin alternate ED1 exon interacts with SR proteins and stimulates U2 snRNP binding. Genes Dev. 7: 2405–2417.

Lee D.Y., Teyssier C., Strahl B.D. and Stallcup M.R. 2005. Role of protein methylation in regulation of transcription. Endocr. Rev. 26: 147–170.

Lee J., Park E., Kim G.H., Kwon I. and Kim K. 2018. A splice variant of human Bmal1 acts as a negative regulator of the molecular circadian clock. Exp. Mol. Med. 50: 159.

Leister R.T. and Katagiri F. 2000. A resistance gene product of the nucleotide binding site - Leucine rich repeats class can form a complex with bacterial avirulence proteins in vivo. Plant J. 22: 345–354.

Li Q., Zhao Y., Yue M., Xue Y. and Bao S. 2016. The Protein Arginine Methylase 5 (PRMT5/SKB1) Gene Is Required for the Maintenance of Root Stem Cells in Response to DNA Damage. J. Genet. Genomics 43: 187–197.

Li X., Jiang D.H., Yong K. and Zhang D.B. 2007. Varied transcriptional efficiencies of multiple Arabidopsis U6 small nuclear RNA genes. J. Integr. Plant Biol. 49: 222–229.

Lim M.H., Kim Joonki, Kim Y.S., Chung K.S., Seo Y.H., Lee I., Kim Jungmook, Hong C.B., Kim H.J. and Park C.M. 2004. A new arabidopsis gene, FLK, encodes an RNA binding protein with K homology motifs and regulates flowering time via Flowering Locus C. Plant Cell 16: 731–740.

Livak K.J. and Schmittgen T.D. 2001. Analysis of relative gene expression data using real-time quantitative PCR and the 2-ΔΔCT method. Methods 25: 402–408.

Long R., Yang Q. and Kang J. 2013. Overexpression of a novel salt stress-induced glycine-rich protein gene from alfalfa causes salt and ABA sensitivity in Arabidopsis 1289–1298.

Lorković Z.J. and Barta A. 2002. Genome analysis: RNA recognition motif (RRM) and K homology (KH) domain RNA-binding proteins from the flowering plant Arabidopsis thaliana. Nucleic Acids Res. 30: 623–635.

Manaa A., Ben Ahmed H., Valot B., Bouchet J.P., Aschi-Smiti S., Causse M. and Faurobert M. 2011. Salt and genotype impact on plant physiology and root proteome variations in tomato. J. Exp. Bot. 62: 2797–2813.

Mangeon A., Junqueira R.M. and Sachetto-Martins G. 2010. Functional diversity of the plant glycine-rich proteins superfamily. Plant Signal. Behav. 5: 99–104.

Marquez Y., Brown J.W.S., Simpson C., Barta A. and Kalyna M. 2012. Transcriptome survey reveals increased complexity of the alternative splicing

landscape in Arabidopsis. Genome Res. 22: 1184–1195.

Marshall C.M., Tartaglio V., Duarte M. and Harmon F.G. 2016. The arabidopsis sickle mutant exhibits altered circadian clock responses to cool temperatures and temperature-dependent alternative splicing. Plant Cell 28: 2560–2575.

Más P. 2008. Circadian clock function in Arabidopsis thaliana: time beyond transcription. Trends Cell Biol. 18: 273–281.

Mastrangelo A.M., Marone D., Laidò G., De Leonardis A.M. and De Vita P. 2012. Alternative splicing: enhancing ability to cope with stress via transcriptome plasticity. Plant Sci. 185–186: 40–49.

Mateos J.L., de Leone M.J., Torchio J., Reichel M. and Staiger D. 2018. Beyond Transcription: Fine-Tuning of Circadian Timekeeping by Post-Transcriptional Regulation. Genes (Basel). 9: E616.

McClung C.R. 2006. Plant Circadian Rhythms. Plant Cell Online 18: 792–803.

Meyer K., Koester T. and Staiger D. 2015. Pre-mRNA Splicing in Plants: In Vivo Functions of RNA-Binding Proteins Implicated in the Splicing Process. Biomolecules 5: 1717–1740.

Meyer K., Köster T., Nolte C., Weinholdt C., Lewinski M., Grosse I. and Staiger D. 2017. Adaptation of iCLIP to plants determines the binding landscape of the clock-regulated RNA-binding protein AtGRP7. Genome Biol. 18: 204.

Michael T.P. and Mcclung C.R. 2003. Enhancer trapping reveals widespread circadian clock transcriptional control in Arabidopsis. Plant Physiol. 132: 629–639.

Moore M.J., Query C.C. and Sharp P.A. 1993. Splicing of precursors to messenger RNAs by the spliceosome. In: The RNA World. pp. 303–357.

Nicaise V., Joe A., Jeong B., Korneli C., Boutrot F., Westedt I., Staiger D., Alfano J.R. and Zipfel C. 2013. Pseudomonas HopU1 modulates plant immune receptor levels by blocking the interaction of their mRNAs with GRP7. EMBO J. 32: 701–712.

Niu L., Lu F., Pei Y., Liu C. and Cao X. 2007. Regulation of flowering time by the protein arginine methyltransferase AtPRMT10. EMBO Rep. 8: 1190–1195.

Niu L., Lu F., Zhao T., Liu C. and Cao X. 2012. The enzymatic activity of Arabidopsis protein arginine methyltransferase 10 is essential for flowering time regulation. Protein Cell 3: 450–459.

Niu L., Zhang Y., Pei Y., Liu C. and Cao X. 2008. Redundant requirement for a pair of Protein Arginine Methyltransferase4 homologs for the proper regulation of Arabidopsis flowering time. Plant Physiol. 148: 490–503.

Nohales M.A. and Kay S.A. 2016. Molecular mechanisms at the core of the plant

circadian oscillator. Nat. Struct. Mol. Biol. 23: 1061–1069.

Nolte C. and Staiger D. 2015. RNA around the clock - regulation at the RNA level in biological timing. Front. Plant Sci. 6: 311.

Pahlich S., Zakaryan R.P. and Gehring H. 2006. Protein arginine methylation: Cellular functions and methods of analysis. Biochim. Biophys. Acta - Proteins Proteomics 1764: 1890–1903.

Paik W.K. and Kim S. 1967. Enzymatic methylation of protein fractions from calf thymus nuclei. Biochem. Biophys. Res. Commun. 29: 14–20.

Pal S., Vishwanath S.N., Erdjument-bromage H., Tempst P. and Sif S. 2004. Human SWI/SNF-Associated PRMT5 Methylates Histone H3 Arginine 8 and Negatively Regulates Expression of ST7 and NM23 Tumor Suppressor Genes. Mol. Cell. Biol. 24: 9630–9645.

Peart J.R., Mestre P., Lu R., Malcuit I. and Baulcombe D.C. 2005. NRG1, a CC-NB-LRR protein, together with N, a TIR-NB-LRR protein, mediates resistance against tobacco mosaic virus. Curr. Biol. 15: 968–973.

Pei Y., Niu L., Lu F., Liu C., Zhai J., Kong X. and Cao X. 2007. Mutations in the Type II protein arginine methyltransferase AtPRMT5 result in pleiotropic developmental defects in Arabidopsis. Plant Physiol. 144: 1913–1923.

Pek J.W., Anand A. and Kai T. 2012. Tudor domain proteins in development. Development 139: 2255–2266.

Pel M.J.C., van Dijken A.J.H., Bardoel B.W., Seidl M.F., van der Ent S., van Strijp J.A.G. and Pieterse C.M.J. 2014. Pseudomonas syringae evades host immunity by degrading flagellin monomers with alkaline protease AprA. Mol. Plant. Microbe. Interact. 27: 603–610.

Perez-Santángelo S., Mancini E., Francey L.J., Schlaen R.G., Chernomoretz A., Hogenesch J.B. and Yanovsky M.J. 2014. Role for LSM genes in the regulation of circadian rhythms. Proc. Natl. Acad. Sci. U. S. A. 111: 15166–15171.

Petrillo E., Godoy Herz M.A., Fuchs A., Reifer D., Fuller J., Yanovsky M.J., Simpson C., Brown J.W.S., Barta A., Kalyna M. and Kornblihtt A.R. 2014. A chloroplast retrograde signal regulates nuclear alternative splicing. Science 344: 427–430.

Posé D., Verhage L., Ott F., Yant L., Mathieu J., Angenent G.C., Immink R.G.H. and Schmid M. 2013. Temperature-dependent regulation of flowering by antagonistic FLM variants. Nature 503: 414–417.

Raczynska K.D., Simpson C.G., Ciesiolka A., Szewc L., Lewandowska D., McNicol J., Szweykowska-Kulinska Z., Brown J.W.S. and Jarmolowski A. 2009. Involvement of the nuclear cap-binding protein complex in alternative splicing in Arabidopsis thaliana. Nucleic Acids Res. 38: 265–278.

Reddy A.S.N. 2007. Alternative splicing of pre-messenger RNAs in plants in the genomic era. Annu. Rev. Plant Biol. 58: 267–294.

Reddy A.S.N., Marquez Y., Kalyna M. and Barta A. 2013. Complexity of the Alternative Splicing Landscape in Plants. Plant Cell 25: 3657–3683.

Remy E., Cabrito T.R., Batista R.A., Hussein M.A.M., Teixeira M.C., Athanasiadis A., Sá-Correia I. and Duque P. 2014. Intron Retention in the 5′UTR of the Novel ZIF2 Transporter Enhances Translation to Promote Zinc Tolerance in Arabidopsis. PLoS Genet. 10: 15–19.

Ren J., Wang Y., Liang Y., Zhang Y., Bao S. and Xu Z. 2010. Methylation of ribosomal protein S10 by protein-arginine methyltransferase 5 regulates ribosome biogenesis. J. Biol. Chem. 285: 12695–12705.

Salomé P.A. and McClung C.R. 2004. The Arabidopsis thaliana clock. J. Biol. Rhythms 19: 425–435.

Sanchez S.E., Petrillo E., Beckwith E.J., Zhang X., Rugnone M.L., Hernando C.E., Cuevas J.C., Godoy Herz M.A., Depetris-Chauvin A., Simpson C.G., Brown J.W.S., Cerdán P.D., Borevitz J.O., Mas P., Ceriani M.F., Kornblihtt A.R. and Yanovsky M.J. 2010. A methyl transferase links the circadian clock to the regulation of alternative splicing. Nature 468: 112–116.

Schaffer R., Ramsay N., Samach A., Corden S., Putterill J., Carré I.A. and Coupland G. 1998. The late elongated hypocotyl mutation of Arabidopsis disrupts circadian rhythms and the photoperiodic control of flowering. Cell 93: 1219–1229.

Schiml S., Fauser F. and Puchta H. 2014. The CRISPR/Cas system can be used as nuclease for in planta gene targeting and as paired nickases for directed mutagenesis in Arabidopsis resulting in heritable progeny. Plant J. 80: 1139–1150.

Schlaen R.G., Mancini E., Sanchez S.E., Perez-Santángelo S., Rugnone M.L., Simpson C.G., Brown J.W.S., Zhang X., Chernomoretz A. and Yanovsky M.J. 2015. The spliceosome assembly factor GEMIN2 attenuates the effects of temperature on alternative splicing and circadian rhythms. Proc. Natl. Acad. Sci. U. S. A. 112: 9382–9387.

Schmal C., Reimann P. and Staiger D. 2013. A circadian clock-regulated toggle switch explains AtGRP7 and AtGRP8 oscillations in Arabidopsis thaliana. PLoS Comput. Biol. 9: e1002986.

Schmidt F., Marnef A., Cheung M.K., Wilson I., Hancock J., Staiger D. and Ladomery M. 2010. A proteomic analysis of oligo(dT)-bound mRNP containing oxidative stress-induced Arabidopsis thaliana RNA-binding proteins ATGRP7 and ATGRP8. Mol. Biol. Rep. 37: 839–845.

Schmitz R.J., Sung S. and Amasino R.M. 2008. Histone arginine methylation is required for vernalization-induced epigenetic silencing of FLC in winter-annual Arabidopsis thaliana. Proc. Natl. Acad. Sci. U. S. A. 105: 411–416.

Schöning J.C. and Staiger D. 2005. At the pulse of time: Protein interactions determine the pace of circadian clocks. FEBS Lett. 579: 3246–3252.

Schöning J.C., Streitner C., Meyer I.M., Gao Y. and Staiger D. 2008. Reciprocal regulation of glycine-rich RNA-binding proteins via an interlocked feedback loop coupling alternative splicing to nonsense-mediated decay in Arabidopsis. Nucleic Acids Res. 36: 6977–6987.

Schöning J.C., Streitner C., Page D.R., Hennig S., Uchida K., Wolf E., Furuya M. and Staiger D. 2007. Auto-regulation of the circadian slave oscillator component AtGRP7 and regulation of its targets is impaired by a single RNA recognition motif point mutation. Plant J. 52: 1119–1130.

Senapathy P., Shapiro M.B. and Harris N.L. 1990. Splice junctions, branch point sites, and exons: Sequence statistics, identification, and applications to genome project. Methods Enzymol. 183: 252–278.

Shakhmantsir I., Nayak S., Grant G.R. and Sehgal A. 2018. Spliceosome factors target timeless (tim) mRNA to control clock protein accumulation and circadian behavior in Drosophila. Elife 7: 1–27.

Shakhmantsir I. and Sehgal A. 2019. Splicing the Clock to Maintain and Entrain Circadian Rhythms. J. Biol. Rhythms 074873041986813.

Shang X., Cao Y. and Ma L. 2017. Alternative Splicing in Plant Genes: A Means of Regulating the Environmental Fitness of Plants. Int. J. Mol. Sci. 18: 432.

Simpson C.G., Fuller J., Maronova M., Kalyna M., Davidson D., McNicol J., Barta A. and Brown J.W.S. 2008. Monitoring changes in alternative precursor messenger RNA splicing in multiple gene transcripts. Plant J. 53: 1035–1048.

Sivakumaran H., van der Horst A., Fulcher A.J., Apolloni A., Lin M.-H., Jans D.A. and Harrich D. 2009. Arginine Methylation Increases the Stability of Human Immunodeficiency Virus Type 1 Tat. J. Virol. 83: 11694–11703.

Smith W.A., Schurter B.T., Wong-Staal F. and David M. 2004. Arginine methylation of RNA helicase A determines its subcellular localization. J. Biol. Chem. 279: 22795–22798.

Staiger D. and Apel K. 1999. Circadian clock-regulated expression of an RNA-binding protein in Arabidopsis: Characterisation of a minimal promoter element. Mol. Gen. Genet. 261: 811–819.

Staiger D. and Brown J.W.S. 2013. Alternative splicing at the intersection of biological timing, development, and stress responses. Plant Cell 25: 3640–3656.

Staiger D. and Köster T. 2011. Spotlight on post-transcriptional control in the circadian system. Cell. Mol. Life Sci. 68: 71–83.

Staiger D., Zecca L., Wieczorek Kirk D.A., Apel K. and Eckstein L. 2003. The circadian clock regulated RNA-binding protein AtGRP7 autoregulates its

expression by influencing alternative splicing of its own pre-mRNA. Plant J. 33: 361–371.

Steffen A., Elgner M. and Staiger D. 2019. Regulation of Flowering Time by the RNA-Binding Proteins AtGRP7 and AtGRP8. Plant Cell Physiol. 60: 2040–2050.

Steinert J., Schiml S., Fauser F. and Puchta H. 2015. Highly efficient heritable plant genome engineering using Cas9 orthologues from Streptococcus thermophilus and Staphylococcus aureus. Plant J. 84: 1295–1305.

Streitner C., Danisman S., Wehrle F., Schöning J.C., Alfano J.R. and Staiger D. 2008. The small glycine-rich RNA binding protein At GRP7 promotes floral transition in Arabidopsis thaliana. Plant J. 56: 239–250.

Streitner C., Hennig L., Korneli C. and Staiger D. 2010. Global transcript profiling of transgenic plants constitutively overexpressing the RNA-binding protein AtGRP7. BMC Plant Biol. 10: 221.

Streitner C., Köster T., Simpson C.G., Shaw P., Danisman S., Brown J.W.S. and Staiger D. 2012. An hnRNP-like RNA-binding protein affects alternative splicing by in vivo interaction with transcripts in Arabidopsis thaliana. Nucleic Acids Res. 40: 11240–11255.

Streitner C., Simpson C.G., Shaw P., Danisman S., Brown J.W.S. and Staiger D. 2013. Small changes in ambient temperature affect alternative splicing in Arabidopsis thaliana. Plant Signal. Behav. 8: e24638.

Sugio A., Dreos R., Aparicio F. and Maule A.J. 2009. The cytosolic protein response as a subcomponent of the wider heat shock response in Arabidopsis. Plant Cell 21: 642–654.

Sun L., Wang M., Lv Z., Yang N., Liu Y., Bao S., Gong W. and Xu R.-M. 2011. Structural insights into protein arginine symmetric dimethylation by PRMT5. Proc. Natl. Acad. Sci. U. S. A. 108: 20538–20543.

Suzuki N., Rizhsky L., Liang H., Shuman J., Shulaev V. and Mittler R. 2005. Enhanced tolerance to environmental stress in transgenic plants expressing the transcriptional coactivator multiprotein bridging factor 1c. Plant Physiol. 139: 1313–1322.

Tan C.P. and Nakielny S. 2006. Control of the DNA Methylation System Component MBD2 by Protein Arginine Methylation. Mol. Cell. Biol. 26: 7224–7235.

Thatcher S.R., Danilevskaya O.N., Meng X., Beatty M., Zastrow-Hayes G., Harris C., Van Allen B., Habben J. and Li B. 2016. Genome-wide analysis of alternative splicing during development and drought stress in maize. Plant Physiol. 170: 586–599.

The Arabidopsis Genome Initiative 2000. Analysis of the genome sequence of the flowering plant Arabidopsis thaliana. Nature 408: 796–815.

Thomma B.P.H.J., Penninckx I.A.M.A., Broekaert W.F. and Cammue B.P.A.

2001. The complexity of disease signaling in Arabidopsis. Curr. Opin. Immunol. 13: 63–68.

Uknes S., Mauch-Mani B., Moyer M., Potter S., Williams S., Dincher S., Chandler D., Slusarenko A., Ward E. and Ryals J. 1992. Acquired Resistance in Arabidopsis. Plant Cell 4: 645–656.

van Nocker S. and Vierstra R.D. 1993. Two cDNAs from Arabidopsis thaliana encode putative RNA binding proteins containing glycine-rich domains. Plant Mol. Biol. 21: 695–699.

Vanden Driessche T. 1966. Circadian rhythms in Acetabularia: Photosynthetic capacity and chloroplast shape. Exp. Cell Res. 42: 18–30.

Wahl M.C., Will C.L. and Lührmann R. 2009. The Spliceosome: Design Principles of a Dynamic RNP Machine. Cell 136: 701–718.

Waibel F. and Filipowicz W. 1990. U6 snRNA genes of Arabidopsis are transcribed by RNA polymerase III but contain the same two upstream promoter elements as RNA polymerase II-transcribed U-snRNA genes. Nucleic Acids Res. 18: 3451–3458.

Wang B.-B. and Brendel V. 2006. Genomewide comparative analysis of alternative splicing in plants. Proc. Natl. Acad. Sci. 103: 7175–7180.

Wang Q., Abruzzi K.C., Rosbash M. and Rio D.C. 2018. Striking circadian neuron diversity and cycling of Drosophila alternative splicing. Elife 7: 1–24.

Wang X., Wu F., Xie Q., Wang H., Wang Y., Yue Y., Gahura O., Ma S., Liu L., Cao Y., Jiao Y., Puta F., McClung C.R., Xu X. and Ma L. 2012. SKIP is a component of the spliceosome linking alternative splicing and the circadian clock in Arabidopsis. Plant Cell 24: 3278–3295.

Wang X., Zhang Y., Ma Q., Zhang Z., Xue Y., Bao S. and Chong K. 2007. SKB1-mediated symmetric dimethylation of histone H4R3 controls flowering time in Arabidopsis. EMBO J. 26: 1934–1941.

Wang Z., Rolish M.E., Yeo G., Tung V., Mawson M. and Burge C.B. 2004. Systematic identification and analysis of exonic splicing silencers. Cell 119: 831–845.

Wang Z. and Tobin E.M. 1998. Constitutive Expression of the CIRCADIAN CLOCK ASSOCIATED 1 (CCA1) Gene Disrupts Circadian Rhythms and Suppresses Its Own Expression. Cell 93: 1207–1217.

Will C.L. and Lührmann R. 2011. Spliceosome structure and function. Cold Spring Harb. Perspect. Biol. 3: a003707.

Williams S.P., Rangarajan P., Donahue J.L., Hess J.E. and Gillaspy G.E. 2014. Regulation of Sucrose non-Fermenting Related Kinase 1 genes in Arabidopsis thaliana. Front. Plant Sci. 5: 324.

Xiao J., Li C., Xu S., Xing L., Xu Y. and Chong K. 2015. JACALIN-LECTIN LIKE1 Regulates the Nuclear Accumulation of GLYCINE-RICH RNA-BINDING PROTEIN7, Influencing the RNA Processing of FLOWERING LOCUS C Antisense Transcripts and Flowering Time in Arabidopsis. Plant Physiol. 169: 2102–2117.

Xing T., Malik K., Martin T. and L. Miki B. 2001. Activation of tomato PR and wound-related genes by a mutagenized tomato MAP kinase through divergent pathways. Plant Mol. Biol. 46: 109–120.

Xue Y., Zhou Y., Wu T., Zhu T., Ji X., Kwon Y., Zhang C., Yeo G., Black D.L., Sun H., Fu X. and Zhang Y. 2009. Genome-wide analysis of PTB-RNA interactions reveals a strategy used by the general splicing repressor to modulate exon inclusion or skipping. Mol. Cell 36: 996–1006.

Yang M., Sun J., Sun X., Shen Q., Gao Z. and Yang C. 2009. Caenorhabditis elegans protein arginine methyltransferase PRMT-5 negatively regulates DNA damage-induced apoptosis. PLoS Genet. 5: e1000514.

Yang W., Wightman R. and Meyerowitz E.M. 2017. Cell Cycle Control by Nuclear Sequestration of CDC20 and CDH1 mRNA in Plant Stem Cells. Mol. Cell 68: 1108-1119.e3.

Yu M.C. 2011. The Role of Protein Arginine Methylation in mRNP Dynamics. Mol. Biol. Int. 2011: 163827.

Zhang F., Qi B., Wang L., Zhao B., Rode S., Riggan N.D., Ecker J.R. and Qiao H. 2016. EIN2-dependent regulation of acetylation of histone H3K14 and non-canonical histone H3K23 in ethylene signalling. Nat. Commun. 7: 13018.

Zhang X.-C. and Gassmann W. 2003. RPS4-mediated disease resistance requires the combined presence of RPS4 transcripts with full-length and truncated open reading frames. Plant Cell 15: 2333–2342.

Zhang X.-C. and Gassmann W. 2007. Alternative Splicing and mRNA Levels of the Disease Resistance Gene RPS4 Are Induced during Defense Responses. Plant Physiol. 145: 1577–1587.

Zhang Z., Zhang S., Zhang Ya, Wang X., Li D., Li Qiuling, Yue M., Li Qun, Zhang Yu-e, Xu Y., Xue Y., Chong K. and Bao S. 2011. Arabidopsis floral initiator SKB1 confers high salt tolerance by regulating transcription and pre-mRNA splicing through altering histone H4R3 and small nuclear ribonucleoprotein LSM4 methylation. Plant Cell 23: 396–411.

Zhao C., Zhang Z., Xie S., Si T., Li Y. and Zhu J.-K. 2016. Mutational Evidence for the Critical Role of CBF Transcription Factors in Cold Acclimation in Arabidopsis. Plant Physiol. 171: 2744–2759.

Zhou Z., Sun X., Zou Z., Sun L., Zhang T., Guo S., Wen Y., Liu L., Wang Y., Qin J., Li L., Gong W. and Bao S. 2010. PRMT5 regulates Golgi apparatus structure through methylation of the golgin GM130. Cell Res. 20: 1023–1033.

Zhu G., Li W., Zhang F. and Guo W. 2018. RNA-seq analysis reveals alternative

splicing under salt stress in cotton, Gossypium davidsonii. BMC Genomics 19: 73.

Zhu X., Xu Y., Yu S., Lu L., Ding M., Cheng J., Song G., Gao X., Yao L., Fan D., Meng S., Zhang X., Hu S. and Tian Y. 2014. An efficient genotyping method for genome-modified animals and human cells generated with CRISPR/Cas9 system. Sci. Rep. 4: 6420.

Ziemienowicz A., Haasen D., Staiger D. and Merkle T. 2003. Arabidopsis transportin1 is the nuclear import receptor for the circadian clock-regulated RNA-binding protein AtGRP7. Plant Mol. Biol. 53: 201–212.

Appendix

All primers used for this work were synthesised by Metabion (Planegg/Steinkirchen, Germany) and they are listed in the following table.

Name	**AGI**	**Primer name**	**Primer sequence (5'→ 3')**
ACT2	AT3G18780	Act2_667	GTTGACTACGAGCAGGAGATGG
ACT2	AT3G18780	Act2_841	AGGTTGTCTCGTGGATTCCAG
AKIN11	AT3G29160	AKIN11_as_for	CCTGACTCAGCTCTGCGTCACC
AKIN11	AT3G29160	AKIN11_as_rev	CCCAATTCCAAGAGTTTTACC
EIF4A	AT3G13920	eIF4a_1033	CAACAAGTCTCCCTGGTTATC
EIF4A	AT3G13920	eIF4a_1169	AGCATCCTCTCATCATCACGG
FLC	AT2G21660	FLC_295	CTTGTGGATAGCAAGCTTGTGGG
FLC	AT2G21660	FLC_417	CATGAGAGTTCGGTCTTCTTGGCTC
FLK	AT3G04610	FLK_Ex1_for	CCTCCATTGTTACCGGAATC
FLK	AT3G04610	FLK_Ex2_rev	TCTTCAGCTTCAGCCATGAC
FRK1	AT2G19190	At2g19190_FRK1_fwd	CAGCGCAAGGACTAGAG
FRK1	AT2G19190	At2g19190_FRK1_rev	CTTCGCTTGGAGCTTCT
GRP7	AT2G21660	Agrp_140	ACATCTCACTGCTCACTACTC
GRP7	AT2G21660	Agrp_121	ATCGTTAATGATCTTGGAATC
GRP8	AT4G39260	CCRB_5'UTR	ACCCTAATTTCTCTTCTTTTCC
GRP8	AT4G39260	Agrp_122	GTCGTTAATGATCTTAGAATC
GRP8	AT4G39260	Agrp_95	CGATGGGACAAATTAAGTAAC
PP2A	AT1G13320	PP2A_for	CGATAGTCGACCAAGCGGTT
PP2A	AT1G13320	PP2A_rev	TACCGAACATCAACATCTGG
PR1	AT2G14610	PR1_175_2011 (fwd)	GCTCGGAGCTACGCAGAACA
PR1	AT2G14610	PR1_402_2011 (rev)	GGCACATCCGAGTCTCACTG
VFP5	AT5G05550	VFP5_as_for	AGAAGCAGAGAATGGAAGTGAC
VFP5	AT5G05550	VFP5_as_rev	GGATCCTCCAATTTCAATGAG
sgRNA	-	F_NotI_pEN	TTGCGGCCGCgctttttttcttcttcttcgttcatac
sgRNA	-	R_NotI_pEN	TTGCGGCCGCAaaaaaaagcaccgactcggtg

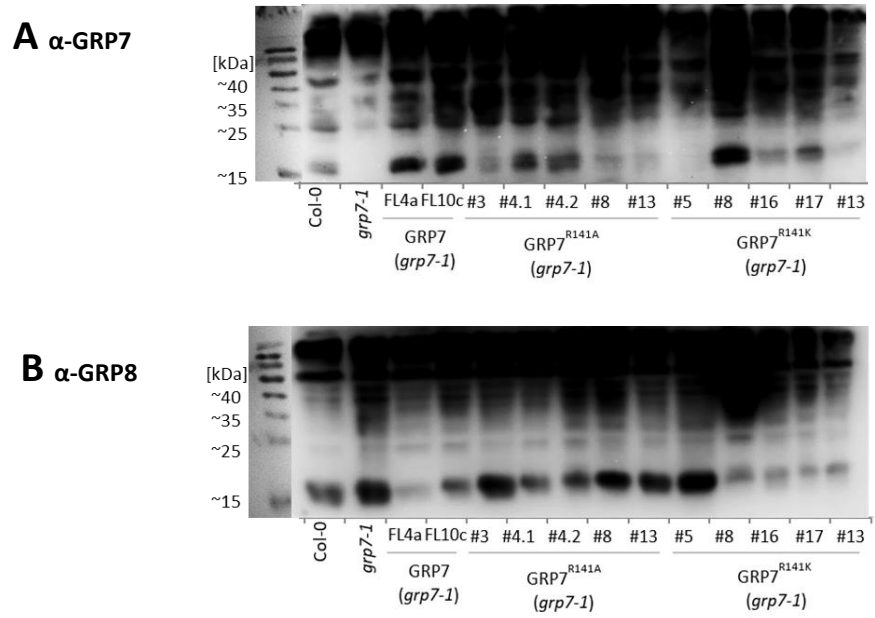

Figure A. 1 Levels of GRP7 and GRP8 proteins in complementation lines GRP7^{R141A} and GRP7^{R141K}. The total protein extracts were isolated from 18-days-old seedlings grown under short day conditions (8 h light and 16 h dark rhythm). The protein level of (**A**) GRP7 and (**B**) GRP8 was examined by Western blot with anti-GRP7 (α-GRP7) and anti-GRP8 (α-GRP8) antibodies, respectively.

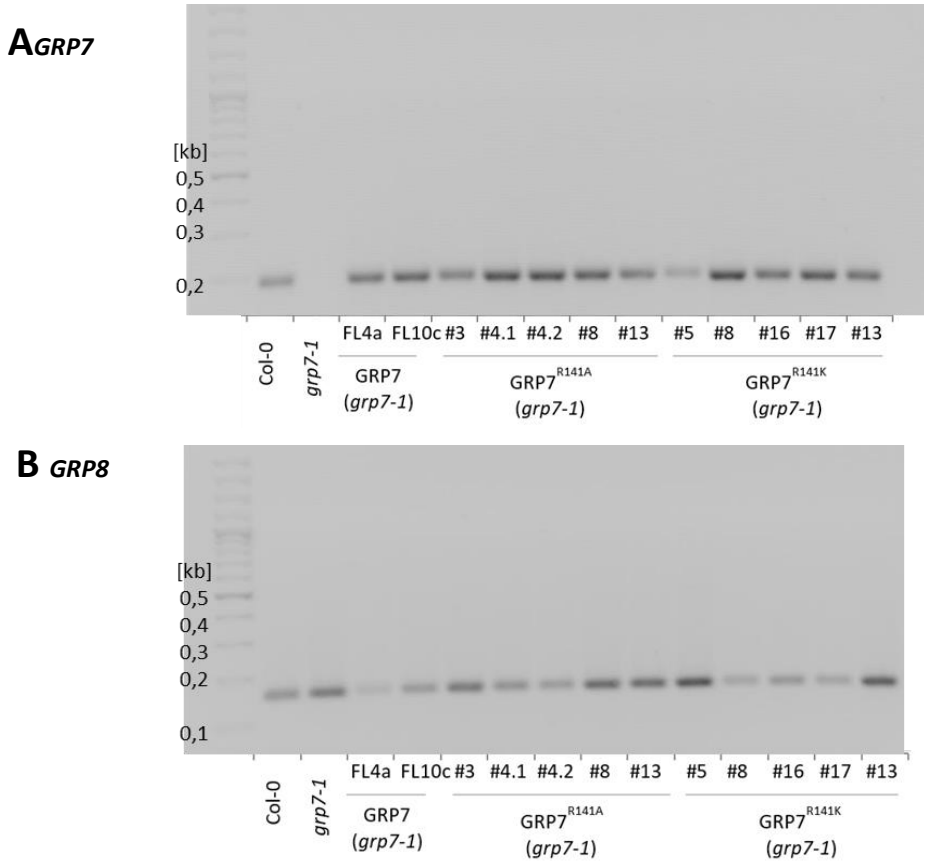

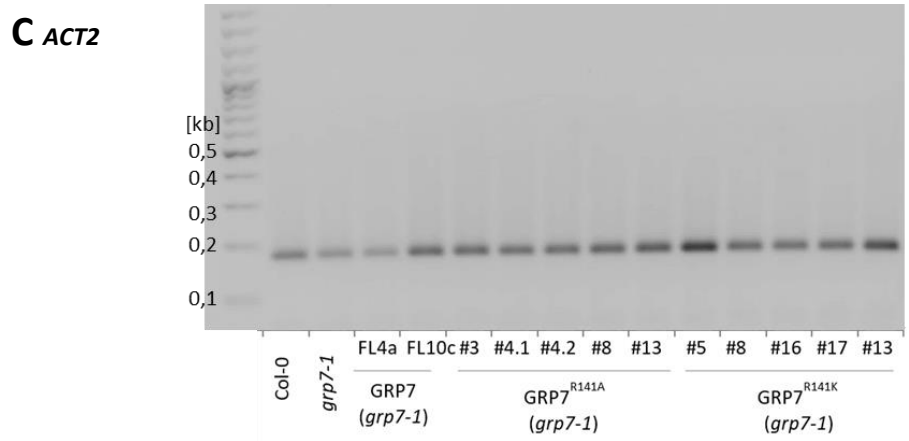

Figure A. 2 Transcript level of *GRP7, GRP8* and *ACT2* in complementation lines GRP7^{R141A} and GRP7^{R141K}. (**A**, **B**, **C**) The RNA samples were isolated from 5-week-old seedlings grown under short day conditions (8 h light and 16 h dark rhythm). Total RNA was reverse transcribed and used for measuring (**A**) *GRP7* and (**B**) *GRP8* levels by semi-quantitative PCR. (**C**) *ACTIN2* (*ACT2*) was used as a loading control.

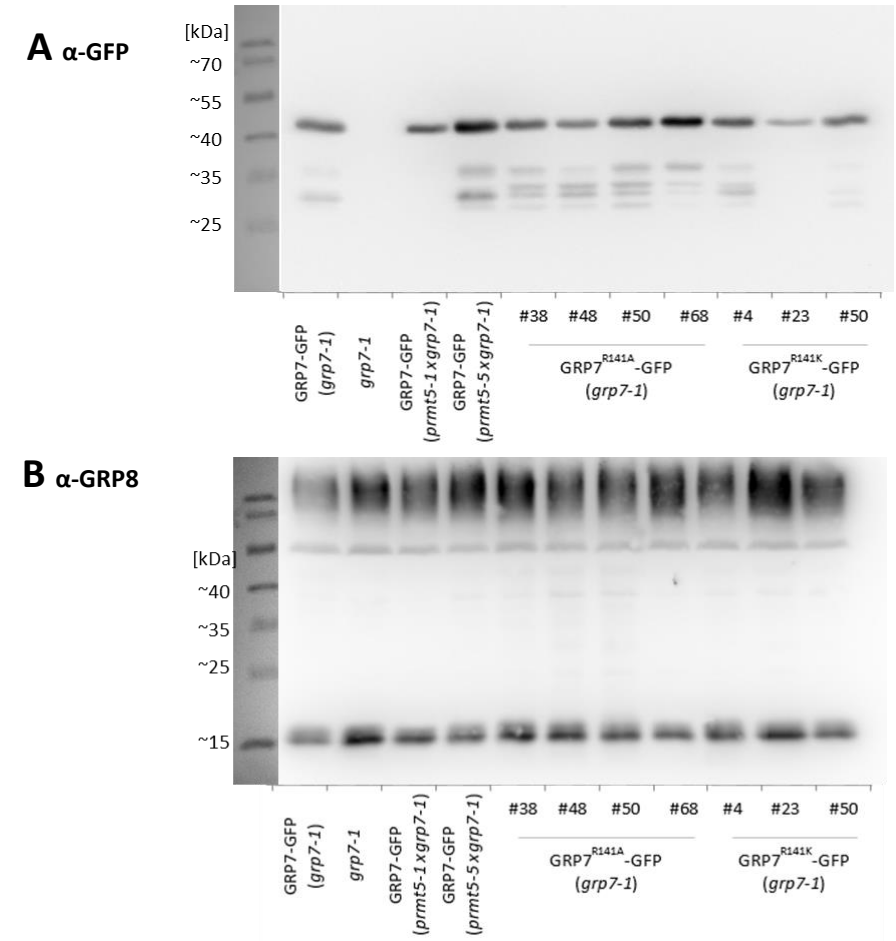

Figure A. 3 Levels of GRP7 and GRP8 proteins in the transgenic GRP7^{R141A}-GFP and GRP7^{R141K}-GFP plants. The total protein extracts were isolated from 18-

days-old seedlings grown under short day conditions (8 h light and 16 h dark rhythm). The protein level of (**A**) GRP7 and (**B**) GRP8 was examined by Western blot with anti-GFP (α-GFP) and anti-GRP8 (α-GRP8) antibodies, respectively.

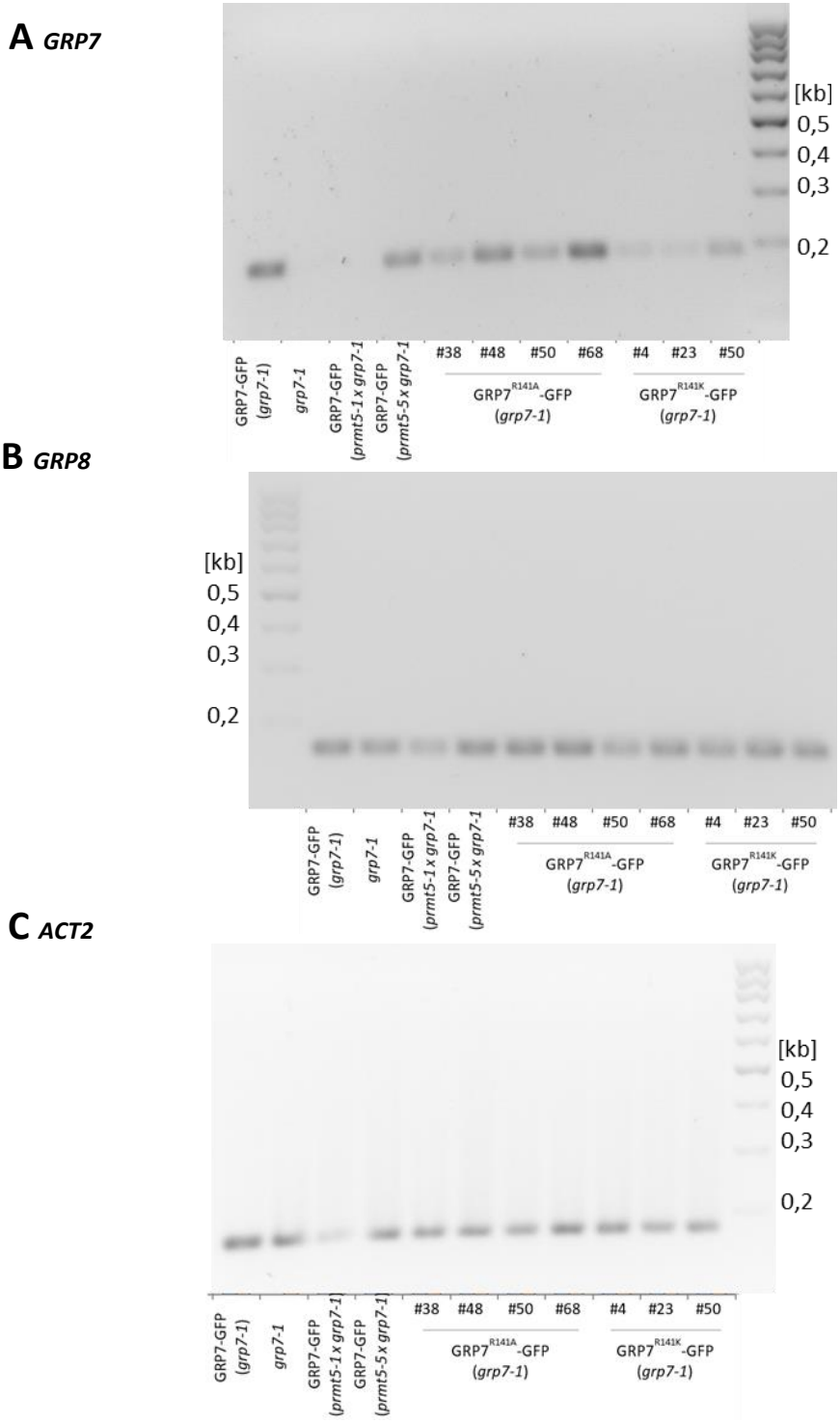

Figure A. 4 Transcript level of *GRP7, GRP8* and *ACT2* in the transgenic GRP7^{R141A}-GFP and GRP7^{R141K}-GFP plants. The RNA samples were isolated from 5-week-old seedlings grown under short day conditions (8 h light and 16 h dark rhythm).

Total RNA was reverse transcribed and used for measuring (**A**) *GRP7* and (**B**) *GRP8* levels by semi-quantitative PCR. (**C**) *ACTIN2* (*ACT2*) was used as a loading control.

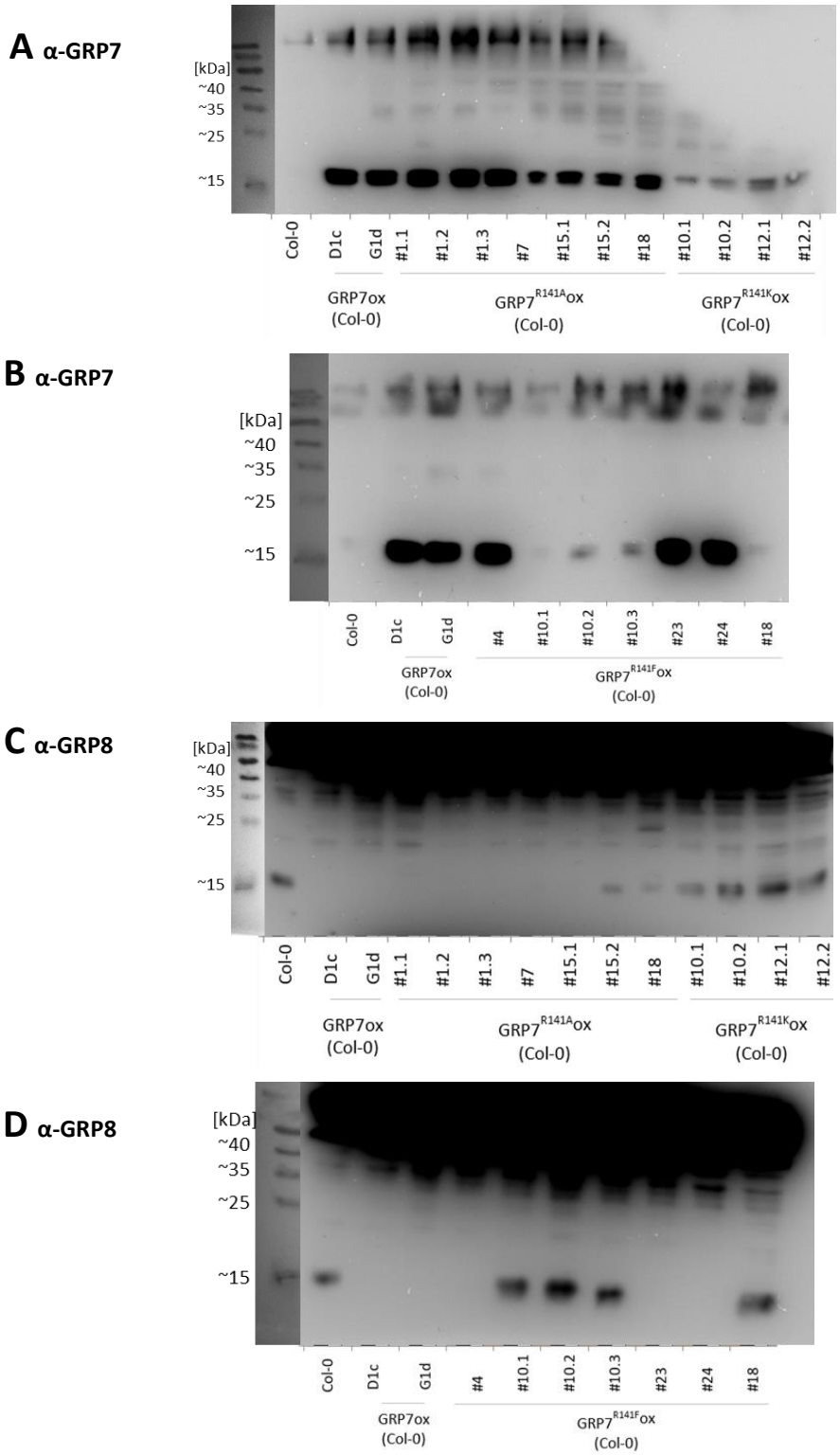

Figure A. 5 Levels of GRP7 and GRP8 proteins in lines overexpressing GRP7^{R141A} and GRP7^{R141K}. The total protein extracts were isolated from 18-days-old

seedlings grown under short day conditions (8 h light and 16 h dark rhythm). The protein level of (**A**, **B**) GRP7 and (**C**, **D**) GRP8 was examined by Western blot with anti-GRP7 (α-GRP7) and anti-GRP8 (α-GRP8) antibodies.

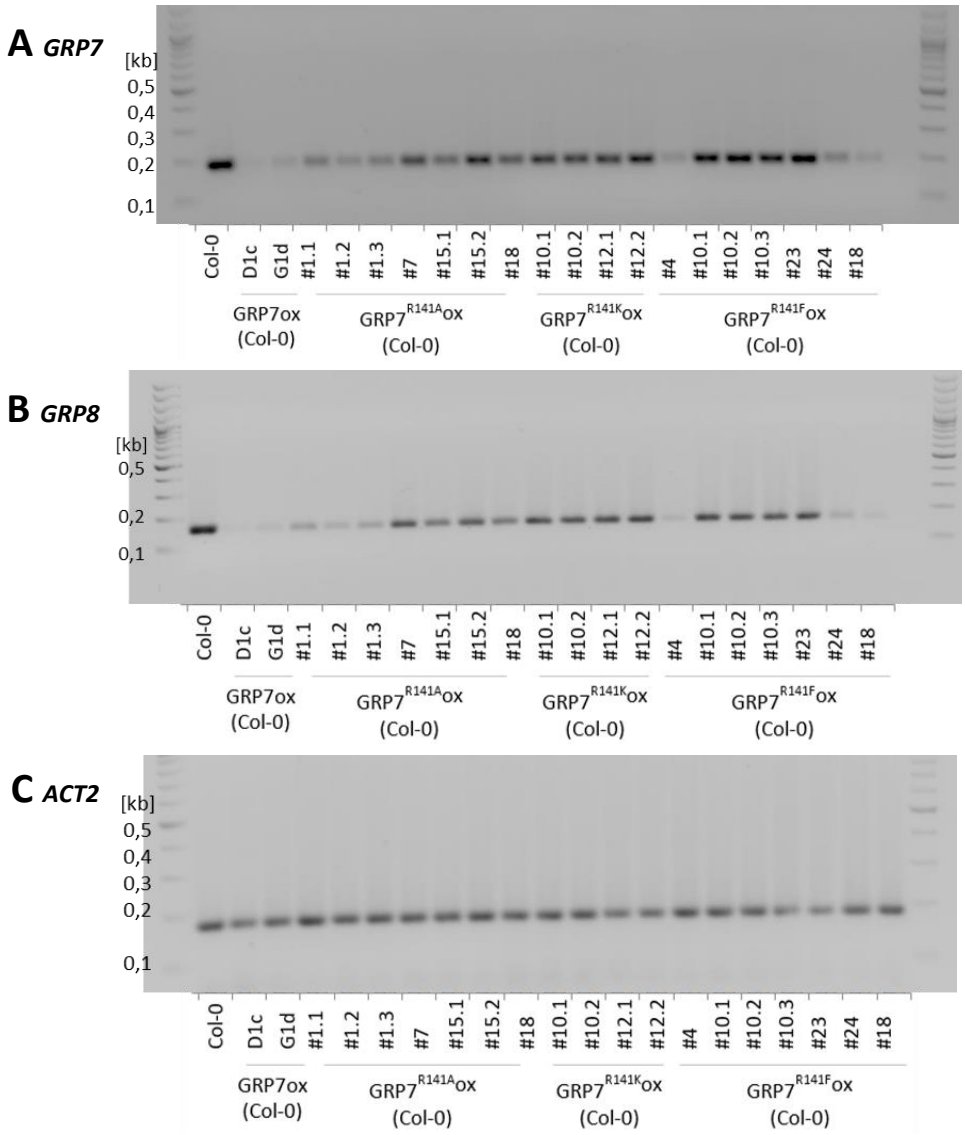

Figure A. 6 Transcript level of *GRP7, GRP8* and *ACT2* in lines overexpressing GRP7^{R141A}, GRP7^{R141K} and GRP7^{R141F}. The RNA samples were isolated from 5-week-old seedlings grown under short day conditions (8 h light and 16 h dark rhythm). Total RNA was reverse transcribed and used for measuring (**A**) *GRP7* and (**B**) *GRP8* levels by semi-quantitative PCR. (**C**) *ACTIN2* (*ACT2*) was used as a loading control.

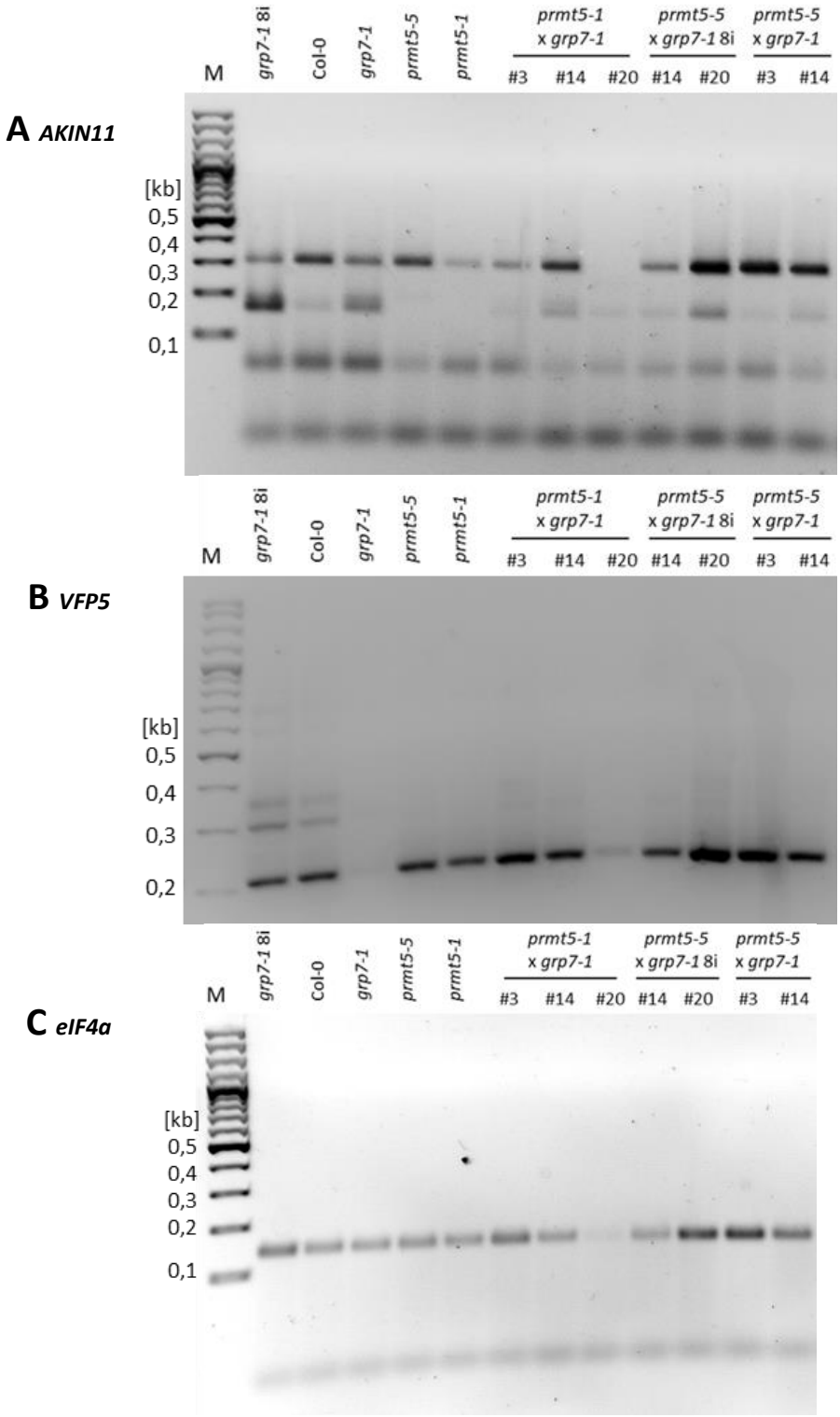

Figure A. 7 Effect of GRP7, GRP8 and PRMT5 on alternative splicing of *AKIN11* and *VFP5*. Pictures **A, B** and **C** represent first biological replicate of AS analyses. RNA was isolated from 16-day-old seedlings and reverse transcribed. Synthesised cDNA was used in sqPCR for amplification of (**A**) *AKIN11* and (**B**) *VFP5* transcripts. M - 100 bp marker. (**C**) *EUKARYOTIC INITIATION FACTOR-4A* (*eIF4a*) was used as a loading control.

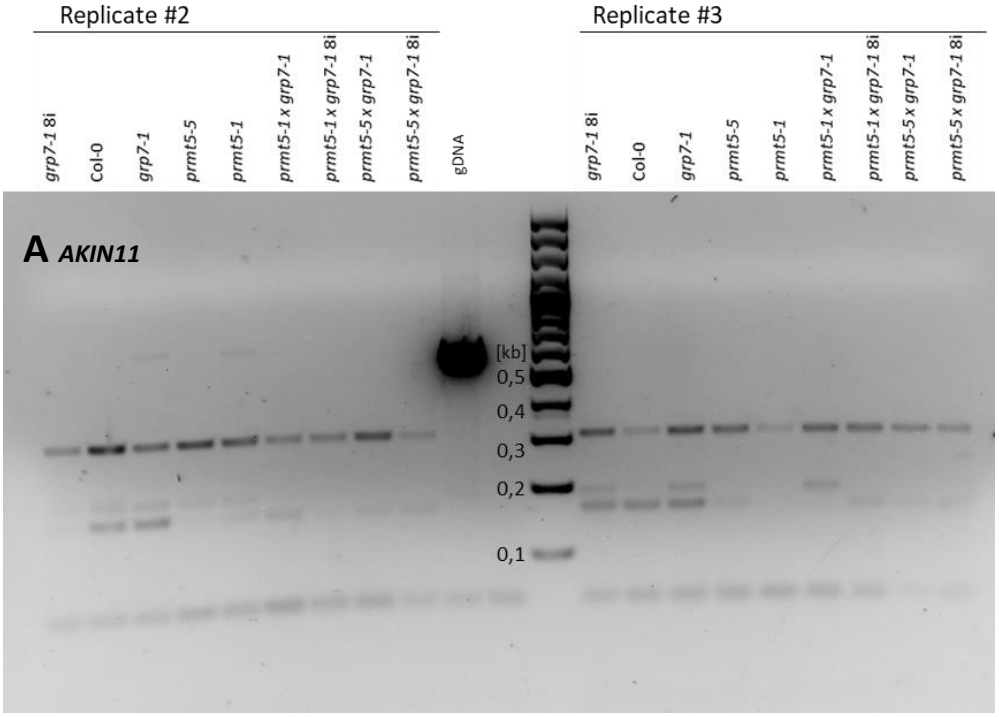
Replicate #2
Replicate #3
grp7-1 8i
Col-0
grp7-1
prmt5-5
prmt5-1
prmt5-1 x grp7-1
prmt5-1 x grp7-1 8i
prmt5-5 x grp7-1
prmt5-5 x grp7-1 8i
gDNA
A AKIN11
[kb]
0,5
0,4
0,3
0,2
0,1

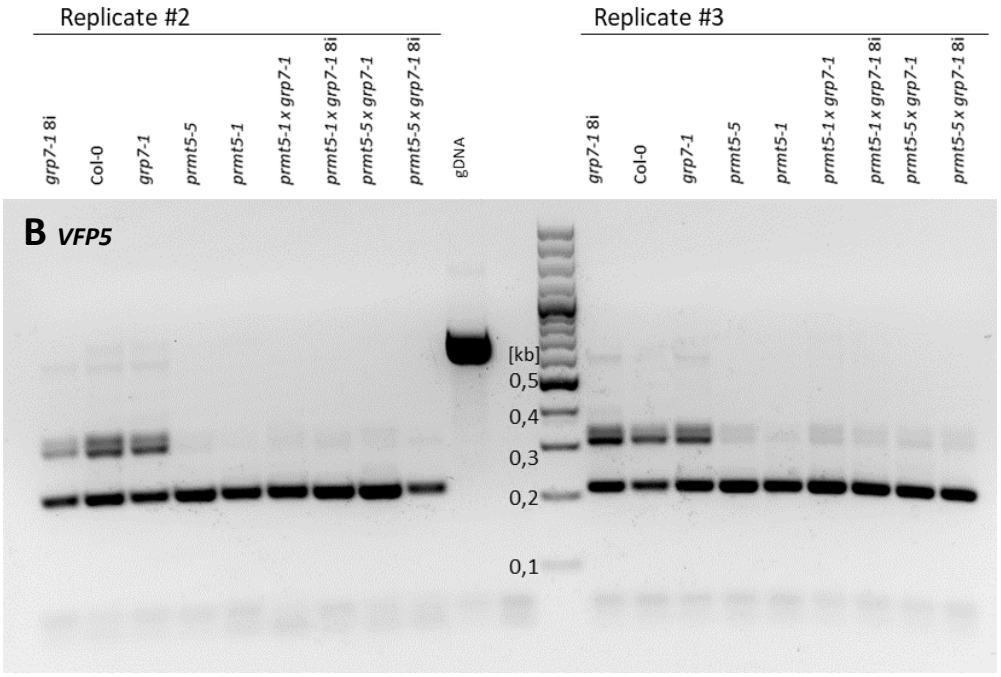
Replicate #2
Replicate #3
grp7-1 8i
Col-0
grp7-1
prmt5-5
prmt5-1
prmt5-1 x grp7-1
prmt5-1 x grp7-1 8i
prmt5-5 x grp7-1
prmt5-5 x grp7-1 8i
gDNA
B VFP5
[kb]
0,5
0,4
0,3
0,2
0,1

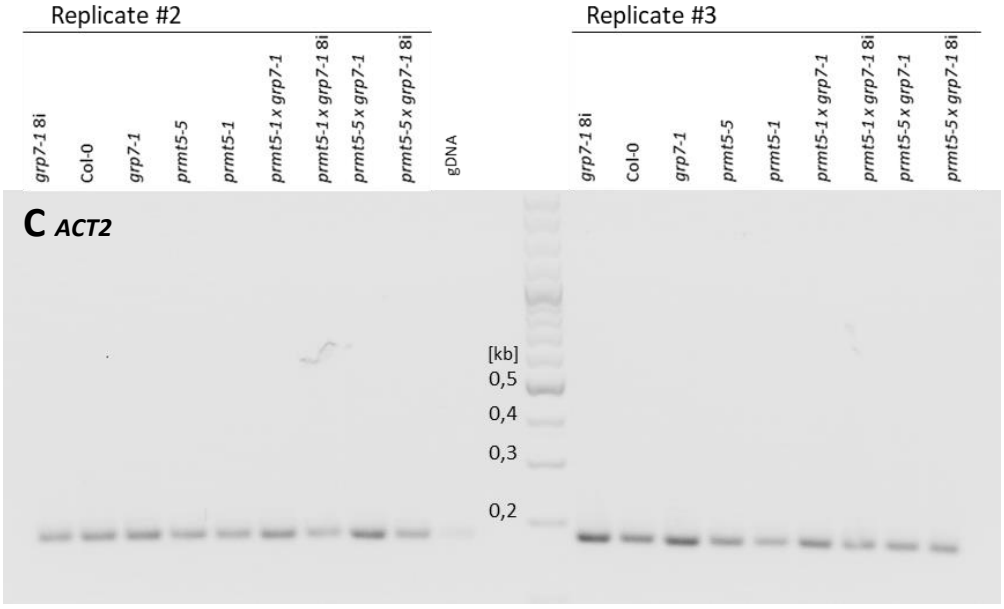

Figure A. 8 Effect of GRP7, GRP8 and PRMT5 on alternative splicing of *AKIN11* and *VFP5*. Pictures **A, B** and **C** represent second and third biological replicate of AS analyses. RNA was isolated from 16-day-old seedlings and reverse transcribed. Synthesised cDNA was used in sqPCR for amplification of (**A**) *AKIN11* and (**B**) *VFP5* transcripts. M - 100 bp marker. (**C**) *ACTIN2* (*ACT2*) was used as a loading control.

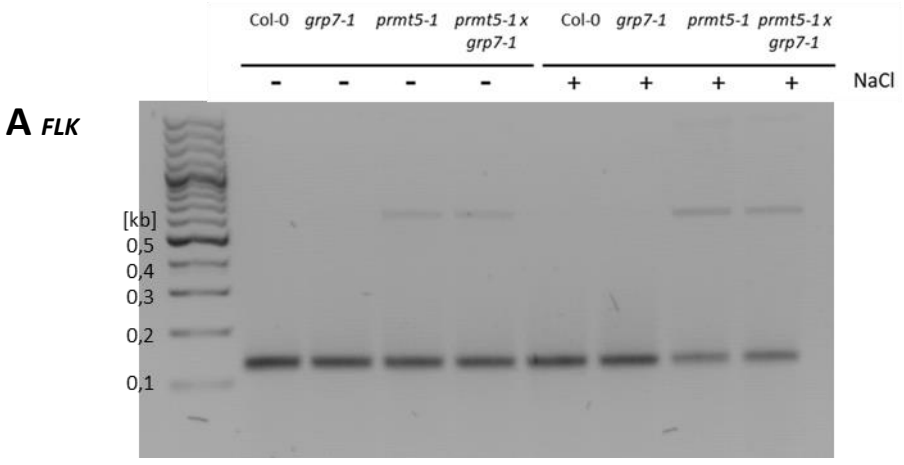

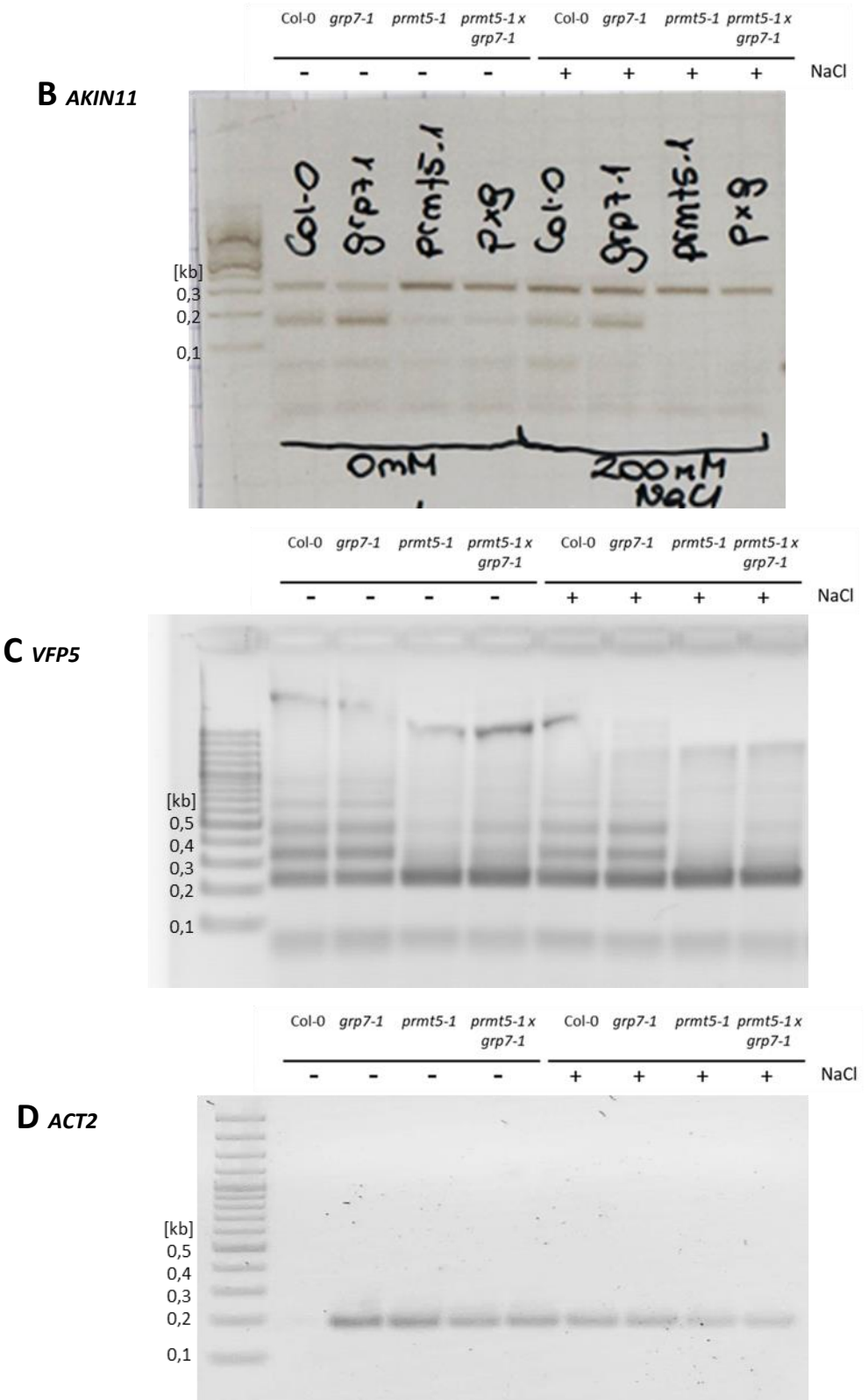

Figure A. 9 Effect of GRP7 and PRMT5 on alternative splicing of *FLK, AKIN11* and *VFP5* under salt stress conditions. Pictures represent first biological replicate of AS under salt stress conditions. 11-day-old seedlings were transferred

on ½ MS plates with or without 200 mM NaCl for 6 h and aerial parts were harvested. Synthesised cDNAs were used in sqPCR for amplification of (**A**) *FLK,* (**B**) *AKIN11* and (**C**) *VFP5* transcripts. (**D**) *ACTIN2* (*ACT2*) was used as a loading control.

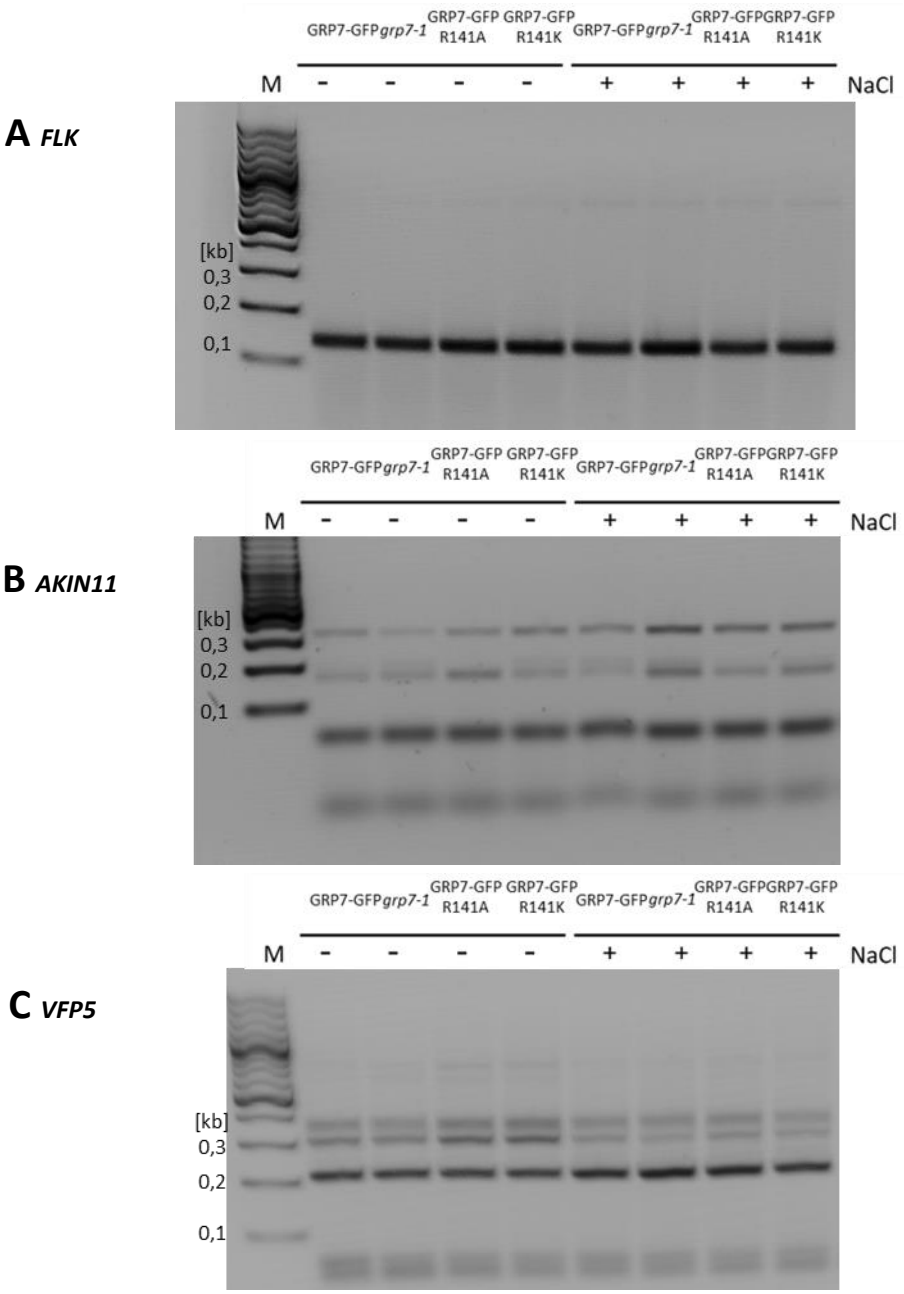

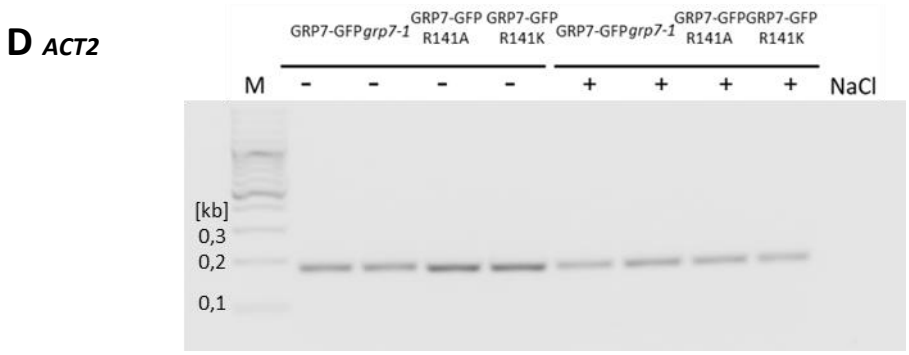

Figure A. 10 Effect of arginine methylation in GRP7 on alternative splicing of *FLK, AKIN11* and *VFP5* under salt stress conditions. Pictures represent first biological replicate of AS under salt stress conditions. 11-day-old seedlings were transferred on ½ MS plates with or without 200 mM NaCl for 6 h and aerial parts were harvested. Synthesised cDNAs were used in sqPCR for amplification of (**A**) *FLK,* (**B**) *AKIN11* and (**C**) *VFP5* transcripts. (**D**) *ACTIN2* (*ACT2*) was used as a loading control.

A ***FLK***

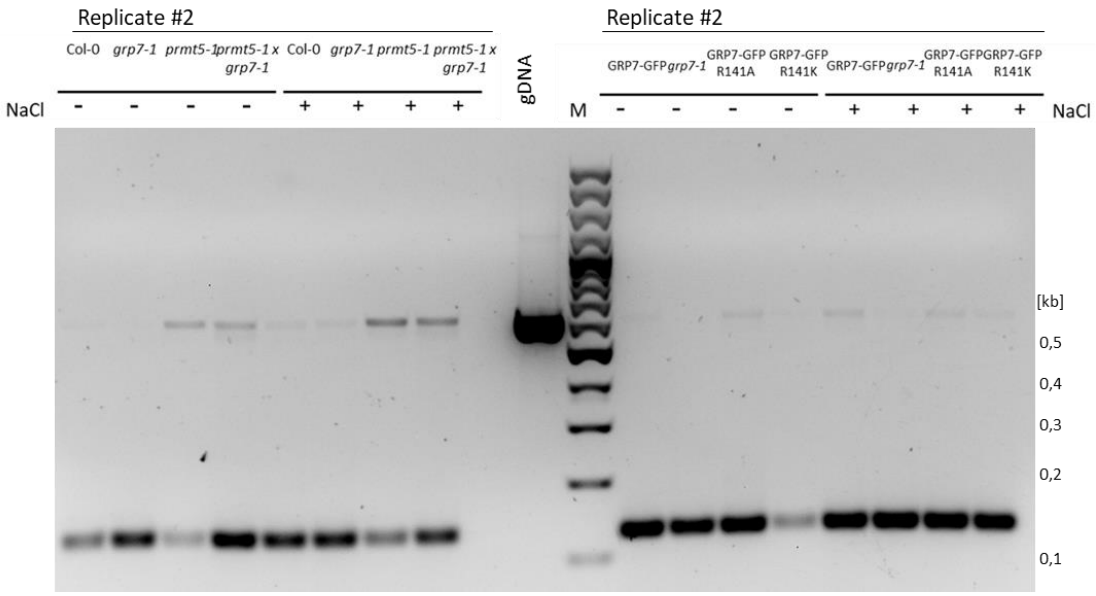

B ***AKIN11***

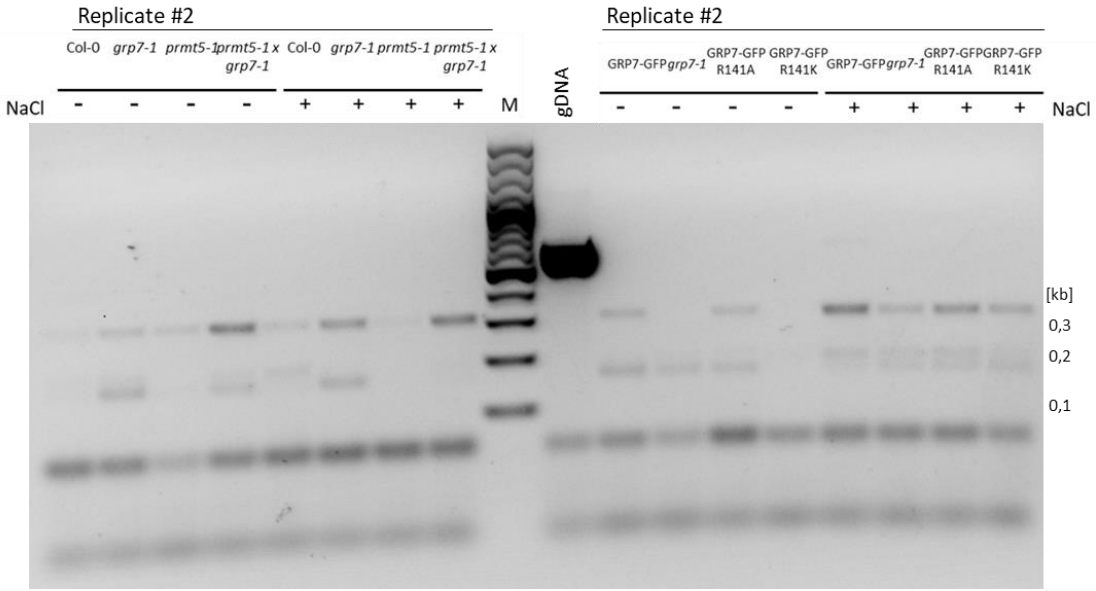

C ***VFP5***

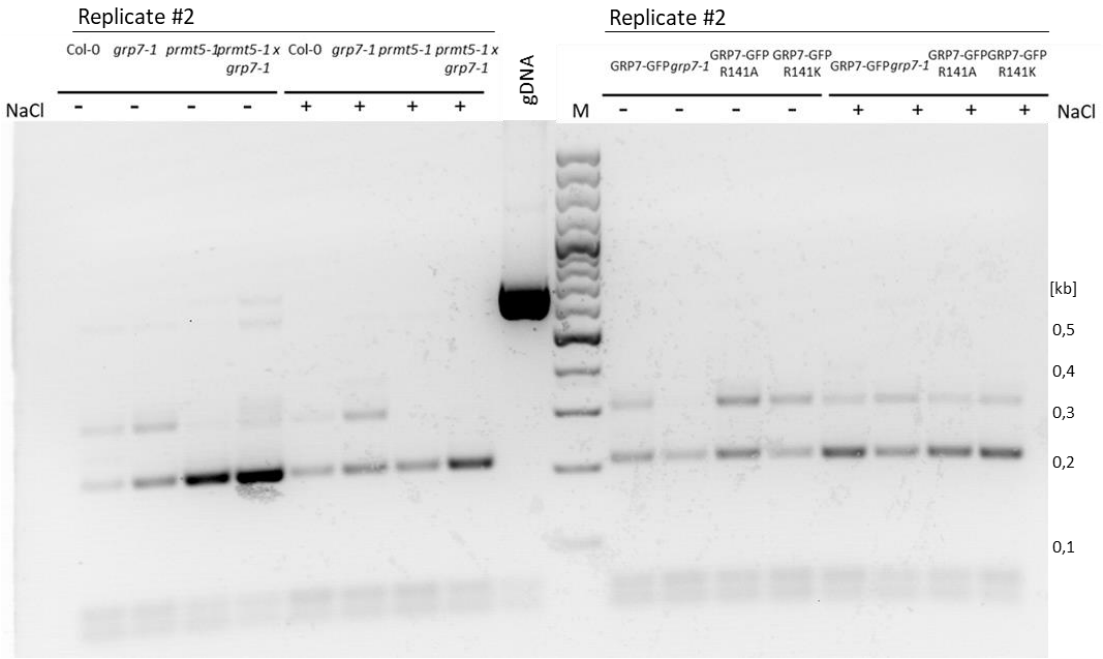

D ***ACT2***

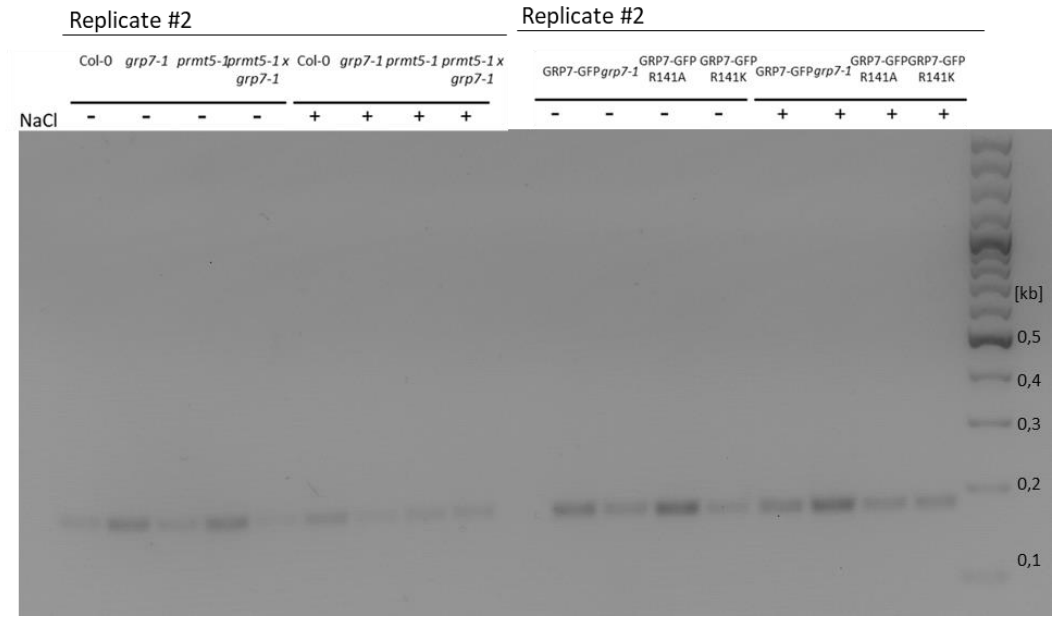

Figure A. 11 Effect of GRP7 and PRMT5 and arginine methylation in GRP7 on alternative splicing of *FLK, AKIN11* and *VFP5* under salt stress conditions. Pictures represent second biological replicate of AS under salt stress conditions. 11-day-old seedlings were transferred on ½ MS plates with or without 200 mM NaCl for 6 h and aerial parts were harvested. Synthesised cDNAs were used in sqPCR for amplification of (**A**) *FLK,* (**B**) *AKIN11* and (**C**) *VFP5* transcripts. (**D**) *ACTIN2* (*ACT2*) was used as a loading control.

A ***FLK***

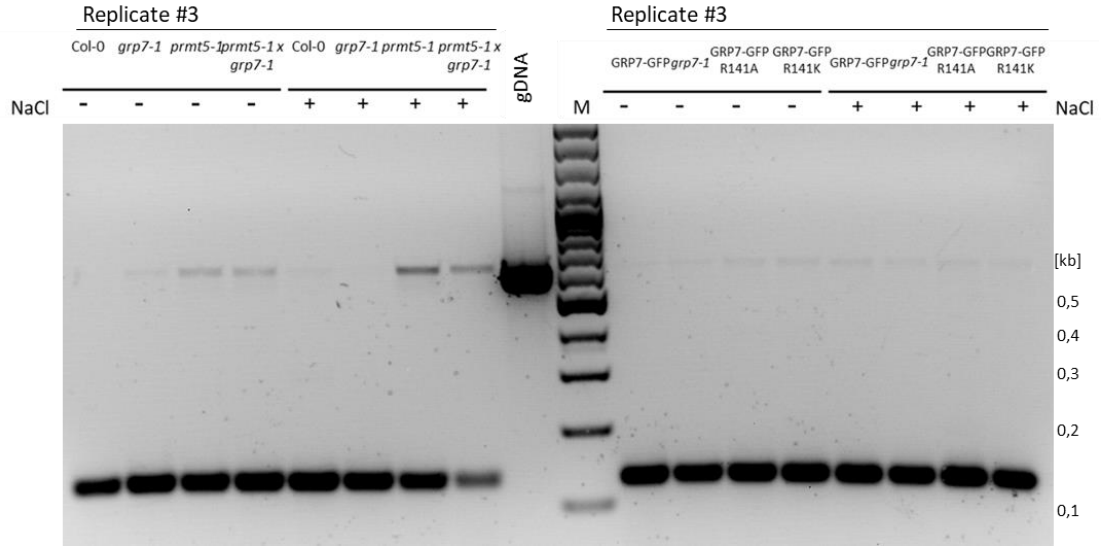

B ***AKIN11***

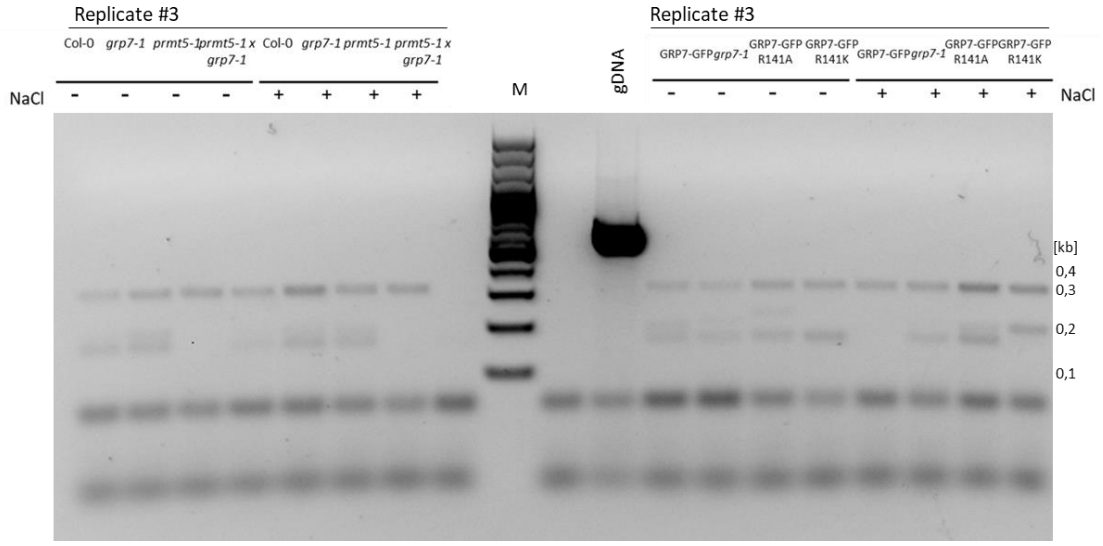

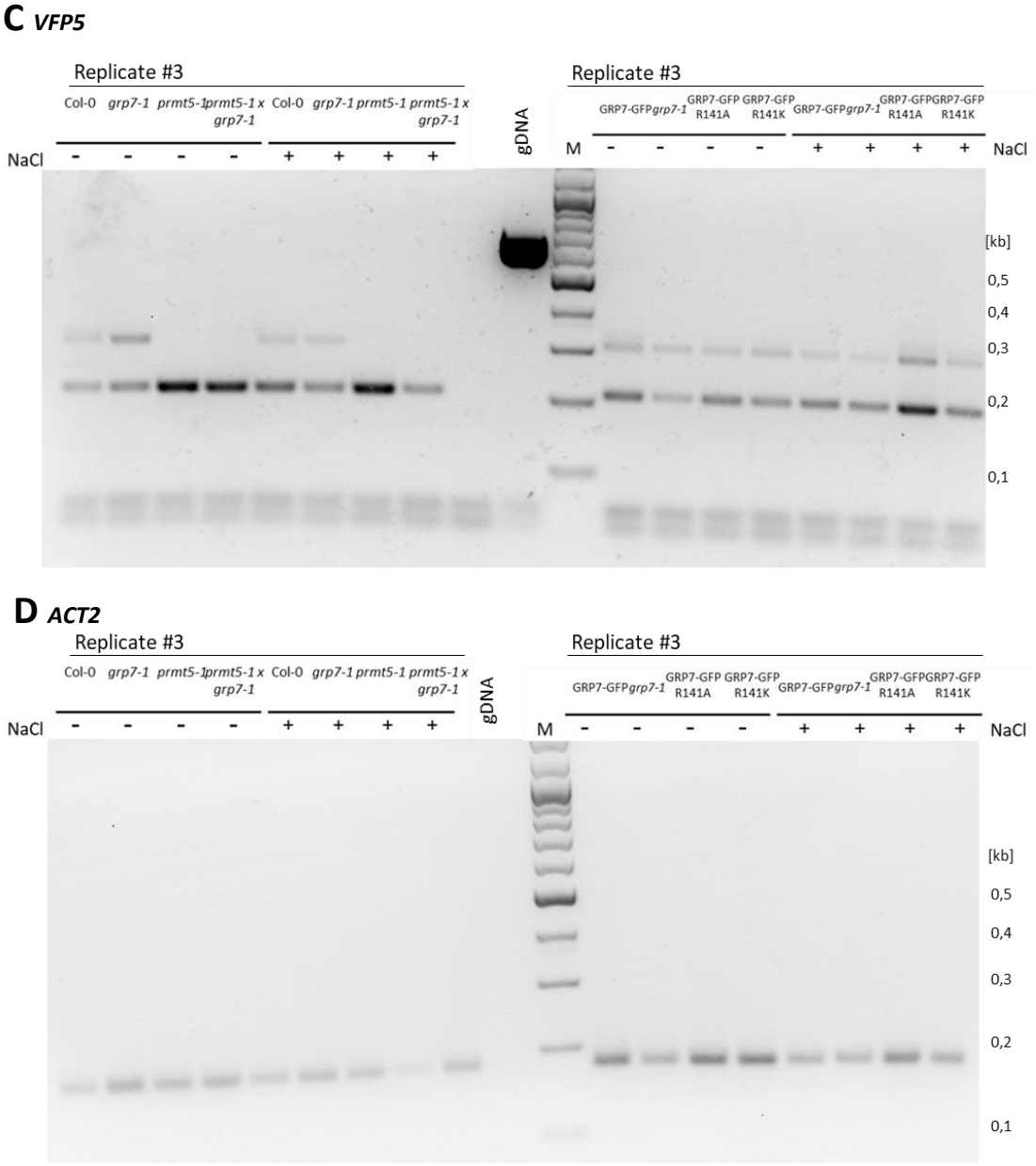

Figure A. 12 Effect of GRP7 and PRMT5 and arginine methylation in GRP7 on alternative splicing of *FLK, AKIN11* and *VFP5* under salt stress conditions. Pictures represent third biological replicate of AS under salt stress conditions. 11-day-old seedlings were transferred on ½ MS plates with or without 200 mM NaCl for 6 h and aerial parts were harvested. Synthesised cDNAs were used in sqPCR for amplification of (**A**) *FLK,* (**B**) *AKIN11* and (**C**) *VFP5* transcripts. (**D**) *ACTIN2* (*ACT2*) was used as a loading control.

A ***FLK***

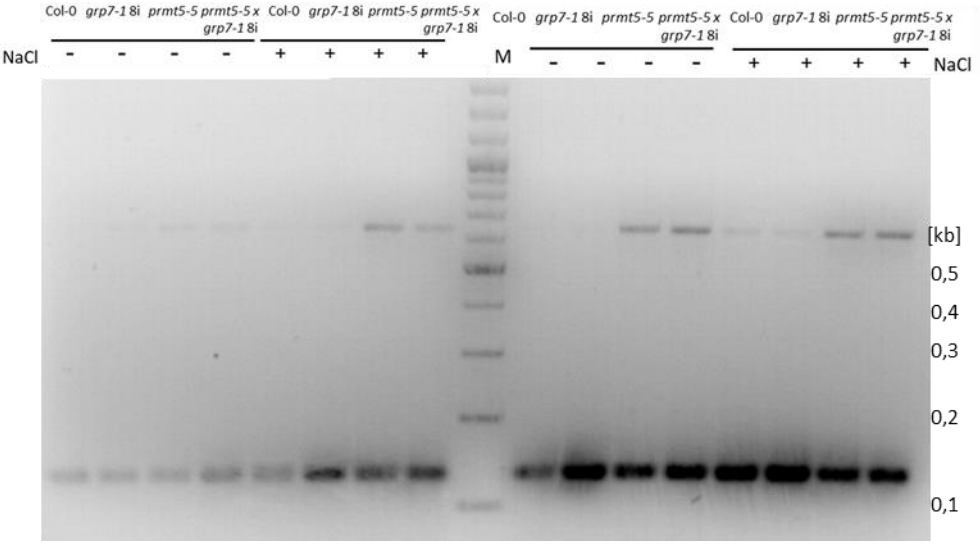

B ***AKIN11***

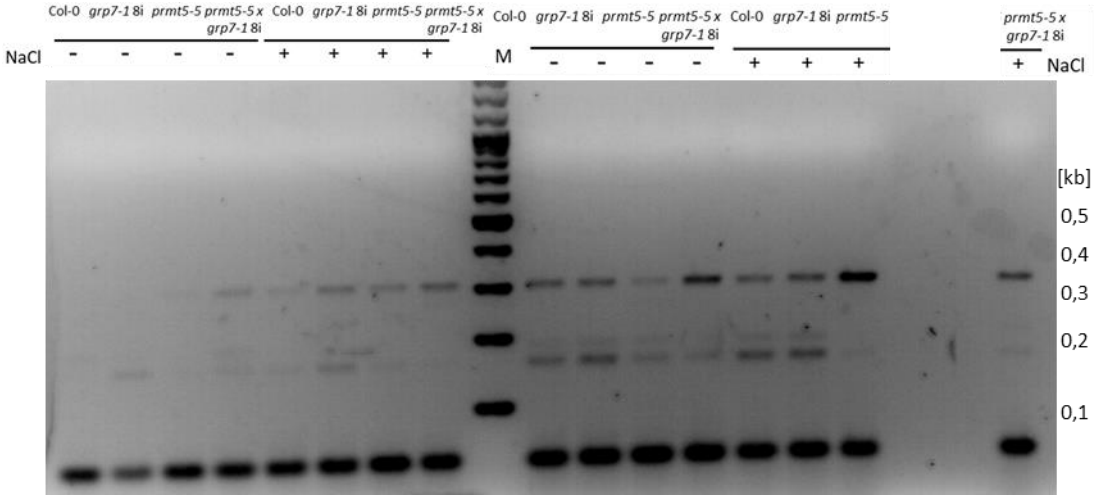

C ***VFP5***

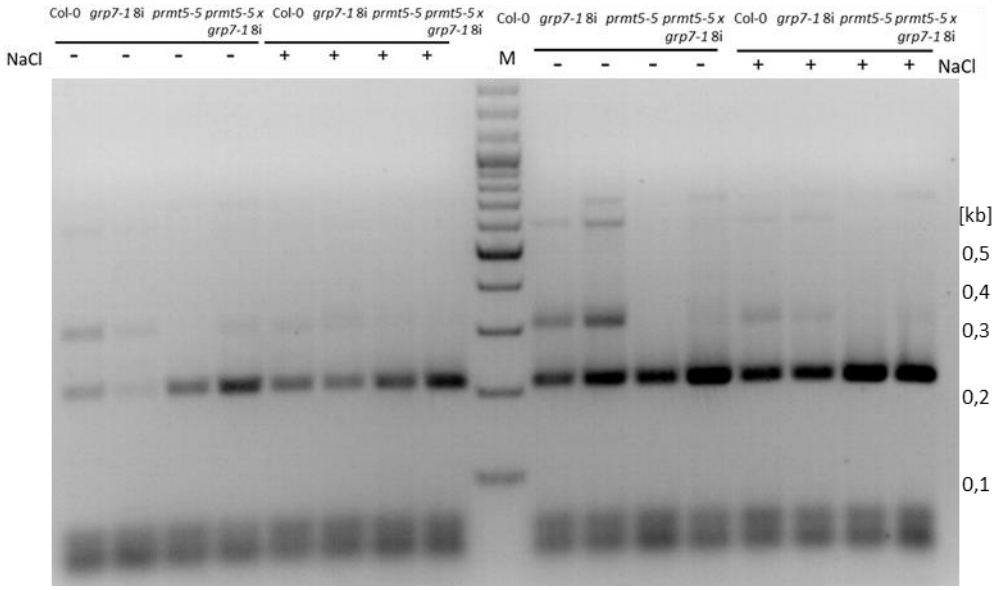

D ***ACT2***

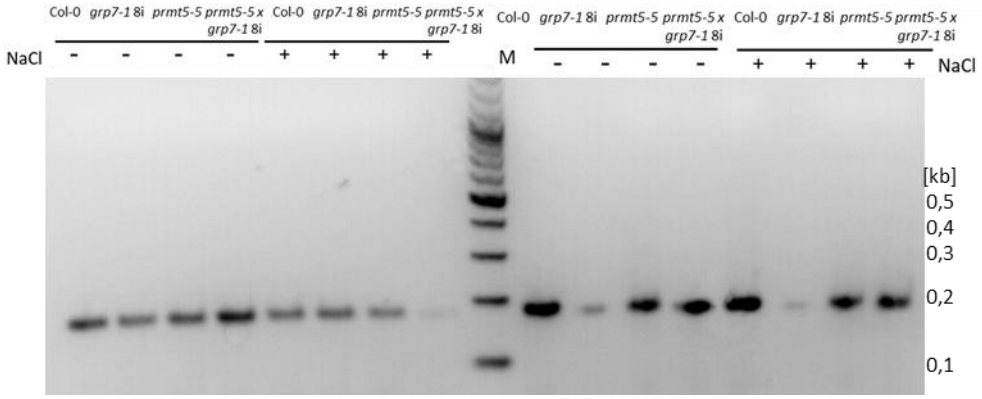

Figure A. 13 Effect of GRP7, GRP8 and PRMT5 on alternative splicing of *FLK*, *AKIN11* and *VFP5* under salt stress conditions. Pictures represent first and second biological replicate of AS under salt stress conditions. 11-day-old seedlings were transferred on ½ MS plates with or without 200 mM NaCl for 6 h and aerial parts were harvested. Synthesised cDNAs were used in sqPCR for amplification of (**A**) *FLK,* (**B**) *AKIN11* and (**C**) *VFP5* transcripts. (**D**) *ACTIN2* (*ACT2*) was used as a loading control.

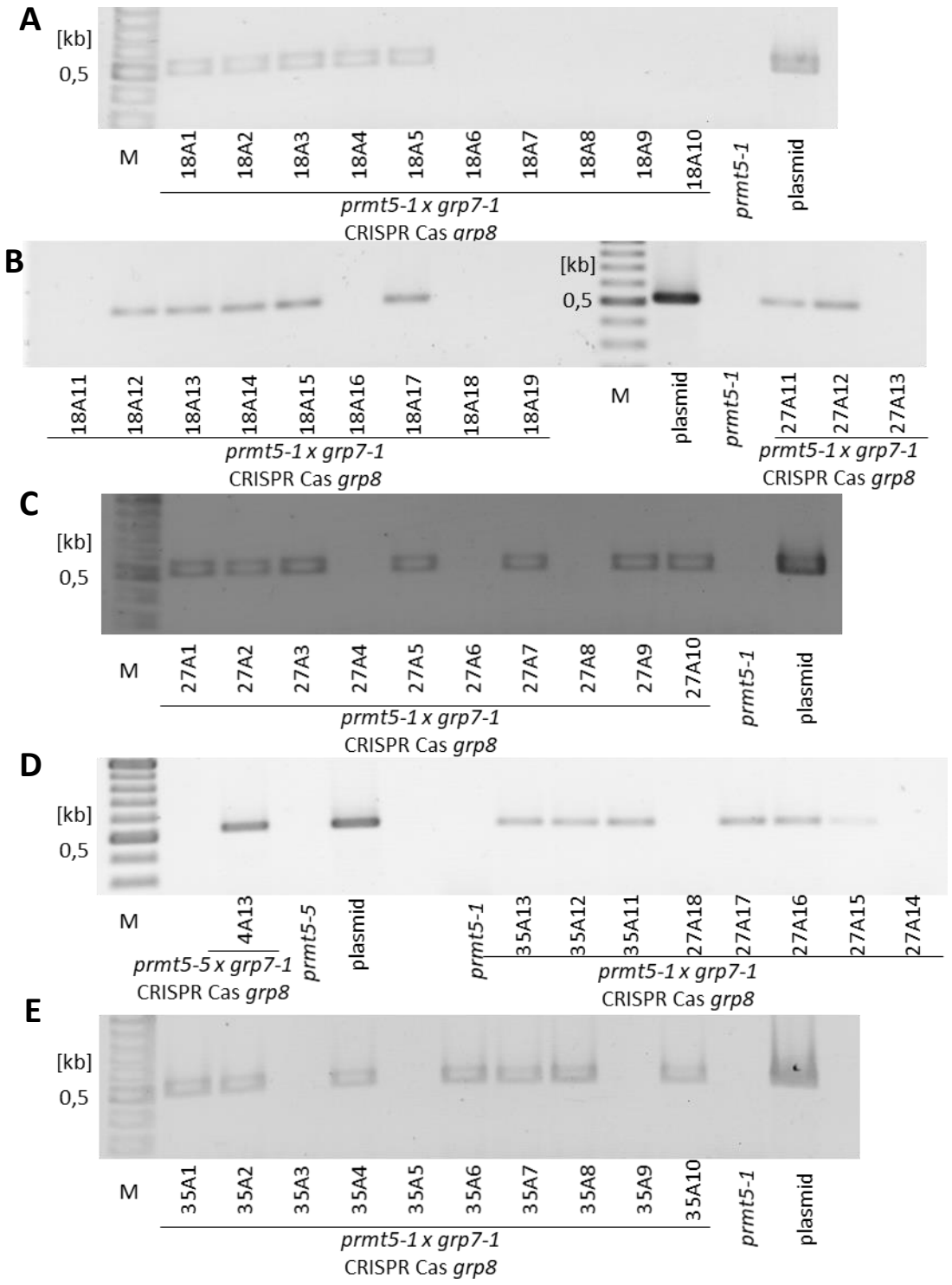

Figure A. 14 Amplification of sgRNA fragments in plants of the T_2 generation. Detection of the T-DNA with the sgRNA in transgenic plants was performed by PCR with F_NotI_pEN and R_NotI_pEN primers using DNA isolated from T_2 plants (**A** and **B**) 18A1-18A19, (**B, C** and **D**) 27A1-27A18, (**D** and **E**) 35A1-35A13. The plasmid #2020 containing the sgRNA sequence served as a positive control, while DNA from the *prmt5-1* mutant was used as a negative control. M- marker 100 bp.

Abbreviations

AGI	Arabidopsis Genome Initiative Identifier
Alt. 3'ss	Alternative 3' splice site
Alt. 5'ss	Alternative 5' splice site
AS	Alternative splicing
ATP	Adenosine-5'-triphosphate
bp	Base Pair
CDS	Coding sequence
cDNA	Complementary DNA
Col	Columbia
Da	Dalton
DNA	Deoxyribonucleic acid
dNTP	Deoxynucleotide Triphosphate
ds	double-stranded
d(T)	Desoxy Thymidine
DTT	Dithiothreitol
EDTA	Ethylenediaminetetraacetic acid
ES	Exon Skipping
EtBr	Ethidium Bromide
gDNA	Genomic DNA
GFP	Green Fluorescent Protein
hnRNP	heterogeneous nuclear RNP
IR	Intron Retention
kb	Kilobase
MOPS	3-(N-morpholino)propanesulfonic acid
mRNA	Messenger Ribonucleic Acid
MS	Murashige-Skoog
NMD	Nonsense-Mediated mRNA Decay
nt	nucleotide
PCR	Polymerase Chain Reaction
Pst	*Pseudomonas syringae pv.* tomato DC3000
PTC	Premature Termination Codon
qPCR	quantitative PCR
RBD	RNA-Binding Domain
RBP	RNA-Binding Protein
Rep	Replicate
RIP	RNA Immunoprecipitation
RNA	Ribonulceic Acid

RNP	Ribonucleoprotein
rpm	Revolutions Per Minute
RRM	RNA Recognition Motif
rRNA	Ribosomal RNA
RT	Reverse Transcription
SDS-PAGE	Sodium Dodecylsulfate Polyacrylamide Gel Electrophoresis
seq	Sequencing
snRNA	Small Nuclear Ribonucleic Acid
snRNP	Small Nuclear Ribonucleoprotein Particle
sqPCR	semiquantitative PCR
SR domain/protein	Serine/Arginine Rich Domain/Protein
TEMED	Tetramethylethylenediamine
UTR	Untranslated Region
v/v	Volume per Volume
WT	Wild Type
w/v	Weight per Volume
zt	zeitgeber time

Acknowledgement

I would like to express my sincere gratitude to Prof. Dr. Dorothee Staiger for her support and guidance of my Ph.D. study. Prof. Staiger has been a tremendous mentor, who allowed me to grow as a scientist and inspired me by her hardworking and passionate attitude. Joining Bio8 team has changed my life and therefore, I will be forever grateful to Prof. Staiger for accepting my application.

I would also like to thank to Dr. Alexander Steffen, whose office door was always open whenever I had a question about my research. His patience, advices and comments helped me not to run into a trouble spot.

My sincere thanks also go to Dr. Marlene Reichel for her unfailing support, insightful comments, advices, constructive criticism and continuous encouragement through the process of writing this thesis. It was a pleasure to see Marlene every day in the lab and a blessing to work with her.

I would like to express sincere gratitude to the Universitätsgesellschaft (UGBI) for supporting me with the Helmut-Skowronek-Stipendium der Universität Bielefeld.

Ein besonderer Dank geht an die zukünftigen Hollywoodstars Elisabeth Klemme und Kristina Neudorf für ihre Hilfe, Geduld, Unterstützung und guten Herzen. Sie sind die Besten und ohne Sie wäre keine Laborarbeit möglich. Vielen Dank auch an alle meine Kollegen vom Bio8-Team für die unschätzbare Unterstützung, die Umarmungen, das Ihr mit mir den Hamstertanz getanzt habt, den Deutschunterricht und Butter bei die Fische. Vielen Dank an Katja Meyer und Christine Nolte, die mir das Leben im Labor beigebracht, Tränen abgewischt und interessante Geschichten erzählt haben. Vielen Dank an Natalie Williams, Olga Schmidt, Marlene Reichel, Christiane Nöh und Martin Lewinski für schöne Momente auch außerhalb des Labors. Ohne euch wäre es nicht dasselbe und ich würde wahrscheinlich mehr als einmal aufgeben. Ich hoffe auf eine lange und großartige Freundschaft. Mein Dank gilt auch meinen ehemaligen Studenten Irina Dück, Pia Gülpen und Katharina Grunert.

Na koniec chciałabym podziękować moim najbliższym, bez których wsparcia nie byłabym w stanie osiągnąć tego wszystkiego i być w miejscu, w którym teraz jestem. Największe i najszczersze podziękowania prosto z całego mojego serca kieruje do mojej Mamy. Bez niej, myśl o pisaniu doktoratu za granicą pozostałaby w swerze marzeń. Dzięki jej wsparciu i dopingowi nigdy się nie poddałam i zyskałam coś więcej niż tylko tytuł doktora. Otóż, w Bielefeld odnalazłam swoją drugą połówkę. Frederykowi Dombertowi, mojemu przyszłemu mężowi dziękuję za bezgraniczne zaufanie, podnoszenie głowy w ciężkich chwilach i sprawienie, że cztery lata przeminęły w mgnieniu oka. Bez jego wsparcia, ukończenie tej pracy byłoby niemożliwe. Z całego serca dziękuję również Edeltraudzie Dombert i Thomasowi Dohnie, za ich dobre rady, kibicowanie i wiarę, że się to wszystko uda.

Erklärung

Hiermit versichere ich, dass ich die vorliegende Arbeit selbstständig und nur mit Hilfe der aufgeführten Quellen und Hilfsmitteln erstellt habe. Anderen Werken entnommene Stellen sind unter Angabe ihrer Quelle gekennzeichnet.

Bielefeld, im Oktober 2019

_____

Katarzyna Krowicka